To the Graduate Council:

I am submitting herewith a thesis written by Cyrus K. Riahi-Nezhad entitled "The Effect of Electric Field on Moving Aqueous Aerosol Suspended in a Dynamic Fluid Chamber." I have examined the final paper copy of this thesis for form and content and recommend that it be accepted in partial fulfillment of the requirements for the degree of Master of Science, with a major in Chemical Engineering.

George C. Frazier

George C. Frazier, Major Professor

We have read this thesis
and recommend its acceptance:

Accepted for the Council:

Vice Provost and
Dean of Graduate Studies

# THE EFFECT OF ELECTRIC FIELD ON MOVING AQUEOUS AEROSOL SUSPENDED IN A DYNAMIC FLUID CHAMBER

**A Thesis**
**Presented for the**
**Master of Science**
**Degree**
**The University of Tennessee, Knoxville**

**Cyrus K. Riahi-Nezhad**
**May 2002**

# ACKNOWLEDGMENTS

Thesis
2002
.R53

The author wishes to thank Oak Ridge National Laboratory for providing the financial support which made this work possible. Several people contributed in significant measure to this program. The author's deepest appreciation and thanks go to the following people:

George C. Frazier (Distinguished Professor), major professor, for his invaluable guidance and friendship.

Jack S. Watson, committee member, for his support and suggestion of preparing slush of methanol and dry-ice for moisture trap.

David W. DePaoli, committee member and supervisor at ORNL, for his kindness, encouragement, understanding and support.

Costas Tsouris, Committee member and supervisor at ORNL, for his technical advice, support, kindness, encouragement and choosing me for this project.

Valmor F. de Almeida, supervisor at ORNL, for his friendship, support and suggestion in fluid dynamics and collaboration in several other topics

Masoud Feizi, for his comments, contributions, kindness and suggestions.

Max Cronan, Larry Cox and coworkers at the Oak Ridge National Laboratory's Plant and Equipment Division for their continuous help with modifications. Also, I wish to thank Linda Moyer and Charlene Burt in the same Division for providing me with dry-ice on a weekly basis.

Betty Frazier and Susan Seymour at University of Tennessee, Linda Puckett at Oak Ridge National Laboratory for their secretarial services.

Finally, I would like to express my appreciation of my parents for their support, love, and encouragement to pursue my education which resulted in this work.

# ABSTRACT

The primarily aim of this research work was to develop a better understanding of electrically driven drop-drop and drop-electrode interactions in an aerosol flow chamber. A particular application of this technology is for treatment processing of radioactive droplets generated in tank waste at Department of Energy sites.

In this research, experimental studies were conducted to explore methods of enhancing the agglomeration of micron sized particles. In such studies, the removal of aerosols by means of DC electric fields was investigated. As a high strength electric field is of importance when building a full-scale agglomerator, agglomeration experiments were carried out with the use of a DC electric field.

An experimental setup was designed and built in which to carry out various aerosol experiments to produce the needed data for this research. The experimental setup consisted of two parallel electrodes, a laser-light-scattering particle sizing system, a rectangular test chamber, dry-ice trap, and a variable high voltage DC power supply. The experimental data were used to accomplish the following tasks:

- Quantify removal of drops from an air stream by an electric field.
- Measure drop size distribution along the flow chamber and determine the effect of an electric field on drop coalescence.

The data indicate that the droplet removal efficiency increases approximately linearly with voltage over the range of voltages investigated, except for one case. In this case, there was no appreciable increase in droplet removal efficiency in the range of 24-

26 kV, suggesting a saturation effect may be occurring. The analysis also shows that in general the removal efficiency is a function of initial droplet concentration. For instance, for a concentration of 24.23 $g/m^3$, the maximum removing efficiency is approximately 85.5 percent while for the concentration of 8.32 $g/m^3$ the maximum removing efficiency is 65.0 percent under the same experimental conditions.

The analysis of the droplet distribution reveals that the mean size of droplets does not always change with voltage; however, the distribution of the number of droplets does change. Appreciable changes in the number of droplets were observed for droplet sizes in a typical range of 4 to 10 μm.

The overall experience and knowledge gained in this research will be useful in developing effective applications of superimposed electric fields for the elimination of mist from air or gaseous streams.

# TABLE OF CONTENTS


| CHAPTER | | PAGE |
|---|---|---|
| 1. | **INTRODUCTION** | **1** |
| | 1.1 Background | 2 |
| | 1.2 Problem Statement and Research Objectives | 3 |
| | 1.3 Thesis Organization | 5 |
| 2. | **REVIEW OF PERTINENT LITERATURE** | **6** |
| | 2.1 Cyclone Collector | 6 |
| | 2.2 Fabric Filters | 7 |
| | 2.3 Electrostatic Precipitators | 8 |
| | 2.4 Venturi Scrubbers | 10 |
| | 2.5 Ionizing Wet Scrubbers | 11 |
| | 2.6 Collision Scrubbers | 12 |
| | 2.7 Electrodynamic Venturis | 12 |
| | 2.8 Inertial Impaction | 13 |
| | 2.9 HEPA Filters | 15 |
| | 2.10 Electrocoalescence | 16 |
| | 2.11Electro-filtration of Aerosols | 19 |
| 3. | **EXPERIMENTAL PROCEDURES** | **22** |
| | 3.1 Experimental Setup | 22 |
| | 3.2 Isokinetic Sampling | 27 |
| | 3.3 Dry-Ice Sampling | 27 |
| | 3.4 Particle Size Distribution Measurement and Control | 32 |
| 4. | **THEORETICAL CONSIDERATIONS** | **37** |
| | 4.1 Equation of Motion for a Single Aerosol Particle | 37 |
| | 4.2 Particle Motion in an Electric Field | 39 |
| | 4.3 Electric field Between Parallel Plates | 43 |
| | 4.4 Theory of Electro-Coalescence | 45 |
| 5. | **RESULTS AND DISCUSSIONS** | **49** |
| | 5.1 Observations | 49 |
| | 5.2 Test Conditions | 50 |
| | 5.3 Effects of Electric Field Strength on Droplet Concentration | 51 |
| | 5.4 Effects of Electric Field Strength on Light Transmission | 54 |
| | 5.5 Effect of Electric Field on Droplet Numbers | 57 |
| | 5.6 Size Distribution | 58 |
| | 5.7 Multiple Elevation Results | 63 |
| | 5.8 Multiple Mist Densities at Constant Flow Rates | 65 |

5.9 Multiple Flow Rates at Constant Mist Concentration ..... 68
5.10 Removing Efficiency of the Droplets ..... 72

**6. SUMMARY and CONCLUSIONS ..... 76**
**7. RECOMMENDATIONS ..... 79**
**REFERENCES ..... 80**
**APENDIX ..... 85**
**VITA ..... 134**

# LIST OF TABLES

Table 5.1 Percent error of measured and calculated mass of collected water rom room's air at variable flow rates ..... 50
Table 5.2 Comparison of percent light transmission at various heights and applied voltages ..... 64
Table 5.3 Effect of applied voltage on droplet concentration for Reynolds Number of 1350 ..... 66
Table 5.4 Effect of applied voltage on droplet concentration for Reynolds Number of 1950 ..... 67
Table 5.5 Constant droplet concentration at Reynolds Numbers of 940, 1350, and 1680 ..... 69
Table 5.6 Exit mist concentrations for Reynolds Numbers of 1230, 1350, and 1680 ..... 70
Table 5.7 Exit mist concentration for Reynolds Numbers of 2400, 2070, 1807 and 937 ..... 71
Table 5.8 Exit mist concentrations for Reynolds Numbers of 2200, 1680, 1350 and 940 ..... 73
Table A.1a Droplet Diameter vs. Cumulative (%) and Volume Frequency (%) Respectively for conditions of Figure A1a ..... 107
Table A.1b Droplet Diameter vs. Cumulative (%) and Volume Frequency (%) Respectively for conditions of Figure A1b ..... 107
Table A.1c Droplet Diameter vs. Cumulative (%) and Volume Frequency (%) Respectively for conditions of Figure A1c ..... 108
Table A.1d Droplet Diameter vs. Cumulative (%) and Volume Frequency (%) Respectively for conditions of Figure A1d ..... 108
Table A.1e Droplet Diameter vs. Cumulative (%) and Volume Frequency (%) Respectively for conditions of Figure A1e ..... 109
Table A.1f Droplet Diameter vs. Cumulative (%) and Volume Frequency (%) Respectively for conditions of Figure A1f ..... 109
Table A.2a Droplet Diameter vs. Cumulative (%) and Volume Frequency (%) Respectively for conditions of Figure A2a ..... 110
Table A.2b Droplet Diameter vs. Cumulative (%) and Volume Frequency (%) Respectively for conditions of Figure A2b ..... 110
Table A.2c Droplet Diameter vs. Cumulative (%) and Volume Frequency (%) Respectively for conditions of Figure A2c ..... 111
Table A.2d Droplet Diameter vs. Cumulative (%) and Volume Frequency (%) Respectively for conditions of Figure A2d ..... 111
Table A.2e Droplet Diameter vs. Cumulative (%) and Volume Frequency (%) Respectively for conditions of Figure A2e ..... 112
Table A.2f Droplet Diameter vs. Cumulative (%) and Volume Frequency (%) Respectively for conditions of Figure A2f ..... 112
Table A.3a Droplet Diameter vs. Cumulative (%) and Volume Frequency (%) Respectively for conditions of Figure A3a ..... 113

Table A.3b Droplet Diameter vs. Cumulative (%) and Volume Frequency (%) Respectively for conditions of Figure A3b ..... 113
Table A.3c Droplet Diameter vs. Cumulative (%) and Volume Frequency (%) Respectively for conditions of Figure A3c ..... 114
Table A.3d Droplet Diameter vs. Cumulative (%) and Volume Frequency (%) Respectively for conditions of Figure A3d ..... 114
Table A.3e Droplet Diameter vs. Cumulative (%) and Volume Frequency (%) Respectively for conditions of Figure A3e ..... 115
Table A.3f Droplet Diameter vs. Cumulative (%) and Volume Frequency (%) Respectively for conditions of Figure A3f ..... 115
Table A.4a Droplet Diameter vs. Cumulative (%) and Volume Frequency (%) Respectively for conditions of Figure A4a ..... 116
Table A.4b Droplet Diameter vs. Cumulative (%) and Volume Frequency (%) Respectively for conditions of Figure A4b ..... 116
Table A.4c Droplet Diameter vs. Cumulative (%) and Volume Frequency (%) Respectively for conditions of Figure A4c ..... 117
Table A.4d Droplet Diameter vs. Cumulative (%) and Volume Frequency (%) Respectively for conditions of Figure A4d ..... 117
Table A.4e Droplet Diameter vs. Cumulative (%) and Volume Frequency (%) Respectively for conditions of Figure A4e ..... 118
Table A.4f Droplet Diameter vs. Cumulative (%) and Volume Frequency (%) Respectively for conditions of Figure A4f ..... 118
Table A.5a Droplet Diameter vs. Cumulative (%) and Volume Frequency (%) Respectively for conditions of Figure A5a ..... 119
Table A.5b Droplet Diameter vs. Cumulative (%) and Volume Frequency (%) Respectively for conditions of Figure A5b ..... 119
Table A.5c Droplet Diameter vs. Cumulative (%) and Volume Frequency (%) Respectively for conditions of Figure A5c ..... 120
Table A.5d Droplet Diameter vs. Cumulative (%) and Volume Frequency (%) Respectively for conditions of Figure A5d ..... 120
Table A.5e Droplet Diameter vs. Cumulative (%) and Volume Frequency (%) Respectively for conditions of Figure A5e ..... 121
Table A.5f Droplet Diameter vs. Cumulative (%) and Volume Frequency (%) Respectively for conditions of Figure A5f ..... 121
Table A.6a Droplet Diameter vs. Cumulative (%) and Volume Frequency (%) Respectively for conditions of Figure A6a ..... 122
Table A.6b Droplet Diameter vs. Cumulative (%) and Volume Frequency (%) Respectively for conditions of Figure A6b ..... 122
Table A.6c Droplet Diameter vs. Cumulative (%) and Volume Frequency (%) Respectively for conditions of Figure A6c ..... 123
Table A.6d Droplet Diameter vs. Cumulative (%) and Volume Frequency (%) Respectively for conditions of Figure A6d ..... 123
Table A.6e Droplet Diameter vs. Cumulative (%) and Volume Frequency (%) Respectively for conditions of Figure A6e ..... 124
Table A.6f Droplet Diameter vs. Cumulative (%) and Volume Frequency (%)

Respectively for conditions of Figure A6f ..... 124
Table A.7a Droplet Diameter vs. Cumulative (%) and Volume Frequency (%)
Respectively for conditions of Figure A7a ..... 125

Table A.7b Droplet Diameter vs. Cumulative (%) and Volume Frequency (%)
Respectively for conditions of Figure A7b ..... 125
Table A.7c Droplet Diameter vs. Cumulative (%) and Volume Frequency (%)
Respectively for conditions of Figure A7c ..... 126
Table A.7d Droplet Diameter vs. Cumulative (%) and Volume Frequency (%)
Respectively for conditions of Figure A7d ..... 126
Table A.7e Droplet Diameter vs. Cumulative (%) and Volume Frequency (%)
Respectively for conditions of Figure A7e ..... 127

Table A.7f Droplet Diameter vs. Cumulative (%) and Volume Frequency (%)
Respectively for conditions of Figure A7f. ..... 127
Table A.8a Effect of Applied Voltage on Droplet Concentration
for a Reynolds Number of 1350 (Run 1) ..... 128
Table A.8b Effect of Applied Voltage on Droplet Concentration
for a Reynolds Number of 1350 (Run 2) ..... 128
Table A.8c Effect of Applied Voltage on Droplet Concentration
for a Reynolds Number of 1350 (Ave.) ..... 128
Table A.9a Effect of Applied Voltage on Droplet Concentration
for a Reynolds Number of 1950 (Run 1) ..... 129
Table A.9b Effect of Applied Voltage on Droplet Concentration
for a Reynolds Number of 1950 (Run 2) ..... 129
Table A.9c Effect of Applied Voltage on Droplet Concentration
for a Reynolds Number of 1950 (Ave.) ..... 129
Table A.10a Constant Droplet Concentration
at Reynolds Number of 940,1350 and 1680 (Run 1) ..... 130
Table A.10b Constant Droplet Concentration
at Reynolds Number of 940,1350 and 1680 (Run 2) ..... 130
Table A.10c Constant Droplet Concentration
at Reynolds Number of 940,1350 and 1680 (Ave.) ..... 130
Table A.11a Exit Mist Concentration
for a Reynolds Number of 1230,1350 and 1680 (Run 1) ..... 131
Table A.11b Exit Mist Concentration
for a Reynolds Number of 1230,1350 and 1680 (Run 2) ..... 131
Table A.11c Exit Mist Concentration
for a Reynolds Number of 1230,1350 and 1680 (Ave.) ..... 131
Table A.12a Exit Mist Concentration
for a Reynolds Number of 2400, 2070, 1810, and 940 (Run 1) ..... 132
Table A.12b Exit Mist Concentration
for a Reynolds Number of 2400, 2070, 1810, and 940 (Run 2) ..... 132
Table A.12c Exit Mist Concentration
for a Reynolds Number of 2400, 2070, 1810, and 940 (Ave.) ..... 132

Table A.13a Exit Mist Concentration
for a Reynolds Number of 2200, 1680,1350, and 940 (Run 1)..... 133
Table A.13b Exit Mist Concentration
for a Reynolds Number of 2200, 1680,1350, and 940 (Run 2)..... 133
Table A.13c Exit Mist Concentration
for a Reynolds Number of 2200, 1680,1350, and 940 (Ave.)..... 133

# LIST OF FIGURES

Figure 3.1 Schematic diagram of Electro-Coalescence Unit System ..... 23
Figure 3.2 Schematic diagram of the experimental setup ..... 24
Figure 3.3 Photograph of the experimental setup ..... 26
Figure 3.4 Schematic diagram of macroscopic mass balance process ..... 28
Figure 3.5 Dimension and components of the Malvern
Spraytec RTS 5000 Series (Malvern Instrument) ..... 33
Figure 3.6 Spraytec RTS 5000 System Layout (Malvern Instrument ..... 33
Figure 4.1 Electric field around an aerosol uncharged particle ..... 40
Figure 4.2 Electric field around a partially charged aerosol particle ..... 40
Figure 4.3 Electric field between parallel plates with plate spacing, d ..... 43
Figure 4.4 Possible relative trajectories of two drops ..... 48
Figure 5.1 Droplets concentration vs. applied voltage at
Reynolds Number of 1350 ..... 52
Figure 5.2 Droplets concentration vs. applied voltage at
Reynolds Number of 1620 ..... 52
Figure 5.3 Droplets concentration vs. applied voltage at
Reynolds Number of 1680 ..... 53
Figure 5.4 Droplets concentration vs. applied voltage at
Reynolds Number of 1950 ..... 53
Figure 5.5 Droplets concentration vs. applied voltage at
Reynolds Number of 2200 ..... 54
Figure 5.6 Droplets concentration vs. percent light transmission at
Reynolds Number of 1350 under varying applied voltage ..... 55
Figure 5.7 Droplets concentration vs. percent light transmission at
Reynolds Number of 1620 under varying applied voltage ..... 55
Figure 5.8 Droplets concentration vs. percent light transmission at
Reynolds Number of 1680 under varying applied voltage ..... 56
Figure 5.9 Droplets concentration vs. percent light transmission at
Reynolds Number of 1950 under varying applied voltage ..... 56
Figure 5.10 Droplets concentration vs. percent light transmission at
Reynolds Number of 2200 under varying applied voltage ..... 57
Figure 5.11 Number droplets vs. particle diameter in micron at inlet
Mist concentration of 12.4 g/m$^3$ and Reynolds Number of 1624 ..... 61
Figure 5.12 Number droplets vs. particle diameter in micron at inlet
Mist concentration of 8.72 g/m$^3$ and Reynolds Number of 2195 .....
Figure 5.13 Droplet size distribution for Reynolds Number of 1345 ..... 60
a. Droplet concentration of 12.11 g/m$^3$ at applied voltage of 0.0 kV
b. Droplet concentration of 5.96 g/m$^3$ at applied voltage of 26 kV
Figure 5.14 Droplet size distribution for Reynolds Number of 1345 ..... 62
a. Droplet concentration of 24.23 g/m$^3$ at applied voltage of 0.0 kV
b. Droplet concentration of 8.17 g/m$^3$ at applied voltage of 26 kV
Figure 5.15 Percent light transmission vs. height of column at Reynolds

Number of 1624 and inlet droplet concentration of 27.27 g/m$^3$ ..... 63
Figure 5.16 Collected Droplets (g/m$^3$) vs. applied voltage (kV)
at Reynolds Number of 1346 ..... 66
Figure 5.17 Collected Droplets (g/m$^3$) vs. applied voltage (kV)
at Reynolds Number of 1946 ..... 67
Figure 5.18 Collected Droplets (g/m$^3$) vs. applied voltage (kV)
at Reynolds Numbers of 937, 1346 and 1682 ..... 69
Figure 5.19 Collected Droplets (g/m$^3$) vs. applied voltage (kV)
at Reynolds Numbers of 1225, 1346 and 1682 ..... 70
Figure 5.20 Collected Droplets (g/m$^3$) vs. applied voltage (kV)
at Reynolds Numbers of 2400, 2070, 1807 and 937 ..... 71
Figure 5.21 Collected Droplets (g/m$^3$) vs. applied voltage (kV)
at Reynolds Numbers of 2195, 1682, 1346 and 937 ..... 73
Figure 5.22 Percent removal efficiency vs. applied voltages (kV)
at Reynolds Number of 1346 ..... 74
Figure 5.23 Percent removal efficiency vs. applied voltages (kV)
at Reynolds Number of 1946 ..... 75
Figure A.1a Droplet size distribution for Reynolds Number of
1345 and concentration of 12.1 g/m$^3$ at V = 0.0 kV ..... 86
Figure A.1b Droplet size distribution for experimental conditions of Figure A1a,
with V = 10.0 kV; Droplet Concentration at exit = 9.2 g/m$^3$ ..... 86
Figure A.1c Droplet size distribution for experimental conditions of Figure A1a,
with V = 15.0 kV; Droplet Concentration at exit = 8.0 g/m$^3$ ..... 87
Figure A.1d Droplet size distribution for experimental conditions of Figure A1a,
with V = 18.0 kV; Droplet Concentration at exit = 6.60 g/m$^3$ ..... 87
Figure A.1e Droplet size distribution for experimental conditions of Figure A1a,
with V = 20.0 kV; Droplet Concentration at exit = 6.16 g/m$^3$ ..... 88
Figure A.1f Droplet size distribution for experimental conditions of Figure A1a,
with V = 26.0 kV; Droplet Concentration at exit = 5.0 g/m$^3$ ..... 88
Figure A.2a Droplet size distribution for Reynolds Number of
1350 and concentration of 24.23 g/m$^3$ at V = 0.0 kV ..... 89
Figure A.2b Droplet size distribution for experimental conditions of Figure A2a,
with V = 10.0 kV; Droplet Concentration at exit = 18.97 g/m$^3$ ..... 89
Figure A.2c Droplet size distribution for experimental conditions of Figure A2a,
with V = 15.0 kV; Droplet Concentration at exit = 15.8 g/m$^3$ ..... 90
Figure A.2d Droplet size distribution for experimental conditions of Figure A2a,
with V = 18.0 kV; Droplet Concentration at exit = 13.7 g/m$^3$ ..... 90
Figure A.2e Droplet size distribution for experimental conditions of Figure A2a,
with V = 20.0 kV; Droplet Concentration at exit = 11.6 g/m$^3$ ..... 91
Figure A.2f Droplet size distribution for experimental conditions of Figure A2a,
with V = 26.0 kV; Droplet Concentration at exit = 5.12 g/m$^3$ ..... 91
Figure A.3a Droplet size distribution for Reynolds Number of
1350 and concentration of 16.3 g/m$^3$ at V = 0.0 kV ..... 92
Figure A.3b Droplet size distribution for experimental conditions of Figure A3a,
with V = 10.0 kV; Droplet Concentration at exit = 11.7 g/m$^3$ ..... 92

Figure A.3c Droplet size distribution for experimental conditions of Figure A3a, with V = 15.0 kV; Droplet Concentration at exit = 9.3 g/m$^3$ ..... 93
Figure A.3d Droplet size distribution for experimental conditions of Figure A3a, with V = 18.0 kV; Droplet Concentration at exit = 8.6 g/m$^3$ ..... 93
Figure A.3e Droplet size distribution for experimental conditions of Figure A3a, with V = 20.0 kV; Droplet Concentration at exit = 8.1 g/m$^3$ ..... 94
Figure A.3f Droplet size distribution for experimental conditions of Figure A3a, with V = 26.0 kV; Droplet Concentration at exit = 5.4 g/m$^3$ ..... 94
Figure A.4a Droplet size distribution for Reynolds Number of 1350 and Droplet Concentration of 8.3 g/m$^3$ at V = 0.0 kV ..... 95
Figure A.4b Droplet size distribution for experimental conditions of Figure A4a, with V = 10.0 kV; Droplet Concentration at exit = 7.3 g/m$^3$ ..... 95
Figure A.4c Droplet size distribution for experimental conditions of Figure A4a, with V = 15.0 kV; Droplet Concentration at exit = 6.0 g/m$^3$ ..... 96
Figure A.4d Droplet size distribution for experimental conditions of Figure A4a, with V = 18.0 kV; Droplet Concentration at exit = 5.4 g/m$^3$ ..... 96
Figure A.4e Droplet size distribution for experimental conditions of Figure A4a, with V = 20.0 kV; Droplet Concentration at exit = 4.6 g/m$^3$ ..... 97
Figure A.4f Droplet size distribution for experimental conditions of Figure A4a, with V = 26.0 kV; Droplet Concentration at exit = 3.0 g/m$^3$ ..... 97
Figure A.5a Droplet size distribution for Reynolds Number of 1950 and Droplet Concentration of 13.3 g/m$^3$ at V = 0.0 kV ..... 98
Figure A.5b Droplet size distribution for experimental conditions of Figure A5a, with V = 10.0 kV; Droplet Concentration at exit = 9.7 g/m$^3$ ..... 98
Figure A.5c Droplet size distribution for experimental conditions of Figure A5a, with V = 15.0 kV; Droplet Concentration at exit = 9.0 g/m$^3$ ..... 99
Figure A.5d Droplet size distribution for experimental conditions of Figure A5a, with V = 18.0 kV; Droplet Concentration at exit = 8.0 g/m$^3$ ..... 99
Figure A.5e Droplet size distribution for experimental conditions of Figure A5a, with V = 20.0 kV; Droplet Concentration at exit = 7.5 g/m$^3$ ..... 100
Figure A.5f Droplet size distribution for experimental conditions of Figure A5a, with V = 26.0 kV; Droplet Concentration at exit = 3.3 g/m$^3$ ..... 100
Figure A.6a Droplet size distribution for Reynolds Number of 1950 and Droplet Concentration of 10.1 g/m$^3$ at V = 0.0 kV ..... 101
Figure A.6b Droplet size distribution for experimental conditions of Figure A6a, with V = 10.0 kV; Droplet Concentration at exit = 8.8 g/m$^3$ ..... 101
Figure A.6c Droplet size distribution for experimental conditions of Figure A6a, with V = 15.0 kV; Droplet Concentration at exit = 7.5 g/m$^3$ ..... 102
Figure A.6d Droplet size distribution for experimental conditions of Figure A6a, with V = 18.0 kV; Droplet Concentration at exit = 6.3 g/m$^3$ ..... 102
Figure A.6e Droplet size distribution for experimental conditions of Figure A6a, with V = 20.0 kV; Droplet Concentration at exit = 5.2 g/m$^3$ ..... 103
Figure A.6f Droplet size distribution for experimental conditions of Figure A6a, with V = 26.0 kV; Droplet Concentration at exit = 3.3 g/m$^3$ ..... 103
Figure A.7a Droplet size distribution for Reynolds Number of 1950

and Droplet Concentration of 8.1 g/m$^3$ at V = 0.0 kV ..... 104
Figure A.7b Droplet size distribution for experimental conditions of Figure A7a, with V = 10.0 kV; Droplet Concentration at exit = 7.3 g/m$^3$ ..... 104
Figure A.7c Droplet size distribution for experimental conditions of Figure A7a, with V = 15.0 kV; Droplet Concentration at exit = 5.9 g/m$^3$ ..... 105
Figure A.7d Droplet size distribution for experimental conditions of Figure A7a, with V = 18.0 kV; Droplet Concentration at exit = 4.6 g/m$^3$ ..... 105
Figure A.7e Droplet size distribution for experimental conditions of Figure A7a, with V = 20.0 kV; Droplet Concentration at exit = 4.4 g/m$^3$ ..... 106
Figure A.7f Droplet size distribution for experimental conditions of Figure A7a, with V = 26.0 kV; Droplet Concentration at exit = 3.3 g/m$^3$ ..... 106

# CHAPTER 1

# INTRODUCTION

The Clean Air Act Amendments of 1990 (CAAA) changed the air quality regulations in the United States. A major component of the CAAA concerns the emissions of hazardous air pollutants (HAPs). After the rules have been implemented by U.S Environmental Protection Agency (EPA), companies must modify their operations and emission control systems to meet the regulatory challenges (Bacon, 1997). These changes are mainly concerned with the control of hazardous aerosol particle sizes and human exposure to such particles. Thus, it is important to characterize these particles in both size and dynamics as accurately as possible. Such characterization will help develop new filtering technologies that could significantly reduce/control the emission of hazardous aerosol particles in a cost effective manner.

For instance, the growing concern regarding the production of radioactive aerosols during treatment and sludge retrieval operations in high-level radioactive waste tanks has led the Department of Energy to an increasing interest in reducing the emissions, worker exposure, cost and increased waste volume from such tanks. Conventional mist eliminators such as High Efficiency Particulate Attenuation (HEPA) filtration were not sufficient to treat off-gas in a recent In-Tank Evaporation process (ITE) at the Oak Ridge National Laboratory, Melton Valley Storage Tank waste, resulting in contamination of system ductwork and wetting and plugging of HEPA filters.

It should be emphasized that the human exposure to hazardous aerosol particles in general and sub-micron particles in particular has been a major health concern over the

past decade. In fact, sub-micron particles including droplets constitute the most serious environmental and health related problems. One problem is that such small particles are able to penetrate into the human lung system where the exchange of gases between blood and air takes place (Brown, 1981). The human lower pulmonary system is unfortunately most efficient in retaining particles in 1 micron range (Davies, 1953 & Cadle, 1965 ). The deposition of small particles in the pulmonary system tends to intensify such respiratory disease as bronchitis, emphysema and lung cancer (Cadle, 1965). In addition, submicron particles will stay in the atmosphere for a considerable period of time, scattering the sunlight and dissipating over large area (Kildesq, 1995).

## 1.1 Background

It is known that the removal of small particles from process or waste streams is costly and often very time consuming (Barker et al.,1991). Elimination of liquid droplets and/or solid particles from gas or vapor streams is a common operation in a variety of chemical and environmental processes. Despite the utilized equipment or separation mechanisms, the mist eliminators are designed to operate as coalescers or agglomerators and thereby form larger droplets that can be removed from the process by gravity or shear forces. Droplets of size smaller than 10 microns are in general difficult to remove from gaseous streams. Current particle removing techniques (cyclone, electrostatic precipitator, scrubbers, etc.) have been used to remove larger droplets/particles from a carrier gas with high efficiency (Fuchs, 1964). An electrically driven process including mechanisms such as electrocoalescence and electrophoresis is the focus of this research. The effect of electric fields on particle agglomeration has been investigated by Loffler &

Gutsch (1993) and Zhang et al. (1995), while Lucker et al. (1995) studied electric-field bed filtration.

In order to design an efficient aerosol removal system, we need a fundamental knowledge of droplet-droplet interactions. The selection and evaluation of an air pollution-control system depends on many criteria such as gas flow rate, gas temperature, moisture content, chemical properties of the gas, properties of particulate matter, available space, system operating pressure, waste generation and economics.

## 1. 2 Problem Statement and Research Objectives

Over the past three decades an extensive effort has been directed to finding new applications of electrical energy in the field of heat and mass transfer operations and phase separation processes. In many situations electrically driven processes, including electrocoalescence and electric filtration, can be considered competitive alongside mechanically or thermally driven operations (Ptasinski, 1992) and powerful for improving aerosol elimination. Electrocoalescence increases the mean droplet size, which is a key for improving the removal efficiency by HEPA filtration.

The primary aim of this research work is at developing a better understanding of electrically driven drop-drop and drop-electrode interactions in an aerosol flow chamber. The overall gained experience and knowledge will be useful in developing effective applications of superimposed electric fields for the elimination of mist from air or gaseous streams.

In this research, experimental studies have been undertaken for enhancing the agglomeration of small droplets. In such studies, the agglomeration of aerosols by means of DC electric fields has been investigated.

Experimental measurements have been conducted in order to accomplish the following tasks:

- Quantify removal of drops by an electric field.
- Measure drop size distribution along the flow chamber and determine the effect of an electric field on drop coalescence.

In this work, a homogeneous DC electric field between two parallel plates was used. It is believed that a well-functioning agglomerator under a DC electric field might have a considerable impact on the control of aerosol emissions from waste treatment operations. This is due to the fact that polarized aerosol particles and droplets are attracted to each other in a DC electric field. This behavior enhances the collision and coalescence rate of particles leading to larger aggregates or droplets, which can be removed easier by a conventional filter. Other mechanisms of particle/drop interactions with the electric field are also possible, such as electrophoresis and dielectrophoresis. The results of these interactions with respect to particle/drop removal by collision with the electrodes, are also investigated in this work.

## 1.3 Thesis Organization

This thesis is organized into six chapters. After this introductory chapter, Chapter 2 presents a review of pertinent literature. Experimental procedures used in this research are described in Chapter 3. The equation of motion for a single particle with and without an electric field, and the macroscopic mass balance equation are discussed in Chapter 4. Chapter 5 presents results and discussion. Conclusions are presented in Chapter 6. Avenues for future work are suggested in Chapter 7.

# CHAPTER 2

# REVIEW OF PERTINENT LITERATURE

## 2.1 Cyclone Collector

The cyclone collector is one of the most common and oldest devices for controlling the emissions of large-diameter particulates. The separator generates two vortices as the gas stream enters the top of the cyclone. Centrifugal action throws the heavier particles to the side of the cyclone. Frictional and gravitational forces act on the particles closest to the wall, causing them to slide down into a collector, while particles of less mass remain closer to the center of the vortex. Inside the lower segment of the cyclone, the direction of the gas-flow vortex is reversed and the inner ascending vortex is formed. The inner vortex is a relatively particulate free air (Wark and Warner, 1981). Cyclone systems are classified as follows: simple, multiple, or multi tube. A simple system is a single cyclone, where a multiple cyclone refers to the series or parallel arrangement of more than one cyclone. A multi-tube system is a group of smaller diameter vane axial parallel cyclones within a common housing which contribute to a common inlet and discharges to a common track. Multi-tube cyclones are used for large gas flow rates (Bacon, 1997). The removal efficiency of cyclones for submicron particulates is low and they require very high energy input. However, they are efficient for emissions of large particulates and effective with no liquid waste streams generated. Cyclones are frequently used as pretreatment devices for high efficiency particulate control devices such as ESPs, venturi scrubers, and baghouse. Cyclone collectors are

used primarily when product recovery is an important issue for a facility's production efficiency.

## 2.2 Fabric Filters

Filters are used in a wide variety of materials and geometries to remove particulates from gas streams. Fabric filters or baghouses consist of a large number of filter bags, arranged so that continuous removal of the collected material is possible, and are very effective removal devices for fine particulate matter (Perkins, 1974). The basic components of a baghouse include a filter medium, a cage to support the bag, a gas tight enclosure and a mechanism to remove accumulated particulates. Gases enter one of several separate baghouse compartments, where they are directed upward through a cell plate and into contact with the tubular bag. The tubular bags are contained in multiple modular units comprising the total baghouse system. Initial particulate collection forms a thick porous cake on the bags, which acts as the filtration medium while the bags support the particulate cake. The accumulated dust cake is removed from the bags periodically.

There are three categories of baghouses depending on their flow rate capacity such as low, medium, and large. The low capacity fabric filters are capable of handling hundreds to a few thousand cfm of process gas. The medium capacity fabric filters are modular units designed to handle about 10,000 cfm. The high capacity fabric filters can handle 50,000 to a million cfm (Bacon, 1997). Baghouses are excellent for controlling the small diameter particulate matter from exhaust stream. For example, medium baghouses have efficiencies of 99 percent or better when collecting 0.5 micron particles and can remove substantial quantities of 0.01 micron. The operating temperatures of

baghouses can vary from 175 to 550 °F depending on the nature of baghouse fabric (e.g; cotton, wool, or glass). One of the disadvantages of fabric filters is the necessity of relatively frequent cleaning to avoid an excessive pressure drop (Wark & Warner, 1981). Normally, these filters need to be cleaned up when the pressure drop approaches 5 to 6 in. water. A reasonable operating pressure drop is about 2 to 3 in. water. These filters are also temperature and moisture sensitive. As a result, the moisture in the inlet gas can form a cake, leading to plugging. This might cause fire and/or explosion in the filters if they are not properly cleaned up. In comparison to other competitive types of removal devices, the overall size of the equipment is large and a large physical space is required.

## 2.3 Electrostatic Precipitators (ESP)

Electrostatic phenomena have been known for the past few hundred years. It is a technique to remove suspended particles in a gas using an electric force (White, 1962, Masuda and Hosokawa, 1997 and Boem, 1982). Recently, It also has been used for cleaning indoor air (Mizuno, 1981). Particulate and aerosol collection by electrostatic precipitation is based on the combined attraction between particles of one electrical charge and a collecting electrode of opposite polarity (Wark & Warner, 1981). The ESP technology used for particulate and trace metal removal can be employed as either a dry or wet system (Bacon et al., 1997). Dry and wet ESPs can vary in shape from concentric to square. The concentric ESPs use high intensity ionization electrodes mounted on the central tube. Uniform flow through the tube can be accomplished by a distributor device. As the gas enters the tube, it passes through a charging zone. Particles are charged by ions diffusing from so-called corona dischargers. As the gas flows farther down the tube,

the charged particles are forced to the tube walls by an electrostatic field. The clean gas exits the tube into a clean air compartment which is located at the bottom of the vessel. Square ESPs are build on the same principle as concentric ESPs but they are configured differently. They can use an alternating array of negatively charged grids and positively charged collection plates. The discharged electrodes are usually metal wires suspended along the center by weights or rigid frames. The dry ESP employs an alternating rapping action to remove particulate matter collected on the surface of opposite charge. Wet-electrostatic precipitators are washed with water sprays to remove collected particles from collection surfaces. The high voltage single stage electrostatic precipitator is used to collect both solid and liquid (mist and fog) particulate matter. Low voltage double stage precipitators are limited fully to the collection of particulates or drops.

The advantages of ESPs include high capacity to handle large gas volumes, high collection efficiencies even for submicron size particles, low energy consumption and ability to operate with relatively high temperature gases. Their collection efficiency for trace metals, mist, and fog is very high. Electrostatic precipitators have been built for volumetric rates from 100 to 4,000,000 cfm, and they are used to remove particles from 0.05 to 200 microns with efficiencies in the range of 98 to 99 percent range in some cases. The pressure drop is quite small, extending from 0.1 to 0.5 inches of water. Gas temperatures up to 1200 $^{0}$F and pressures up to 150 psi can be accommodated.

Electrostatic precipitators also have problems. Ionization of the gas occurs only in a limited temperature range so that the device can suffer a loss in efficiency if sudden changes occur in the operating conditions. Build-up of collected material can cause "spark-over" between the electrodes which in turn causes a high current flow and

excessive power use. Build-up of collected material on the negative electrode can suppress the corona discharge and reduce efficiency. The resistivity of the gas-particulate combination also affects the corona and the collection efficiency. Reentrainment of the collected material can interfere with the particle charging and result in direct release of particulate at the exit stream (Perkins, 1974). The other disadvantages of electrostatic precipitators include high costs of operation, maintenance, equipment and energy requirements. In addition, they require large metallic collection surface and expensive corrosion resistant alloys.

## 2.4 Venturi Scrubbers

A venturi is defined as a rectangular or circular flow channel which converges to a narrow throat section and then diverges back to its original cross-section area. In the converging section, the fluid flow is converted into kinetic energy, with a decrease in static pressure and rise in velocity. Venturi scrubbers are designed to serve as control devices for applications requiring very high collection efficiencies of particles between 0.5 and 5.0 micron in diameter. The collection efficiency depends on the length of the throat. A liquid, usually water, is introduced upstream of the throat and flows down the converging sides into the throat where it is atomized by the gas stream. Once the liquid is atomized, it begins to collect particles from the gas impacting into the liquid as a result of the difference in velocities of the gas stream and the atomized droplets. As the mixture decelerates in the diverging section, further contact occurs, causing the droplets to agglomerate. Once the particles have been trapped by the liquid, a separator such as cyclone or mist eliminator can readily remove the scrubbing liquid from the cleaned gas

stream. Venturi scrubbers are excellent fine particulate control devices to a corrosive process stream. Also, they can operate in high temperature and high moisture environments. The disadvantages of this control device are the expensive materials of construction and costly operation and maintenance.

## 2.5 Ionizing Wet Scrubbers

The ionizing wet scrubber uses the principle of electrostatic particle charging, inertial impaction, and gas absorption to collect submicron solid and liquid particles. It uses high voltage ionization to electrostatically charge particulate matter in the gas stream before the particles enter a packed bed scrubber section. At that point, they are removed by attraction of the charged particles by neutral surfaces. Collection of particles of three to five microns and larger can take place by inertial impaction. The smaller particles flow through the scrubber where they pass over the surfaces of packing material and scrubbing liquid droplets. The electrostatic charge of the particles causes them to be attracted to neutral surfaces. The scrubbing liquid and packing material act as collection surfaces. The shell and most internal parts are made of fiberglass and thermoplastic materials to prevent corrosion in the presence of acid gases (Bacon et al., 1997). Collection of submicron particles, mist, and fog by this technique is very effective. Operation and maintenance costs are relatively low, whereas the capital costs are very high and liquid waste streams are generated.

## 2.6 Collision Scrubbers

The collision scrubber has better efficiency than the wet scrubber. It has three scrubber throats arranged in a "T". The gas enters the collision scrubber then splits into two gas streams prior to entering a pair of scrubber throats. At the entrance of each throat, water is injected and then it is atomized by the gas stream. The droplets collect particles as they are accelerated toward the center of the throat. Because of their inertia, they travel into the opposing gas stream with high velocity and turning into finer droplets, which more effectively collect submicron particles and produce a larger liquid surface area for gas absorption. A multi-stage collision scrubber takes the gas/water mixture and removes the water, letting the clean gas to exit the system. The collected water returns to the scrubber throat by a centrifugal pump (Bacon et al., 1997). The collision scrubber can collect trace metal and submicron particulates from process exhaust streams, but its capital and operating costs are high and liquid waste streams are generated.

## 2.7 Electrodynamic Venturis

This air pollution control device consists of a sequence of steps which include saturation, expansion, condensation, ionization, and filtration. Saturation takes place in a quench/ spray tower. The additional steps take place in the main unit. The saturated gas stream leaving the spray tower enters the main unit, then travels into a converging/ diverging section causing an adiabatic expansion of the gas which results in a change in the state of energy (Bacon et al., 1997). As the kinetic energy of the gas increases in the converging section, the static pressure energy decreases. The reduced pressure of the gas

saturated with water vapor creates supersaturation in the diverging section. The suspended particulates in the gas act as condensation nuclei and a film of a water is formed on the surface of the particles. The presence of a water film ensures that the composite particle is capable of receiving and retaining an electric charge. For ionization, the divergent section of the main unit is designed to minimize pressure loss and ensure suitable ionization conditions. On the axial centerline of the main unit, an electrode is mounted and creates a corona within the flow of gas stream. In the final filtration and collection step, two separate mechanisms take place, physical impaction and electrostatic attraction. A hollow cone spray nozzle is located at the center and positioned adjacent to the recovery section of the main unit. The water curtain by the nozzle is positively charged under the influence of the electric field which is generated by the electrode. The carrier gas passes through the charged droplet curtain. The mist eliminator collects the particulate bearing water droplets. Then, large particulates are separated from gas stream by the physical impaction of the spray droplets enhanced by the electrostatic attraction effect. Finally, at the filtration step, the total water droplets are removed from the gas stream and clean gas exits the system (Bacon et al. 1997). The electrodynamic venturi can remove submicron particulate matter from the exhaust streams effectively. On the other hand, the capital costs are relatively high, and it generates a lot of liquid waste.

## 2.8 Inertial Impaction

Inertial impaction units capture tiny liquid droplets entrained in a gas or vapor by impingement on solid surfaces. In vane-type units, the gas flows either horizontally or

upward and vanes direct the flowing gas back and forth in a twisting pattern. Mist droplets are carried along by the gas. Because of their momentum due to their higher density, the droplets tend to move in straight lines than the bulk of the gas. At every change in the gas direction, some droplets strike and stick to the surface. The captured droplets coalesce on the vanes, forming larger drops which have enough weight to drip down. With horizontal flow, a drainage path is provided from the bottom of the vanes. With vertical flow, collected liquid drips from the bottom of the vane unit and falls on the rising gas (Hansen et al., 1983).

Separation of liquid droplets from gas or vapor stream is one of the most common operations in chemical plants. Separation of liquid is not only to recover valuable products or to protect the equipment from corrosive liquids, also it is necessary to improve emissions controls. Knitted wire mesh mist eliminators are used extensively in many industrial plants. Their widespread application is due to the low cost and efficient removal of entrained liquid droplets from vapor and gas streams. They can be classified as "impingement type separators" and their working principle is based on inertial force (Brunazzi, 1999). They are designed to operate as coalescers or agglomerators, i.e..to combine small liquid particles into larger drops which can be readily removed from the process by gravity (Hansen et al., 1983). They are efficient for capturing droplets in the range of 5-100 microns. One of principle limitation of mesh pad is flooding, meaning choking with liquid due to excessive quantities of mist.

## 2.9 HEPA Filters

High Efficiency Particulate Attenuation (HEPA) filters are used to prevent the emissions of particulates and mists into the environment. Filters are often made of 0.013-inch thick glass fiber materials. These filters are efficient to capture 99.97% of 0.3 micron diameter aerosol particles. Water is the major problem for HEPA. Usually, a preheater is installed in the air ducts of waste stream to prevent condensation which damage the HEPA. Construction of HEPA with sintered stainless steel will provide a filter which is not subject to water damages and can be installed with built in water jets to wash the filter to reduce radiation and to eliminate the dirt accumulation. Preliminary tests showed that the use of such filters gives the same efficiency as filtration with a fiberglass filter medium. This medium resulted in data indicating that it was efficient to capture 99.97% of aerosol with 0.3 micron in diameter. Test data indicated that removal of water from the clean side of the filter is required for normal filter operation. Water on the clean side of filter flows by gravity and air movement out of the bottom of the cylindrical filter. Using a vacuum pump, clean air will be drawn out of the cylindrical filter. Water sprayed on the dirty side of a vertical filter flushes the accumulated aerosol down the dirty side. One of the advantages is the formation of a very thin filter medium which stops particle transmission at the exposed surface of the medium. The collected particles can be easily removed from the relatively smooth surface compared to a thicker medium, such as wire mesh. In addition, the stainless steel construction makes the filter resistant to mechanical damage, high pressure, and temperature. On the other hand, washing the dirty side of filter increases the waste volume.

## 2.10 Electrocoalescence

The problem of efficient removal of dispersed droplets from gas or vapor stream is important and extensive in many industrial processes. One of the many proposed different improvements of phase separation (Berger, 1986), the application of an electric field seems to be the most promising. Fundamentally, the strong electric fields induce a dipole in the aerosol particles. Adjacent particles experience an attractive force, which can lead to agglomeration or coalescence. Electrical coalescers have been successfully used for many years from the late 1950's and early 1960's for removal of water during desalting of crude oil in the petroleum industry (Waterman, 1965). Recently, electrical coalescence has been considered as the most promising technique in such fields as the liquid membrane extraction process, where the breaking of a liquid emulsion is a key step in this technology (Hsu, 1985, Hauertmann, 1989, & Kataoka, 1990), direct liquid-liquid emulsion heat transfer, separation of two liquid phases formed as the product, and emulsion phase contactor (EPC) for desulfurization of crude oil (Tsouris et al., 1998).

The coalescence of suspended aqueous droplets in an insulating liquid under electric field has been influenced by the field strength, the droplet size, and the viscous resistance (Zhang, 1995). The mechanism of electrical coalescene is poorly understood because of the complexity of hydrodynamic and electrical phenomena.

A number of mechanisms have been proposed and they involve such effects as electromigration (electrophoresis), drop-drop coalescence, drop-electrode collision, dielectrophoresis, and dipole coalescence (Waterman, 1965 & Bailes, 1982). The formation of droplets oriented along the electric field lines originates from the induced

polarization forces ((Hsu & Li, 1985). It suggests that electric field should be an effective means for droplets coalescence.

When two droplets move toward each other, the strength of electric field at the closest point between them can reach several times of applied electric field, as a result of shared interaction between the induced charges on the drop surfaces (Latham & Roxburgh, 1966). Davis developed a separation technique to solve the Laplace equation which dominates the electric field outside the droplets for electrohydrostatic problems of two conducting sphere (Davis, 1964). The induced charges on the surfaces of two different sized droplets were determined under an arbitrary electric field and different separation of two drops. The induced electric field forces on two conducting droplets with radii of $a_1$ and $a_2$ and net charges of $Q_1$and $Q_2$ can be decomposed into two components, along and normal to the line-of-centers of the droplets, $F^{r}_{E,12}$ and $F^{\theta}_{E,12}$, respectively.

$$F^{r}_{E,12} = 4\pi\varepsilon a_2^2 E_0^2 (F_1\cos^2\Psi + F_2\sin^2\Psi) + E_0\cos\Psi(F_3Q_1 + F_4Q_2) + \frac{1}{4\pi\varepsilon a_2^2}(F_5Q_1^2 + F_6Q_1Q_2 + F_7Q_2^2) + E_0Q_2\cos\Psi \quad (1)$$

$$F^{\theta}_{E,12} = 4\pi\varepsilon a_2^2 E_0^2 F_8\sin 2\Psi + E_0\sin\Psi(F_9Q_1 + F_{10}Q_2) + E_0Q_2\sin\Psi \quad (2)$$

where $E_0$ is the magnitude of the external electric field and $\Psi$ is the angle between the electric field and the droplet center line. The force coefficients, $F_i$ (i=1, 2, …, 10), are complicated series of expressions that depend on the relative geometry of the two droplets. The solution for the force coefficients, $F_i$, diverge when the distance between

the two drops tends to zero, indicating a dramatic increase in the electric-field-induced forces between two drops in Latham & Roxburgh (1966) experiment. Erker and Baygents have examined the electrohydrodynamic interactions between two dielectric spherical drops using the bispherical coordinates technique to solve the Laplace equation for the electric potential and the Stokes equations for the velocity field (Erker & Baygents, 1996). Their results showed that the induced electrical interaction between two drops by an imposed electric field is always attractive when the drops are in close contact. Recently, Keh & Chen (1989a & 1989b) have studied the electrohydrodynamics of two charged, dielectric spheres for the electrophoretic motion along and normal to the drop center line, Loewenberg & Davis (1995) studied a similar problem for near contact axisymmetric electrophoretic motion. Their results showed that the electrophoresis motion is at least three times greater than buoyancy-driven motion when they are in close contact. Depending on their polarity and free charge, two droplets may respond differently to an electric field. They concluded that the motion of the drops can be changed when they are in close contact.

In an external electric field, the enhanced coalescence of conducting spheres was examined by Williams & Bailey (1983 & 1986) theoretically and experimentally. They used an approximate solution which is not valid when two drops are close together. They did not account the viscous interactions which is significant for the coalescence rate. To resolve this problem, Zhang (1995) used a trajectory method to predict the coalescence rate of spherical conducting drops without charge. In their work, they accounted for viscous and electrostatic interactions of the droplets. They concluded that the rate of

coalescence can be increased by application of electric field especially when the field acts perpendicular to the gravity.

A natural practical extension of drop electro-coalescence is electro-filtration. A more detailed discussion of the basic operation of electro-filtration processes will be provided in the following section. Zhang et al. (1995) added theoretical justification to quantitatively predict collision and coalescence rates of conducting, charge-free spherical drops and their growth induced by combined gravitational and electric-field-induced forces.

## 2.11 Electro-filtration of Aerosols

The removal of sub-micron particles from processed waste streams is ineffective and requires a significant amount of energy. Several reports on investigations of electrically enhanced aerosol filtration in fiber filters have been published. Silverman (1954), Thomas and Woodfin (1959) empirically showed that fiber filtration efficiency was enhanced by the application of an electric field. They used a bank of metal screens (Silverman et al., 1954) and several layers of nylon hosiery (Thomas & Woodfin, 1959) placed between high voltage electrodes as a filter. They measured filtration efficiency with and without electric field. The filtration efficiency was much higher with electric field.

Bogardus (1974) and Fielding (1975) studied the performance of commercial fiber filters when placed in an electric field. Their experiment showed a great improvements of filtration efficiency over non-electrified filters.

Granular filtration (deep-bed filtration) is mechanically simple and consumes little energy. However, it relies principally on the mechanisms of interception, sedimentation, diffusion, inertia, and surface forces, which yield low collision efficiency between particle and collectors (Barker, 1988). It is well known that the efficiency of aerosol filtration in fiber mats (Silverman et al., 1954) and in granular bed (Harriott et al., 1980) can be improved by the application of an electric field to the filter media. Filtration efficiency greater than 99% are repoted in the literature (Watermam, 1951).

A granular electrofilter is simply a bed of coarse particles (diameter ≈1mm), with electrodes arranged so that a strong electric field can be applied to the bed. The electric field polarizes the packing granules, and the combined electric field causes the charged suspended particles to deviate from the fluid streamline and be collected on the oppositely charged surface of the granules. In a different concept of electrofiltration, the electric charge is applied directly to the granules (Muller, 1982). In this case, the granular electrofilter operates much like an electrostatic precipitator, but with more complex flow paths. This type of electrofiltration is more suitable with less densely packed beds, such as fiber filled beds. The filter media is also restricted to a conducting medium.

Applied electric field across fibrous filters have enhanced performance with gas filtration, and successful mathematical analyses have been presented (Henry, 1986, Van Osdell, 1986, & Accomazzo, 1986). There are two differences between fibrous and granular filters: first, the geometry of the collecting solids, and second, in fibrous filtration of gaseous streams, the drag on suspending particles is more likely to be dominated by inertial rather than viscous forces.

Local electric fields are essentially in the direction of the applied field and important deviations occur near the granule or fiber packing. If the granules/fiber packing are non-conducting, the field lines will be diverted around the granules or fibers. If the packing is a better conductor than the fluid, the field lines will be diverted toward the granules or fibers. Since the electric forces on the particulates act along the electric field lines, it is desirable to have the lines diverted into (rather than around) the granules or fibers. This is similar to the concept of using conducting granules or fibers which can be considered to have a very high dielectric constant than the fluid. When both fluid and packing are conductors, it is desirable for the granules or fibers to have a higher conductivity than the fluid. In the case, the packing materials are highly conductive, more or less packed fibers may be needed to prevent unnecessary current through the bed. Cleaner granules could be obtained by vigorously backwashing, but the particles could be obtained in a more concentrated suspension by slow backwashing when the field is off (Barker et al., 1991).

In summary, many parameters can have a major effect on the electric filtration process such as geometry of packing and density, orientation and strength of the electric field, particle charge, dielectric constant and conductivity of the packing material and fluid, and particle size. It is in our best interest to take all of the major parameters into account in order to achieve the highest separation efficiency.

# CHAPTER 3

# EXPERIMENTAL PROCEDURES

## 3.1 Experimental Setup

The primary objective of this research project is to develop a better understanding of electrically driven drop-drop and drop-electrode interactions and agglomeration of droplets in an aerosol flow chamber. To accomplish this objective, an experimental setup was designed to carry out a series of experiments to:

- Characterize the size distribution of aerosol droplets under the influence of a strong DC electric field
- Measure the removal of drops by an electric field.

Using the experimental setup described below, a sequence of procedures was followed in each experiment in order to ensure repeatable results.

The experimental setup for this study is shown schematically in Figures 3.1 and 3.2. The aerosol observation chamber unit was designed as a small, controlled environment in which the flow-through water aerosol could be excited into additional motion by a relatively strong electric field. The chamber unit is made of clear Lexan with a cross-sectional area of 10x10 cm and approximately 94 cm long. Two 9x60 cm steel electrodes are mounted vertically inside the chamber on opposite sides of the test window. The rectangular test view window is made of flat optical glass (non-reflecting) whose dimensions are 2x60 cm (Figure 3.1). A heating tape is attached to the glass to prevent accumulation of moisture during operation.

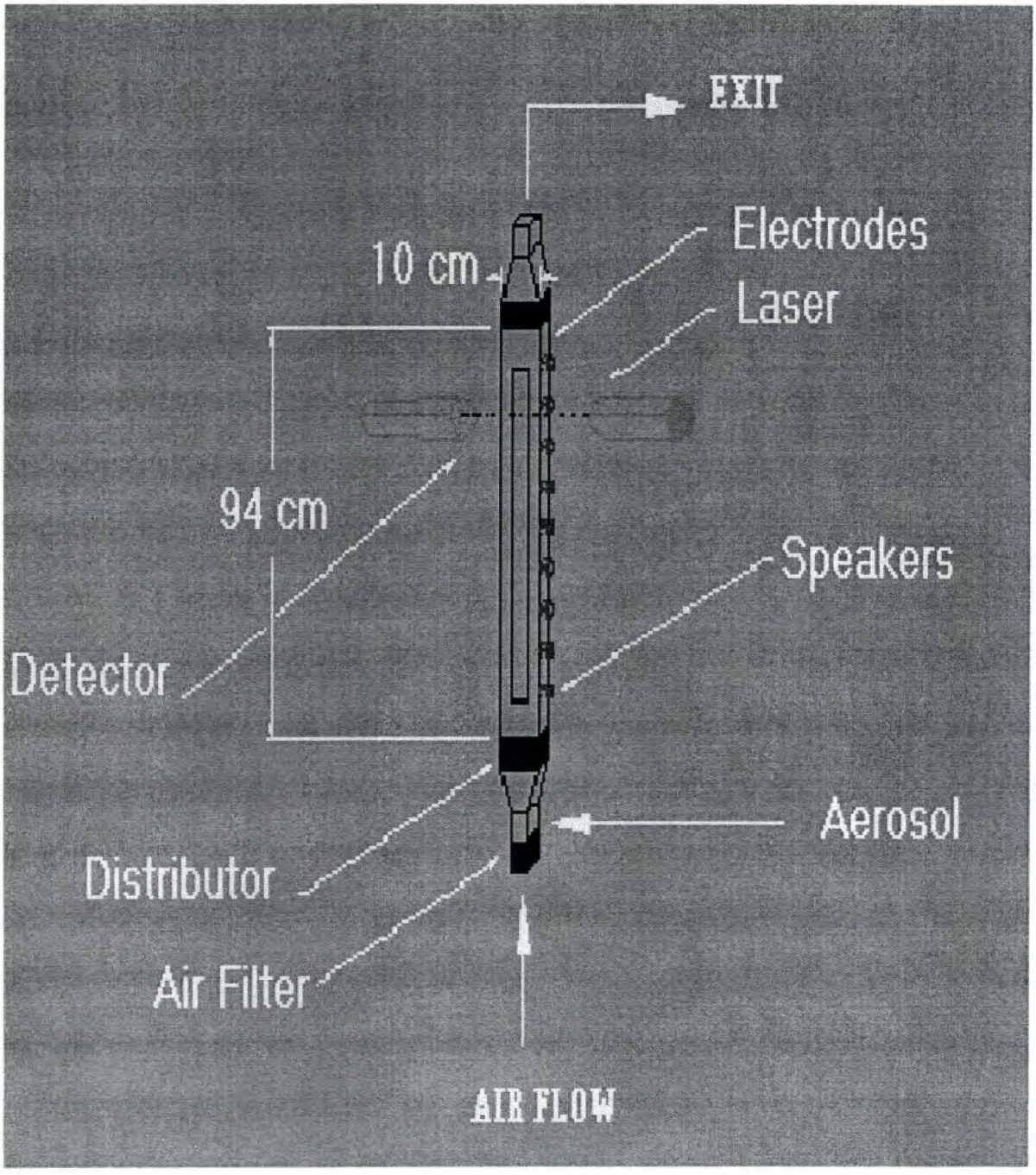



Figure 3.1: Schematic diagram of Electro-Coalescence Unit System

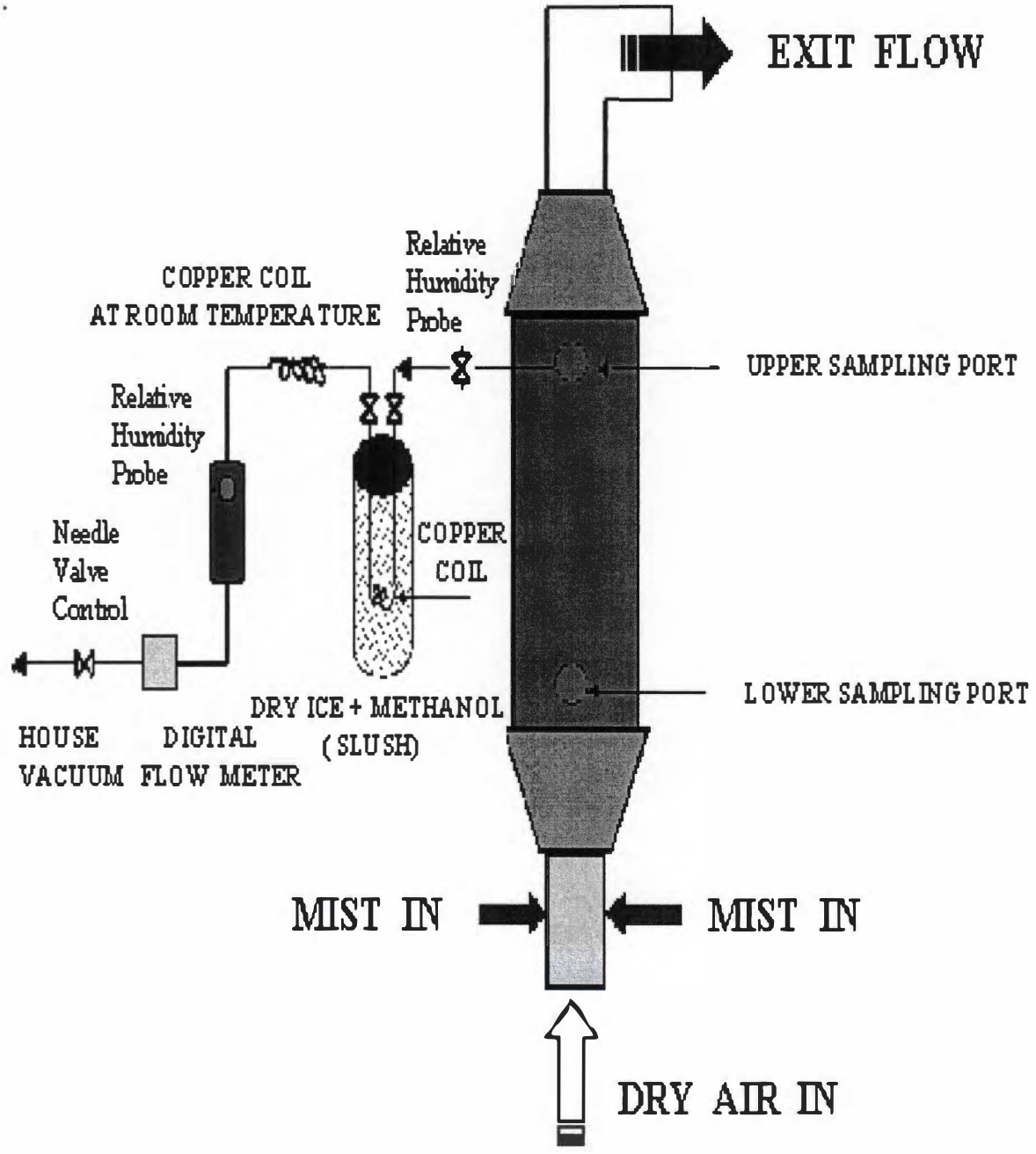



Figure 3.2: Schematic diagram of the experimental setup.

The top section of chamber is connected by flexible ductwork to the exhaust in a hood Two sampling ports are available on the test section of the chamber. At the bottom of the tunnel, mist from two ultrasonic humidifiers is introduced into the air stream by a diffuser, as shown in Figure 3.2. The bottom part of test section is connected to the steel duct which is heated before the experiment for condensation prevention. The supplied house air is passed through a flow meter and air filter before delivering the mist through the test section of the chamber. At the entrance of the test section, a honeycomb baffle is placed for constant and evenly distributed air flow. It should be noted that distilled water was used for the two ultrasonic humidifiers (Electro-Tech System, Model 5612) that generated the aerosol flowing through the test chamber. A probe is used to measure the relative humidity/temperature of flowing air at the exit of the test section. A high voltage of up to 26 kV is applied to the positive electrode during the experiment by a DC power supply. The aerosol size distribution in the test chamber is determined by laser-light scattering using a Malvern Spraytec RTS 5006 droplet sizing system which is mounted on a movable stage. A moisture trap of dry ice and methanol slush is prepared in a dewar flask to remove the moisture from the sampled fluid. By using this technique, a controlled flow rate of gas is drawn from the sampling port by the house vacuum through a copper coil which is immersed in the slush. A scale (Mettler PJ 3600 Delta Range) is used to determine the weight of collected mist. Sampling of the gas was carried out

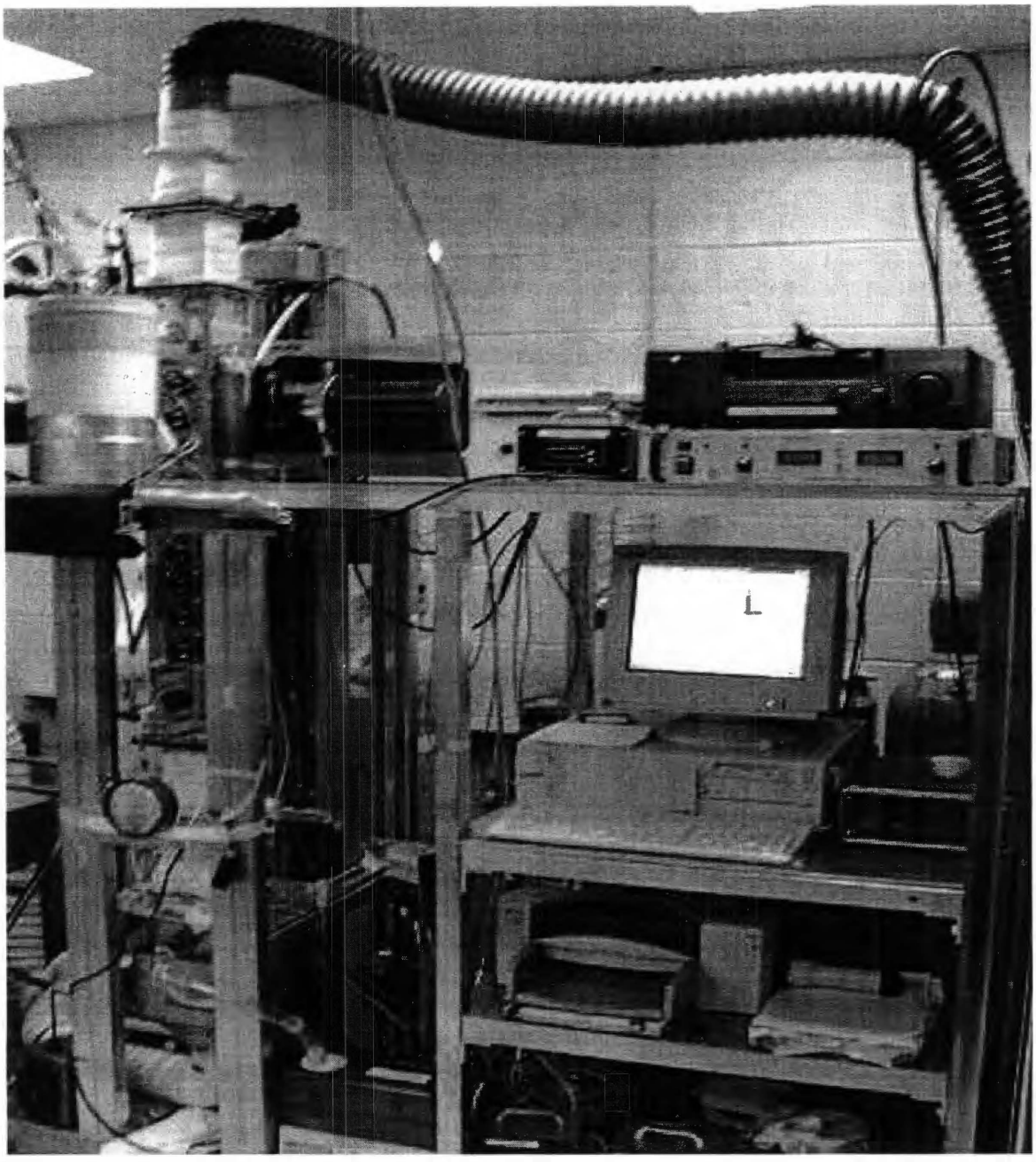


Figure 3.3: Photograph of experimental setup used in this study.

isokinetically as discussed in the following section. A photograph of the laboratory test set up is provided as Figure 3.3.

## 3.2 Isokinetic Sampling

In aerosol sampling, the measured concentration and size distribution should represent as closely as possible the concentration and size distribution of the original aerosol. There are several reasons why the measured concentration can differ from the true concentration. One reason is that gravitational or inertial deposition of the sample as it flows into the sampling tube can result in loss of the larger-sized particles. Also, deposition or selective collection at the entrance of the sampling tube can yield either greater or lesser amounts of larger particles. If the sampling probe is aligned with the flow and the sample velocity is equal to the stream velocity, sampling is said to be isokinetic, and the collected sample should match the actual concentration and size distribution. For this purpose, the flow rate of the sampling stream was set such that the velocity at the sampling line entrance was equal to the average velocity in the chamber. In addition, the copper sampling probe was heated to evaporate the deposited water droplets at the edge and inside the probe, so that the experimental error can be reduced.

## 3.3 Dry-Ice Sampling

For capturing the water droplets from isokinetic sampling probe, a slush of dry-ice and methanol was prepared in a dewar flask. During the sampling events, a

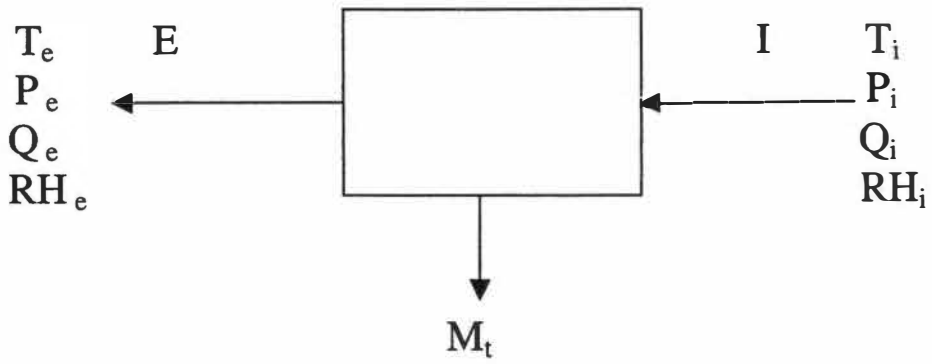



Figure 3.4: Schematic diagram of macroscopic mass balance process

controlled flow rate of gas was pulled out by house vacuum through a copper coil (2.0 m long and 1.25 cm ID) immersed in the slush. The copper coil was weighed before and after sampling on a sensitive balance ($\pm 0.001$ g). A long sampling time was used to achieve a higher mass loading in the copper coil for a low flow rate. In contrast, a short sampling time was used for a higher flow rate. A battery-powered relative humidity/temperature probe (ALNOR APM-360) was utilized to monitor the inlet and exit relative humidity for mass balance calculations. The exit air was first passed through a 3.0 m long copper coil before going into the chamber to reach room temperature before the relative humidity and temperature were measured. A pressure device (SENSOTEC SC Series) was also connected to the relative humidity/temperature probe chamber to monitor the pressure drop in the dry-ice system.

The net droplet mass is calculated using the accumulated water weight in the copper coil (A), mass of the water vapor in the humid air exiting from the copper coil (B), and the mass of water vapor contained in the humid air flowing through the test

chamber at the sampling port (C). Thus, the mathematical description of the net droplet mass in the air stream is as follows.

$$Net\ droplet\ mass = A + B - C$$

The masses of B and C are calculated using relative humidity and temperature measurements and A is directly obtained from the balance. The equations for a mass balance around the dry-ice trap (Figure 3.4) used in this study are similar to the equations obtained in studies of a ***dehumidification*** process. Assuming that dispersion is negligible, a material mass balance equation can be written as

$$\text{Accumulation rate} = \text{Flow in} - \text{Flow out}$$

Where

$$\text{Accumulation due to mist collection} = M_t$$

$$\text{Flow in} = I$$

And

$$\text{Flow out} = E$$

Or

$$M_t = I - E \tag{3.1}$$

Symbolic notation has been chosen to be consistent as possible with the ***dehumidification*** process. $T_i$ is the temperature of inlet, $P_i$ is the inlet pressure, $Q_i$ is the inlet flow rate and $(RH)_i$ is the relative humidity of inlet air. $M_t$ is the total mass accumulated. $T_e$ is the temperature of exit air, $P_e$ is the exit pressure, $Q_e$ is the exit flow rate and $(RH)_i$ is the relative humidity of exit air.

The ideal gas law can be derived from the theory of gases by assuming that gas molecules have a negligible volume, exert no forces on one another, and collide

elastically with the walls of their container (Felder and Rousseau). The law usually appears in the form

$$PV = n\,RT \tag{3.2}$$

Where

P = absolute pressure of a gas

V = volume or volumetric flow rate of the gas

n = number of moles or molar flow rate of the gas

R = the gas constant , whose value depends on the units of P, V, n, and T

T = absolute temperature of the gas

Assuming ideal gas behavior,

$$P_I^A V_I = n_I^A RT_I \tag{3.3}$$

$$P_I^W V_I = n_I^W RT_I \tag{3.4}$$

Where the subscript I represents inlet and superscript A and W represent air and water vapor respectively, through the dry-ice trap.

The density of a fluid can be used to convert a known volumetric flow rate of a process stream to the mass flow rate of that stream or vice versa. Therefore:

$$M_I = \rho_I Q_I \tag{3.5}$$

$$M_E = \rho_E Q_E \tag{3.6}$$

Where $M_I$ and $M_E$ are the mass flow rate and $\rho_I$ and $\rho_E$ are the densities of inlet and outlet fluid respectively. Recalling the material balance equation in terms of mass;

$$M_t = M_I - M_E \tag{3.7}$$

In terms of moles

$$n_t = n_t^A + n_t^W = n_I - n_E = n_I^A + n_I^W - \left(n_E^A - n_E^W\right) \tag{3.8}$$

Substituting the equation 3.8 into the above equation and using the ideal gas law,

$$n_t^A + n_t^W = \left(\frac{P_I^A V_I}{RT_I}\right) + \left(\frac{P_I^W V_I}{RT_I}\right) - \left(\frac{P_E^W V_E}{RT_E}\right) \tag{3.9}$$

$$\boxed{n_t^W = \left(\frac{P_I^W V_I}{RT_I}\right) - \left(\frac{P_E^W V_E}{RT_E}\right)} \tag{3.10}$$

The above equation gives the moles of water at large sampling time. Also, this can be written in terms of relative humidity as

$$n_t^W = \left(\frac{RH_I . P_I^*(T_I) Q_I}{RT_I}\right) - \left(\frac{RH_E . P_E^*(T_E) Q_E}{RT_E}\right) \tag{3.11}$$

where $RH_I$ and $RH_E$ are the relative humidity, $P_I^*$ and $P_E^*$ are the water vapor pressure of inlet and outlet flow, respectively. The relationship between relative humidity and vapor pressure is described such that a gas at temperature T and pressure P contains a vapor whose partial pressure is $p_v$ and whose vapor pressure is $p_v^*(T)$. It is given as

$$RH = \frac{p_v}{p_v^*(T)} \times 100\% \tag{3.12}$$

A relative humidity of 50%, for example, signifies that the partial pressure of water vapor equals 0.50 of the vapor pressure of water at the system temperature. Equation (3.10) also can be written for a period of experiment as follows:

$$n_t^w = \frac{RH_I . P_I^*(T_I) Q_I}{RT_I} - \frac{P_E^* Q_E}{RT_E} \int_{t_i}^{t_f} RH_I \, dt \tag{3.13}$$

In terms of mass, it can be written as

$$M_t^w = \frac{M}{R}\left[\frac{P_I^*(T_I) Q_I}{T_I} - \frac{P_E^*(T_E) Q_E}{T_E} \int_{t_i}^{t_f} RH_E \, dt\right] \tag{3.14}$$

For the case $T_I = T_E = T$, the above equation can be written as

$$M_t^w = \frac{M}{RT}\left[P_I^*(T_I) Q_I - P_E^*(T_E) Q_E \int_{t_i}^{t_f} RH_E dt\right] \tag{3.15}$$

Where:

M = molecular weight of water

R = the gas constant

$t_i$ = initial time of dry-ice trap experiment

$t_f$ = final time of dry-ice trap experiment

The above equation gives the theoretical value of collected mass of water vapor in the air.

## 3.4 Particle Size Distribution Measurements and Control

The aerosol size distribution in the test chamber is determined by laser-light scattering using a Malvern Spraytec RTS 5006 (Figure 3.5) droplet sizing system which is mounted on a movable stage for measurements at various heights along the column. The system is designed to continuously measure and present in real time particle size distribution information from a stream of aerosol.

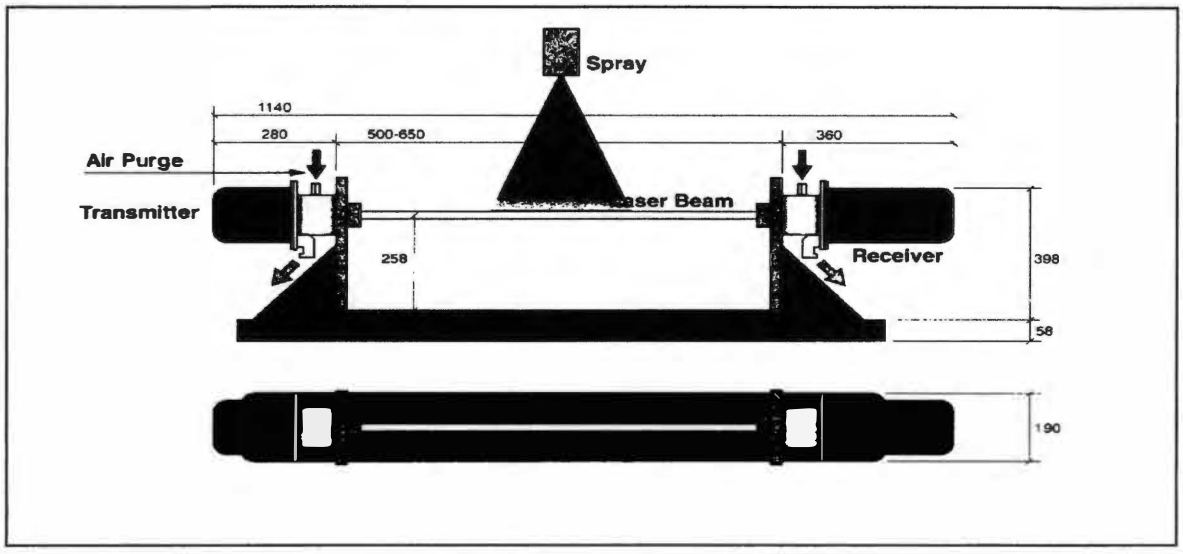



Figure 3.5: Dimension and components of the Malvern Spraytec RTS 5000 Series (Malvern Instrument)

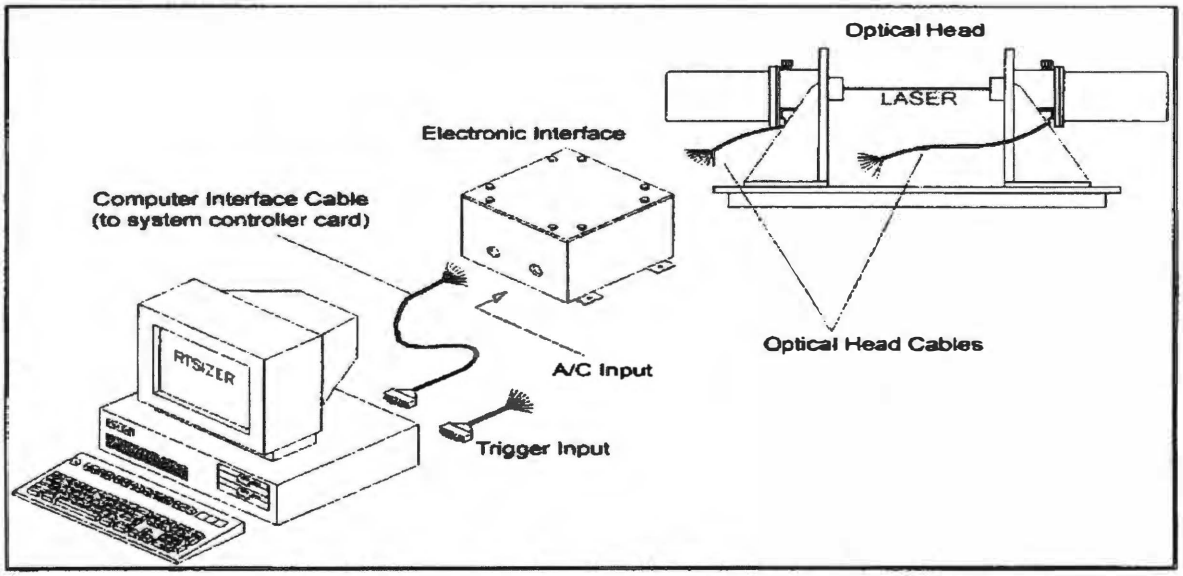



Figure 3.6: Spraytec RTS 5000 System Layout (Malvern Instrument)

The main components of the RTS 5006 system include the optical head, interface box, computer and software (Figure 3.6). The particle sensing region or sample volume forward direction is collected by the receiver lens and focused onto an annular ring detector. The detector is scanned at high speed by the interface card which records the signal levels on each ring. Each ring on the detector measures the total signal intensity. Each particle scatters light on all rings of the detector. Therefore, the measured signal is the summation of the light scattered from all particles. Once a significant number of detector scans are acquired, the software uses a non-linear inversion technique to solve for the relative particle concentration. No assumptions are required about the shape of the size distribution, which is obtained directly from the experimental scattering information.

The chamber design for the experiments (See Figure 3.1) was guided by the goal to achieve a small and controlled volume in which the droplets could be subjected to a relatively high electric field. A number of design criteria had to be taken into consideration.

1. It was desired to generate a homogeneous electric field within the observation chamber to simplify the geometry. Such a field can be generated between two parallel flat steel electrodes mounted vertically inside the chamber on opposing sides of the test section.
2. Care was taken that the two mist feeding ports, two sampling ports, and the two flat optical windows would minimize possible disturbances of air flow due to sharp edges within the enclosure.

3. To improve visualization of droplets and reduce the error in drop size measurements, two removable flat optical windows were designed so that they could be easily removed and cleaned after each experiment.
4. The mist feeding system was designed to distribute the produced mist uniformly by using a rubber diffuser which connects the two outputs from two ultrasonic humidifiers just below the honeycomb baffle.
5. Moisture accumulation on the optical window was prevented by heating, using ultra thin heating tape.
6. The construction was such to avoid vibrations of the setup during the experiments.

The following steps were carried out before drop size distribution measurements in each run:

- Reference Noise Measurement: This is a permanent acquisition module that allows us to record the reference noise. The reference noise is a dark background measurement, or a measurement of the electronic noise present in the system.
- Background Measurement: This is a permanent acquisition module that allows us to record a background measurement. The background is a measure of stray light in the optical system and most importantly, particulate contamination of the windows. A good background measurement is critical to insure accurate and precise drop size distribution measurements. RTSizer uses the background to compensate for any particulate contamination by using the background as a baseline that is subtracted from all drop size distribution measurements. Background was recorded for each different experiment.

- Time History: The time history is an advantage offered by the RTSizer. The computer records and saves drop size distribution data continuously. Data are stored in a circular data base file with a fixed maximum size. Once the maximum size is reached, the oldest data acquired is overwritten by new data. The time history allows us to determine variables such as light transmission, particle diameter (μm) vs. cumulative volume (%) and volume frequency (%) for each run.

# CHAPTER 4

# THEORETICAL CONSIDERATIONS

The theoretical approach traditionally used to describe the particle behavior under an electric field is conceptually simple, although detailed application of the concept is complex. Specifically, the approach consists of the equation of motion for a single spherical aerosol particle in the absent and present of an electric field, a basic electric field mechanism for particle removal from a flowing suspension, electro-coalescence of particles, and macroscopic material balance, which may be based on drop population dynamics.

## 4.1 Equation of motion for a single aerosol particle

This problem was originally studied by Stokes and the expression for force since has become known as "Stokes' law" (Reist, 1993). Modifications have been made over the years by Basset (1888), Boussinesq (1885), and Oseen (1927). All three studied a spherical particle with motion induced by an arbitrary acceleration in a Newtonian fluid and arrived at their conclusion by neglecting convective acceleration in the Navier-Stokes equations which is called Basset-Boussinesq-Oseen (BBO) equation. More comprehensive studies were performed by Corrsin and Lumley (1956), and Maxey and Riley (1983). A familiar form of the equation in terms of a force balance on a spherical particle is

$$F_{drag} + F_{bouyancy} = F_{gravity} \tag{4.1}$$

The gravity force may be replaced by Newton's second law, $F = m_p g$. The Stokes drag force is correlated to other physical variables through a drag coefficient, $C_D$. The buoyancy force known as the force due to the added mass of the fluid (Maxey and Riley (1983), Panton (1996)).

The overall force balance is written as:

$$\frac{\rho_g A V_t^2 C_D}{2} + m_p\left(\frac{\rho_g}{\rho_p}\right)g = m_p g \tag{4.2}$$

Where $\rho_g$ is the fluid density, $\rho_p$ is the particulate density, $V_t$ is the terminal or settling velocity, $m_p$ is the mass of the particle, A is the frontal cross-sectional area, and g is the local acceleration of gravity. In terms of terminal velocity,

$$V_t = \left[\frac{2m_p g(\rho_p - \rho_g)}{AC_D\rho_p\rho_g}\right]^{1/2} \tag{4.3}$$

The drag coefficient $C_D$ is a function of the shape of the object. Assuming spherical particles, equation (4.3) becomes

$$V_t = \left[\frac{4gd_p(\rho_p - \rho_g)}{3\rho_g C_D}\right]^{1/2} \tag{4.4}$$

Where $d_p$ is the particle diameter. The drag coefficient for the spherical particles are usually plotted as a function of Reynolds number, Re, and is available from literature. By definition, $Re = \rho_g V d / \mu$, where d is a characteristic length such as a diameter and $\mu$ is

the fluid dynamic viscosity. A Stokes time scale can be derived from drag force equation, as

$$\tau = \frac{(\rho_p - \rho_g) d_p^2}{18 \mu} \tag{4.5}$$

Since for air $\rho_p >> \rho_g$, $\tau$ is usually written as

$$\tau = \frac{1}{18} \frac{d_p^2}{\mu} \rho_p \tag{4.6}$$

The factor $\tau$ has units of seconds. It represents a relaxation time for the aerosol particle.

## 4.2 Particle motion in an electric field

When an uncharged spherical conducting aerosol particle is placed in a uniform electric field, the field near the particle is distorted, as illustrated in Fig. 4.1, so that gas ion following the field lines would immediately begin to charge the particle. The dashed lines indicate the limits of the field which passes through the sphere. When the particle becomes charged, it repels some of the incoming ions. This repulsion results in an alteration of the field configuration which accordingly reduces the charging rate. A point will be reached where no further charging of the particle takes place. This point is known as the ***saturation charge*** of the particle. When one-half the saturation charge on the particle is reached, the electric field surrounding the particle is similar to that shown in Fig. 4.2 (Rohmann, 1923; Pauthenier and Moreau-Hanot, 1923).

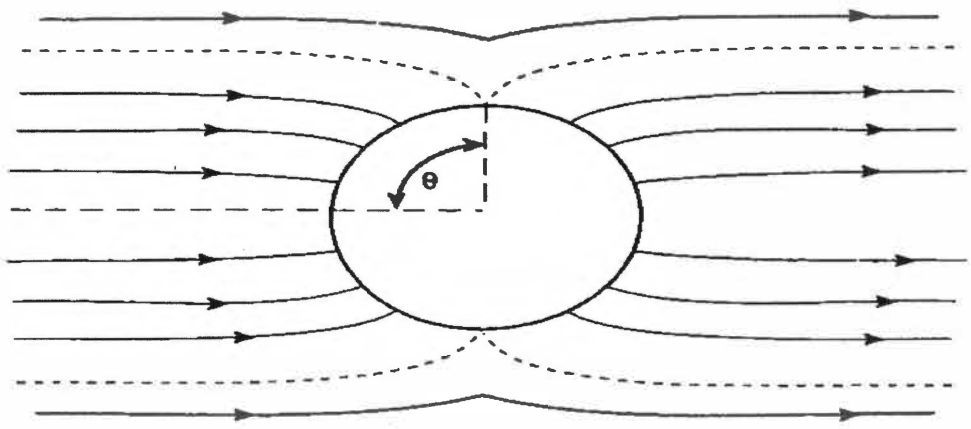



Figure 4.1 Electric field around an aerosol uncharged particle (Reist, 1993).

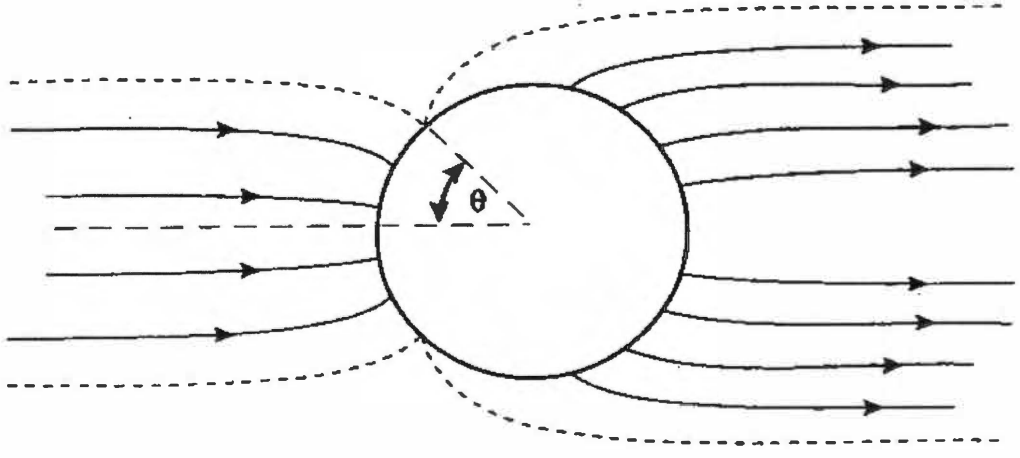



Figure 4.2 Electric field around a partially charged aerosol particle (Reist, 1993)

The main reason for evaluating the charge on aerosol particles and the electric fields that act on these charges is to develop models which describe the effect on particle motion of the electric force. The equation of motion for a spherical aerosol particle in a homogeneous air stream at the presence of only gravity can be written as

$$m\frac{dv}{dt} = F_D + F_G \tag{4.7}$$

where m is the mass of the particle and v is the velocity of the center of gravity of the aerosol particle. $F_D$ is the steady Stokes drag force on the particle represented as

$$F_D = 3\pi\mu d(u - v) \tag{4.8}$$

where u is the velocity of the air stream near the particle. Therefore, (u-v) is the particle velocity relative to the medium velocity. The force of gravity can be written as

$$F_G = mg \tag{4.9}$$

Dividing the equation 4.7 by $3\pi\mu d$ and rearranging terms gives

$$\tau\frac{dv}{dt} = (u - v) + \tau g \tag{4.10}$$

where

$$\tau = \frac{m}{3\pi\mu d} \tag{4.11}$$

The equation of motion for an aerosol particle at the present of an electric force can be written as

$$m\frac{dv}{dt} = F_D + F_G + F_E \tag{4.12}$$

which becomes

$$\tau\frac{dv}{dt} = (u - v) + \tau g - EqB \tag{4.13}$$

where E is the electric field, q is the particle charge and B is the particle mobility and can be written as

$$B = \frac{C_c}{3\pi\mu d} \tag{4.14}$$

Where $C_c$ is the Cunningham correction factor and is available from literature.

Let $u_0 = u + \tau g$ (4.15)

Then equation 4.14 becomes

$$\tau\frac{dv}{dt} + v = u_0 - EqB \tag{4.16}$$

In terms of a dimensionless velocity $v' = \frac{v}{u_0}$, we can write the above equation as

$$\tau\frac{dv'}{dt} + v' = 1 - \Gamma \tag{4.17}$$

the dimensionless parameter $\Gamma$ (can be either positive or negative) is equal to $EqB/u_0$ and indicates the ratio of the particle velocity in an electric field to the constant velocity $u_0$. If $|\Gamma| >> 1$, then electric forces predominate, whereas when $|\Gamma| << 1$, gravity and inertial effects predominate. When $|\Gamma| >> 1$, $\tau$ is very small and the inertia term $\tau dv'/dt$ can be ignored. The equation 4.16 can be simplified as

$v' \cong -\Gamma$ (4.18)

$v \cong -EqB$ (4.19)

where v is the electrical drift velocity. Assuming a saturation or field charge, the equation 4.18 can be written as

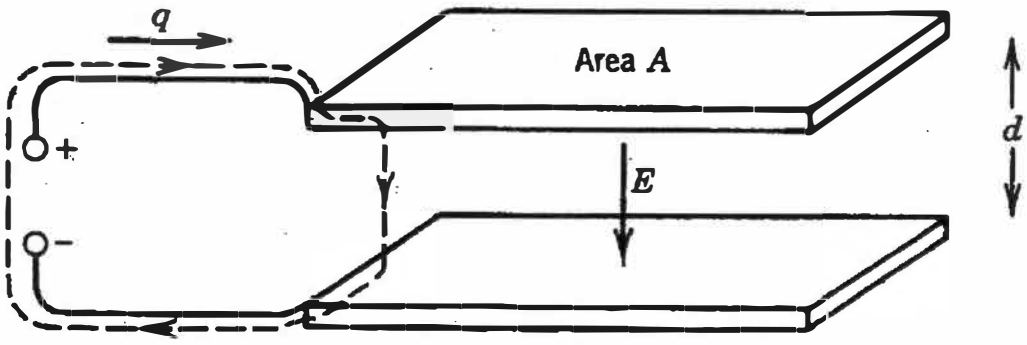



Figure 4.3: Electric field between parallel plates with plate spacing, d (Crowley, 1986)

$$w = E\left(\frac{xE_0d^2}{4}\right)\left(\frac{C_c}{3\pi\mu d}\right) \tag{4.20}$$

or

$$w = \frac{xEE_0dC_c}{12\pi\mu} \tag{4.21}$$

where $x = 3\varepsilon_0/(\varepsilon_0 + 2)$ and $\varepsilon_0$ is the dielectric constant of the spherical aerosol particle and $w$ is the particle velocity in an electric field. The term E0 is the field generating the particle charge and E is the collecting field strength.

## 4.3 Electric filed between parallel plates

Electrostatics involves charges in motion as well as at rest. The most fundamental quantities in electrostatics are voltage, charge, and current. Voltages or electromotive forces (EMF) are the most important fundamental quantities for engineers. The word

force reflects the fact that voltage is related to the force applied to a charge and is derived from the electrostatic force law

$$F = q\,E \tag{4.22}$$

The F vector is the force experienced by a unit charge. This force can be expressed by

$$\oint qE \bullet dr = 0 \tag{4.23}$$

When a voltage is applied across a gap between two parallel plates (Figure 4.1), the electric field can be specified by (Crowley, 1986),

$$\oint E \bullet dr = \int_{-ter\,min\,al}^{+ter\,min\,al} E \bullet dr + \int_{wires} E \bullet dr + \int_{gap} E \bullet dr = 0 \tag{4.24}$$

The integral inside the wires vanishes because the electric field inside a good conductor is very small. The electric field E is uniform inside the capacitor, so only two line integrals are left to evaluate.

The integral becomes

$$\int_{gap} E \bullet dr = Ed \tag{4.25}$$

The E field between the terminals can be described as the voltage across the terminals:

$$V = -\int_{-terminal}^{+terminal} E \bullet dr \tag{4.26}$$

Thus, in this example, the terminal voltage is given by

$$V = Ed \tag{4.27}$$

Breakdown usually occurs at high electric field within the material. It should be noted that there are two criteria for breakdown to become possible, one based on voltage and one on electric field. Generally, both limits must be exceeded before breakdown. For air, the breakdown voltage is 300 volts, and the breakdown electric field is $3 \times 10^6$ v/m.

Below this voltage, the components can be placed as close as a few microns apart. Above this voltage, corona and sparking must be considered in the design which increase both cost and size. Breakdown actually occurs when the insulation properties of the material break down and the material acts like a conductor. If the air acts like a conductor, the current can actually surge across the gap which is known as sparking. A corona discharge usually occur near a conductor with sharp points, or a small radius of curvature. This breakdown is usually manifested by a blue glow. The corona is said to be negative if a cloud of negative ions is formed and positive if positive ions are formed. Corona characteristics will depend on the predominant gas and impurities present. In our experimental system, only water aerosol was tested at various mist and air flow rates.

Williams and Bailey (1983) describe that in their experiment that the permittivity of the particles is larger than that of the fluid. Also, the inter-particle force depends only on the permittivity of the fluid and the size of the particle. Therefore, the size of the particle, electric field strength, separation distance between particles and the fluid permittivity are very important properties which influence the electro-coalescence.

## 4.4 Theory of electro-coalescence

A number of external physical factors can act to enhance the coagulation of aerosols. One important factor is electrical effects such as the attraction or mutual repulsion of charged or polarized particles. In an electric field, particles diffuse toward one another until they are close enough for electric forces to come into play. Then the motion of the particles assumes an ordered nature.

As two drops approach one another, the strength of the electric field in the region between their points of closest separation can attain values many times larger than that acting by the applied electric field on drops, when they are far from each other. This is a result of the mutual interactions between the induced charges on the drop surfaces (Latham & Roxburgh, 1966).

The model of Zhang et al., (1995) has been developed to quantitatively predict collision and coalescence rates of conducting, charge-free spherical drops and their growth induced by combined gravitational and electric-field-induced forces. Yiacoumi et al., (1996) developed a similar model for particle coagulation in magnetic field.

$$V_{12} = V_{12}^{0}\left(-L\cos\theta e_r + M\sin\theta e_\theta\right) - \frac{D_{12}^{0}}{kT}\left(GF_{E,12}^{2} e_r - HF_{E,12}^{\theta} e_\theta\right) - \frac{D_{12}^{0}}{kT} GF_{p,12} e_r \qquad (4.28)$$

gravity electric field van der Waals

where $V_{12}^{0}$ is the relative velocity of two widely separated drops/particles due to gravity which is given by the Hadamard-Rybezynski formula (Kim & Karrila, 1991), $e_r$ and $e_\theta$ are unit vectors along and normal to the line of centers, respectively, $D_{12}^{0}$ is the relative diffusivity of two widely separated drops, k is Boltzmann constant, T is the absolute temperature, $L, M, G,$ and $H$ are the relative mobility functions describing the viscous effects on drop motion, and $F_{E,12}$ and $F_{P,12}$ are electric-field induced forces (See Equations 1 & 2 in chapter 2) and interparticle forces, respectively.

Recently, Ezekoye and Wibowo (1999) used a discretized general dynamic equation (Smoluchowski's equation) in the absence of sedimentation and breakup as,

$$\frac{dn_k}{dt} = \frac{1}{2}\sum_{i+j-k}\beta(v_i, v_j)n_i n_j - n_k\sum_{i-1}\beta(v_i, v_k)n_i \tag{4.29}$$

The first term represents the rate of conversion of particles of size $i$ and $j$ into size $k$ such that the sum of the volumes of the $i$ and $j$ particles is to the volume of the $k$ particle. The second term represents the conversion of $k$ sized particles to larger particles through collisions with the rest of the distribution. The evaluation of β for various types of collisional processes is essential to properly modeling/characterizing the aerosol dynamics and in terms of relative velocity between particles, it can be shown as,

$$\beta n_1 n_2 = \pi r^2 V_{12} n_1 n_2 = \pi r^2 (1_1 - V_2) n_1 n_2 \tag{4.30}$$

where β is the collision rate, $n_1$ and $n_2$ are number densities of droplets 1 and 2, respectively, $V_{12}$ is the relative velocity between two droplets (equation 4.27), r is the radius of the collision volume.

A limiting trajectory can be determined along which two drops approach each other with the largest possible horizontal displacement, $y_c$, such that they will collide, as shown in Figure 4.4 which is duplicated from Zhang et al. (1991). Any relative trajectories that are inside this limiting trajectory end with the drops colliding, whereas those outside the limiting trajectory end with the drop separating. The collision or coalescence efficiency can be calculated to describe the effects of electric-field induced and van der Waals attractive forces and viscous resistances, which can be defined as :

$$\beta = \frac{y_c^2}{(a_1 + a_2)^2} \tag{4.31}$$

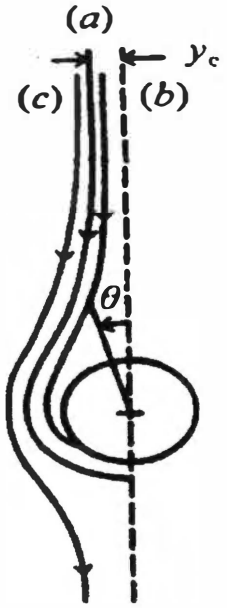



Figure 4.4: Possible relative trajectories of two drops: (a) the limiting trajectory; (b) a trajectory terminating with contact; and (c) a trajectory for which two drops move past one another and separate (Zhang et al., 1991).

where $a_1$ and $a_2$ are the radii of the two conducting droplets respectively. The resultant coalescence efficiency can be used to compute the evolution of a population of drops in a homogeneous, isotropic dispersion by solving the population balance equation (4.28).

This equation was also solved by Tsouris et al., (1995) to include coagulation of magnetic particles in a magnetic field. This model can be readily employed to describe coalescence of polarized droplets.

# CHAPTER 5

# RESULTS AND DISCUSSION

## 5.1 Observations

Prior to the discussion of experimental results, it is important to point out the following observations when the experimental set up was turned on to conduct experiments of this research.

- At zero voltage, the mist distribution was uniform through out the test chamber.
- At a given voltage level, the water droplets were deposited first on the lower end of positive electrode, principally. As the experiment progressed over time, the droplet formation was observed to progress up the surfaces of both electrodes. Droplets drained down the electrodes and formed pools on the bottom of the test unit.
- The electric field caused the mist motion to change from a uniform pattern to a somewhat random pattern with some jetting toward the positive electrode. This more or less chaotic droplet motion was especially intense in the voltage range of 20 kV and above.
- In all cases, at high voltages, the droplets build up at the lower level of the test chamber, causing short circuit between positive and negative electrodes, resulting in sparks and thereby shutting down the system. It was therefore necessary to limit the voltage drop across the electrodes to 26 kV in these experiments in the test apparatus.

## 5.2 Test conditions

All experimental measurements were obtained at room temperature of approximately $23^0$C and ambient pressure of 750-mm Hg. The air density $\rho_{air} = 1.187\ kg/m^3$, air dynamic viscosity $\mu_{air} = 1.86 \times 10^{-5}\ kg/m.s$, and tunnel equivalent diameter $D_e = 0.1146\ m$ were assumed for the calculation of Reynolds Numbers in all experiments. The accuracy of dry-ice-trap was tested by measuring the mass of water vapor in the air passed through the trap and the material balance equation presented in Chapter 4 (Equation (3.15)). Assuming that the air behaves as an ideal gas, the mass of collected water from the room's air in the trap and calculated mass by using the material balance equation were compared and the range of error was within 6 percent. This range was confirmed at different flow rates used in the experiments (Table 5.1).

Table 5.1: Percent error of measured and calculated mass of collected water from room's air at variable flow rates.

| Run | Flow Rate (l/min) | Measured mass during 33 min (g) | Calculated mass during 33 min (g) | Percent Error |
|---|---|---|---|---|
| 1 | 3.0 | 0.38 | 0.40 | 5.00 |
| 2 | 4.5 | 0.50 | 0.53 | 5.66 |
| 3 | 5.0 | 0.58 | 0.62 | 6.50 |
| 4 | 5.5 | 0.48 | 0.50 | 4.00 |
| 5 | 6.0 | 0.50 | 0.53 | 5.70 |
| 6 | 7.0 | 0.63 | 0.65 | 3.08 |

Each experimental run was made at a fixed value of the air flow rate and mist flow rate. The range of Reynolds Number was from 940 to 2400 in all experiments. The raw experimental data were converted into a mist concentration as described in the dry-ice procedure (Sections 3.2 and 3.3). The mist concentration was plotted vs. applied voltage and light transmissions for each experiment. The applied voltages were 0, 10, 15, 18, 20, 22, 24, and 26 kilovolts. These values were selected based on the power supply and the test chamber limitations.

## 5.3 Effects of electric field strength on droplet concentration

Figures 5.1 through 5.5 show experimental data obtained by the method isokinetic/dry-ice sampling at Reynolds Numbers 1350, 1620, 1680, 1950, and 2200 respectively. The figures indicate that the electric field has an effect on the flowing mist in the wind tunnel. They also reveal that as the applied electric potential increases, the quantity of the mist in the air stream decreases. This is due to the increasing number of collisions between droplets (agglomeration), droplets and electrodes and droplets with the chamber walls as the droplets flow in the tunnel under the influence of electric field. Note in Figure 5.3 that the quantity of droplets collected levels off above an applied voltage of 24 kV. This effect is reproducible in this case suggesting that no further reduction of droplets take place. The standard deviation for all experimental data is shown in the form of error bar.

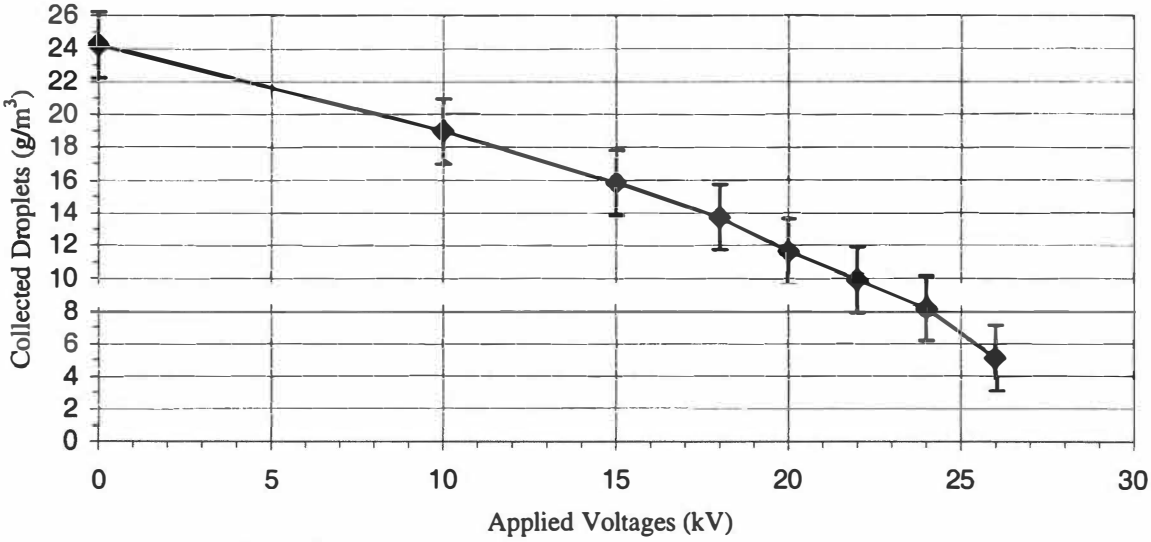



Figure 5.1: Droplets Concentration ($g/m^3$) vs. Applied Voltage (kV) at Reynolds Number of 1350

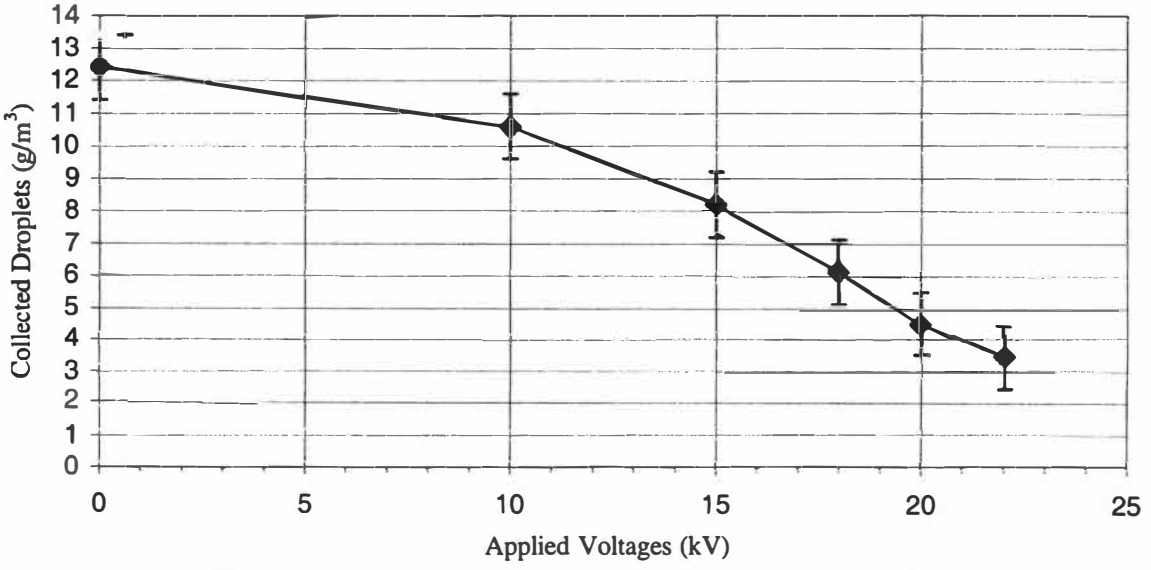



Figure 5.2: Droplets Concentration ($g/m^3$) vs. Applied Voltage (kV) at Reynolds Number of 1620

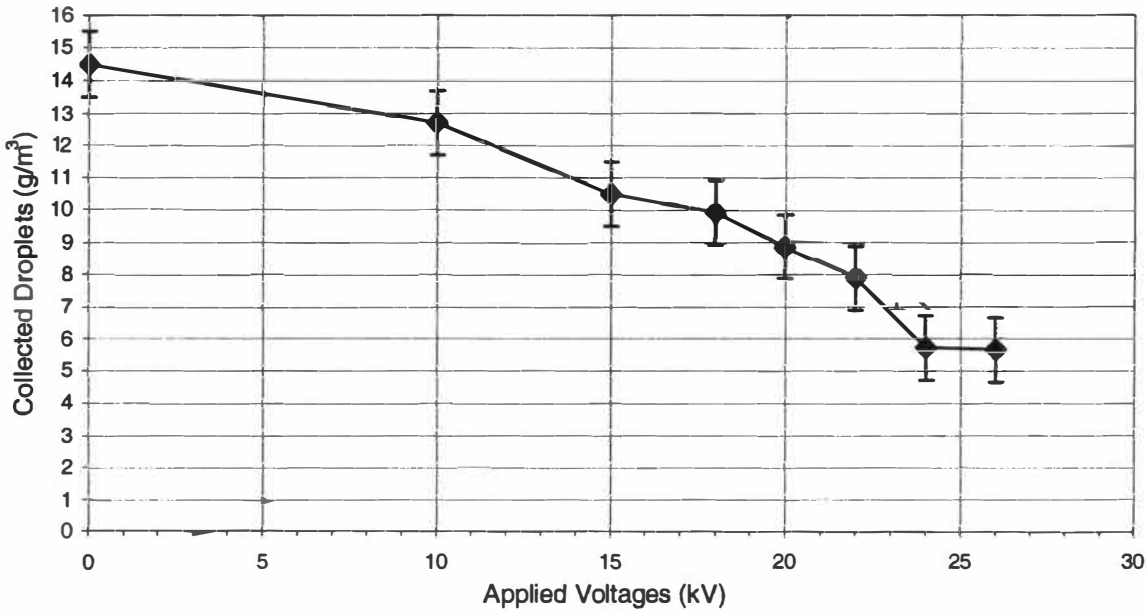



Figure 5.3: Droplets Concentration ($g/m^3$) vs. Applied Voltage (kV) at Reynolds Number of 1680

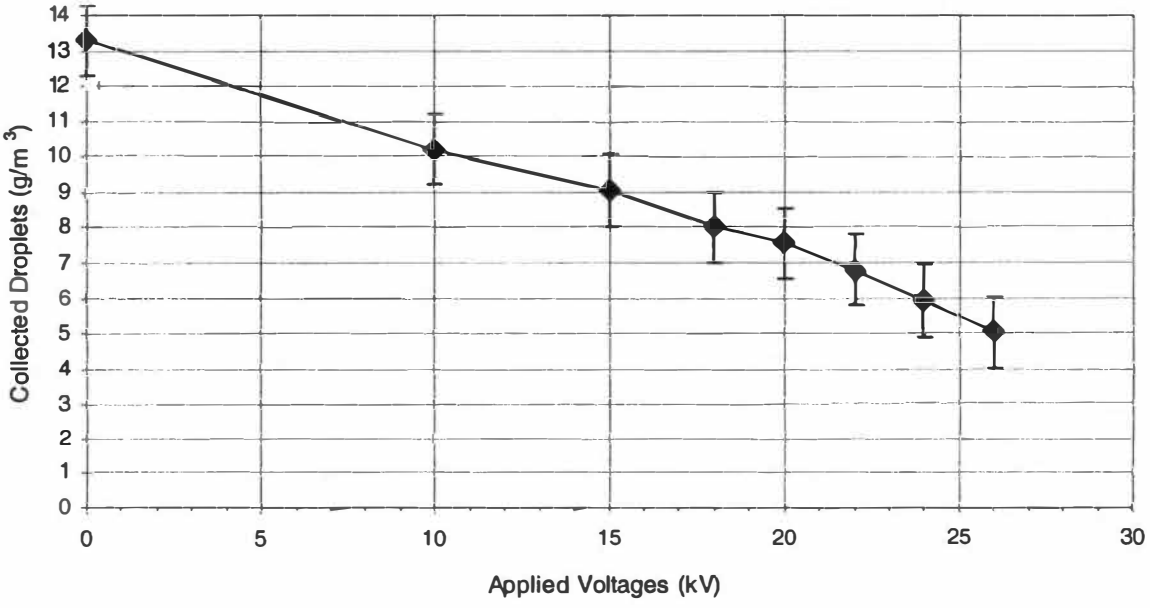



Figure 5.4: Droplets Concentration ($g/m^3$) vs. Applied Voltage (kV) at Reynolds Number of 1950

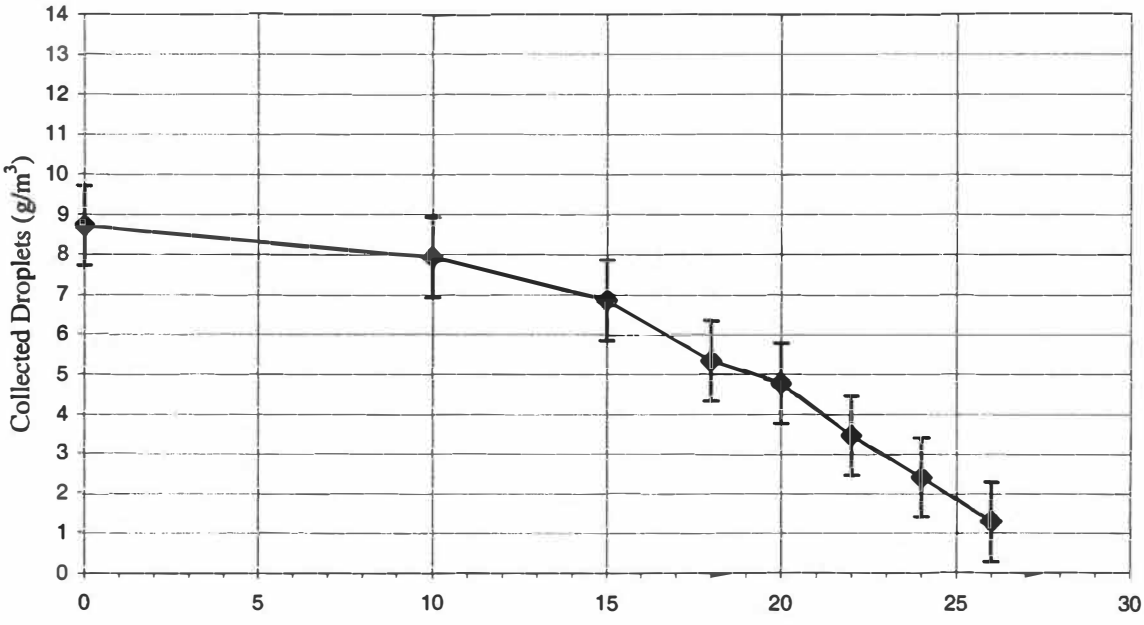



Figure 5.5: Droplets Concentration ($g/m^3$) vs. Applied Voltage (kV) at Reynolds Number of 2200

## 5.4 Effects of electric field strength on light transmission reduction

Figures 5.6 through 5.10 show the relationship between the concentration of collected droplets and light transmission. The investigation of each individual data point reveals that the light transmission is related directly to mist concentration. This could be due to the increasing number of collisions as described in the previous section.

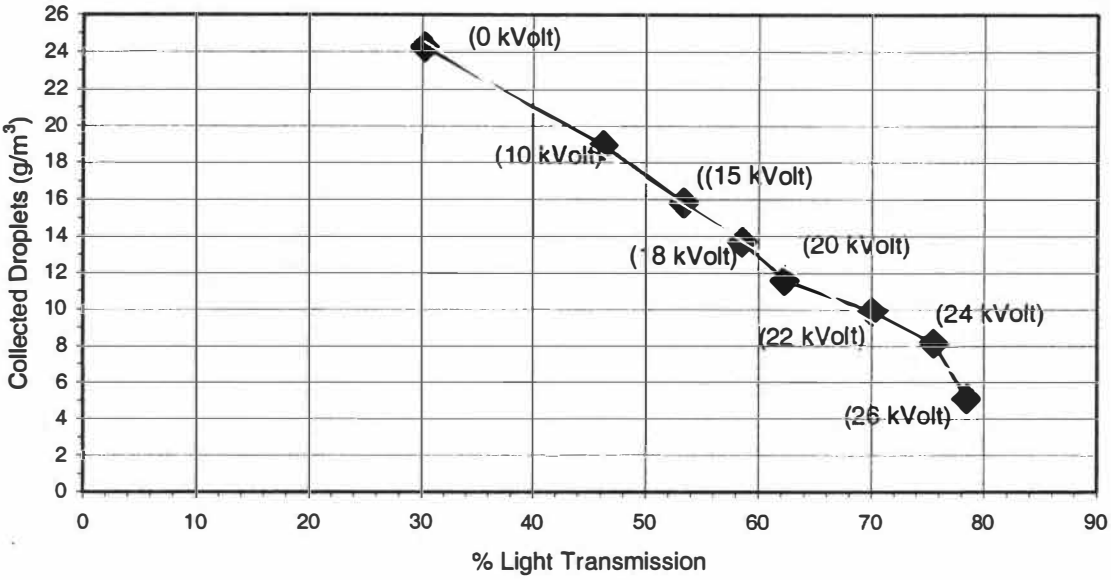



Figure 5.6: Droplets Concentration ($g/m^3$) vs. Percent Light Transmission at Reynolds Number of 1350 under Varying Applied Voltage

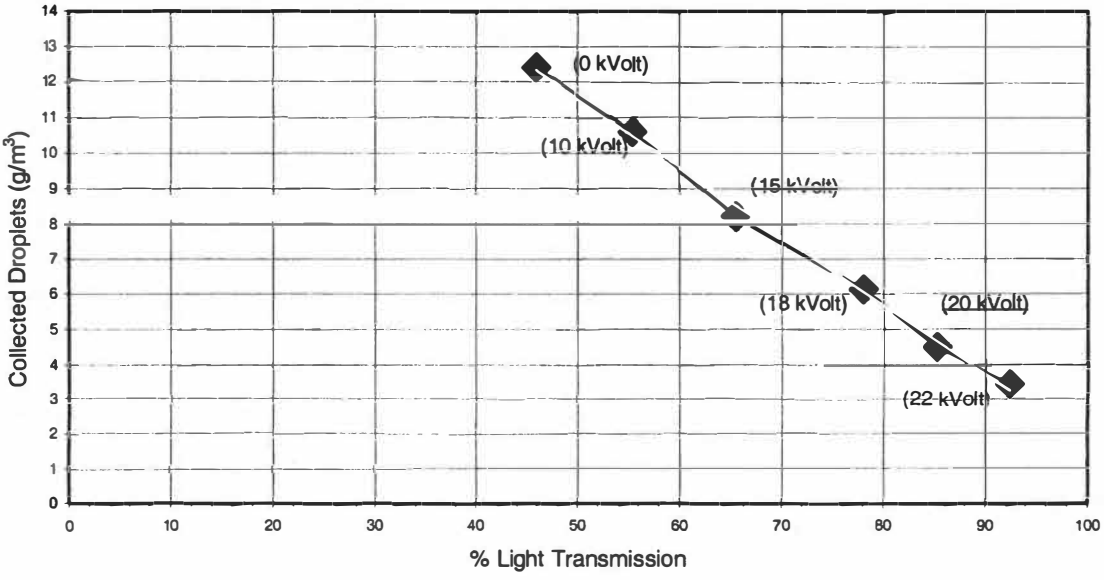



Figure 5.7: Droplets Concentration ($g/m^3$) vs. Percent Light Transmission at Reynolds Number of 1620 under varying Applied Voltage

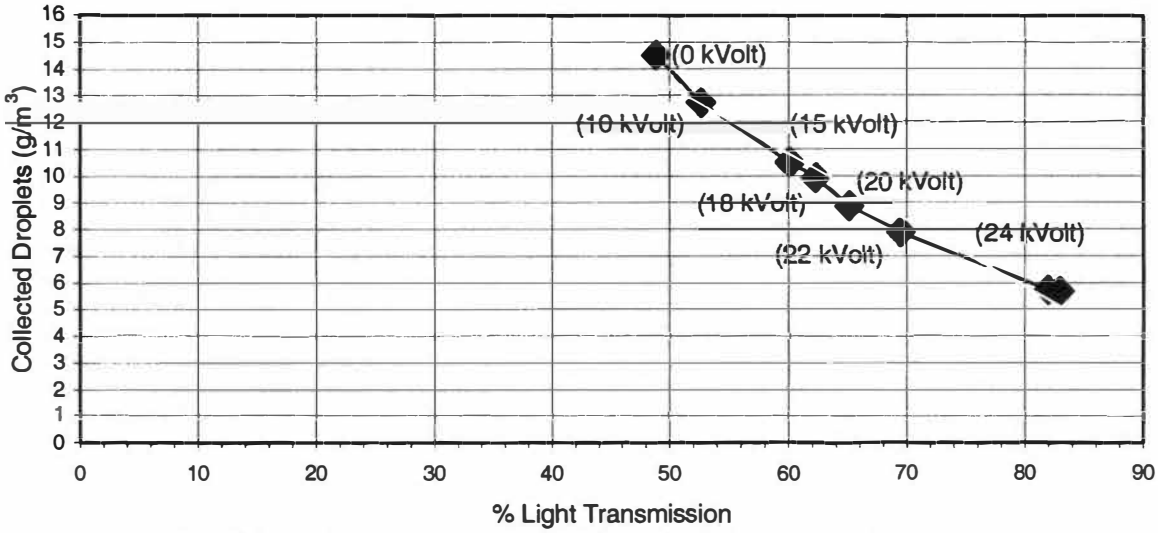



Figure 5.8: Droplets Concentration ($g/m^3$) vs. Percent Light Transmission at Reynolds Number of 1680 under Varying Applied Voltage

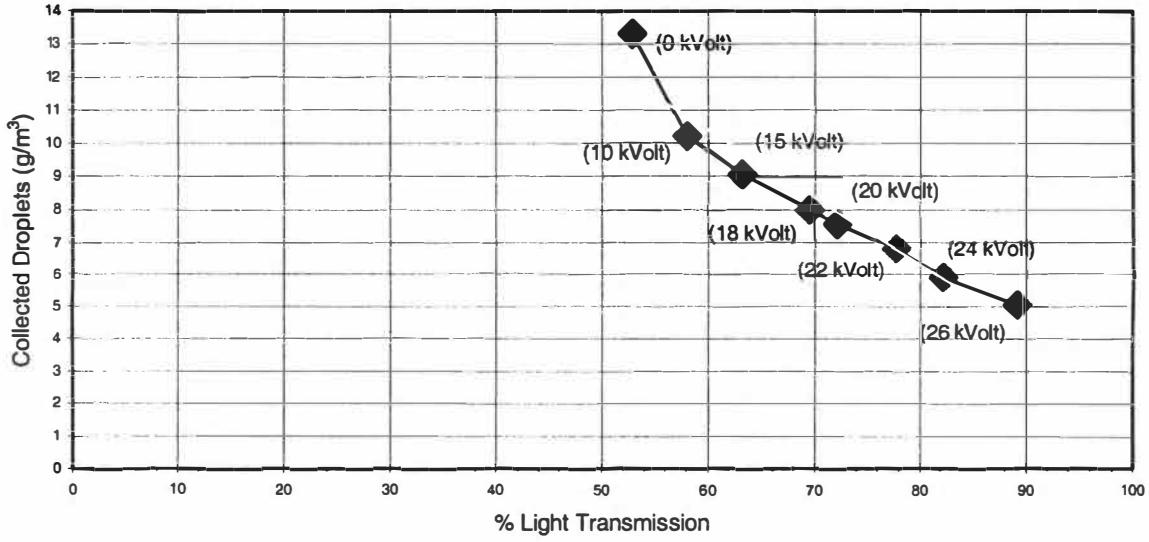



Figure 5.9: Droplets Concentration ($g/m^3$) vs. Percent Light Transmission at Reynolds Number of 1950 under Varing Applied Voltage

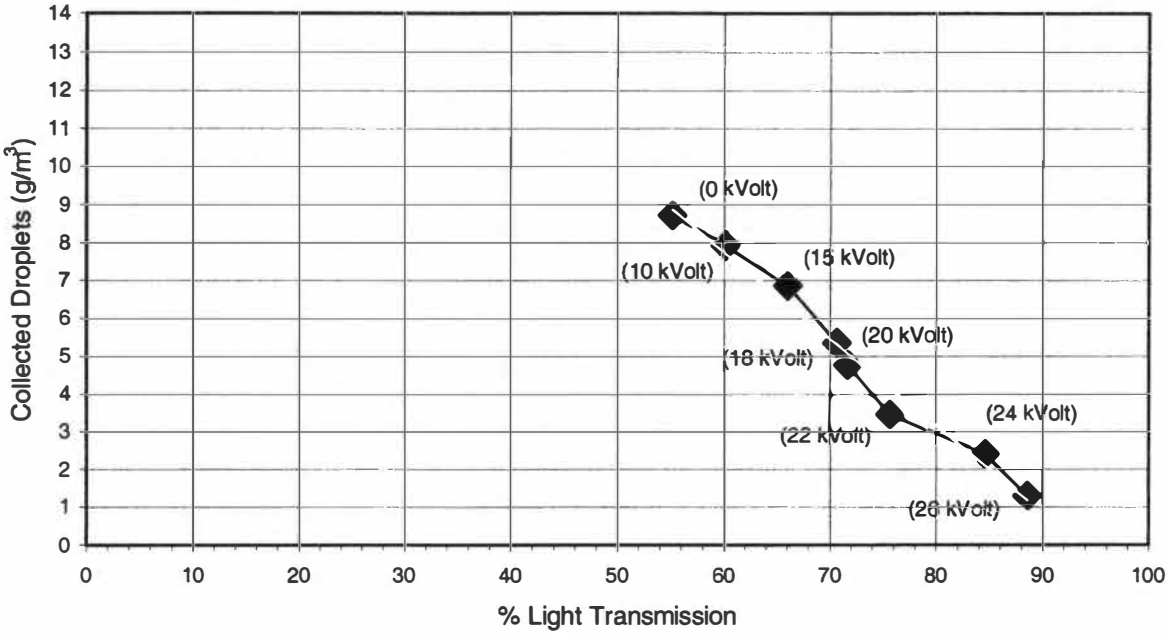



Figure 5.10: Droplets Concentration ($g/m^3$) vs. Percent Light Transmission at Reynolds Number of 2200 under Varying Applied Voltage

## 5.5 Effect of electric field on droplet numbers

A number of experiments were conducted to understand the effect of electric field on both average droplet size and droplet distribution. The average droplet size ($d_{ave}$) was calculated by averaging all sizes of droplets that passed through the laser path. The number of droplets was determined in the following manner

- Calculated the average droplet size, $d_{ave}$
- Determined the average droplet volume, $V_{ave} = 4\pi /3 \, (d_{ave} / 2)^3$
- Measured the mist density obtained from isokentic/dry-ice method

- Multiplied the volume frequency obtained from RTSizer instrument by mist density to determine the total water volume fraction, $V_x$, for droplet size.
- Estimated the number of droplets by dividing $V_x$ over $V_{ave}$

Figure 5.11 shows the distributions of number of droplets versus the averaged droplet size at Reynolds number 1620 and the inlet mist concentration of 12.4 ($g/m^3$) for a range of applied voltages. The figure reveals that the size range of droplets does not change significantly with voltage; however, the distribution of the number of droplets does change. The changes are rather significant for droplet sizes in the range of 4 to 8 □m. For instance, when the applied voltage increases from 0 to 22 kV, the number of droplets reduces from $1.3x10^{10}$ to $4.0x10^{8}$ for the droplet size 5.23 □m. The main reason for this large reduction is attributed to the collision of droplets with the electrodes and the test chamber walls. As a result of these collisions, many droplets attach to the wall and electrodes, and they eventually flow downward to the chamber floor because of gravitational forces. The same experiment was conducted with a Reynolds number of 2200. Figure 5.12 shows a very similar behavior as seen in figure 5.11. It was also observed that the mist concentration reduces from 12.4 to 8.7 ($g/m^3$) when the Reynolds Number increases from 1620 to 2200.

## 5.6 Size distribution

A number of experiments were conducted to determine whether or not the size of droplets could vary as the Reynolds number and mist concentration change under different voltage levels. In one experiment, the air flow rate was arbitrarily changed to a specific value corresponding to a Reynolds Number of 1230. At this number, the

measured droplet concentration using dry-ice trap method was 12.1 (g/m3) for a zero voltage.

The droplet size distributions for 0 and 26 kV are shown in Figures 5.13a and 5.13b. A comparison between the two figures indicates that the size distribution range is increased from [3.97-31.56] μm to [3.97-47.78] μm. It also reveals that the light transmission percent is increased from 63.5 to 94.4. The reason for these differences could be attributed to the enhanced agglomeration and droplet removal at higher voltages.

A similar experiment was carried out with a different droplet concentration but with the same flow rate value of the first experiment. In this experiment the droplet concentration was increased by twice as much as the first experiment. The results of this experiment are shown in Figures 5.14a and 5.14b. The results indicate that the change in size distribution in this experiment are more pronounced than those seen in Figure 5.13a and 5.13b. This is due to the fact that at higher mist concentration rates, the relative distances between droplets are shorter in a fixed volume. This causes enhanced mutual interactions between the droplets (Latham & Roxburgh, 1966). In both experiments, it was observed that the droplet concentration was reduced when the applied voltage increased from 0 to 26 kV. A complete set of graphical results at various voltages (0 – 26 kV) is shown in the Appendix at Reynolds Number of 1350 for starting droplet concentrations of 12.1 g / $m^3$ and 24.2 g/$m^3$ respectively.

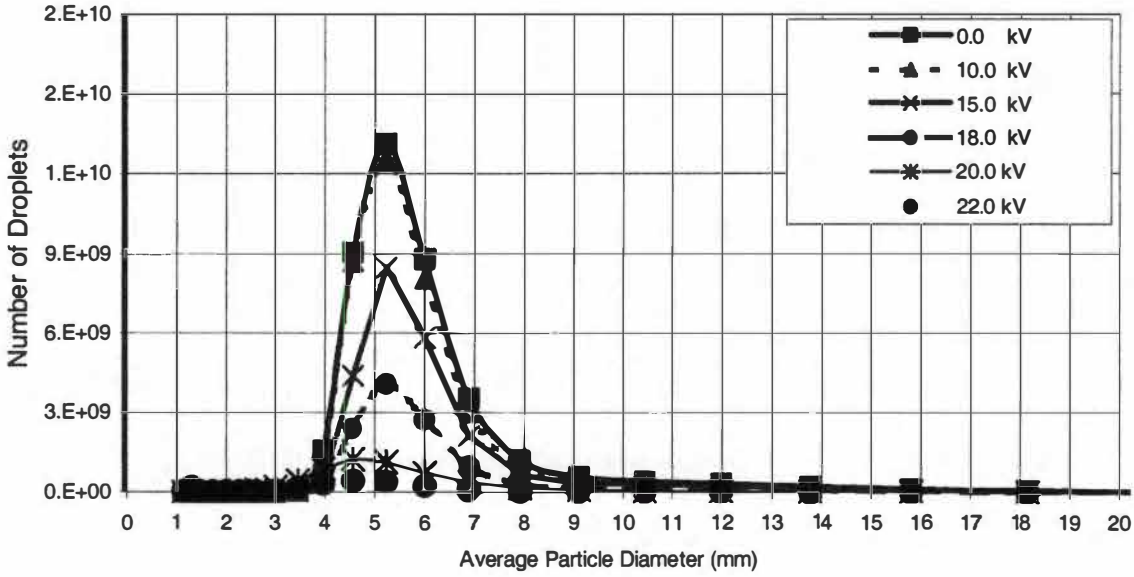



Figure 5.11: Number of Droplets vs. Particle Diameter in Microns at Inlet Mist Concentration of 12.4 g / $m^3$ and Reynolds Number of 1620

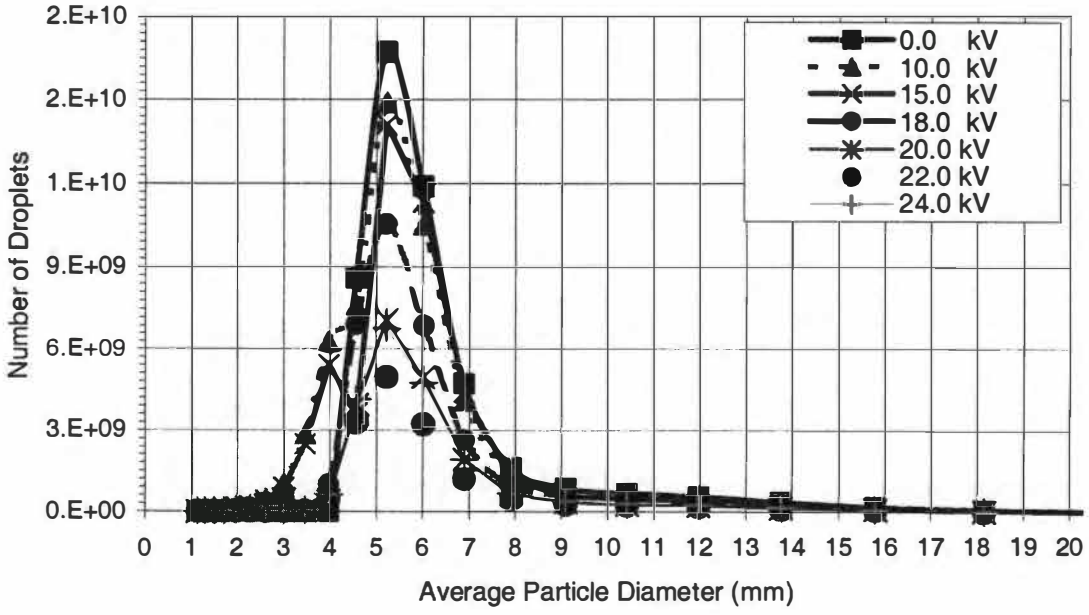
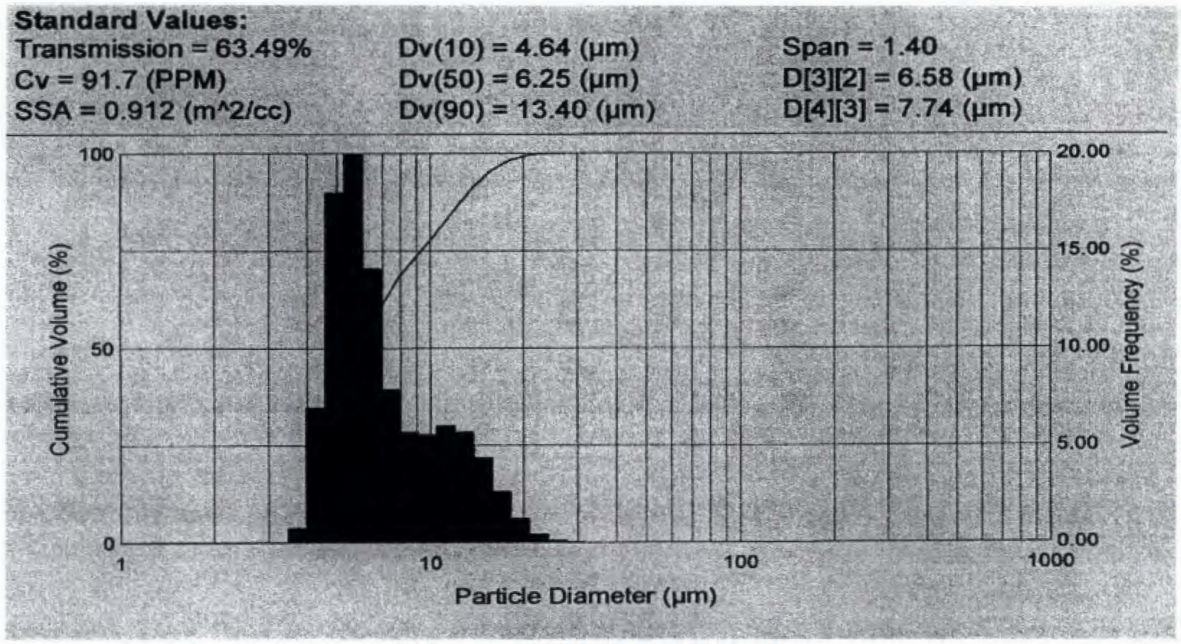
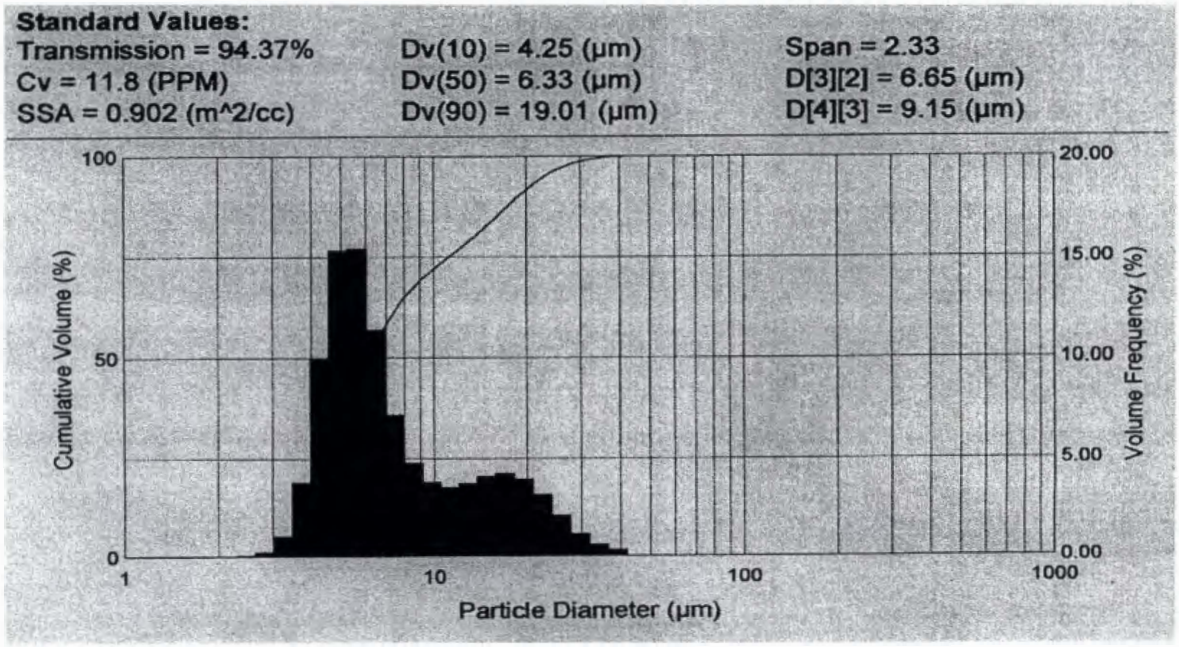



Figure 5.12: Number of Droplets vs. Particle Diameter in Microns at Inlet Mist Concentration of 8.72 g / $m^3$ and Reynolds Number of 2200

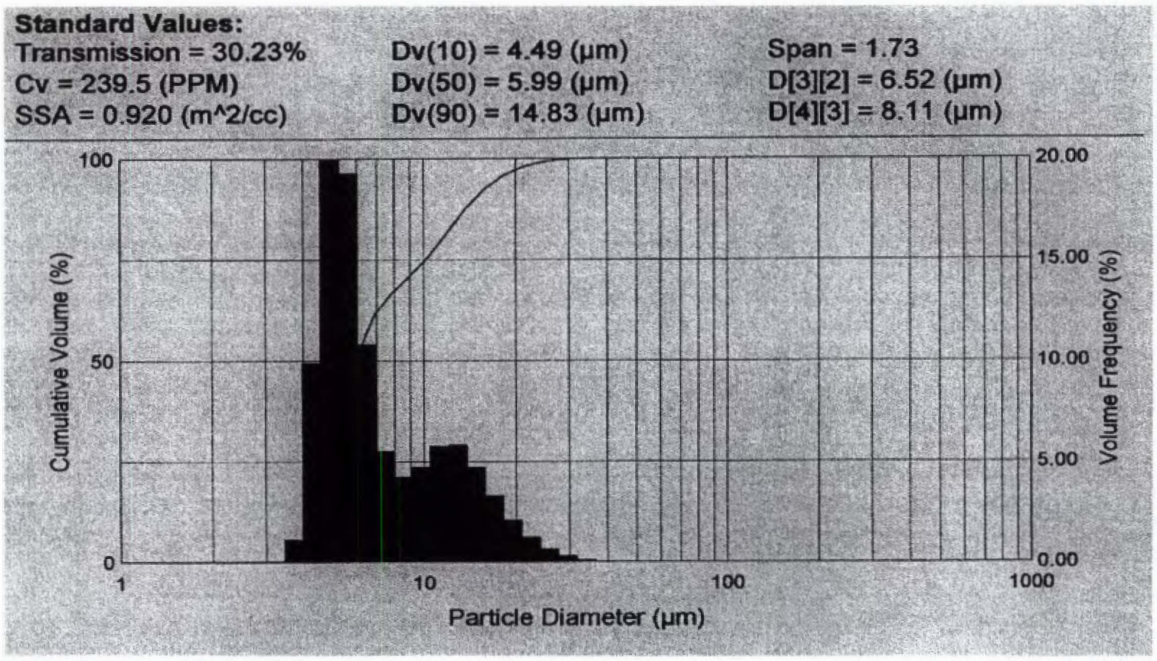



a) Voltage = 0.0 kV and Initial Droplet Concentration = 12.1 g / $m^3$

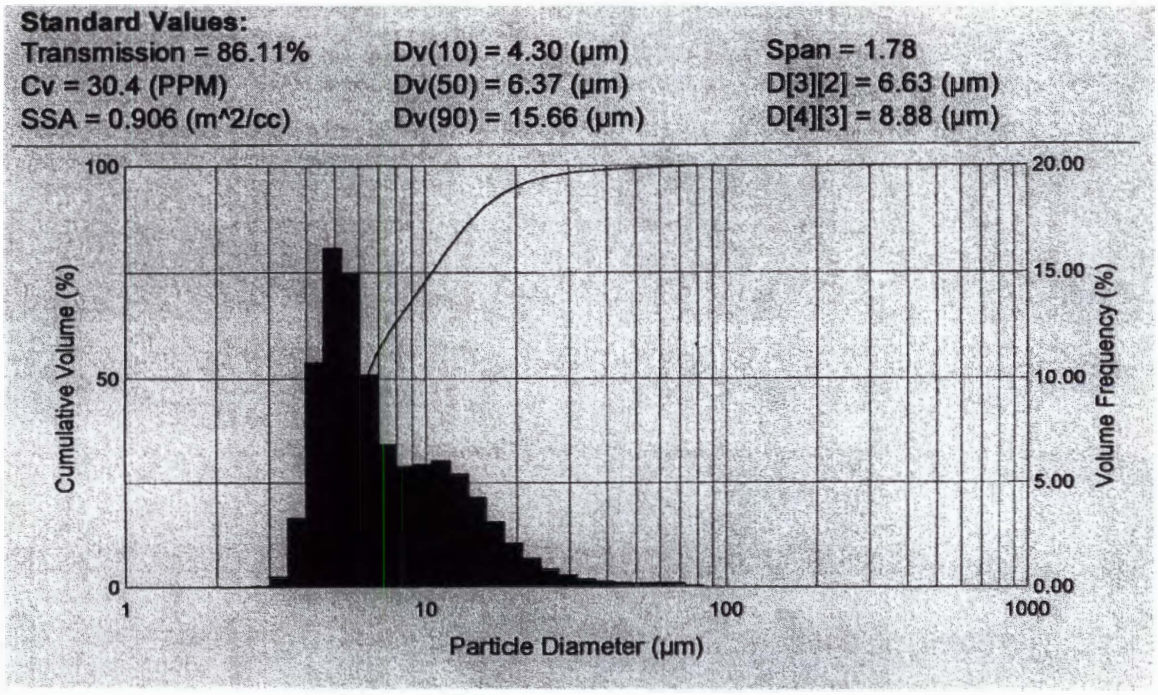



b) Voltage = 26 kV and Droplet Concentration = 5.96 g / $m^3$

Figure 5.13: Droplet size distribution for Reynolds Number of 1350




a) Voltage = 0.0 kV and Initial Droplet Concentration = 24.2 g/m$^3$




b) Voltage = 26.0 kV and Droplet Concentration = 8.17 g/m$^3$

Figure 5.14: Droplet size distribution at Reynolds Number of 1350

## 5.7 Multiple elevation results

A number of experiments were carried out to investigate the effect of distance down electrodes on the light transmission with and without electric field using a constant flow rate. The results of this experiment are shown in Figure 5.15 and Table 5.1. In the figure, the light transmission percent generally increases with the elevation. However, at low voltages the increase is not significant as compared to high voltages. This behavior may be explained as follows. When the droplets travel along the test chamber and between the electrodes, they experience a longer residence time at higher elevations as compared to those at lower elevations. As the residence time increases, the chances for coalescence become greater and thereby reducing the droplet concentration that in turn increases the light transmission percent.

The standard deviation for all experimental data is shown in the form of error bars on each two averaged data point as shown in Figure 5.15. A large error bar indicates poor repeatability of the experiments. The lack of repeatability could be attributed to the heat generated in the medium, resulting in local temperature gradients which in turn give rise to gradients in the conductivity and permittivity of the medium. These can induce fluid unwanted movements that cause errors in measured data. Another reason could be the collision of the droplets on the laser observation window that causes moisture appearance on the window and thereby resulting in incorrect measurement.

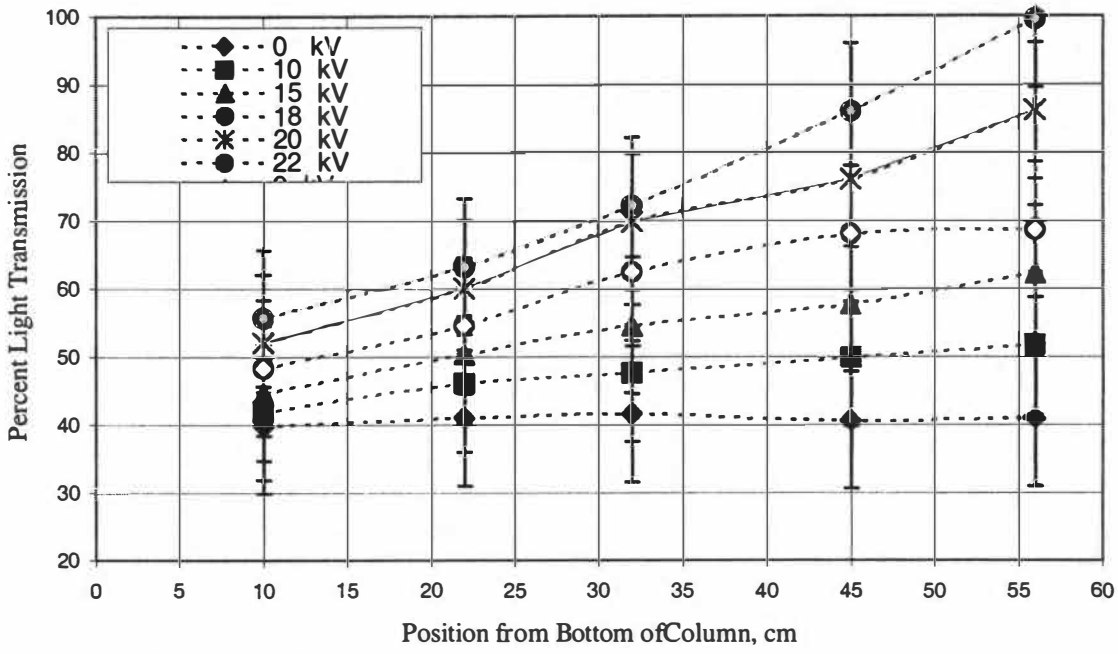



Figure 5.15: Percent Light Transmission vs Height of Column at Reynolds Number of 1620and inlet mist concentration of 27.3 g/m$^3$

Table 5.2: Comparison of percent light transmission at various heights and applied voltages.

| Electric Potential (kV) | Height (cm) | | | | |
|---|---|---|---|---|---|
| | 10 | 22 | 32 | 45 | 56 |
| **0** | 39.8 | 41.0 | 41.6 | 40.6 | 41.0 |
| **10** | 41.8 | 46.0 | 47.6 | 49.8 | 51.7 |
| **15** | 44.7 | 50.3 | 54.6 | 57.7 | 62.3 |
| **18** | 48.2 | 54.6 | 62.4 | 68.0 | 68.7 |
| **20** | 52.2 | 60.0 | 69.8 | 76.2 | 86.2 |
| **22** | 55.7 | 63.2 | 72.3 | 86.1 | 99.5 |

## 5.8 Multiple mist densities at constant flow rates.

A number of experiments were carried out to understand the influence of electric field on various droplet concentrations at a constant flow rate. In this regard, three different droplet concentrations were used under a variable electric field that changed from 0 to 26 kV. The results of these experiments are shown in Figure 5.16 and Table 5.2. The figure indicates that as the voltage increases, the droplet concentrations uniformly decrease from the three different starting levels and converge to a specific levels.

The same experiments were repeated at higher Reynolds numbers and they all indicated the same trend. The results of these experiments are shown in Figures 5.17 and Table 5.3. In Figure 5.17, at the droplet concentration of 8.09 $g/m^3$, saturation occurs at voltages above 22 kV. Therefore, the trend in the data for this particular concentration at voltages above 22 kV was leveled off and did not change in a uniform manner that was the case with the other voltages. The standard deviation for all experimental data is shown in the form of error bars in Figures 5.16 and 5.17.

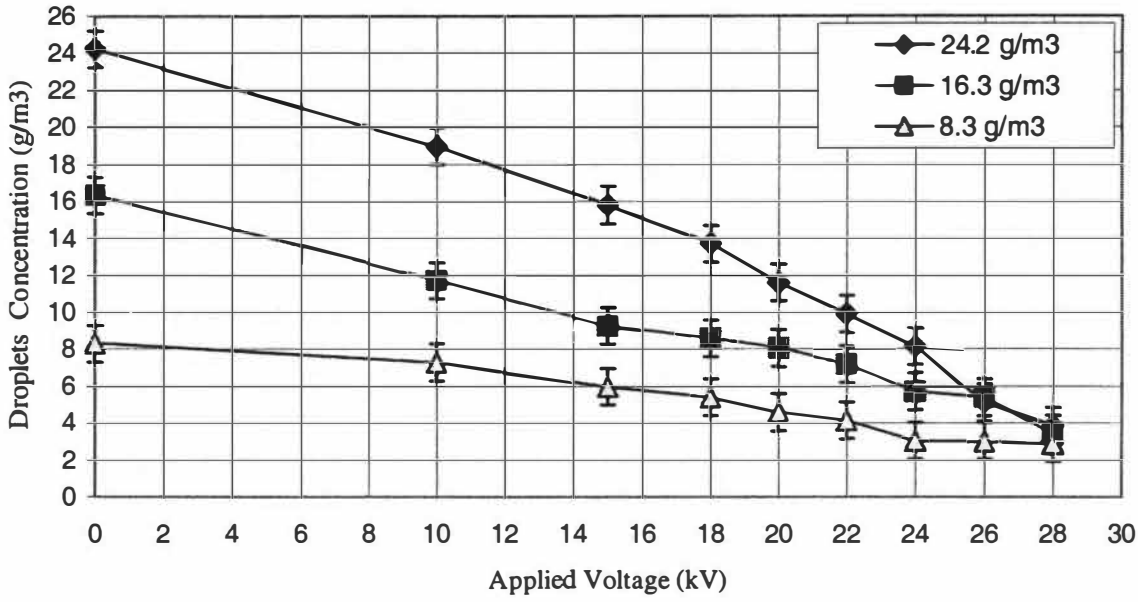



Figure 5.16: Collected Droplets ($g/m^3$) vs. Applied Voltage (kV) at Reynolds Number of 1350

Table 5.3: Effect of Applied Voltage on Droplet Concentration for a Reynolds Number of 1350

| Applied Voltage (Kv) | 0 | 10 | 15 | 18 | 20 | 22 | 24 | 26 | 28 |
|---|---|---|---|---|---|---|---|---|---|
| Ave. Droplet Concentration ($g/m^3$) | 24.23 | 18.97 | 15.82 | 13.72 | 11.62 | 9.92 | 8.17 | 5.12 | 3.86 |
| Ave. Droplet Concentration ($g/m^3$) | 16.33 | 11.73 | 9.28 | 8.60 | 8.08 | 7.20 | 5.73 | 5.40 | 3.42 |
| Ave. Droplet Concentration ($g/m^3$) | 8.32 | 7.30 | 5.97 | 5.41 | 4.60 | 4.16 | 3.04 | 3.04 | 2.90 |

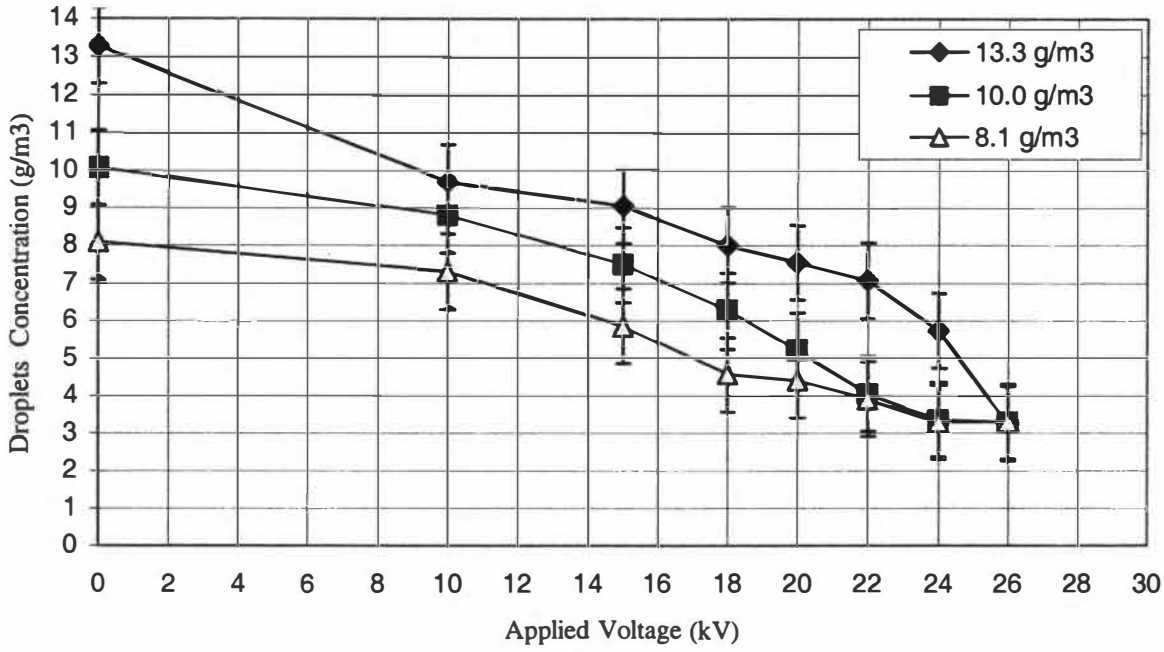



Figure 5.17: Collected Droplets ($g/m^3$) vs. Applied Voltage (kV) at Reynolds Number of 1950

Table 5.4: Effect of Applied Voltage on Droplet Concentration for a Reynolds Number of 1950

| Applied Voltage (Kv) | 0 | 10 | 15 | 18 | 20 | 22 | 24 | 26 |
|---|---|---|---|---|---|---|---|---|
| Ave. Droplet Concentration ($g/m^3$) | 13.30 | 9.70 | 9.05 | 8.01 | 7.56 | 7.07 | 5.74 | 3.26 |
| Ave. Droplet Concentration ($g/m^3$) | 10.10 | 8.81 | 7.50 | 6.28 | 5.20 | 4.05 | 3.37 | 3.30 |
| Ave. Droplet Concentration ($g/m^3$) | 8.10 | 7.31 | 5.86 | 4.58 | 4.41 | 3.92 | 3.30 | 3.32 |

## 5.9 Multiple flow rates at constant mist concentration

Experiments were conducted to investigate the effect of variable flow rate on droplet concentration under various electric field strengths. In each set of experiment the starting droplet concentration was the same. The results of these experiments for a starting droplet concentration of 14.5 ($g/m^3$) and Reynolds numbers of 940, 1350, and 1680 are shown in Figure 5.18 and Table 5.4. As it is seen in the figure, the droplet concentration uniformly reduces with voltage to a certain value. However, after this point further increases in the voltage no longer change the droplet concentration. This appears to be due to charge saturation, as described in the Section 4.2.

Figure 5.19 and Table 5.5 show the results of a similar experiment but with a higher starting droplet concentration and Reynolds number. The figure indicates that at a Reynolds number of 1230 and voltages beyond 22 kV, no further reduction of droplets takes place, in contrast to what was expected. To ensure that the experimental procedure was correct, these experiments were repeated three times with the same outcome. The reason for this behavior is not known at this point.

Figure 5.20 and Table 5.6 show the results of similar experiments with Reynolds numbers of 2400, 2070, 1810, and 940 and a starting droplet concentration of approximately 3.4 ($g/m^3$). The results reveal that the droplet concentration decreases with applied voltage for all Reynolds numbers as expected. The results also reveal that maximum reduction in concentration occurs at 22 kV for all Reynolds numbers. The reduction is more significant for the Reynolds number of 940. The figure also indicates that beyond this voltage no further reduction of droplets take place.

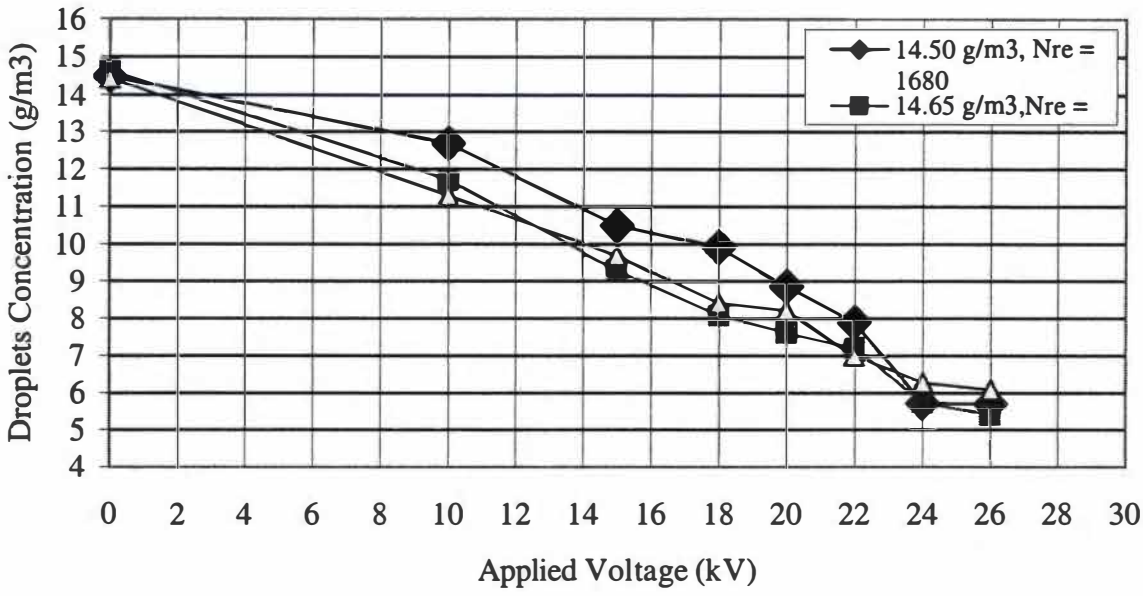



Figure 15.18: Collected Droplets (g/m$^3$) vs. Applied Voltage (kV) at Reynolds Numbers of 940, 1350 and 1680.

Table 5.5: Constant droplet concentration at Reynolds Numbers of 940, 1350 and 1680

| Reynolds Numbers | Applied Voltage (kV) | 0 | 10 | 15 | 18 | 20 | 22 | 24 | 26 |
|---|---|---|---|---|---|---|---|---|---|
| 940 | Ave.Droplet Concentration (g/m$^3$) | 14.5 | 12.7 | 10.5 | 9.9 | 8.9 | 7.9 | 5.7 | 5.7 |
| 1350 | Ave. Droplet Concentration (g/m$^3$) | 14.7 | 11.7 | 9.3 | 8.1 | 7.6 | 7.2 | 5.7 | 5.4 |
| 1680 | Ave. Droplet Concentration (g/m$^3$) | 14.5 | 11.3 | 9.7 | 8.4 | 8.2 | 7.0 | 6.3 | 6.0 |

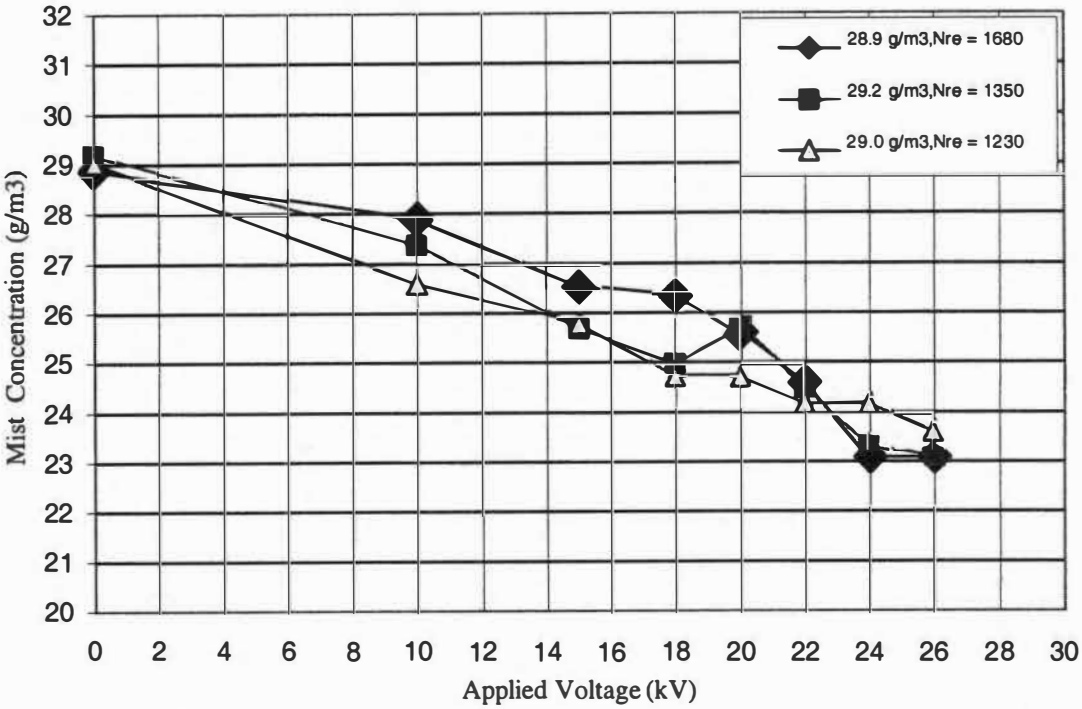



Figure 5.19: Collected Mist ($g/m^3$) vs. Applied Voltage (kV) at Reynolds Number of 1230,1350, and 1680

Table 5.6: Exit mist concentrations for Reynolds Numbers of 1230, 1350, and 1680

| Reynolds Numbers | Applied Voltage (Kv) | 0 | 10 | 15 | 18 | 20 | 22 | 24 | 26 |
|---|---|---|---|---|---|---|---|---|---|
| 1230 | Ave. Droplet Concentration ($g/m^3$) | 28.87 | 27.90 | 26.56 | 26.36 | 25.60 | 24.63 | 23.09 | 23.09 |
| 1350 | Ave. Droplet Concentration ($g/m^3$) | 29.20 | 27.40 | 25.71 | 25.00 | 25.71 | 24.52 | 23.34 | 23.10 |
| 1680 | Ave. Droplet Concentration ($g/m^3$) | 29.03 | 26.61 | 25.80 | 24.74 | 24.74 | 24.20 | 24.20 | 23.65 |

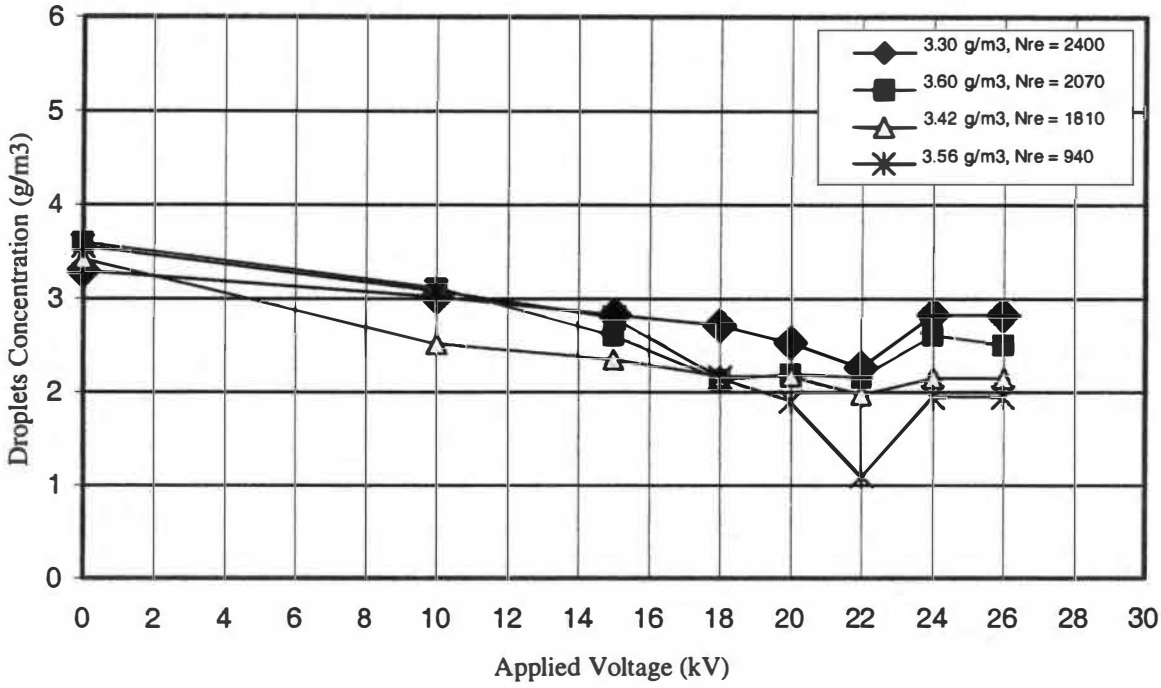



Figure 5.20: Collected Droplets ($g/m^3$) vs. Applied Voltage (kV) at Reynolds Numbers of 2400, 2070, 1810, and 940

Table 5.7: Exit mist concentrations for Reynolds Numbers of 2400, 2070, 1810, and 940

| Reynolds Numbers | Applied Voltage (kV) | 0 | 10 | 15 | 18 | 20 | 22 | 24 | 26 |
|---|---|---|---|---|---|---|---|---|---|
| 2400 | Ave. Droplet Concentration ($g/m^3$) | 3.30 | 3.02 | 2.83 | 2.72 | 2.53 | 2.26 | 2.83 | 2.83 |
| 2070 | Ave. Droplet Concentration ($g/m^3$) | 3.60 | 3.12 | 2.61 | 2.14 | 2.19 | 2.16 | 2.61 | 2.51 |
| 1810 | Ave. Droplet Concentration ($g/m^3$) | 3.42 | 2.52 | 2.35 | 2.17 | 2.17 | 1.97 | 2.15 | 2.15 |
| 940 | Ave. Droplet Concentration ($g/m^3$) | 3.56 | 3.08 | 2.80 | 2.16 | 1.90 | 1.10 | 1.95 | 1.95 |

These experiments were also used to identify a Reynolds number that maximizes the removal of droplets so that a minimum concentration is achieved at a certain applied voltage. Figure 5.20 shows that this phenomenon takes place at a Reynolds number of 940 and applied voltage of 22 kV. This minimum at 22 kV was repeated in 2 runs.

Similarly, additional experiments were carried out but with different starting droplet concentration and Reynolds numbers. The results of these experiments are shown in Figure 5.21 and Table 5.7. In these experiments, it was noticed that for the Reynolds number 940, the droplet concentration did not decrease beyond 20 kV as compared to the other Reynolds numbers. Since this was the smallest Reynolds number used in this experiment, we expected to see the droplet concentration decreasing more than at other Reynolds numbers for all voltages. However, this was not the case when the voltage went beyond 20 kV. The reason for this behavior is not known.

## 5.10 Removal efficiency of the droplets

A key objective of this research work was to quantify the removing efficiency of droplets from an air stream at constant flow rate under a DC electric field. To achieve this objective several experiments were carried out. In this regard, three different droplet concentrations were used under a variable electric field that change from 0 to 28 kV. The results of these experiments are shown in Figure 5.22. The figure reveals that the removal efficiency of all three droplet concentrations vary approximately linearly related with the applied voltage. At the droplet concentration of 8.3 $g/m^3$ , saturation occurred at voltages above 24 kV and the removal efficiency was steady at 63.5 percent.

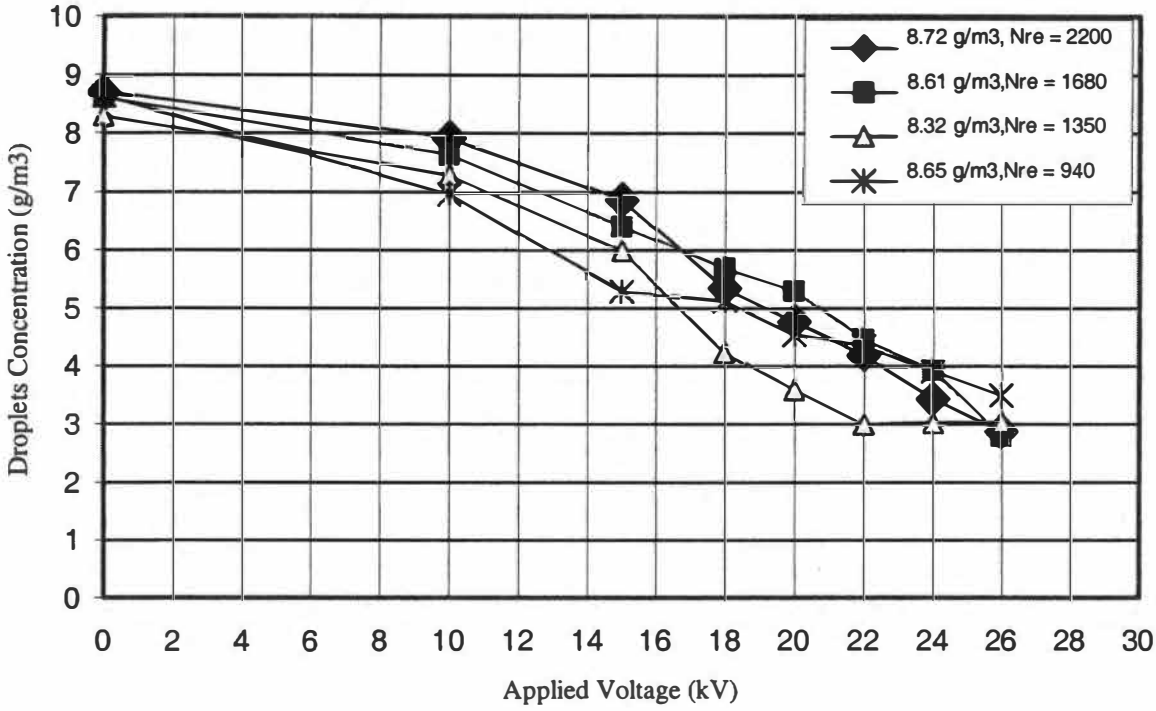



Figure 5.21: Collected Droplets ($g/m^3$) vs. Applied Voltage (kV) at Reynolds Numbers of 2200, 1680, 1350, and 940

Table 5.8: Exit mist concentrations for Reynolds Numbers of 2200, 1680, 1350, and 940

| Reynolds Numbers | Applied Voltage (kV) | 0 | 10 | 15 | 18 | 20 | 22 | 24 | 26 |
|---|---|---|---|---|---|---|---|---|---|
| 2200 | Ave. Droplet Concentration ($g/m^3$) | 8.72 | 7.93 | 6.87 | 5.35 | 4.78 | 4.20 | 3.45 | 2.88 |
| 1680 | Ave. Droplet Concentration ($g/m^3$) | 8.61 | 7.65 | 6.42 | 5.70 | 5.31 | 4.48 | 3.95 | 2.80 |
| 1350 | Ave. Droplet Concentration ($g/m^3$) | 8.32 | 7.30 | 6.00 | 4.25 | 3.60 | 3.00 | 3.04 | 3.04 |
| 940 | Ave. Droplet Concentration ($g/m^3$) | 8.65 | 6.97 | 5.30 | 5.13 | 4.56 | 4.37 | 3.93 | 3.50 |

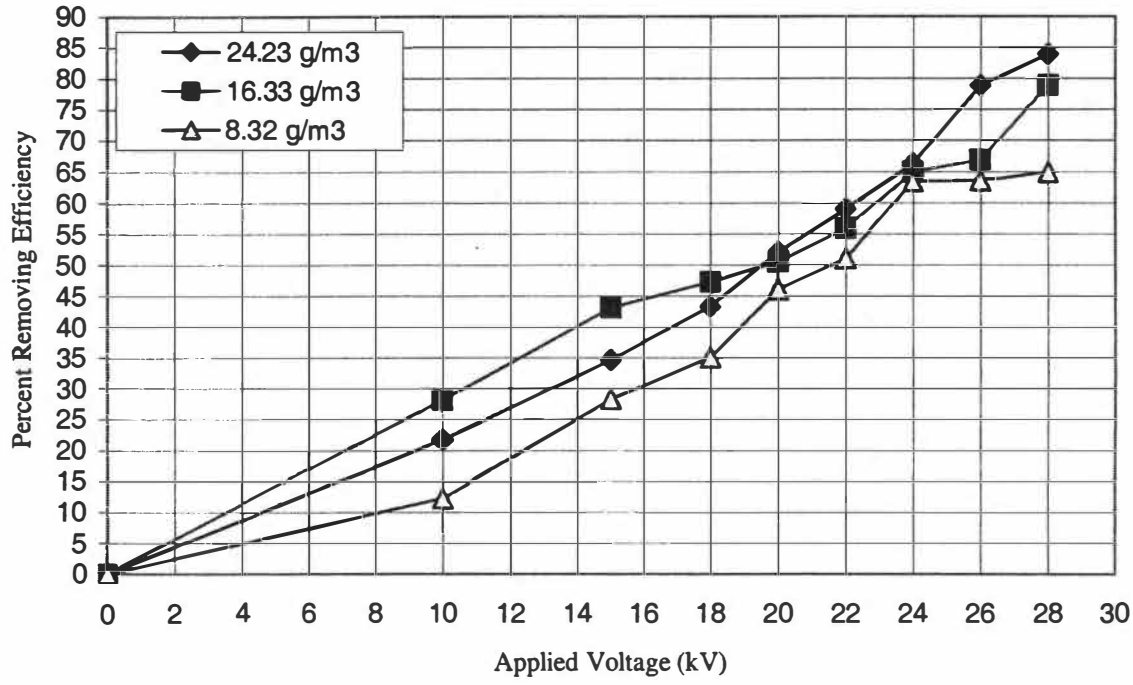



Figure 5.22: Percent removal efficiency vs. applied voltages (kV) at Reynolds Numbers of 1350

At droplet concentrations of 24.2 and 16.3 g/m$^3$ , the removal efficiency of 84.0 and 79.0 percent was achieved, respectively.

The same experiments were repeated at a higher Reynolds number and they all indicated similar results. The results of these experiments are shown in Figure 5.23. In this Figure, at droplet concentrations of 10.1 and 8.1 g/m$^3$ , a maximum efficiency of 67.0 and 59.0 percent was achieved at 24.0 kV. Above 24 kV, saturation occurred and therefore, the efficiency remained constant with further increase in voltage. At a droplet concentration of 13.3 g/m$^3$, the maximum removal efficiency of 75.5 percent was achieved.

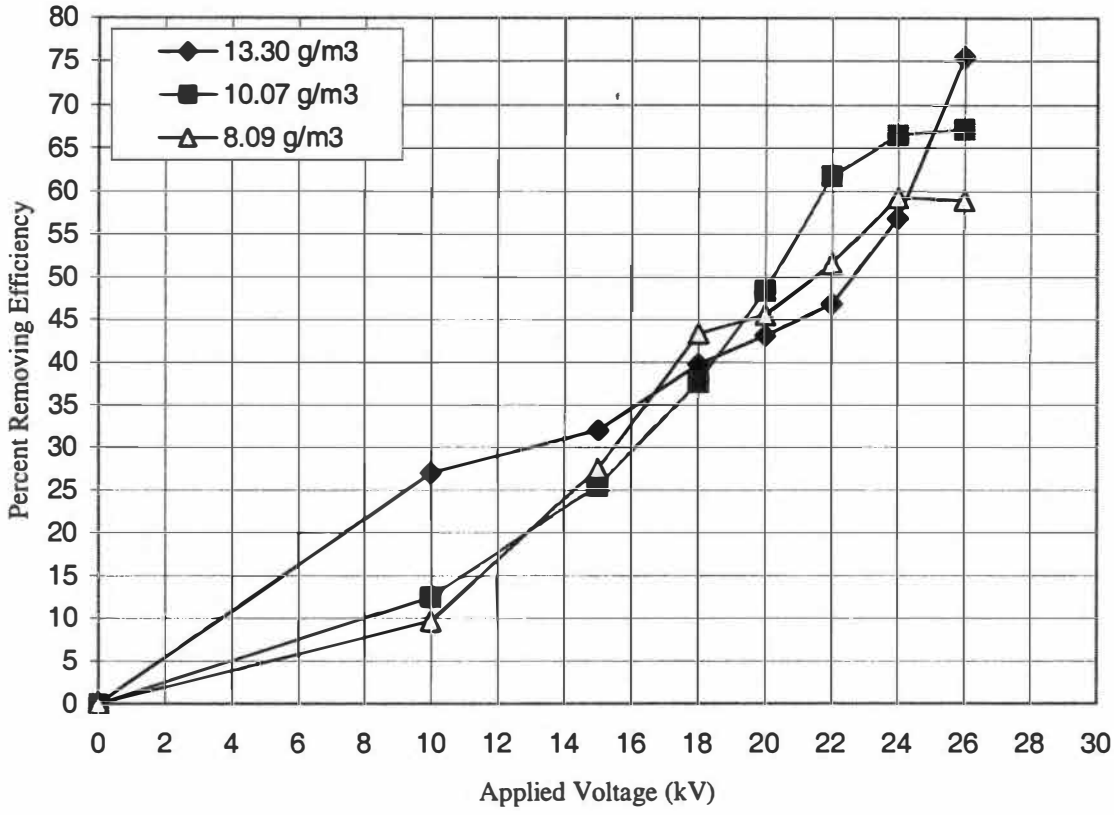



Figure 5.23: Percent removing efficiency vs. applied aoltage (kV) at Reynolds numbers of 1946

Also, it was observed that no saturation was occurred under these experimental conditions.

Comparing the two figures, we can conclude that the higher droplet concentration gives higher removal efficiency presumably due to higher number of droplet collision.

# CHAPTER 6

# SUMMARY and CONCLUSIONS

A series of experiments was conducted in a carefully designed section in order to quantify the effect of an applied electric potential on the water droplet content in simulated moist air streams. The test chamber is clear Lexan with a cross section of 10 cm x 10 cm and approximately 94 cm long mounted vertically, with the air flow from bottom to top through the unit. The two 9 cm x 60 cm electrodes are mounted vertically approximately 8 cm apart on opposite sides of the test window. The applied electric potential gradients were thus normal to the air, mist flow direction. The applied electric potentials ranged from 0 to 26 kV in all experiments.

The mist containing air streams were forced through the test chamber at Reynolds Numbers whose nominal values ranged from 940 to 2200, which correspond to residence times in the test section of 7 seconds to 3 seconds. The droplets are produced by an aerosol generator fed with distilled water, and the size distribution of the resulting mist determined by laser-light scattering using a Malvern Spraytec RTS 5000 Series droplet sizing system mounted on a movable stage. Analysis of the data show that the water droplets in the mist range in diameter from a few micrometers to about 20 micrometers, more or less, in each of the test experiments. The droplet loadings in the air streams, determined by freezing samples withdrawn isokinetically, range from nominal values of 8 to 24 g mass per cubic meter.

The following conclusions are drawn from experimental results and observations:

1. The applied electric potentials reduced the mist content of the air exiting the test unit as the potential is increased from 0 to 26 kV, in all but one of the cases investigated. In this case there is no further reduction in water droplet content of the air stream when the potential is increased from 24 to 26 kV, suggesting that a saturation effect may be occurring in this case.
2. The efficiency of the droplet removal process ranges from about 65% to 85% on a mass basis for the series of runs at a nominal Reynolds Numbers of 1350, with the higher efficiencies corresponding to the higher nominal initial droplet loading of 24 g mass per cubic meter. The removal efficiency of 65% was achieved for a nominal droplet loading of 8 g mass per cubic meter.
3. In a strict sense, the effect of the applied electric potential on the water droplet content of the air stream is not linear. However, fitting the data with a linear model may be useful for preliminary engineering design purposes.
4. The water droplets migrate to the electrodes when the electric potential is applied across the plates, as evidenced by water accumulation on the plate surfaces. Although not quantified, it appeared that more water accumulated on the positive electrode than the negative one. Accumulation of mist on the plates results in draining of water down the plates and pooling at the bottom of the unit. Fogging begins near the bottom of the electrode plates and progresses in time up the plates. This migration of mist from the air stream to the plates due to the influence of the electric potential is the principal mechanism of droplet removal from the air stream in these experiments.

5. Experiments show that the droplet content of the air stream decreases approximately linearly with distance up the test unit. This result suggests that further increases in removal efficiencies can be achieved by the use of electrode plates longer than the 60 cm used in these experiments.
6. There is limited evidence that the electric potential promotes droplet coalescence in the size range of approximately 10 to 20 micrometers, at least. This process should improve droplet collection efficiency in a filter installed downstream of an electric potential demisting unit in an actual application, although sufficient data are not provided here for quantifying the extent to which the overall droplet collection efficiency may be improved.

# CHAPTER 7

# RECOMMENDATIONS

A suggestion for improving the repeatability of the experiments is to use a Laser Mass Velocimeter instead of using a dry-ice trap for measuring droplet concentrations in the air stream. Also, it would be helpful to find a better way to clean the observation windows of the test chamber. Additional experiments are required for determining the exact power consumption in order to characterize the relationship between power consumption and droplet removal efficiency.

It would be interesting also to conduct similar experiments with two additional electrodes between the two original electrodes used in these experiments to promote droplet collisions and preventing the short circuits.

Experiments should be conducted to examine the effects of an acoustic field and a combination of an electric field and an acoustic field in the coalescence unit as illustrated in Figure 3.1.

Finally, it is recommended that the effect of diffusion on the particle collision process be examined theoretically. The diffusion of particles relative to each other and its interaction with the electrically induced collisions apparently has not been investigated in the past. This may cause problems for small particles which have larger diffusivity.

# REFERENCES

1. Accomazzo, M.A. and Grant D.C. "*Mechanisms and devices for filtration of critical Process gases*". *Fluid Filtration: Gas,* **1**, ASTM STP *975, 402*, 1986.
2. ACS Industries, Inc. Bulletin B-124 March, 1990.
3. Bacon, G., Ramon, L., and Liang, K., "*Control Particulate and Metal HAPs*" Chem.Eng. Prog., December 1997.
4. Bailes, P. J, and Larkai, S. K. L, "*Liquid Phase Separation in Pulsed D.C. Fields*".

   Ibid., 60, 115, 1982.
5. Barker, R. E, Granular electrofiltration. Ph.D. Diss., University of Tennessee, 1988.
6. Barker, R. E, Brunson, R. R, Clinton, S. D, and Watson J. D, Granular electrofiltration. *Separations Technology*, vol. 1, 1991.
7. Basset, A.B*Treatise on hydrodynamics.* Deighton Bell, London, 1888.
8. Berger, R, Koaleszensprobleme in chemischen Prozessen,"Chem.,Ing.,Tech"., 58, 449, 1986.
9. Boem, J. *Electrostatic Precipitation*, Elsevier Scientific, 1982.
10. Bogarduos, H. F., R.C. Clark, J. K. Thomspon, and G. H. Fielding, "*Enhancement of filter media performance by corona-free electric fields*", Presented at the 13th AEC Air Cleaning Conference, August 1974.
11. Brown, R. C., "*Capture of dust particles in filters by line-dipole charged filter*", *J. Aerosol Sci.*, 12, 349, 1981.
12. Brunazzi, E. and Paglianti, A. *Design of complex wire mesh mist eliminators. AIChE J.* **24**,1199,2000. 1999.

13. Cadle, R. D, Particle Size: *Theory and Industrial Applications, Reinhold Publishing Corporation*, New York, 1965.

14. Corrsin, S. and Lumley, *J. Appl. Sci.* Res. A6, 114, 1956.

15. Crowley, J. M., *Fundamentals of Applied Electrostatics*, John Wiley and Sons, New York, 1986.

16. Davies, R. N, *Dust is Dangerous*, Faker & Faker Limited, London, 1953.

17. Davis, M.H. Two charged Spherical Conductors in a Uniform Electric Field Forces and Field Strength. *Quart. J. Mech. Appl. Math.* **17**,499, 1964.

18. Erker, J.A. and Baygents, J.C. *NASA Conference publication* **3338**, 731, 1996.

19. Ezekoye, O. A. and Wibowo, Y. W., *Simulation of Acoustic Agglomeration Processes using a Sectional Algorithm, J. Aerosol Sci.* **30**, 1117-1138, 1999.

20. Felder, R. M. and Rousseau, R. W. *Elementry principles of Chemical Processes.* John Wiley & Sons, New York, 1978.

21. Fuchs, N.A, *Mechanics of Aerosols, Pergamon, New York*, 1964.

22. Fielding, G.H.,H.F. Bogardus, R.C. Clark, and J.K. Thompson, "Electrically Augmented Filtration of Aerosols", in ACS Symp. Ser. **17**, 1975.

23. Hansen, O. V, Reid, J. L, CPI-100 NOV-DEC, 1983.

24. Harriott, G.M. and Saville D.A. "*Electrically stimulated aerosol filtration in packed beds*", *AIChE J,* **26**, 325, 1971.

25. Hauertmann, H. B, Degener, W. and Schugerl, Electrostatic Coalescence: Reactor Process Control and Important Parameters, *lbid.*,**24**, 253, 1989.

26. Henry, F.S. and Ariman T. "*Numeric modeling of electrically enhanced fibrous filtration*". ASTM Committee F-21, *Fluid Filtration: Gas,* **1**, 13, 1986.

27. Hsu, E. C. and Li, N. N. "*Membrane Recovery in Liquid Membrane Separation Processes*", *Sep. Sci. Technol.*, **20**, 115, 1985.

28. Kataoka, T. and Nishiki, T." *Development of a Continuous Electric Coalescence of W/O Emulsions in Liquid Surfactant Membrane Proces*". *lbid.*, **25**, 171, 1990.

29. Keh H.J. and Chen, S.B., *J. Colloid Interf. Sci.* **130**, 542, 1989a.

30. Keh H.J. and Chen, S.B., J. *Colloid Interf. Sci.* **130**, 556, 1989b.

31. Kildesg, J., Bhatia, V., Lind, L., Johnson, E., and Johansen, A. *An Experimental Investigation for Agglomeration of Aerosols in Alternating Electric Fields. Aerosol Science and Technology* 23:603-610, 1995.

32. Latham, J. and Roxburgh, I.W. *Proc. Roy. Soc.* **A 295**, 84. Maxey, M.R. and Riley, J.J. (1983) *Equation of motion for a small rigid sphere in a non-uniform flow. Phys. Fluids.* 26(4): 883-888, 1966.

33. Loewvenberg, M and Davis, R.H., *J. Fluid Mech.* **89**, 123, 1995.

34. Loffler, F. and Gutsch, A., *J. Aerosol Sci.*, **24**, S505, 1993.

35. Luckner, J., *J. Aerosol Sci.* **25**, S915, 1995.

36. Maxey, M.R. *and Riely, J.J.*, "*Equation of motion for a small rigid sphere in a nonuniform flow*", *Phys. Fluids*, **26**(4): 883-888, 1983.

37. Mizuno, A., *Review of Particle charging Research*, Proc. 1st Int. Conf. On Electrostatic Precipitation, pp. 304-325, 1981.

38. Muller, D.J., "*Electrostatic granular bed filter development program*", Paper presented at 2nd Annual Contractors' Meeting on Contaminant Control in Hot Coal Derived Gas Streams, pp. 75-85, Morgantown, WV, 17-19 February 1982.

39. Panton, R.L, *Incompressible Flow.* John Wiley and Sons, New York, 1996.

40. Pauthenier, M. M., and Moreau-Hanot, M.,*J. Phys. et Rad., Ser. 7,* **3,** pp. 590, 1932.

41. Perkins, H.C *Air Pollution,* McGraw-Hill, Inc. New York, 1974.

42. Ptasinski, K.J. and Kerkhof, P.J.A.M.,*Sep. Sci. Technoloy.*, **27**, Sep. 1992.

43. Reist, P.C., *Aerosol Science and Technology*, McGraw-Hill, New York, 1993.

44. Rohmann, H., Zeit. *Fur Phys.,* **17,** pp. 253, 1923.

45. Silverman, L., Billings, C.E. and Dennis, R., "*Performance of the model K electro-polar filte", USAEC Report NYO* 1592, Harvard University, 1954.

46. Thomas, J. W., and E. J. Woodfin, "*Electrified fibrous air filter*", *AIEE Transactions*, **78**, 276, 1959.

47. Tsouris, C., Yiacoumi, S., and Scott, T.C., Chem. Eng. Commun. **137**, 147, 1995.

48. Van de Hulst, H. C., *Light Scattering by Small Particles*, Wiley, New York, 1957.

49. Wark, K. and Warner, C.F., *Air Pollution: Its Origin and Control*, Harper and Row, New York, 1981.

50. Waterman, L. C. "*Electrical Coalescers*", *Chem. Eng. Prog.*, **61**, 51-57,1965.

51. White, H. J., *Industrial Electrostatic Precipitation*, Addison-Wesley Publishing Co., 1962.

52. Williams, T.J. and Bailey, A.G. *Inst. Phys. Conf. Ser.* **66-**II, 39, 1983.

53. Zhang, X. and Davis, R.H., *The Rate of Collisions Due to Brownian or Gravitational Motion of Small Drops. J. Fluid Mech.* **230**, 479-504, 1991.

54. Zhang, X., Davis, R.H. and Ruth, M.F., *J. Fluid Mech.* **249**, 227, 1993.

55. Zhang, X., Basaran, O.A. and Wham, R.M. "*Theoretical Prediction of Electric Field-Enhanced Coalescence of Spherical Drops*". *AIChE J.* **41**, 1629, 1995.

# APPENDIX

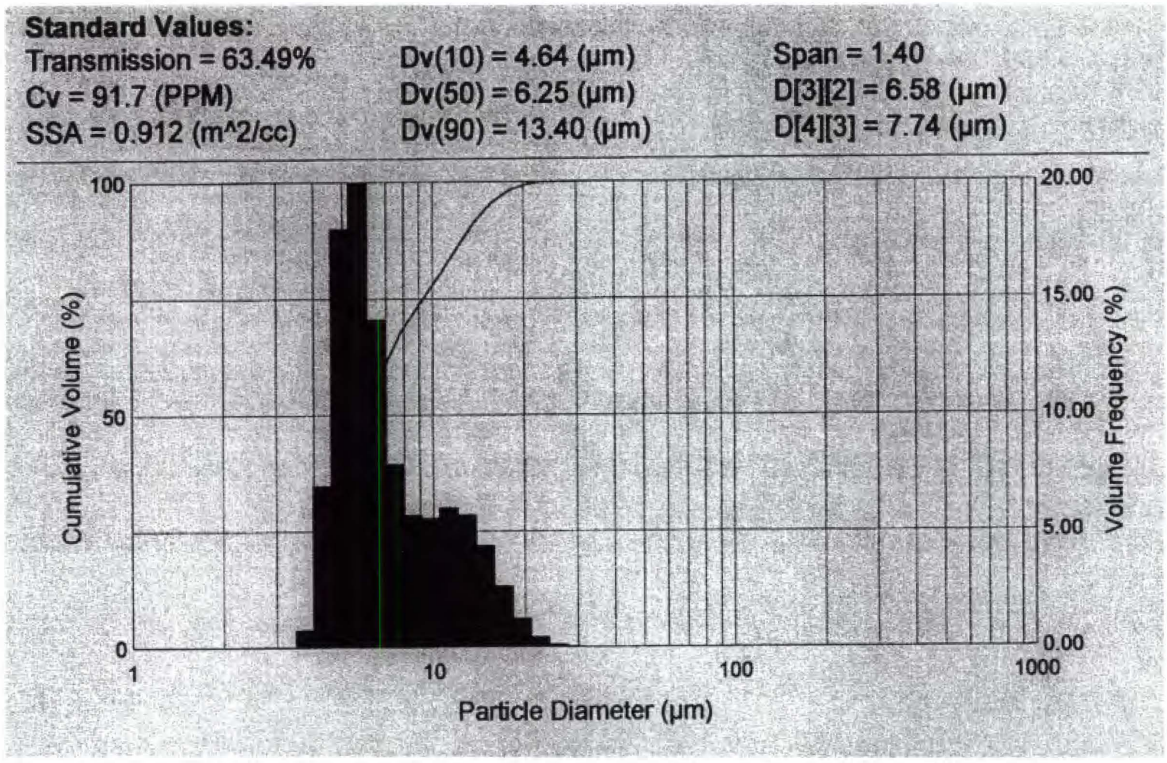



Figure A.1a: Droplet size distribution for Reynolds Number of 1350 and Droplet Concentration of 12.1 g / $m^3$ at V=0.0 kV

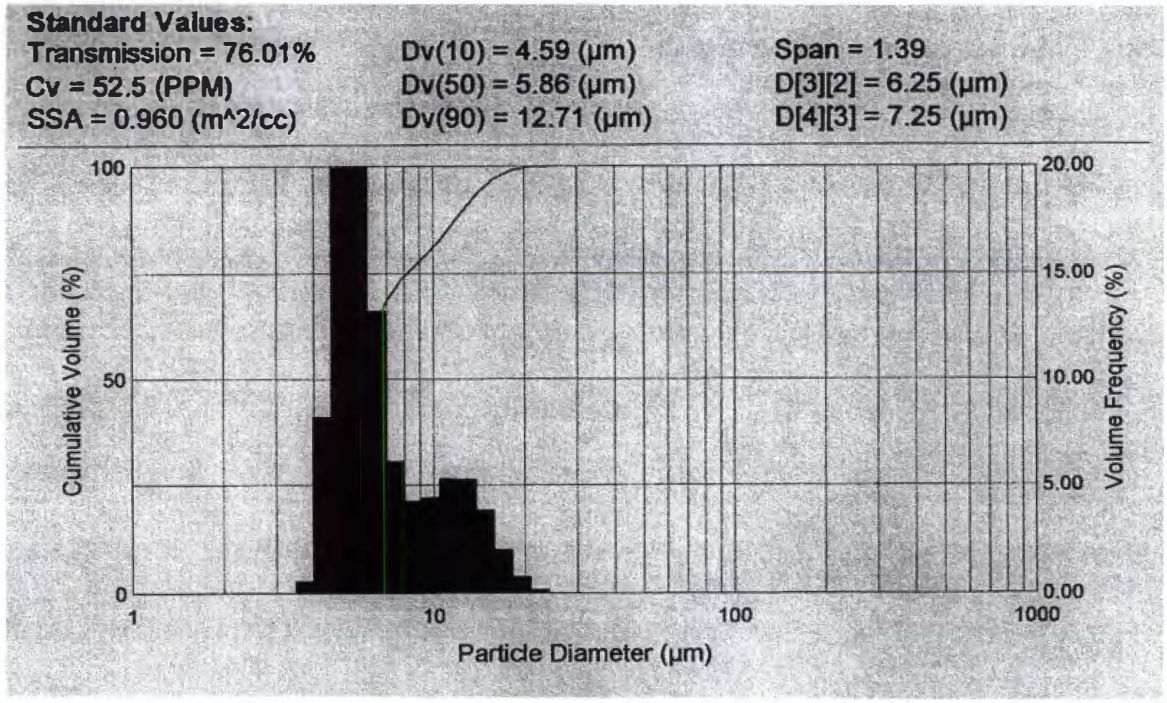



Figure A.1b: Droplet size distribution for experimental conditions of Figure A1a, with V=10.0 kV; Droplet Concentration at exit = 9.2 g / $m^3$

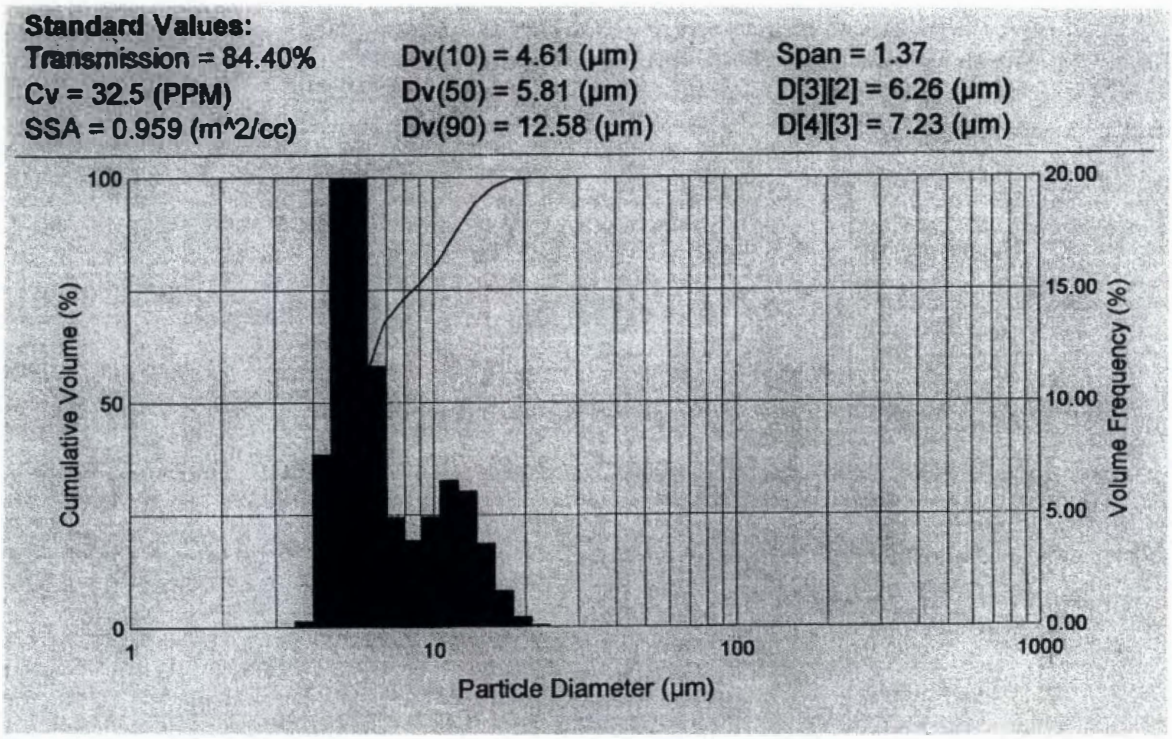



Figure A.1c: Droplet size distribution for experimental conditions of Figure A1a, with V=15.0 kV; Droplet Concentration at exit = 8.0 g / $m^3$

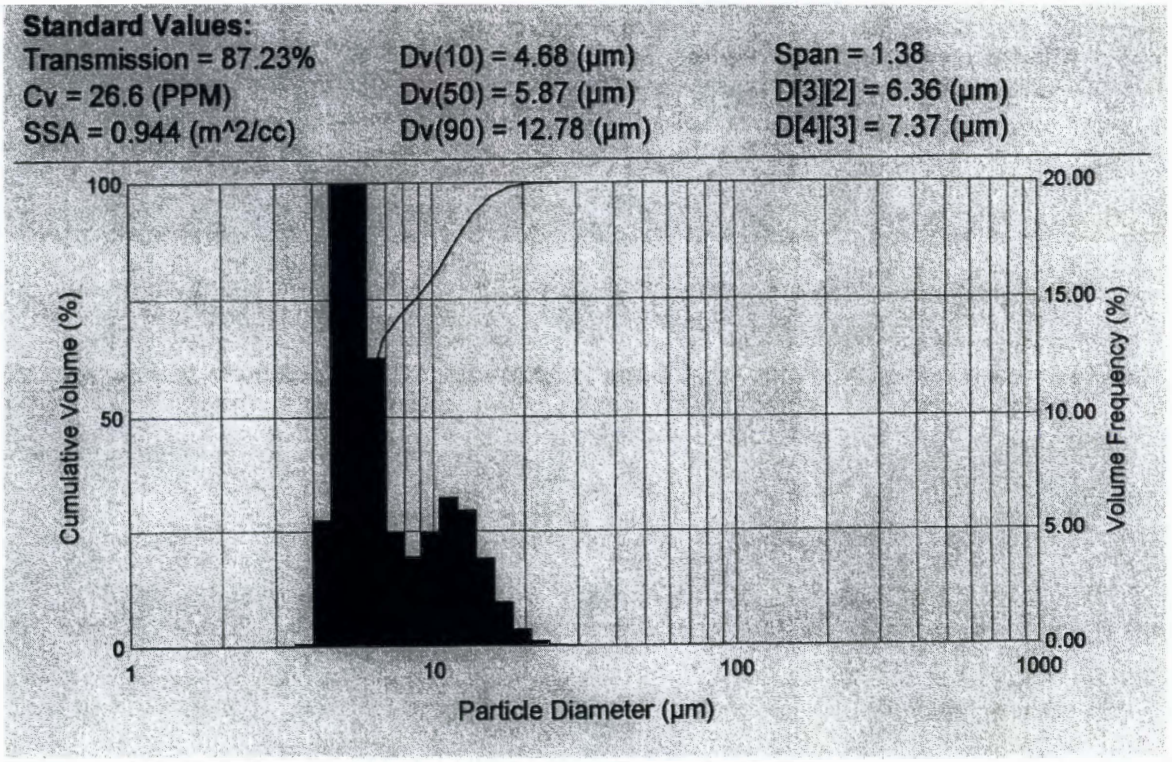



Figure A.1d: Droplet size distribution for experimental conditions of Figure A1a, with V = 18.0 kV; Droplet Concentration at exit = 6.60 g / $m^3$

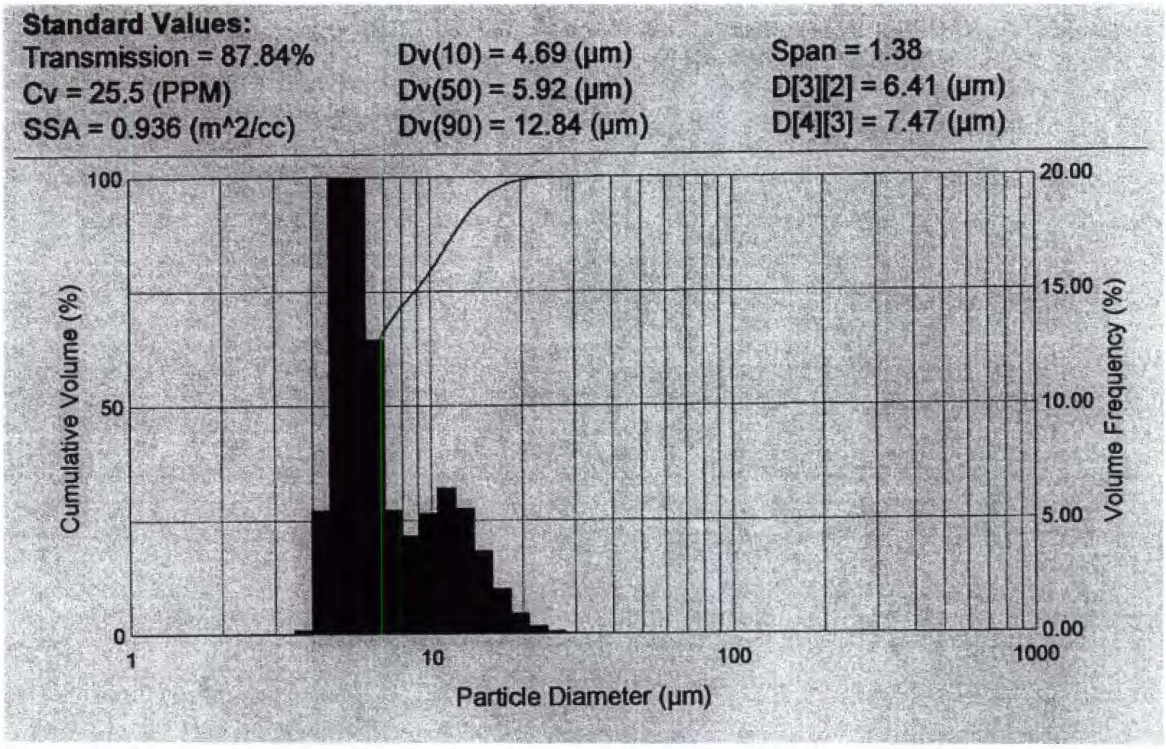



Figure A.1e: Droplet size distribution for experimental conditions of Figure A1a, with V = 20.0 kV; Droplet Concentration at exit = 6.16 g / $m^3$

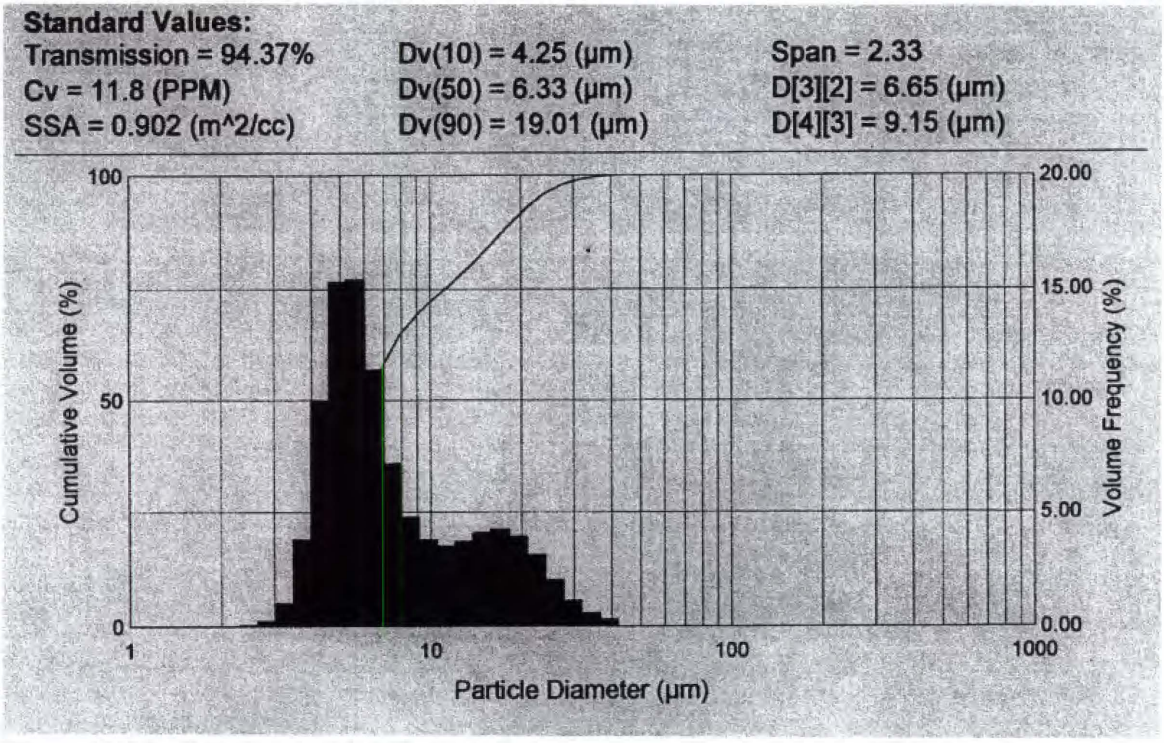



Figure A.1f: Droplet size distribution for experimental conditions of Figure A1a, with V = 26.0 kV; Droplet Concentration at exit = 5.0 g / $m^3$

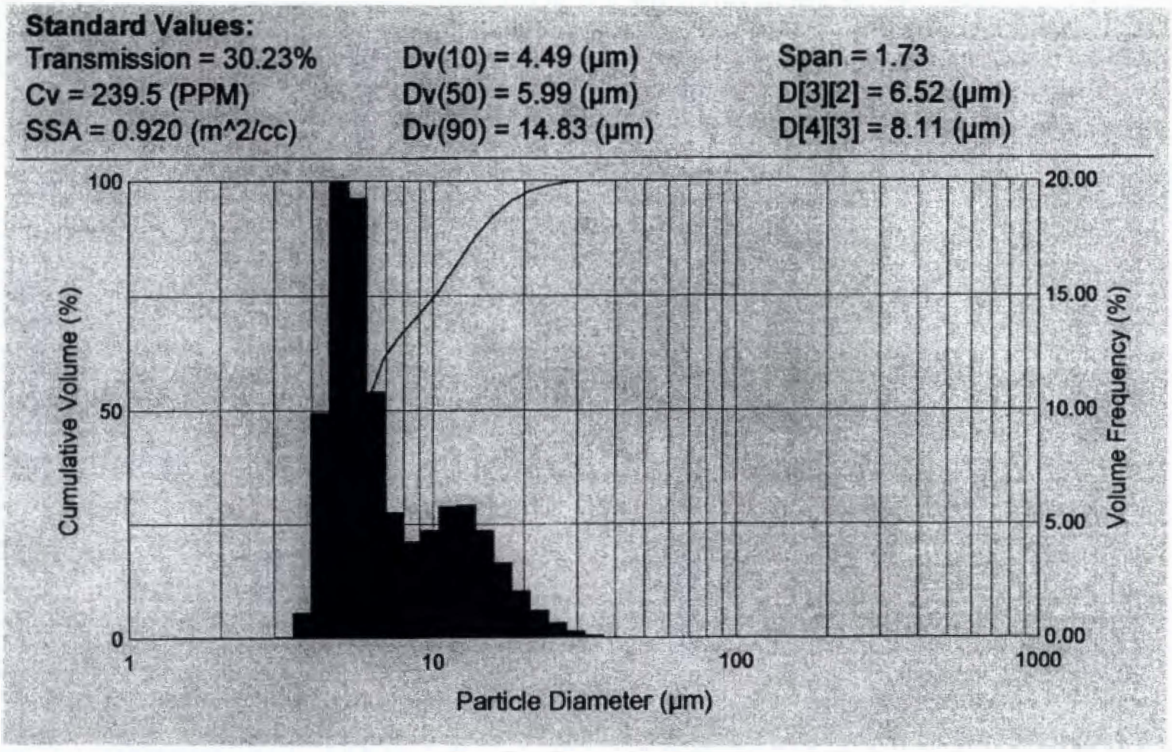



Figure A.2a: Droplet size distribution for Reynolds Number of 1350 and Droplet Concentration of 24.2 g / $m^3$ at V=0.0 kV

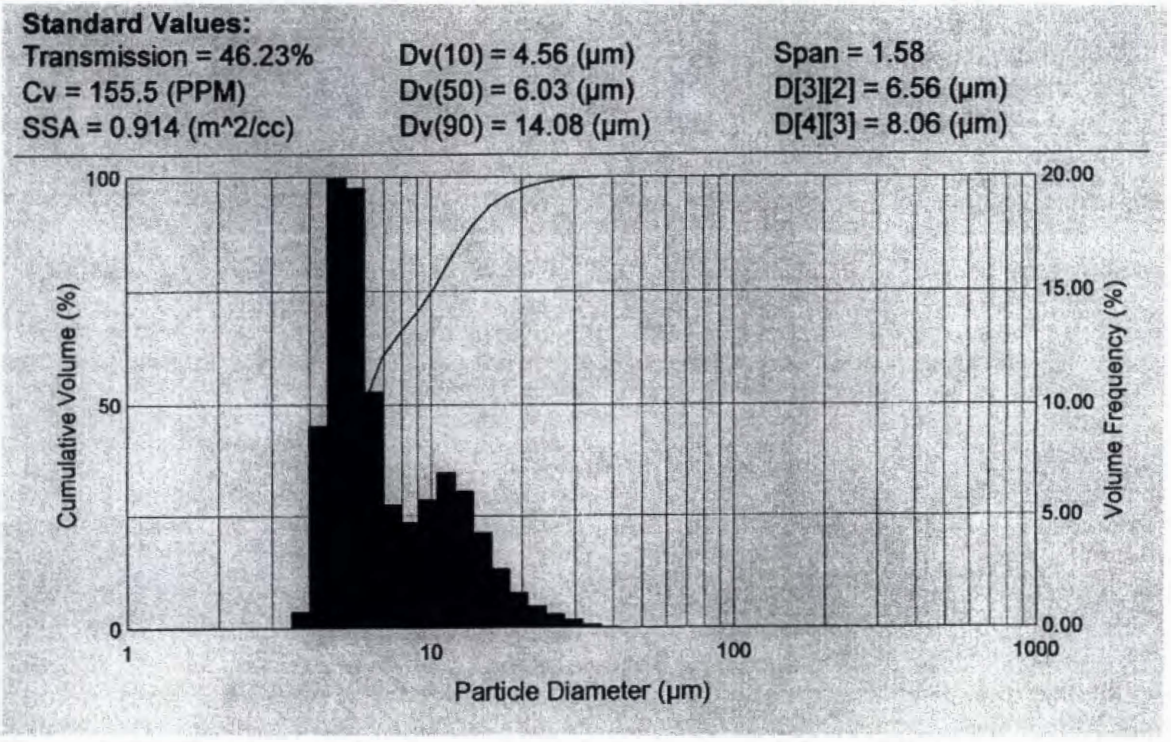



Figure A.2b: Droplet size distribution for experimental conditions of Figure A2a, with V=10.0 kV; Droplet Concentration at exit = 18.97 g / $m^3$

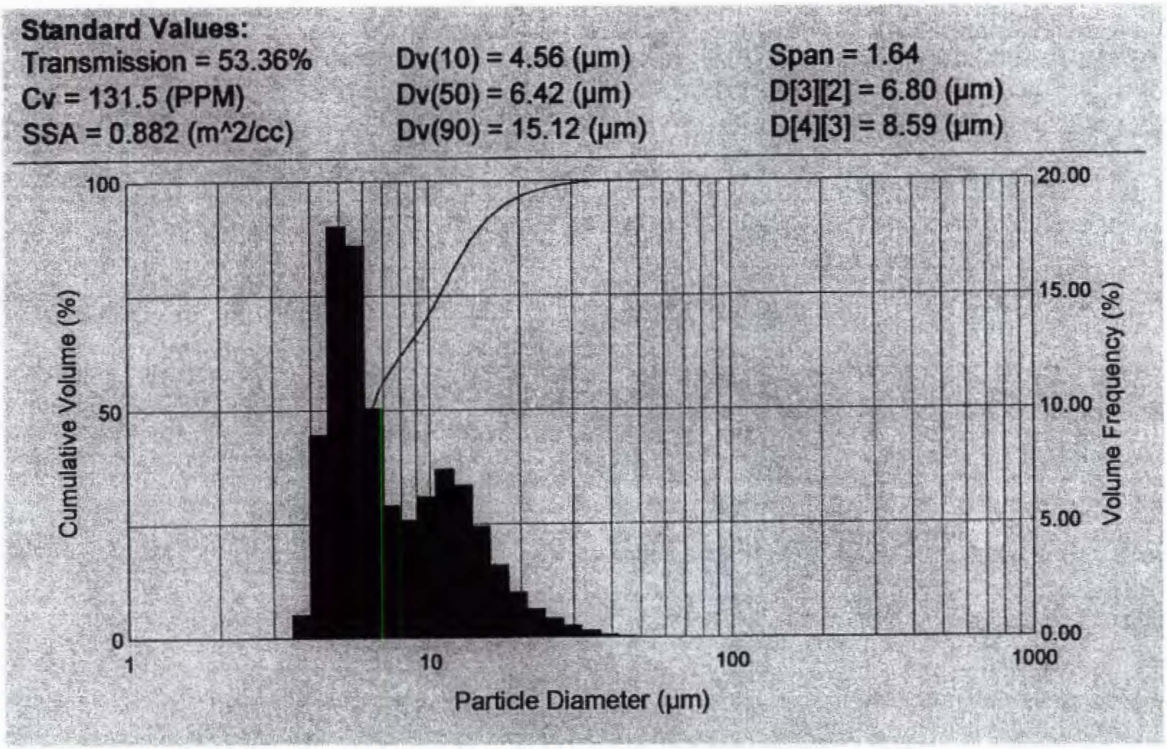



Figure A.2c: Droplet size distribution for experimental conditions of Figure A2a, with V = 15.0 kV; Droplet Concentration at exit = 15.8 g / $m^3$

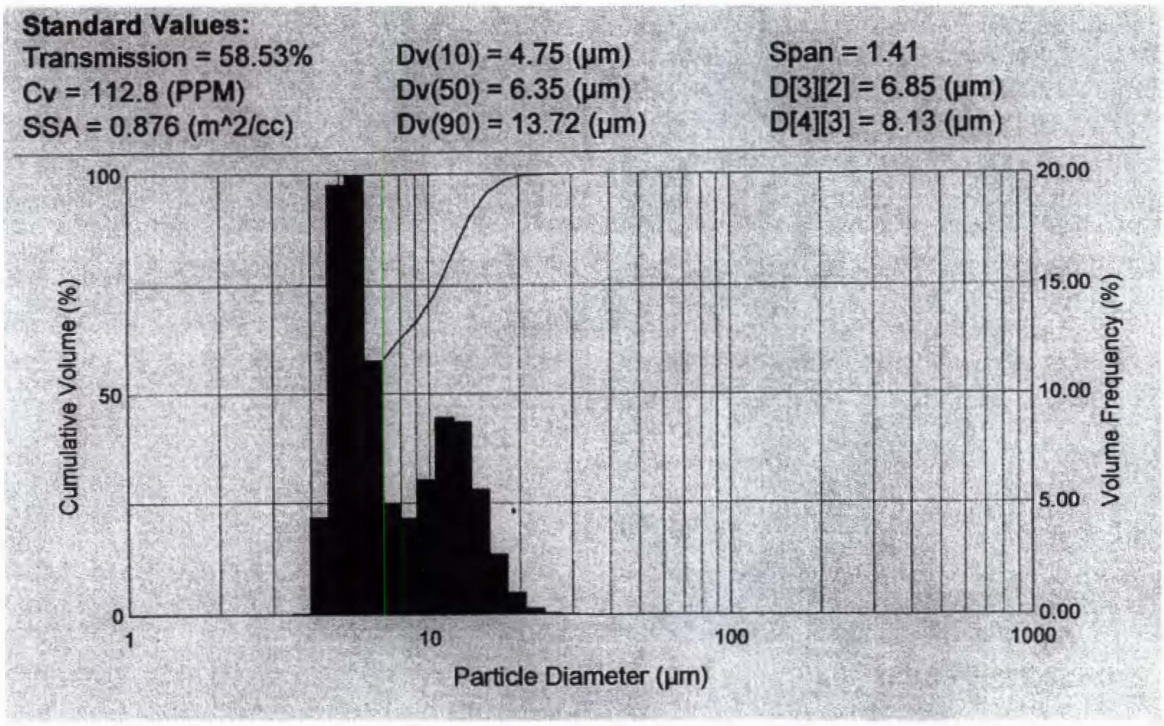



Figure A.2d: Droplet size distribution for experimental conditions of Figure A2a, with V=18.0 kV; Droplet Concentration at exit = 13.7 g / $m^3$

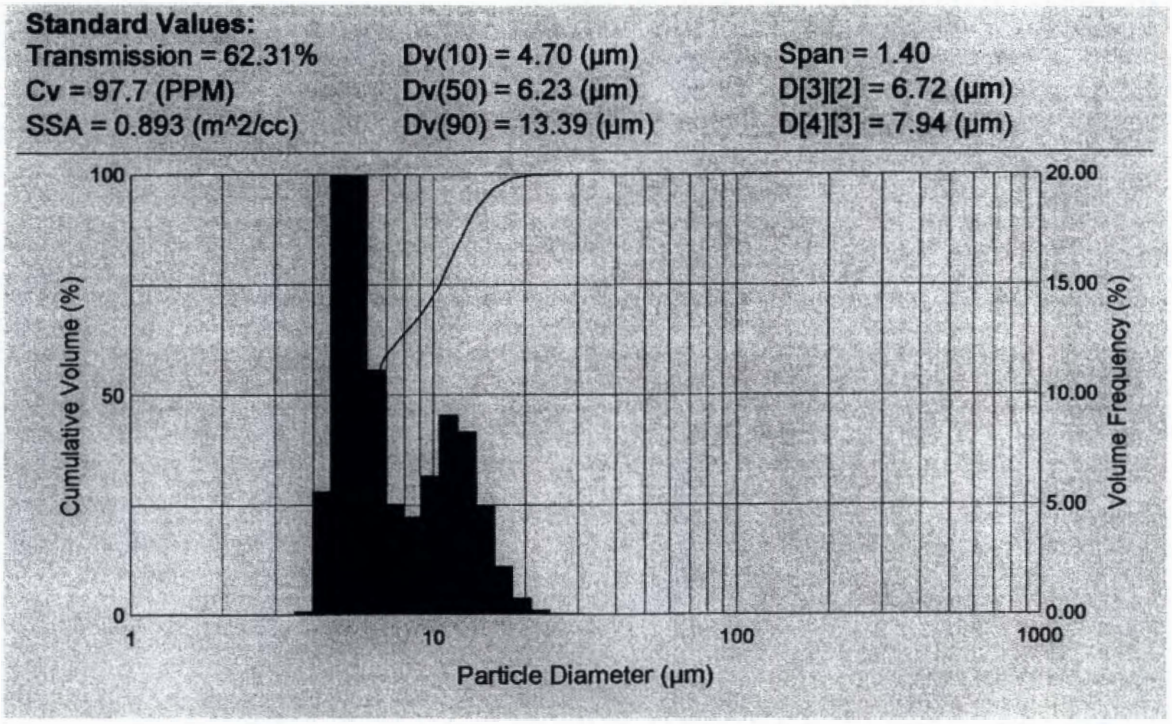



Figure A.2e: Droplet size distribution for experimental conditions of Figure A2a, with V= 20.0 kV; Droplet Concentration at exit = 11.6 g / $m^3$

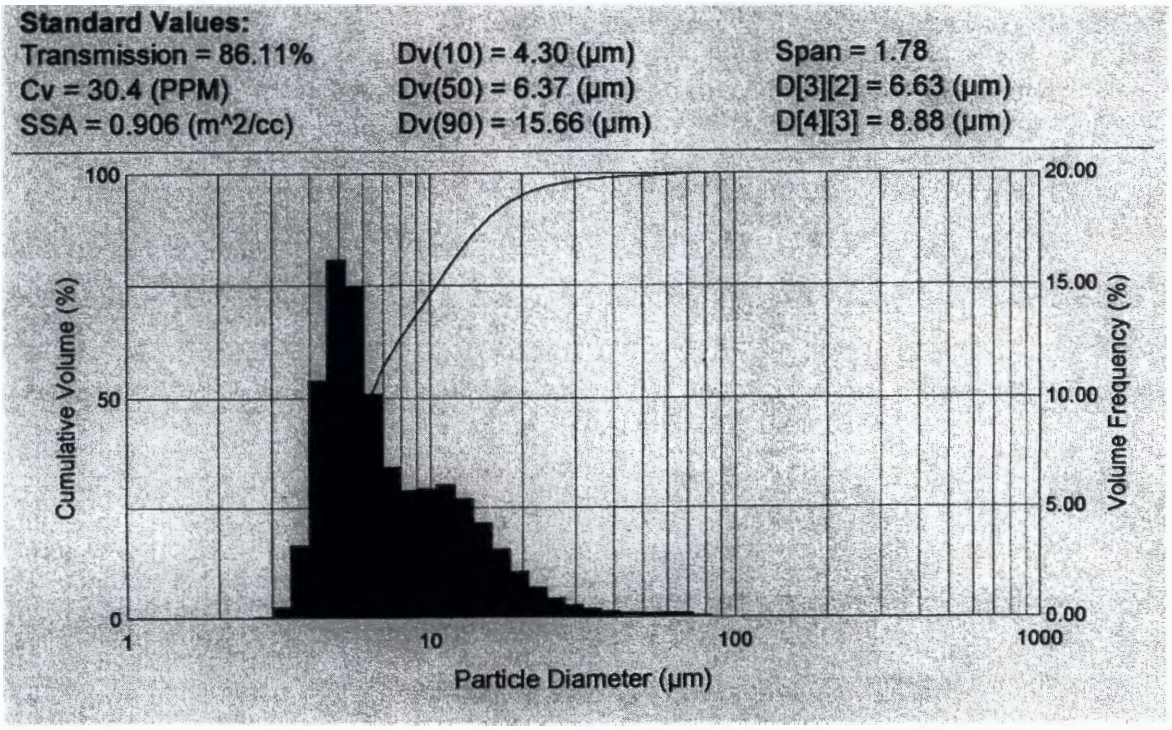



Figure A.2f: Droplet size distribution for experimental conditions of Figure A2a, with V=26.0 kV; Droplet Concentration at exit = 5.12 g / $m^3$

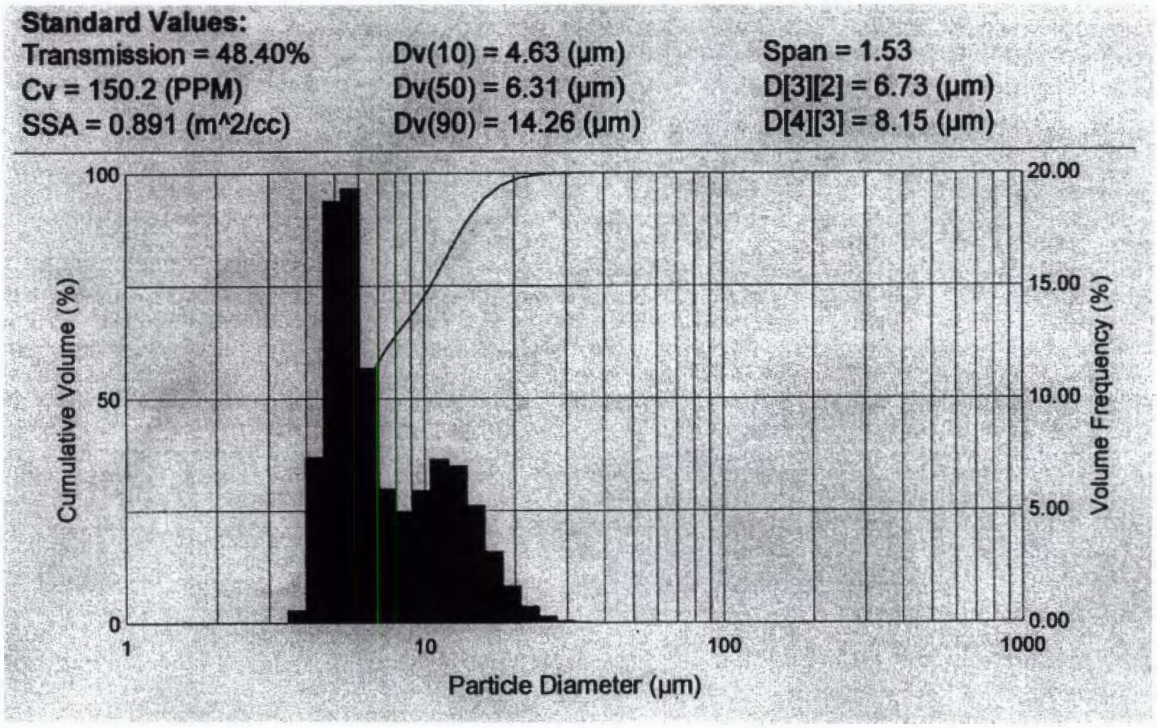



Figure A.3a: Droplet size distribution for Reynolds Number of 1350 and Droplet Concentration of 16.3 g/m$^3$ at V = 0.0 kV

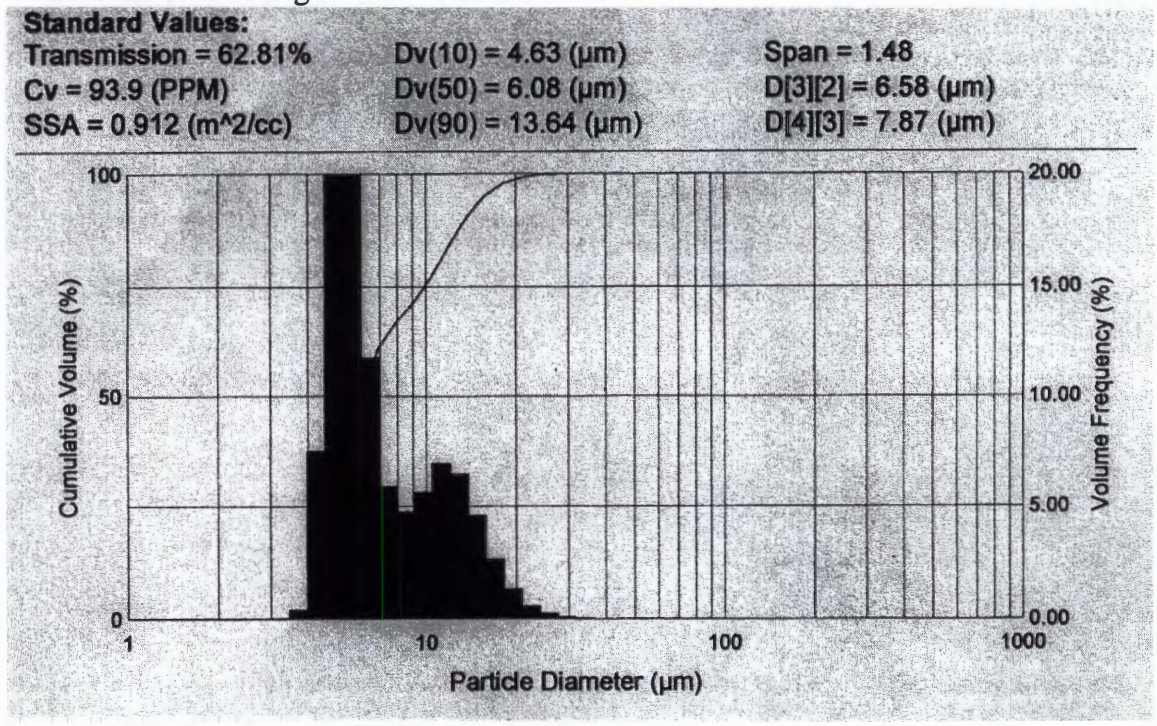



Figure A.3b: Droplet size distribution for experimental conditions of Figure A3a, with V=10.0 kV; Droplet Concentration at exit = 11.7 g / m$^3$

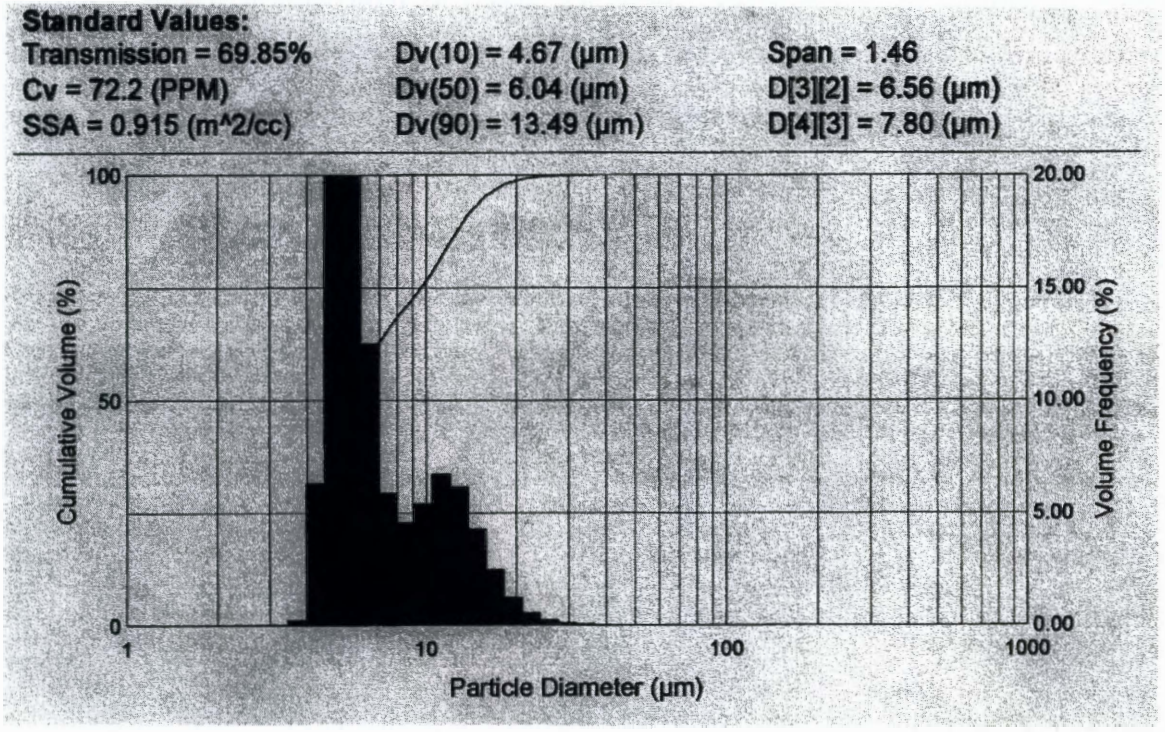



Figure A.3c: Droplet size distribution for experimental conditions of Figure A3a, with V=15.0 kV; Droplet Concentration at exit = 9.3 g / $m^3$

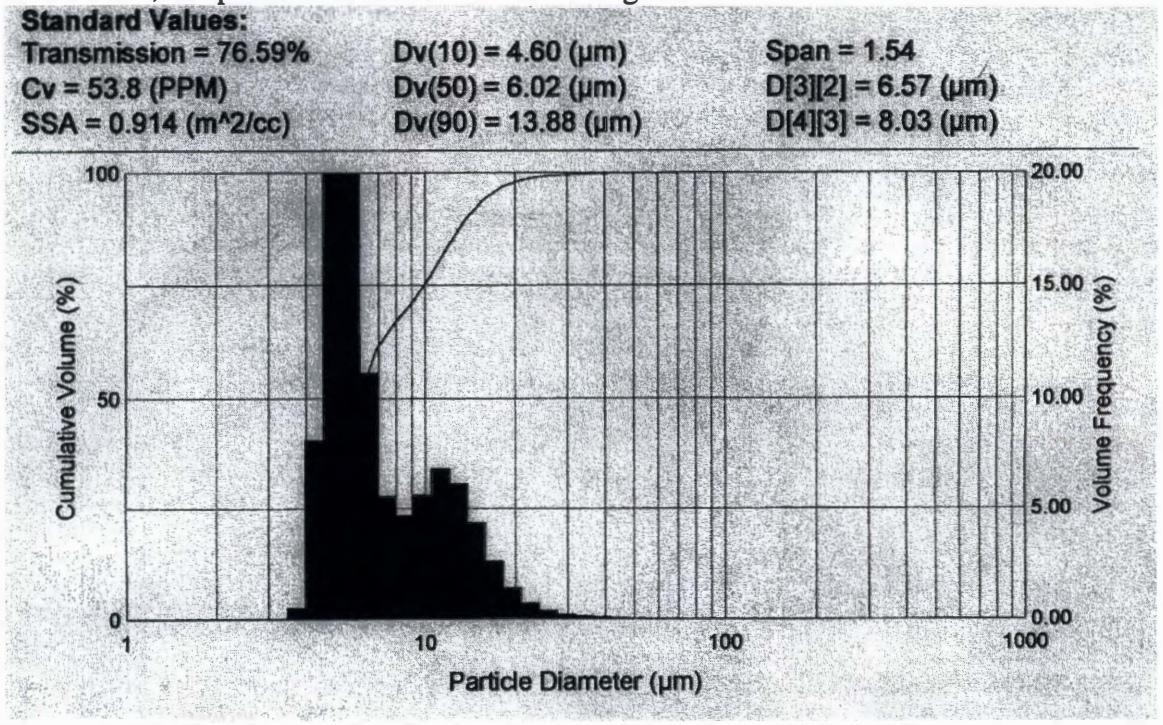



Figure A.3d: Droplet size distribution for experimental conditions of Figure A3a, with V=18.0 kV; Droplet Concentration at exit = 8.6 g / $m^3$

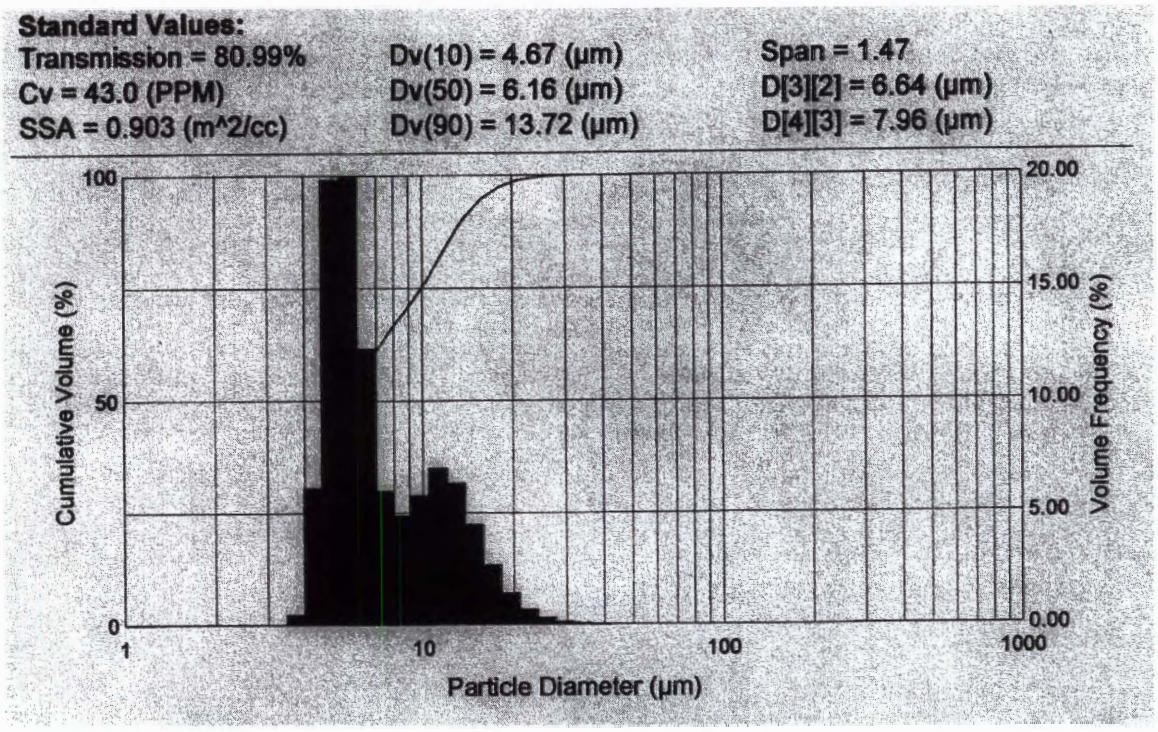



Figure A.3e: Droplet size distribution for experimental conditions of Figure A3a, with V=20.0 kV; Droplet Concentration at exit = 8.1 g / $m^3$

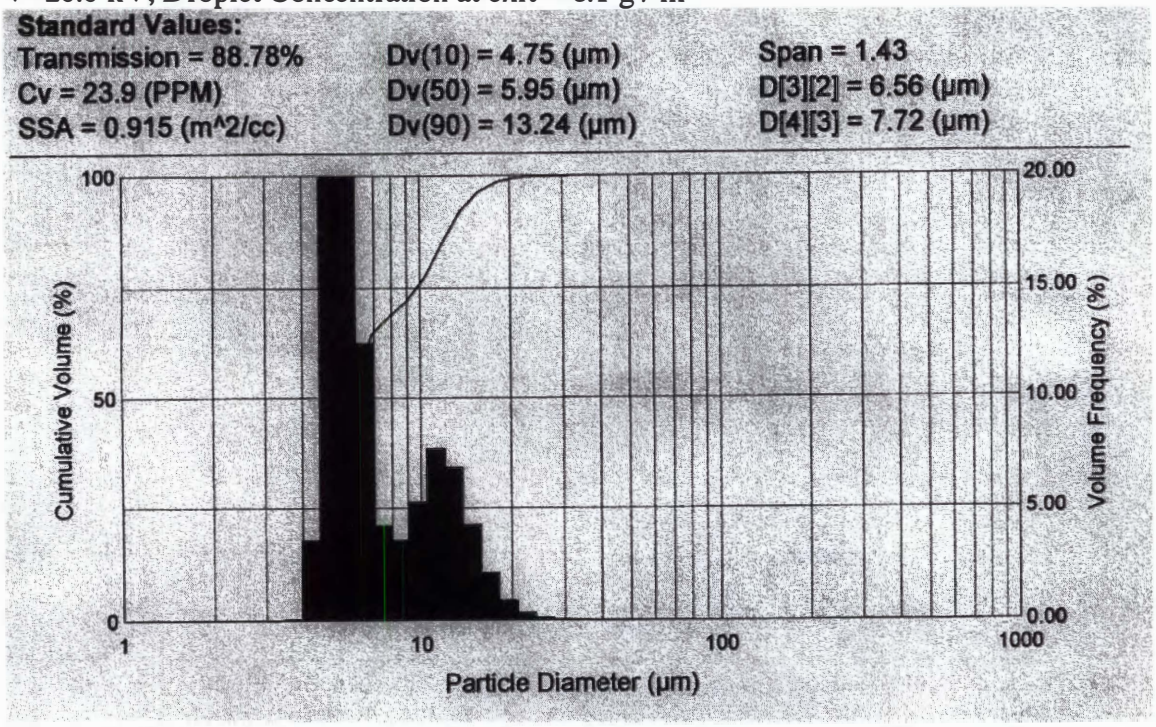



Figure A.3f: Droplet size distribution for experimental conditions of Figure A3a, with V=26.0 kV; Droplet Concentration at exit = 5.4 g / $m^3$

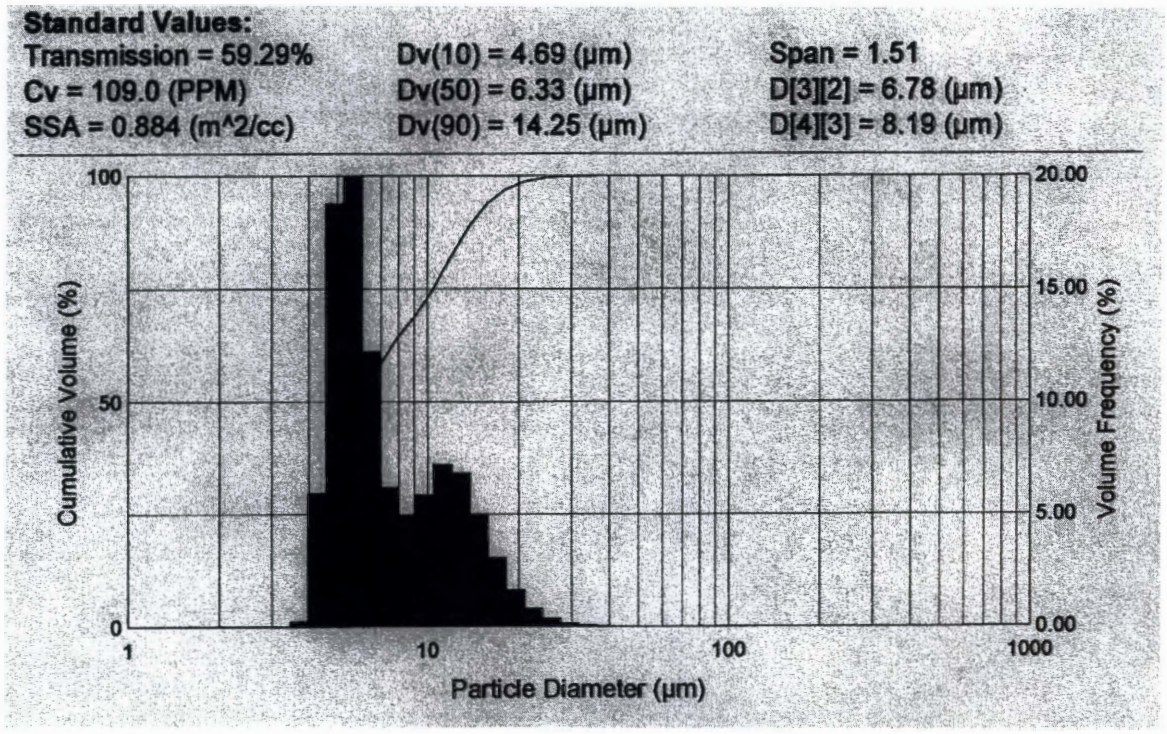



Figure A.4a: Droplet size distribution for Reynolds Number of 1350 and Droplet Concentration of 8.3 $g/m^3$ at V = 0.0 kV

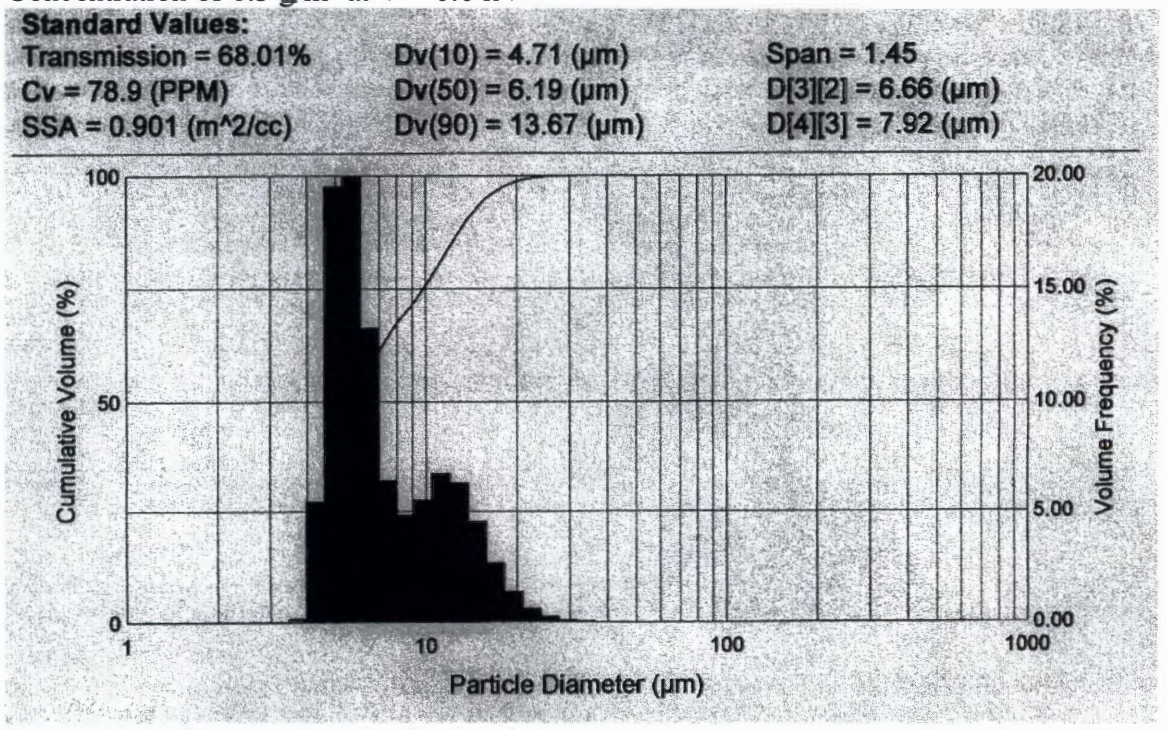



Figure A.4b: Droplet size distribution for experimental conditions of Figure A4a, with V=10.0 kV; Droplet Concentration at exit = 7.3 g / $m^3$

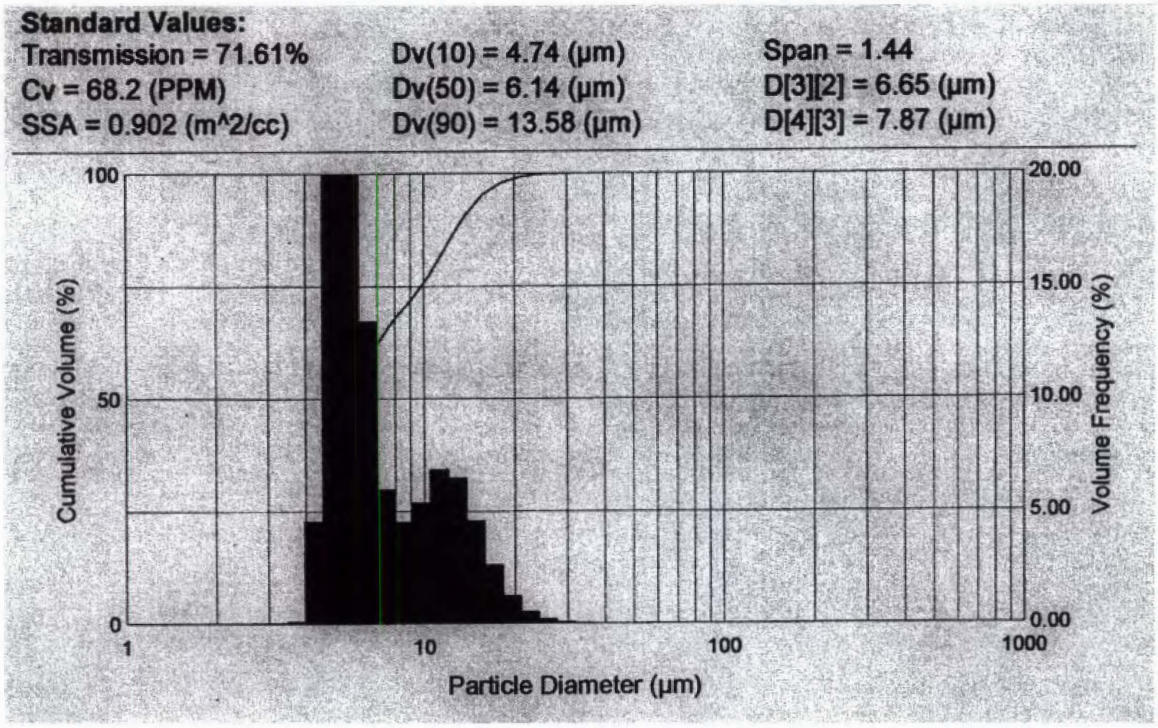



Figure A.4c: Droplet size distribution for experimental conditions of Figure A4a, with V=15.0 kV; Droplet Concentration at exit = 6.0 g / $m^3$

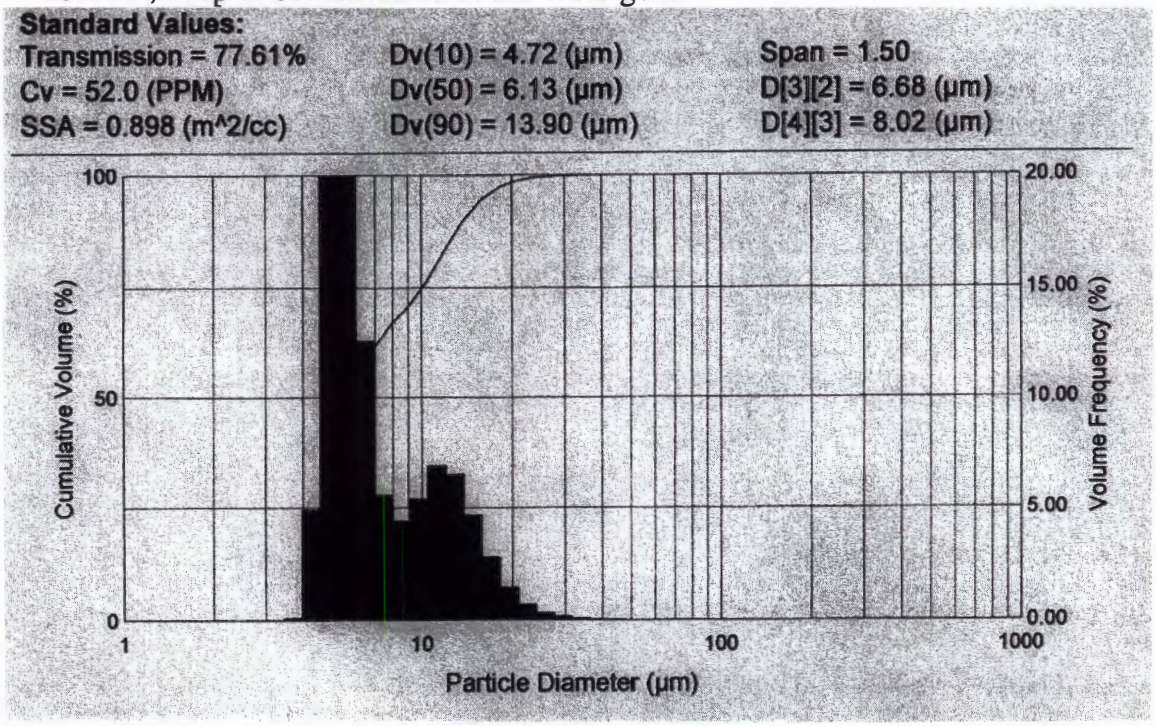



Figure A.4d: Droplet size distribution for experimental conditions of Figure A4a, with V=18.0 kV; Droplet Concentration at exit = 5.4 g / $m^3$

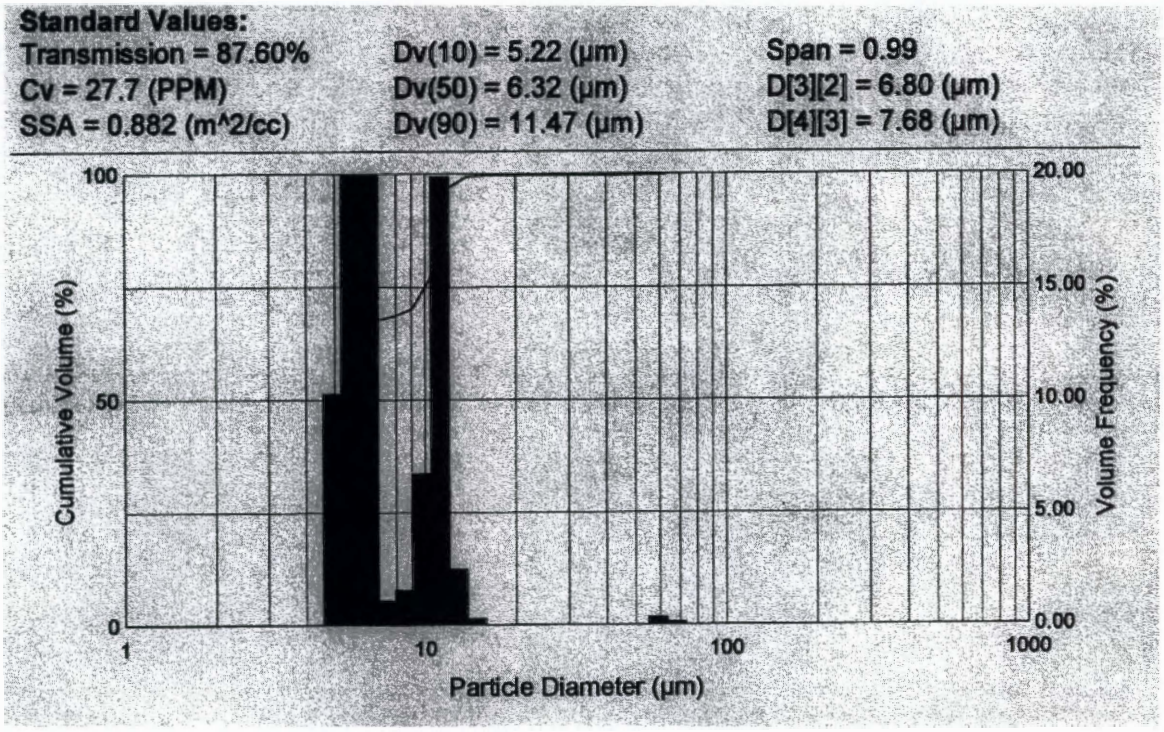



Figure A.4e: Droplet size distribution for experimental conditions of Figure A4a, with V=20.0 kV; Droplet Concentration at exit = 4.6 g / $m^3$

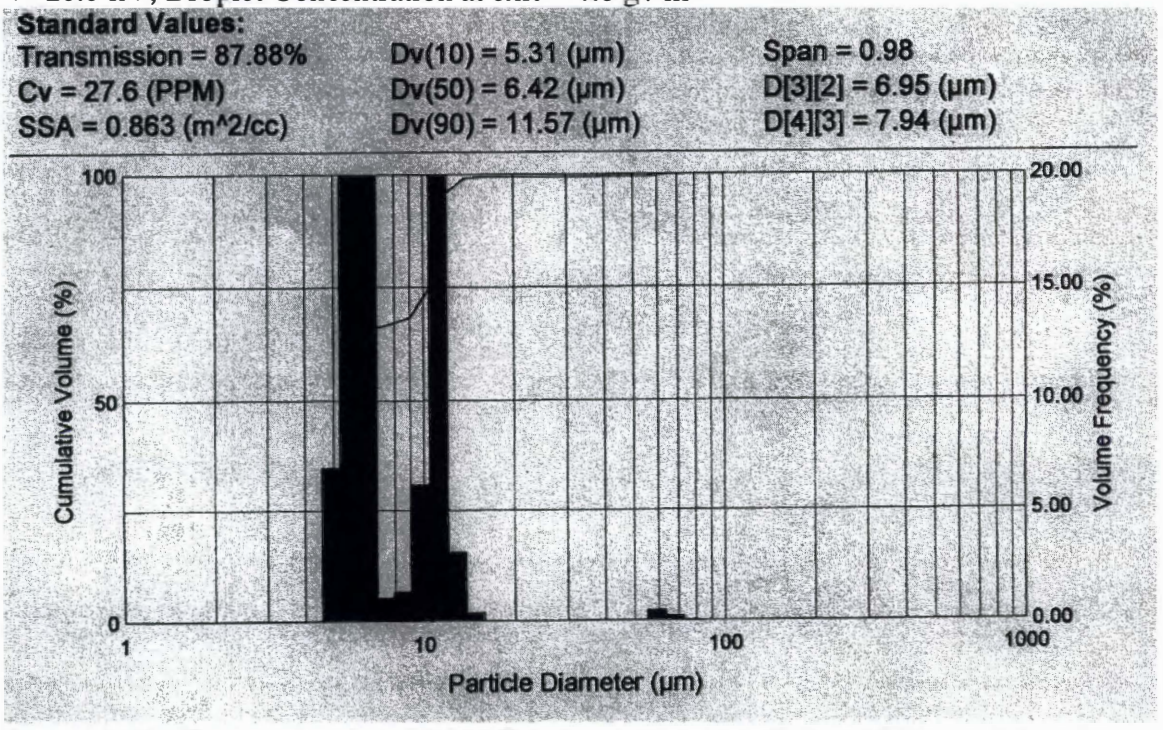



Figure A.4f: Droplet size distribution for experimental conditions of Figure A4a, with V=26.0 kV; Droplet Concentration at exit = 3.0 g / $m^3$

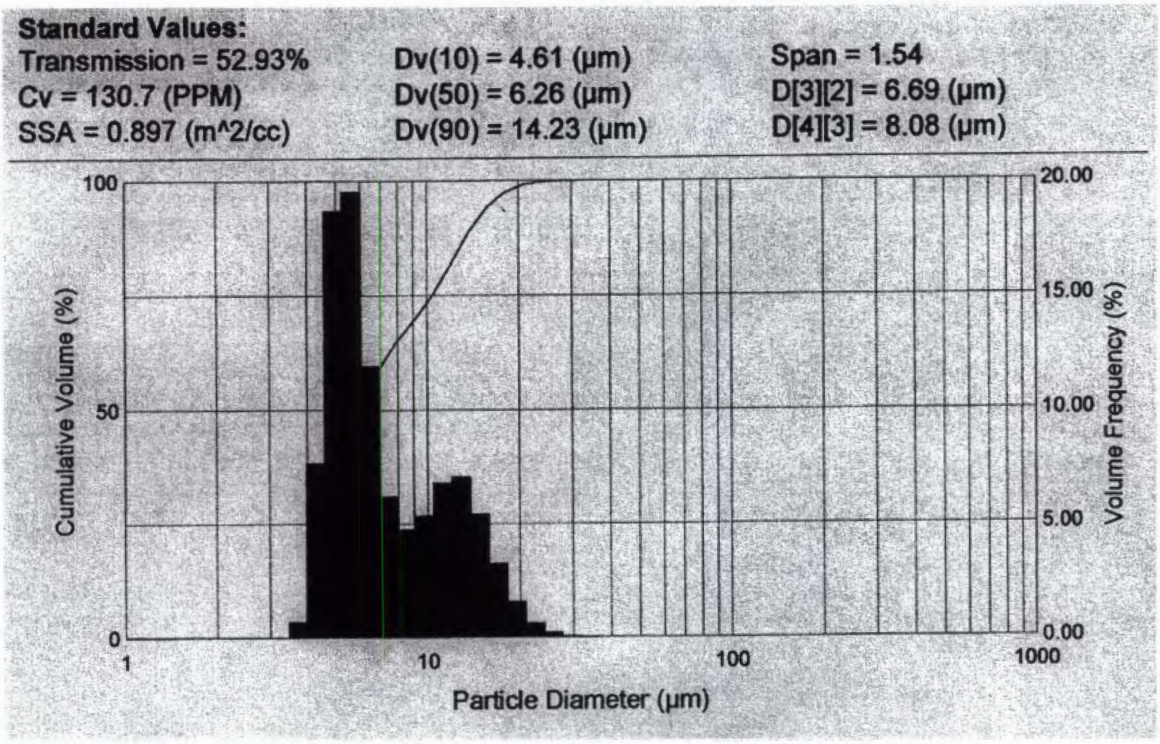



Figure A.5a: Droplet size distribution for Reynolds Number of 1950 and Droplet Concentration of 13.3 g/m$^3$ at V = 0.0 kV

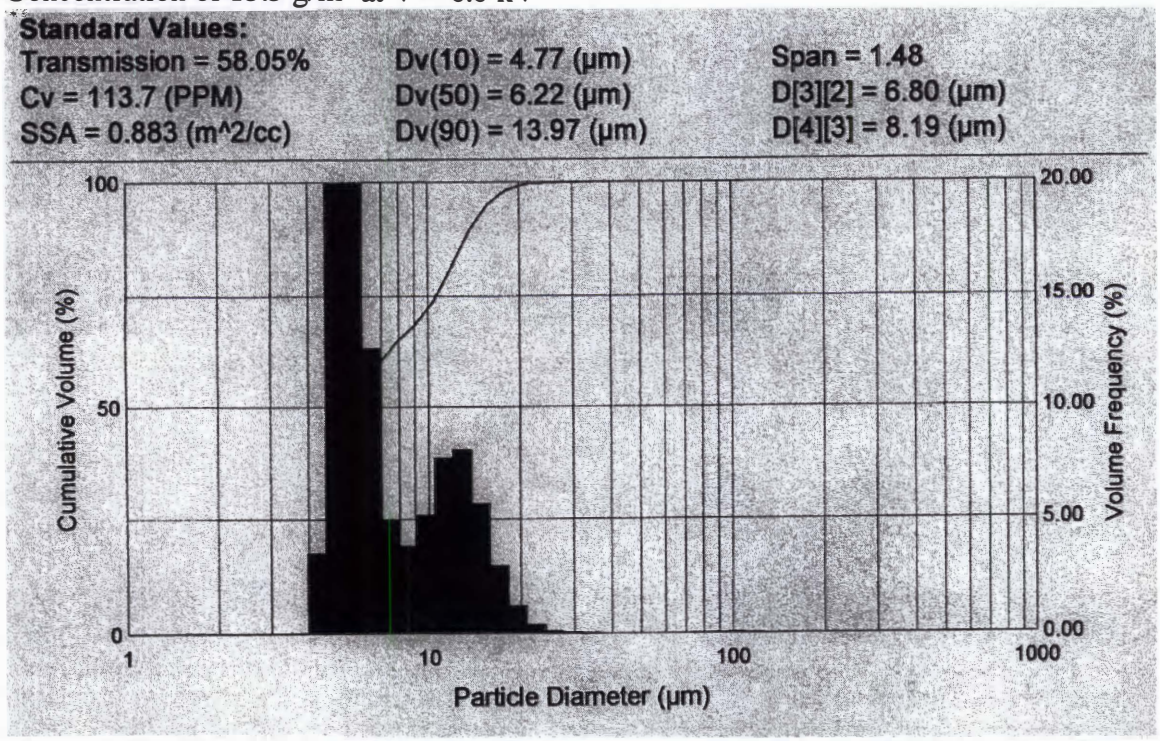



Figure A.5b: Droplet size distribution for experimental conditions of Figure A5a, with V=10.0 kV; Droplet Concentration at exit = 9.7 g / m$^3$

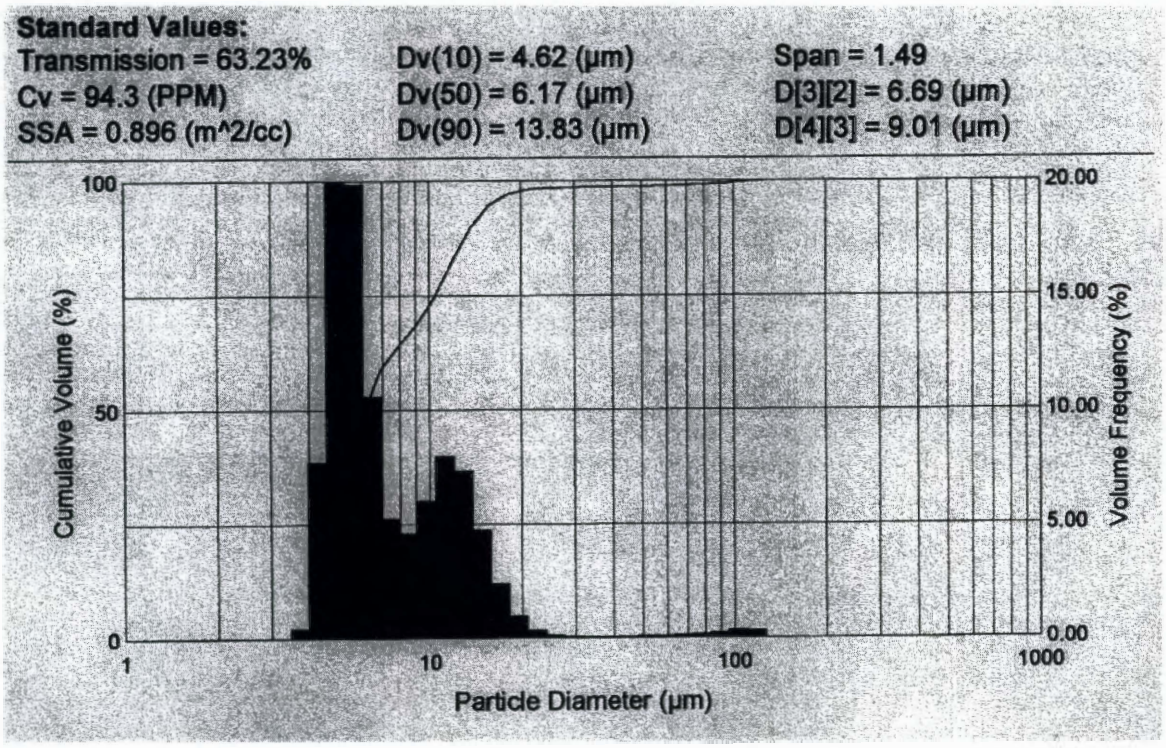



Figure A.5c: Droplet size distribution for experimental conditions of Figure A5a, with V=15.0 kV; Droplet Concentration at exit = 9.0 g / $m^3$

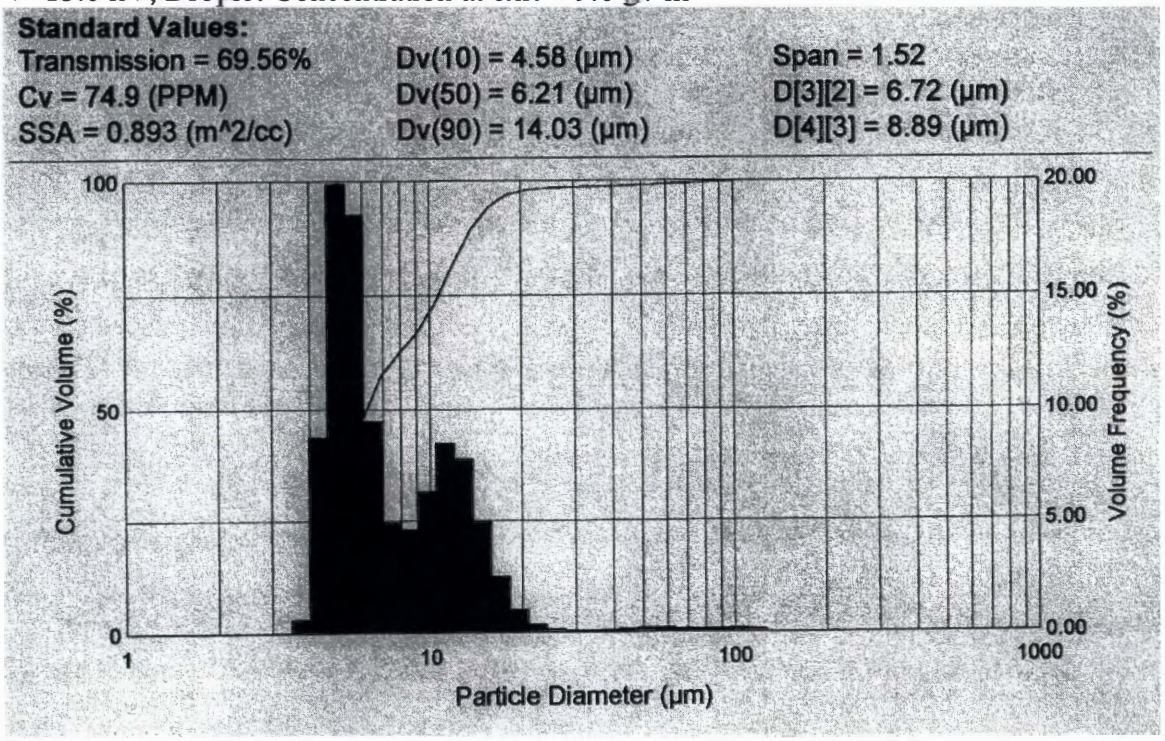



Figure A.5d: Droplet size distribution for experimental conditions of Figure A5a, with V=18.0 kV; Droplet Concentration at exit = 8.0 g / $m^3$

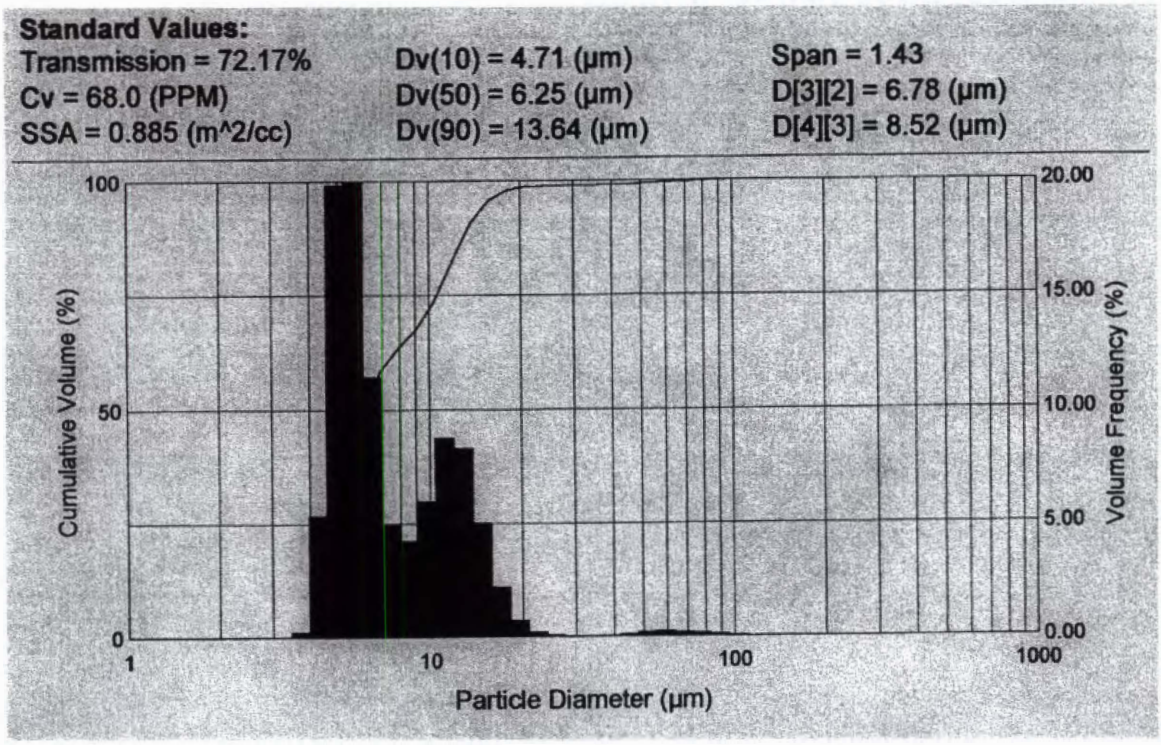



Figure A.5e: Droplet size distribution for experimental conditions of Figure A5a, with V=20.0 kV; Droplet Concentration at exit = 7.5 g / $m^3$

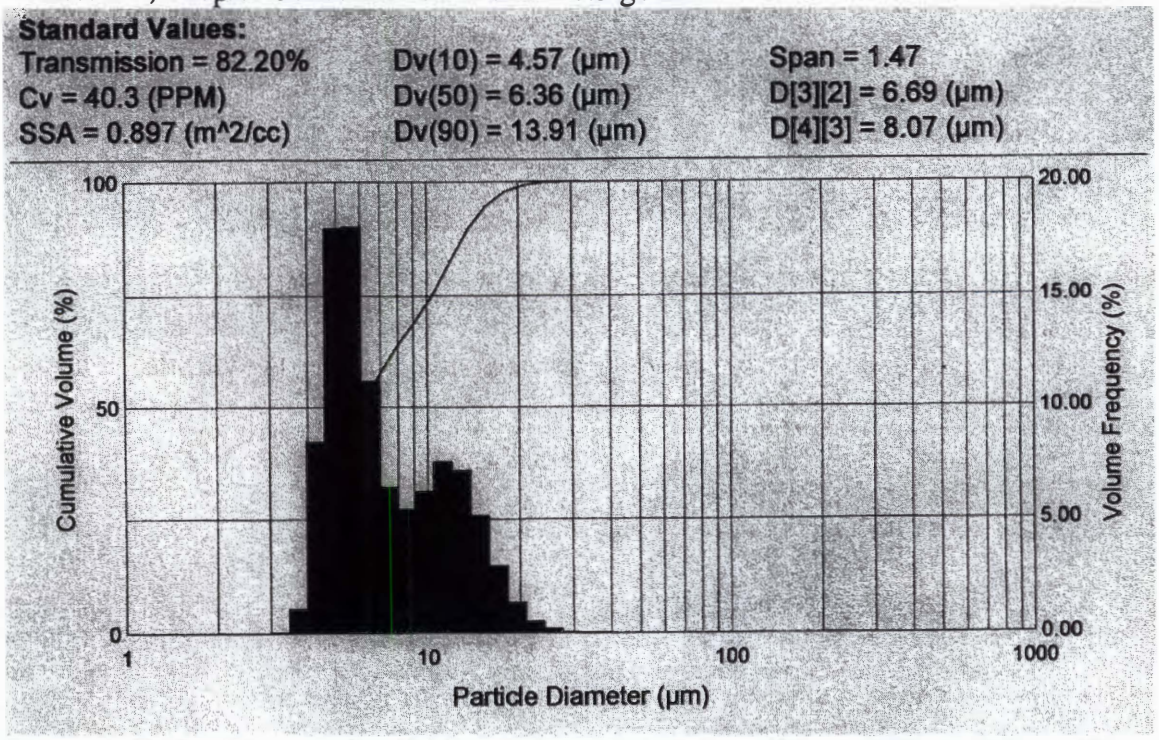



Figure A.5f: Droplet size distribution for experimental conditions of Figure A5a, with V=26.0 kV; Droplet Concentration at exit = 3.3 g / $m^3$

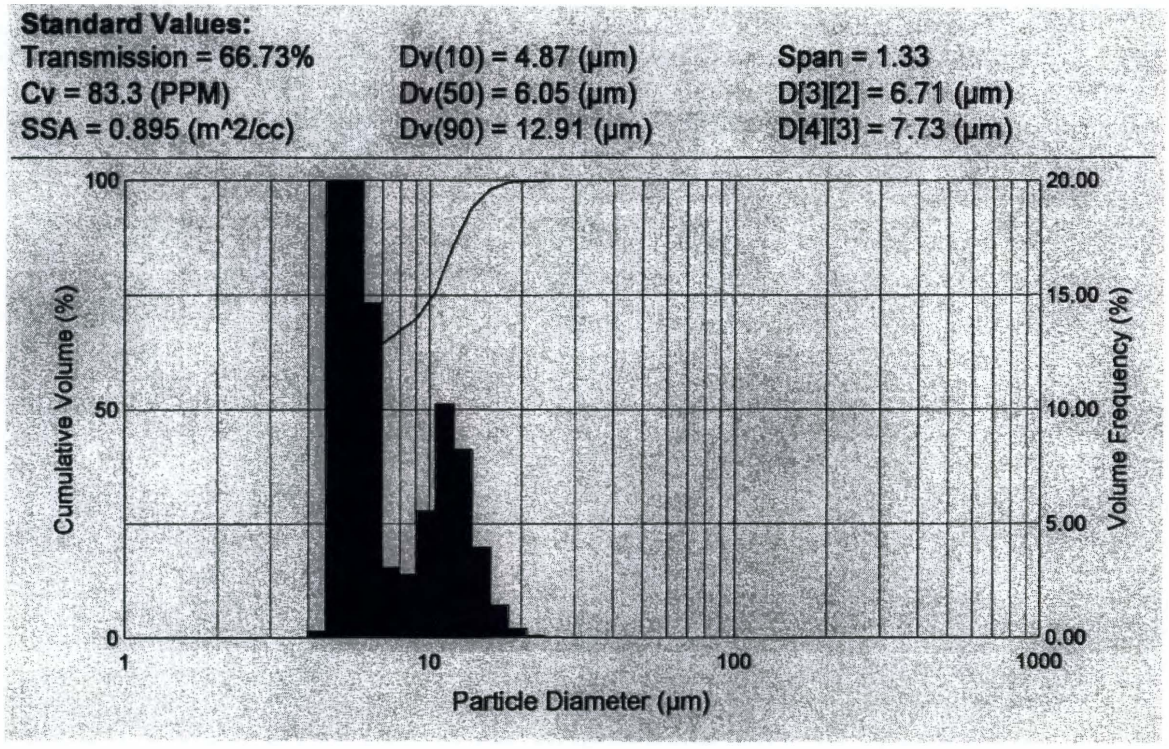



Figure A.6a: Droplet size distribution for Reynolds Number of 1950 and Droplet Concentration of 10.1 g/m$^3$ at V = 0.0 kV

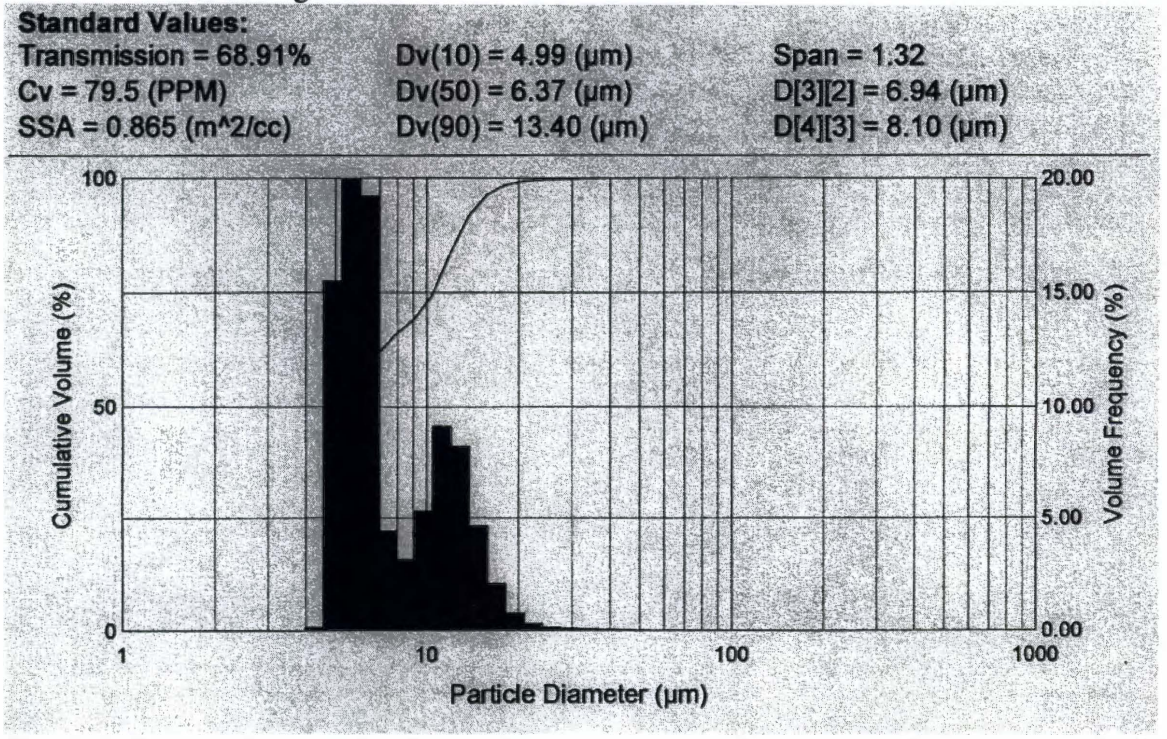



Figure A.6b: Droplet size distribution for experimental conditions of Figure A6a, with V=10.0 kV; Droplet Concentration at exit = 8.8 g / m$^3$

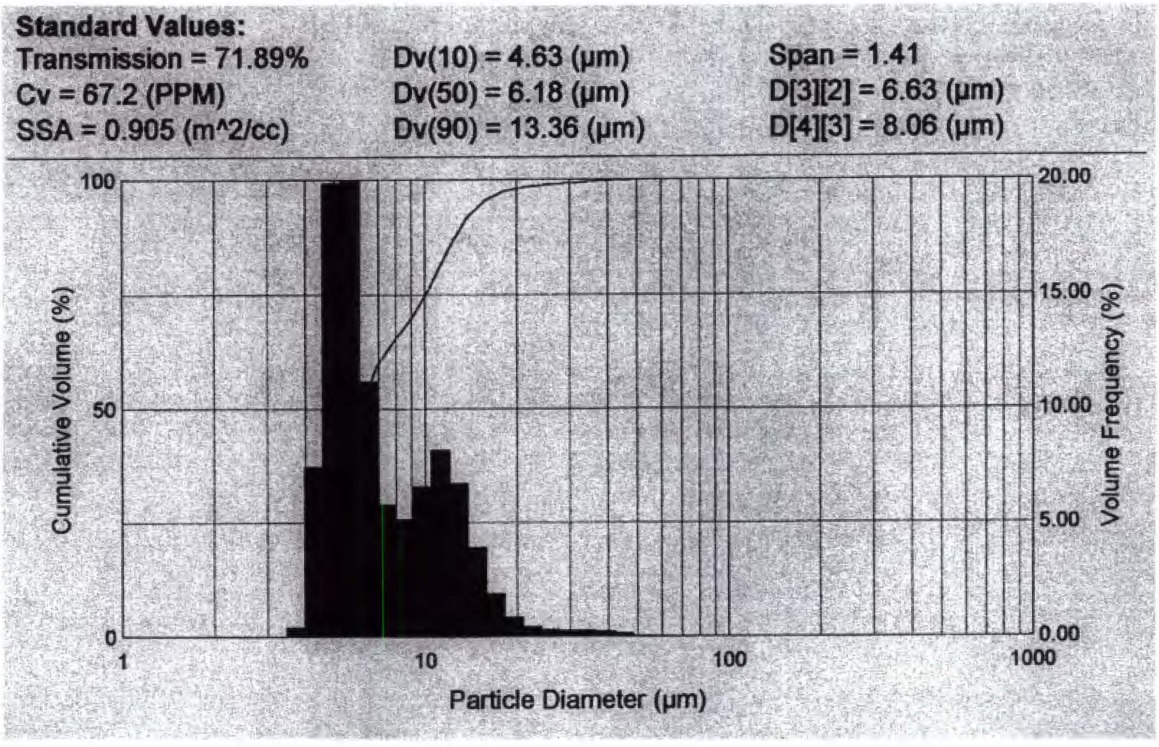



Figure A.6c: Droplet size distribution for experimental conditions of Figure A6a, with V=15.0 kV; Droplet Concentration at exit = 7.5 g / $m^3$

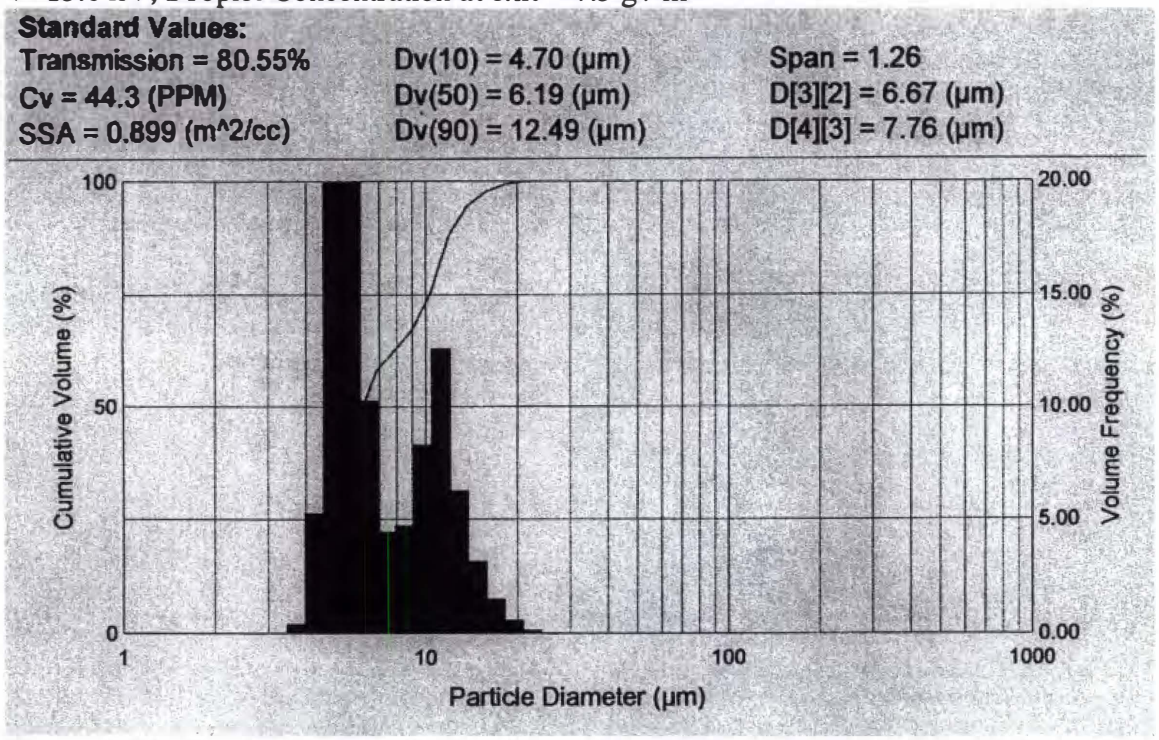



Figure A.6d: Droplet size distribution for experimental conditions of Figure A6a, with V=18.0 kV; Droplet Concentration at exit = 6.3 g / $m^3$

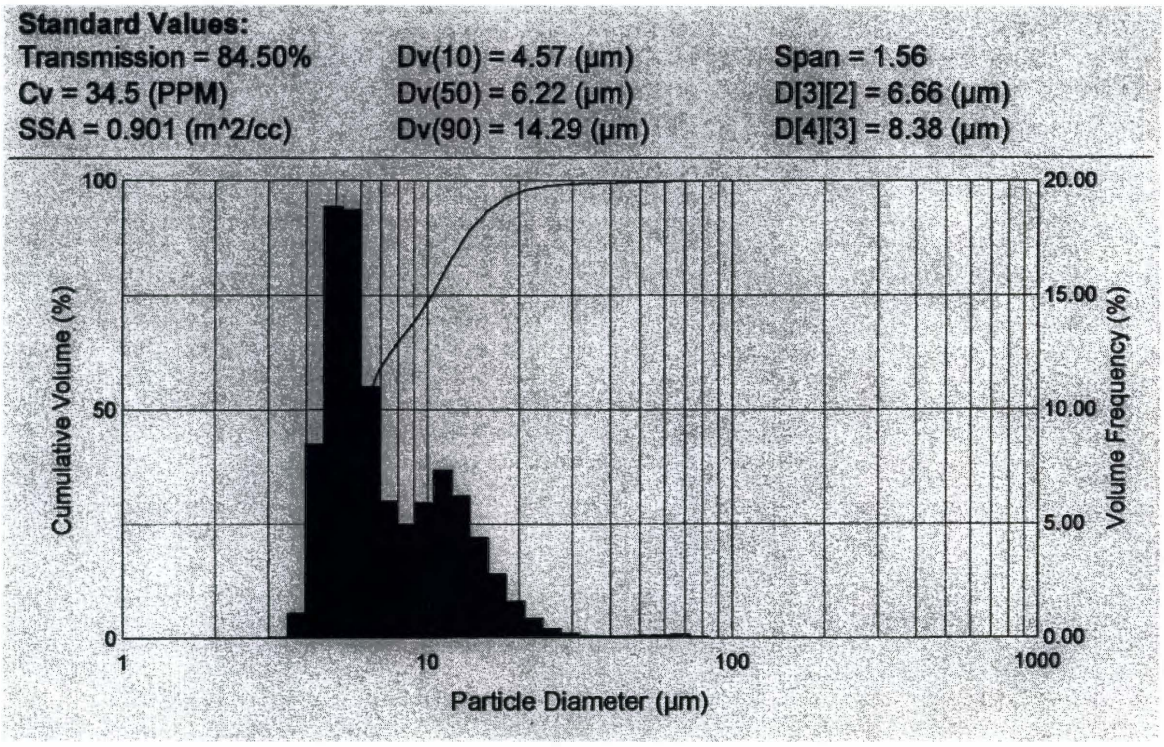



Figure A.6e: Droplet size distribution for experimental conditions of Figure A6a, with V=20.0 kV; Droplet Concentration at exit = 5.2 g / $m^3$

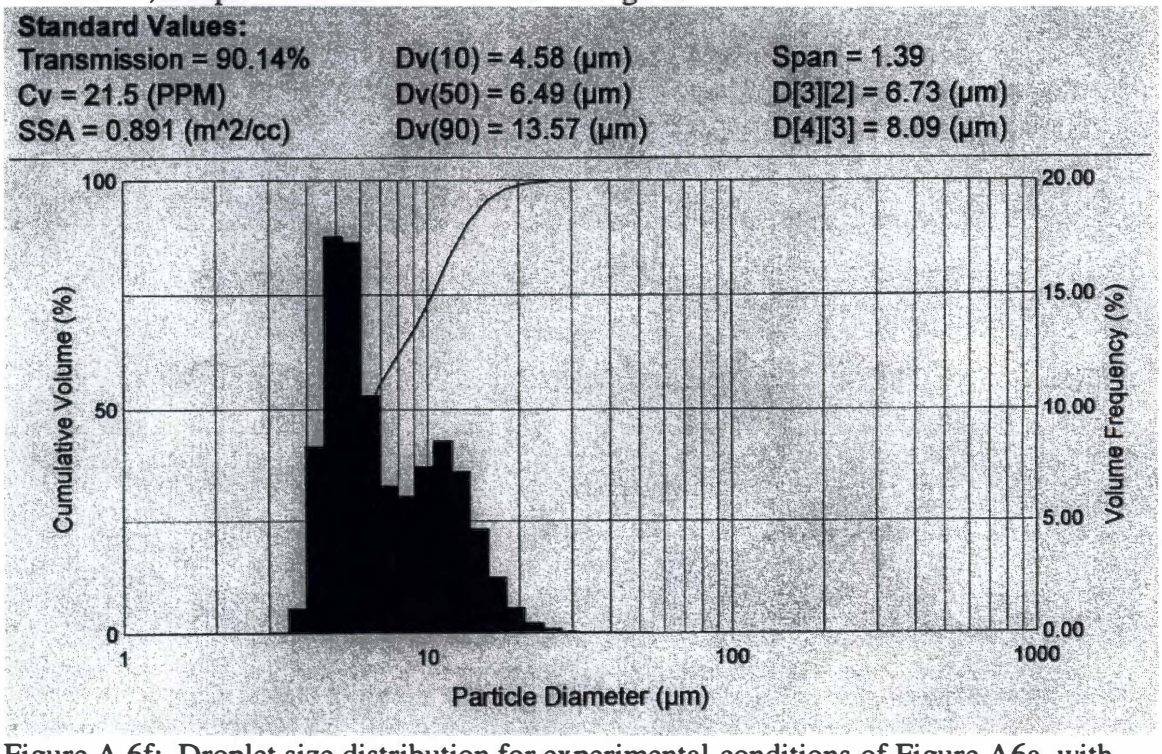



Figure A.6f: Droplet size distribution for experimental conditions of Figure A6a, with V=26.0 kV; Droplet Concentration at exit = 3.3 g / $m^3$

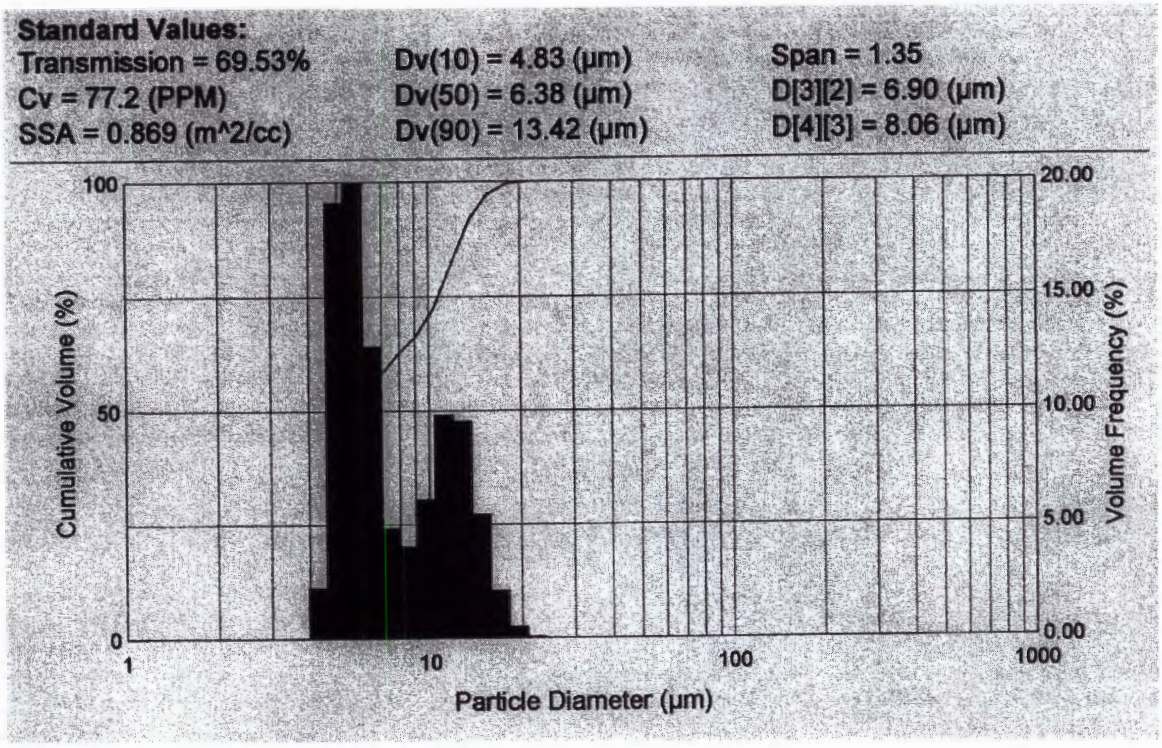



Figure A.7a: Droplet size distribution for Reynolds Number of 1950 and Droplet Concentration of 8.1 g/m$^3$ at V = 0.0 kV

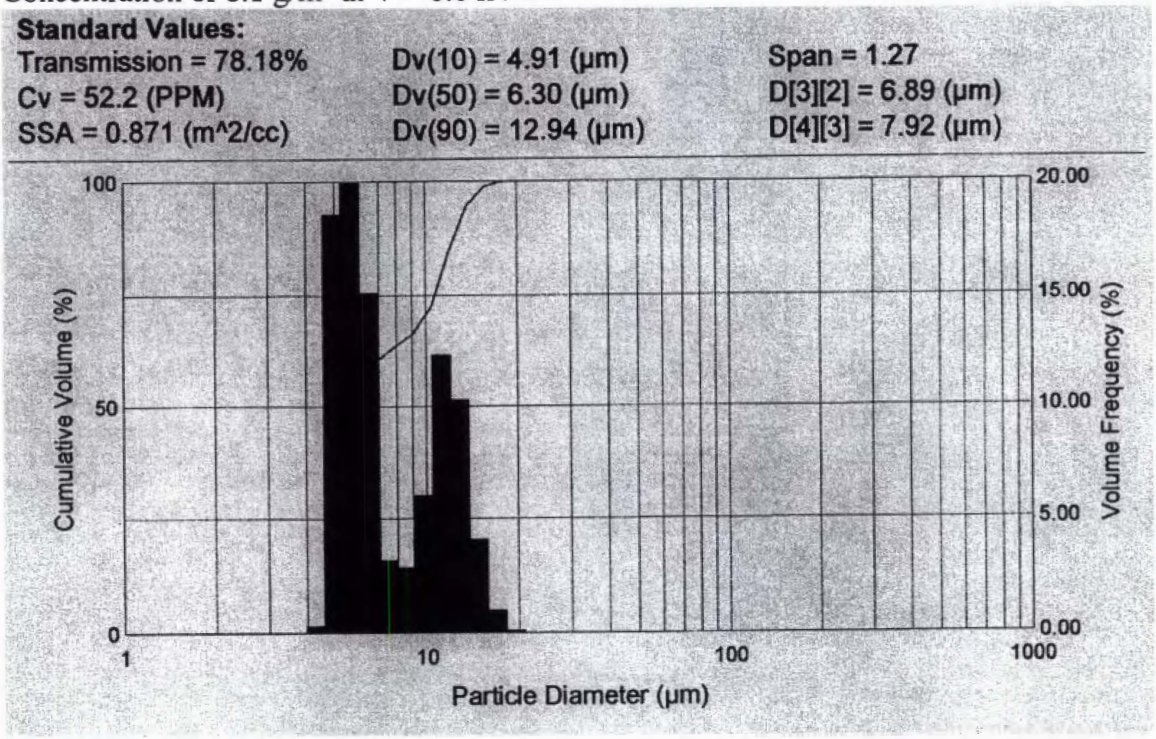



Figure A.7b: Droplet size distribution for experimental conditions of Figure A7a, with V=10.0 kV; Droplet Concentration at exit = 7.3 g / m$^3$

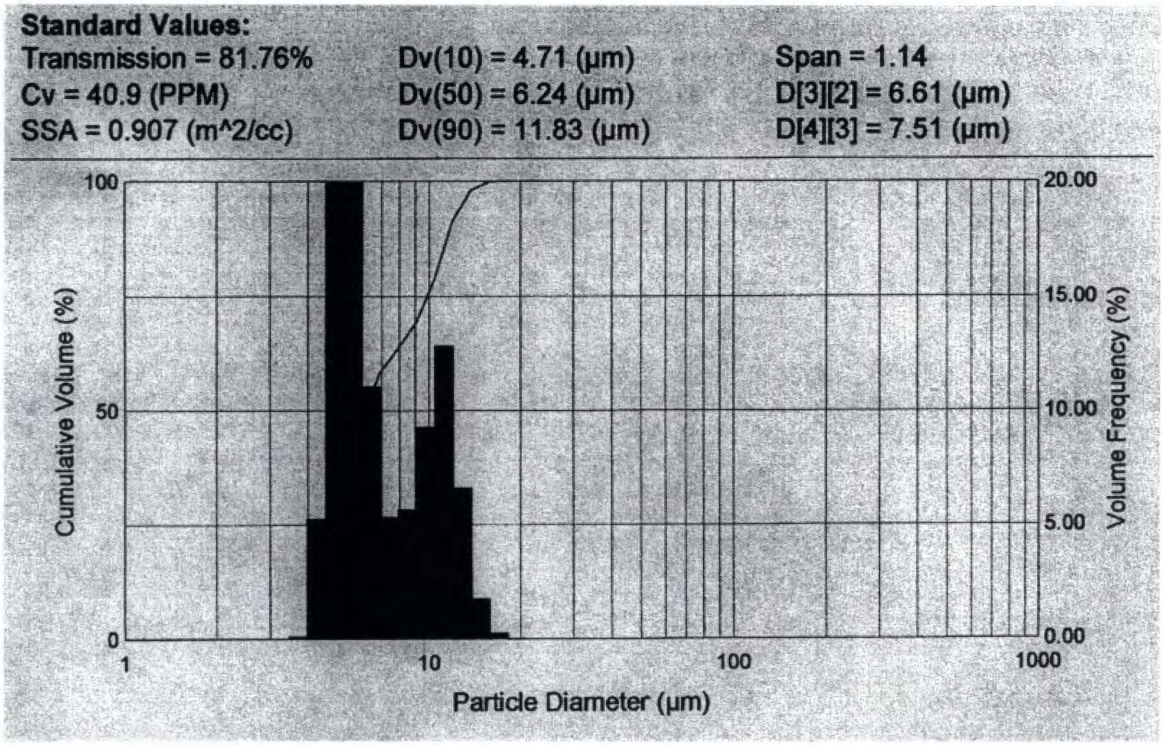



Figure A.7c: Droplet size distribution for experimental conditions of Figure A7a, with V=15.0 kV; Droplet Concentration at exit = 5.9 g / $m^3$

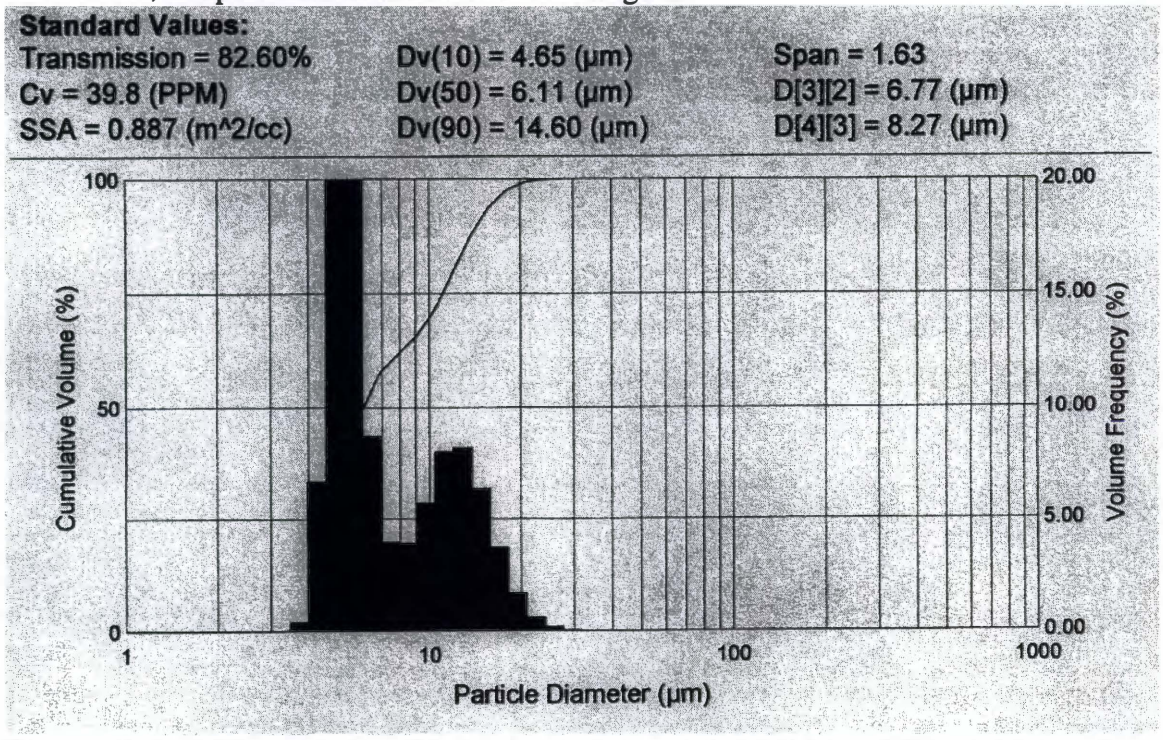



Figure A.7d: Droplet size distribution for experimental conditions of Figure A7a, with V=18.0 kV; Droplet Concentration at exit = 4.6 g / $m^3$

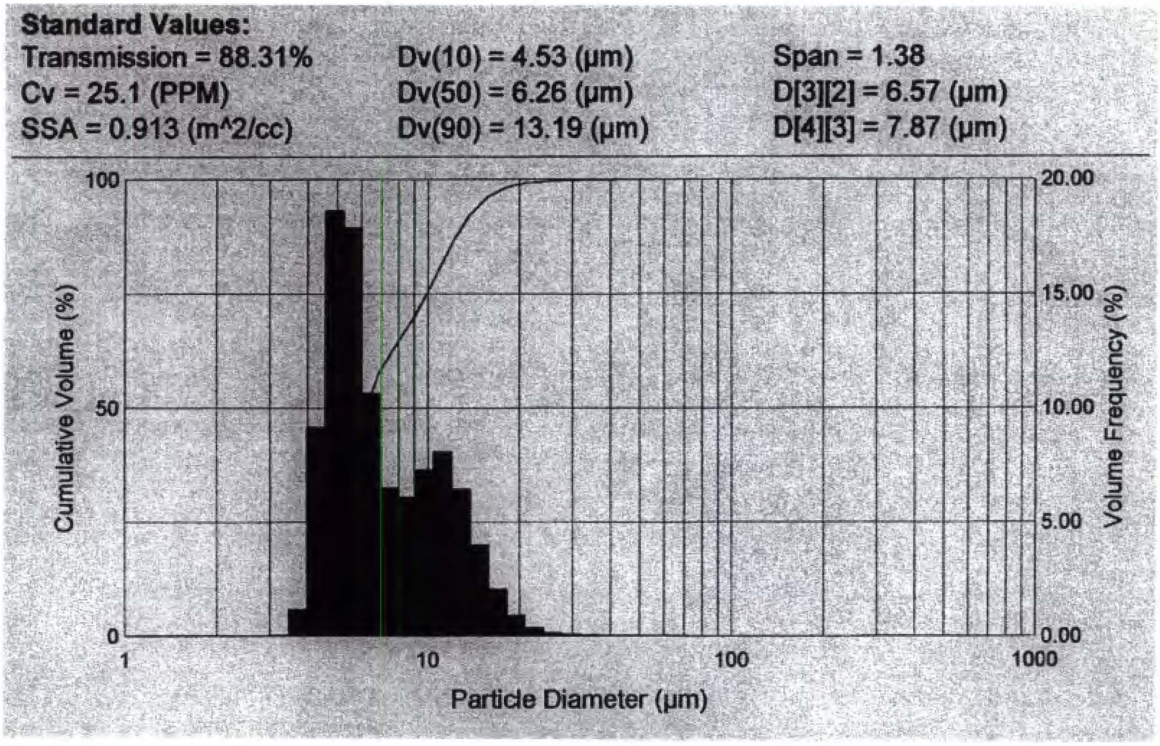



Figure A.7e: Droplet size distribution for experimental conditions of Figure A7a, with V=20.0 kV; Droplet Concentration at exit = 4.4 g / $m^3$

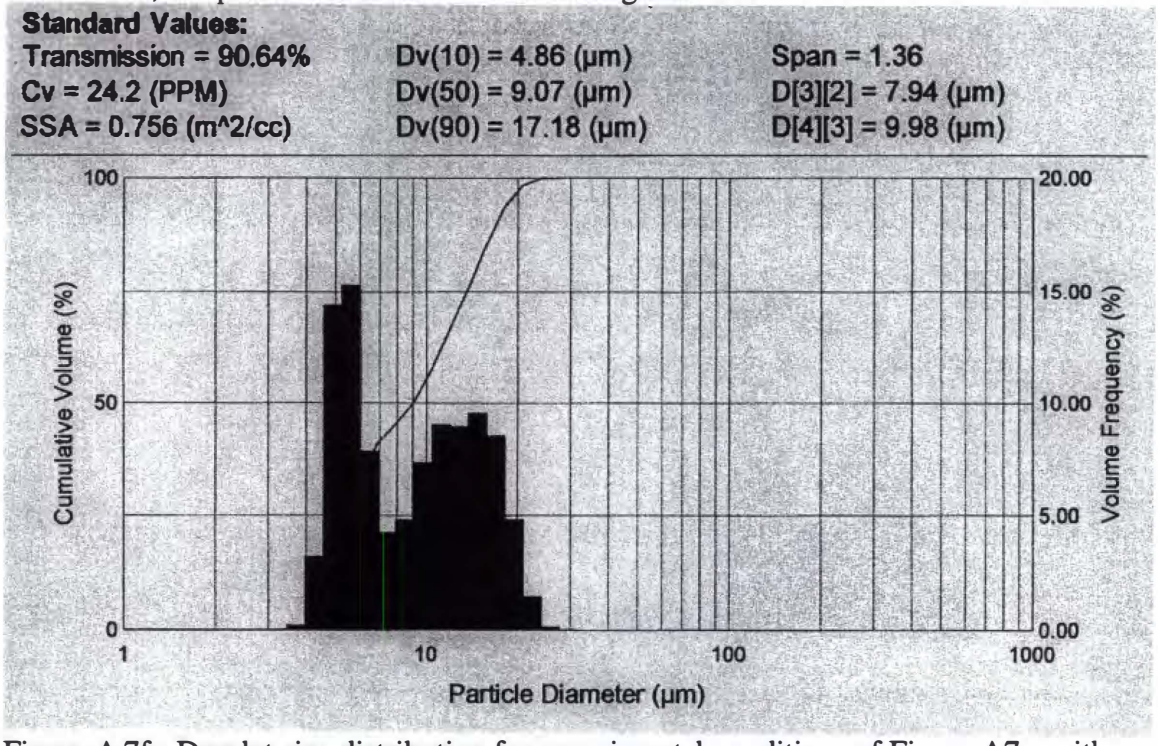



Figure A.7f: Droplet size distribution for experimental conditions of Figure A7a, with V=26.0 kV; Droplet Concentration at exit = 3.3 g / $m^3$

Table A.1a: Droplet Diameter vs. Cumulative (%) and Volume Frequency (%) respectively for conditions of Figure A1a

| Size (µm) | % < | % In | Size (µm) | % < | % In | Size (µm) | % < | % In |
|---|---|---|---|---|---|---|---|---|
| 0.287 | 0.00 | 0.00 | 4.56 | 7.73 | 6.96 | 72.33 | 100.00 | 0.00 |
| 0.330 | 0.00 | 0.00 | 5.23 | 25.72 | 17.99 | 83.06 | 100.00 | 0.00 |
| 0.378 | 0.00 | 0.00 | 6.01 | 46.17 | 20.45 | 95.37 | 100.00 | 0.00 |
| 0.435 | 0.00 | 0.00 | 6.90 | 60.28 | 14.11 | 109.51 | 100.00 | 0.00 |
| 0.499 | 0.00 | 0.00 | 7.92 | 68.18 | 7.90 | 125.74 | 100.00 | 0.00 |
| 0.573 | 0.00 | 0.00 | 9.10 | 73.90 | 5.71 | 144.38 | 100.00 | 0.00 |
| 0.658 | 0.00 | 0.00 | 10.44 | 79.46 | 5.57 | 165.79 | 100.00 | 0.00 |
| 0.755 | 0.00 | 0.00 | 11.99 | 85.48 | 6.02 | 190.37 | 100.00 | 0.00 |
| 0.867 | 0.00 | 0.00 | 13.77 | 91.19 | 5.71 | 218.59 | 100.00 | 0.00 |
| 0.996 | 0.00 | 0.00 | 15.81 | 95.56 | 4.37 | 250.99 | 100.00 | 0.00 |
| 1.14 | 0.00 | 0.00 | 18.16 | 98.19 | 2.63 | 288.20 | 100.00 | 0.00 |
| 1.31 | 0.00 | 0.00 | 20.85 | 99.43 | 1.24 | 330.92 | 100.00 | 0.00 |
| 1.51 | 0.00 | 0.00 | 23.94 | 99.86 | 0.44 | 379.98 | 100.00 | 0.00 |
| 1.73 | 0.00 | 0.00 | 27.49 | 99.98 | 0.11 | 436.31 | 100.00 | 0.00 |
| 1.99 | 0.00 | 0.00 | 31.56 | 100.00 | 0.02 | 500.99 | 100.00 | 0.00 |
| 2.28 | 0.00 | 0.00 | 36.24 | 100.00 | 0.00 | 575.26 | 100.00 | 0.00 |
| 2.62 | 0.00 | 0.00 | 41.61 | 100.00 | 0.00 | 660.54 | 100.00 | 0.00 |
| 3.01 | 0.00 | 0.00 | 47.78 | 100.00 | 0.00 | 758.46 | 100.00 | 0.00 |
| 3.46 | 0.03 | 0.03 | 54.86 | 100.00 | 0.00 | 870.89 | 100.00 | 0.00 |
| 3.97 | 0.78 | 0.75 | 63.00 | 100.00 | 0.00 | 1000.00 | 100.00 | 0.00 |

Table A.1b: Droplet Diameter vs. Cumulative (%) and Volume Frequency (%) respectively for conditions of Figure A1b

| Size (µm) | % < | % In | Size (µm) | % < | % In | Size (µm) | % < | % In |
|---|---|---|---|---|---|---|---|---|
| 0.287 | 0.00 | 0.00 | 4.56 | 8.78 | 8.20 | 72.33 | 100.00 | 0.00 |
| 0.330 | 0.00 | 0.00 | 5.23 | 31.21 | 22.43 | 83.06 | 100.00 | 0.00 |
| 0.378 | 0.00 | 0.00 | 6.01 | 54.57 | 23.37 | 95.37 | 100.00 | 0.00 |
| 0.435 | 0.00 | 0.00 | 6.90 | 67.82 | 13.25 | 109.51 | 100.00 | 0.00 |
| 0.499 | 0.00 | 0.00 | 7.92 | 73.92 | 6.10 | 125.74 | 100.00 | 0.00 |
| 0.573 | 0.00 | 0.00 | 9.10 | 78.16 | 4.24 | 144.38 | 100.00 | 0.00 |
| 0.658 | 0.00 | 0.00 | 10.44 | 82.59 | 4.43 | 165.79 | 100.00 | 0.00 |
| 0.755 | 0.00 | 0.00 | 11.99 | 87.88 | 5.29 | 190.37 | 100.00 | 0.00 |
| 0.867 | 0.00 | 0.00 | 13.77 | 93.15 | 5.26 | 218.59 | 100.00 | 0.00 |
| 0.996 | 0.00 | 0.00 | 15.81 | 96.99 | 3.84 | 250.99 | 100.00 | 0.00 |
| 1.14 | 0.00 | 0.00 | 18.16 | 99.02 | 2.03 | 288.20 | 100.00 | 0.00 |
| 1.31 | 0.00 | 0.00 | 20.85 | 99.78 | 0.76 | 330.92 | 100.00 | 0.00 |
| 1.51 | 0.00 | 0.00 | 23.94 | 99.97 | 0.19 | 379.98 | 100.00 | 0.00 |
| 1.73 | 0.00 | 0.00 | 27.49 | 100.00 | 0.03 | 436.31 | 100.00 | 0.00 |
| 1.99 | 0.00 | 0.00 | 31.56 | 100.00 | 0.00 | 500.99 | 100.00 | 0.00 |
| 2.28 | 0.00 | 0.00 | 36.24 | 100.00 | 0.00 | 575.26 | 100.00 | 0.00 |
| 2.62 | 0.00 | 0.00 | 41.61 | 100.00 | 0.00 | 660.54 | 100.00 | 0.00 |
| 3.01 | 0.00 | 0.00 | 47.78 | 100.00 | 0.00 | 758.46 | 100.00 | 0.00 |
| 3.46 | 0.01 | 0.01 | 54.86 | 100.00 | 0.00 | 870.89 | 100.00 | 0.00 |
| 3.97 | 0.58 | 0.57 | 63.00 | 100.00 | 0.00 | 1000.00 | 100.00 | 0.00 |

Table A.1c: Droplet Diameter vs. Cumulative (%) and Volume Frequency (%) respectively for conditions of Figure A1c

| Size (µm) | % < | % In | Size (µm) | % < | % In | Size (µm) | % < | % In |
|---|---|---|---|---|---|---|---|---|
| 0.287 | 0.00 | 0.00 | 4.56 | 8.01 | 7.71 | 72.33 | 100.00 | 0.00 |
| 0.330 | 0.00 | 0.00 | 5.23 | 32.13 | 24.12 | 83.06 | 100.00 | 0.00 |
| 0.378 | 0.00 | 0.00 | 6.01 | 56.14 | 24.02 | 95.37 | 100.00 | 0.00 |
| 0.435 | 0.00 | 0.00 | 6.90 | 67.78 | 11.64 | 109.51 | 100.00 | 0.00 |
| 0.499 | 0.00 | 0.00 | 7.92 | 72.68 | 4.89 | 125.74 | 100.00 | 0.00 |
| 0.573 | 0.00 | 0.00 | 9.10 | 76.56 | 3.88 | 144.38 | 100.00 | 0.00 |
| 0.658 | 0.00 | 0.00 | 10.44 | 81.46 | 4.91 | 165.79 | 100.00 | 0.00 |
| 0.755 | 0.00 | 0.00 | 11.99 | 88.00 | 6.54 | 190.37 | 100.00 | 0.00 |
| 0.867 | 0.00 | 0.00 | 13.77 | 94.08 | 6.07 | 218.59 | 100.00 | 0.00 |
| 0.996 | 0.00 | 0.00 | 15.81 | 97.81 | 3.74 | 250.99 | 100.00 | 0.00 |
| 1.14 | 0.00 | 0.00 | 18.16 | 99.43 | 1.62 | 288.20 | 100.00 | 0.00 |
| 1.31 | 0.00 | 0.00 | 20.85 | 99.90 | 0.47 | 330.92 | 100.00 | 0.00 |
| 1.51 | 0.00 | 0.00 | 23.94 | 99.99 | 0.09 | 379.98 | 100.00 | 0.00 |
| 1.73 | 0.00 | 0.00 | 27.49 | 100.00 | 0.01 | 436.31 | 100.00 | 0.00 |
| 1.99 | 0.00 | 0.00 | 31.56 | 100.00 | 0.00 | 500.99 | 100.00 | 0.00 |
| 2.28 | 0.00 | 0.00 | 36.24 | 100.00 | 0.00 | 575.26 | 100.00 | 0.00 |
| 2.62 | 0.00 | 0.00 | 41.61 | 100.00 | 0.00 | 660.54 | 100.00 | 0.00 |
| 3.01 | 0.00 | 0.00 | 47.78 | 100.00 | 0.00 | 758.46 | 100.00 | 0.00 |
| 3.46 | 0.00 | 0.00 | 54.86 | 100.00 | 0.00 | 870.89 | 100.00 | 0.00 |
| 3.97 | 0.30 | 0.29 | 63.00 | 100.00 | 0.00 | 1000.00 | 100.00 | 0.00 |

Table A.1d: Droplet Diameter vs. Cumulative (%) and Volume Frequency (%) respectively for conditions of Figure A1d

| Size (µm) | % < | % In | Size (µm) | % < | % In | Size (µm) | % < | % In |
|---|---|---|---|---|---|---|---|---|
| 0.287 | 0.00 | 0.00 | 4.56 | 5.64 | 5.50 | 72.33 | 100.00 | 0.00 |
| 0.330 | 0.00 | 0.00 | 5.23 | 29.31 | 23.68 | 83.06 | 100.00 | 0.00 |
| 0.378 | 0.00 | 0.00 | 6.01 | 54.56 | 25.25 | 95.37 | 100.00 | 0.00 |
| 0.435 | 0.00 | 0.00 | 6.90 | 67.09 | 12.53 | 109.51 | 100.00 | 0.00 |
| 0.499 | 0.00 | 0.00 | 7.92 | 72.08 | 4.99 | 125.74 | 100.00 | 0.00 |
| 0.573 | 0.00 | 0.00 | 9.10 | 75.98 | 3.90 | 144.38 | 100.00 | 0.00 |
| 0.658 | 0.00 | 0.00 | 10.44 | 80.92 | 4.94 | 165.79 | 100.00 | 0.00 |
| 0.755 | 0.00 | 0.00 | 11.99 | 87.39 | 6.47 | 190.37 | 100.00 | 0.00 |
| 0.867 | 0.00 | 0.00 | 13.77 | 93.30 | 5.91 | 218.59 | 100.00 | 0.00 |
| 0.996 | 0.00 | 0.00 | 15.81 | 97.13 | 3.83 | 250.99 | 100.00 | 0.00 |
| 1.14 | 0.00 | 0.00 | 18.16 | 99.01 | 1.88 | 288.20 | 100.00 | 0.00 |
| 1.31 | 0.00 | 0.00 | 20.85 | 99.71 | 0.71 | 330.92 | 100.00 | 0.00 |
| 1.51 | 0.00 | 0.00 | 23.94 | 99.92 | 0.21 | 379.98 | 100.00 | 0.00 |
| 1.73 | 0.00 | 0.00 | 27.49 | 99.98 | 0.05 | 436.31 | 100.00 | 0.00 |
| 1.99 | 0.00 | 0.00 | 31.56 | 99.99 | 0.01 | 500.99 | 100.00 | 0.00 |
| 2.28 | 0.00 | 0.00 | 36.24 | 100.00 | 0.00 | 575.26 | 100.00 | 0.00 |
| 2.62 | 0.00 | 0.00 | 41.61 | 100.00 | 0.00 | 660.54 | 100.00 | 0.00 |
| 3.01 | 0.00 | 0.00 | 47.78 | 100.00 | 0.00 | 758.46 | 100.00 | 0.00 |
| 3.46 | 0.00 | 0.00 | 54.86 | 100.00 | 0.00 | 870.89 | 100.00 | 0.00 |
| 3.97 | 0.14 | 0.14 | 63.00 | 100.00 | 0.00 | 1000.00 | 100.00 | 0.00 |

Table A.1e: Droplet Diameter vs. Cumulative (%) and Volume Frequency (%) respectively for conditions of Figure A1e

| Size (µm) | % < | % In | Size (µm) | % < | % In | Size (µm) | % < | % In |
|---|---|---|---|---|---|---|---|---|
| 0.287 | 0.00 | 0.00 | 4.56 | 5.63 | 5.44 | 72.33 | 100.00 | 0.00 |
| 0.330 | 0.00 | 0.00 | 5.23 | 28.31 | 22.68 | 83.06 | 100.00 | 0.00 |
| 0.378 | 0.00 | 0.00 | 6.01 | 52.95 | 24.64 | 95.37 | 100.00 | 0.00 |
| 0.435 | 0.00 | 0.00 | 6.90 | 65.86 | 12.90 | 109.51 | 100.00 | 0.00 |
| 0.499 | 0.00 | 0.00 | 7.92 | 71.32 | 5.47 | 125.74 | 100.00 | 0.00 |
| 0.573 | 0.00 | 0.00 | 9.10 | 75.66 | 4.33 | 144.38 | 100.00 | 0.00 |
| 0.658 | 0.00 | 0.00 | 10.44 | 80.95 | 5.29 | 165.79 | 100.00 | 0.00 |
| 0.755 | 0.00 | 0.00 | 11.99 | 87.38 | 6.43 | 190.37 | 100.00 | 0.00 |
| 0.867 | 0.00 | 0.00 | 13.77 | 92.89 | 5.51 | 218.59 | 100.00 | 0.00 |
| 0.996 | 0.00 | 0.00 | 15.81 | 96.54 | 3.65 | 250.99 | 100.00 | 0.00 |
| 1.14 | 0.00 | 0.00 | 18.16 | 98.53 | 1.99 | 288.20 | 100.00 | 0.00 |
| 1.31 | 0.00 | 0.00 | 20.85 | 99.44 | 0.91 | 330.92 | 100.00 | 0.00 |
| 1.51 | 0.00 | 0.00 | 23.94 | 99.80 | 0.36 | 379.98 | 100.00 | 0.00 |
| 1.73 | 0.00 | 0.00 | 27.49 | 99.92 | 0.12 | 436.31 | 100.00 | 0.00 |
| 1.99 | 0.00 | 0.00 | 31.56 | 99.96 | 0.04 | 500.99 | 100.00 | 0.00 |
| 2.28 | 0.00 | 0.00 | 36.24 | 99.98 | 0.01 | 575.26 | 100.00 | 0.00 |
| 2.62 | 0.00 | 0.00 | 41.61 | 99.98 | 0.01 | 660.54 | 100.00 | 0.00 |
| 3.01 | 0.00 | 0.00 | 47.78 | 99.99 | 0.00 | 758.46 | 100.00 | 0.00 |
| 3.46 | 0.00 | 0.00 | 54.86 | 99.99 | 0.00 | 870.89 | 100.00 | 0.00 |
| 3.97 | 0.19 | 0.19 | 63.00 | 100.00 | 0.01 | 1000.00 | 100.00 | 0.00 |

Table A.1f: Droplet Diameter vs. Cumulative (%) and Volume Frequency (%) respectively for conditions of Figure A1f

| Size (µm) | % < | % In | Size (µm) | % < | % In | Size (µm) | % < | % In |
|---|---|---|---|---|---|---|---|---|
| 0.287 | 0.00 | 0.00 | 4.56 | 15.17 | 9.99 | 72.33 | 100.00 | 0.00 |
| 0.330 | 0.00 | 0.00 | 5.23 | 30.51 | 15.34 | 83.06 | 100.00 | 0.00 |
| 0.378 | 0.00 | 0.00 | 6.01 | 45.94 | 15.43 | 95.37 | 100.00 | 0.00 |
| 0.435 | 0.00 | 0.00 | 6.90 | 57.33 | 11.39 | 109.51 | 100.00 | 0.00 |
| 0.499 | 0.00 | 0.00 | 7.92 | 64.51 | 7.18 | 125.74 | 100.00 | 0.00 |
| 0.573 | 0.00 | 0.00 | 9.10 | 69.31 | 4.80 | 144.38 | 100.00 | 0.00 |
| 0.658 | 0.00 | 0.00 | 10.44 | 73.10 | 3.79 | 165.79 | 100.00 | 0.00 |
| 0.755 | 0.00 | 0.00 | 11.99 | 76.63 | 3.53 | 190.37 | 100.00 | 0.00 |
| 0.867 | 0.00 | 0.00 | 13.77 | 80.37 | 3.74 | 218.59 | 100.00 | 0.00 |
| 0.996 | 0.00 | 0.00 | 15.81 | 84.47 | 4.10 | 250.99 | 100.00 | 0.00 |
| 1.14 | 0.00 | 0.00 | 18.16 | 88.74 | 4.27 | 288.20 | 100.00 | 0.00 |
| 1.31 | 0.00 | 0.00 | 20.85 | 92.70 | 3.96 | 330.92 | 100.00 | 0.00 |
| 1.51 | 0.00 | 0.00 | 23.94 | 95.83 | 3.14 | 379.98 | 100.00 | 0.00 |
| 1.73 | 0.00 | 0.00 | 27.49 | 97.91 | 2.07 | 436.31 | 100.00 | 0.00 |
| 1.99 | 0.01 | 0.01 | 31.56 | 99.05 | 1.14 | 500.99 | 100.00 | 0.00 |
| 2.28 | 0.03 | 0.02 | 36.24 | 99.65 | 0.59 | 575.26 | 100.00 | 0.00 |
| 2.62 | 0.11 | 0.08 | 41.61 | 99.99 | 0.34 | 660.54 | 100.00 | 0.00 |
| 3.01 | 0.35 | 0.24 | 47.78 | 100.00 | 0.01 | 758.46 | 100.00 | 0.00 |
| 3.46 | 1.36 | 1.02 | 54.86 | 100.00 | 0.00 | 870.89 | 100.00 | 0.00 |
| 3.97 | 5.17 | 3.81 | 63.00 | 100.00 | 0.00 | 1000.00 | 100.00 | 0.00 |

Table A.2a: Droplet Diameter vs. Cumulative (%) and Volume Frequency (%) respectively for Conditions of Figure A2a

| Size (µm) | % < | % in | Size (µm) | % < | % in | Size (µm) | % < | % in |
|---|---|---|---|---|---|---|---|---|
| 0.287 | 0.00 | 0.00 | 4.56 | 11.06 | 9.90 | 72.33 | 100.00 | 0.00 |
| 0.330 | 0.00 | 0.00 | 5.23 | 31.31 | 20.26 | 83.06 | 100.00 | 0.00 |
| 0.378 | 0.00 | 0.00 | 6.01 | 50.57 | 19.26 | 95.37 | 100.00 | 0.00 |
| 0.435 | 0.00 | 0.00 | 6.90 | 61.40 | 10.83 | 109.51 | 100.00 | 0.00 |
| 0.499 | 0.00 | 0.00 | 7.92 | 66.92 | 5.52 | 125.74 | 100.00 | 0.00 |
| 0.573 | 0.00 | 0.00 | 9.10 | 71.18 | 4.25 | 144.38 | 100.00 | 0.00 |
| 0.658 | 0.00 | 0.00 | 10.44 | 75.91 | 4.73 | 165.79 | 100.00 | 0.00 |
| 0.755 | 0.00 | 0.00 | 11.99 | 81.69 | 5.78 | 190.37 | 100.00 | 0.00 |
| 0.867 | 0.00 | 0.00 | 13.77 | 87.54 | 5.84 | 218.59 | 100.00 | 0.00 |
| 0.996 | 0.00 | 0.00 | 15.81 | 92.27 | 4.74 | 250.99 | 100.00 | 0.00 |
| 1.14 | 0.00 | 0.00 | 18.16 | 95.58 | 3.31 | 288.20 | 100.00 | 0.00 |
| 1.31 | 0.00 | 0.00 | 20.85 | 97.67 | 2.09 | 330.92 | 100.00 | 0.00 |
| 1.51 | 0.00 | 0.00 | 23.94 | 98.90 | 1.23 | 379.98 | 100.00 | 0.00 |
| 1.73 | 0.00 | 0.00 | 27.49 | 99.56 | 0.66 | 436.31 | 100.00 | 0.00 |
| 1.99 | 0.00 | 0.00 | 31.56 | 99.87 | 0.31 | 500.99 | 100.00 | 0.00 |
| 2.28 | 0.00 | 0.00 | 36.24 | 99.97 | 0.11 | 575.26 | 100.00 | 0.00 |
| 2.62 | 0.00 | 0.00 | 41.61 | 100.00 | 0.02 | 660.54 | 100.00 | 0.00 |
| 3.01 | 0.00 | 0.00 | 47.78 | 100.00 | 0.00 | 758.46 | 100.00 | 0.00 |
| 3.46 | 0.03 | 0.03 | 54.86 | 100.00 | 0.00 | 870.89 | 100.00 | 0.00 |
| 3.97 | 1.15 | 1.12 | 63.00 | 100.00 | 0.00 | 1000.00 | 100.00 | 0.00 |

Table A.2b: Droplet Diameter vs. Cumulative (%) and Volume Frequency (%) respectively for conditions of Figure A2b

| Size (µm) | % < | % in | Size (µm) | % < | % in | Size (µm) | % < | % in |
|---|---|---|---|---|---|---|---|---|
| 0.287 | 0.00 | 0.00 | 4.56 | 9.81 | 9.05 | 72.33 | 100.00 | 0.00 |
| 0.330 | 0.00 | 0.00 | 5.23 | 30.21 | 20.40 | 83.06 | 100.00 | 0.00 |
| 0.378 | 0.00 | 0.00 | 6.01 | 49.74 | 19.53 | 95.37 | 100.00 | 0.00 |
| 0.435 | 0.00 | 0.00 | 6.90 | 60.34 | 10.59 | 109.51 | 100.00 | 0.00 |
| 0.499 | 0.00 | 0.00 | 7.92 | 65.85 | 5.51 | 125.74 | 100.00 | 0.00 |
| 0.573 | 0.00 | 0.00 | 9.10 | 70.57 | 4.73 | 144.38 | 100.00 | 0.00 |
| 0.658 | 0.00 | 0.00 | 10.44 | 76.32 | 5.74 | 165.79 | 100.00 | 0.00 |
| 0.755 | 0.00 | 0.00 | 11.99 | 83.25 | 6.94 | 190.37 | 100.00 | 0.00 |
| 0.867 | 0.00 | 0.00 | 13.77 | 89.36 | 6.11 | 218.59 | 100.00 | 0.00 |
| 0.996 | 0.00 | 0.00 | 15.81 | 93.62 | 4.26 | 250.99 | 100.00 | 0.00 |
| 1.14 | 0.00 | 0.00 | 18.16 | 96.25 | 2.63 | 288.20 | 100.00 | 0.00 |
| 1.31 | 0.00 | 0.00 | 20.85 | 97.82 | 1.57 | 330.92 | 100.00 | 0.00 |
| 1.51 | 0.00 | 0.00 | 23.94 | 98.80 | 0.98 | 379.98 | 100.00 | 0.00 |
| 1.73 | 0.00 | 0.00 | 27.49 | 99.43 | 0.63 | 436.31 | 100.00 | 0.00 |
| 1.99 | 0.00 | 0.00 | 31.56 | 99.79 | 0.37 | 500.99 | 100.00 | 0.00 |
| 2.28 | 0.00 | 0.00 | 36.24 | 99.95 | 0.16 | 575.26 | 100.00 | 0.00 |
| 2.62 | 0.00 | 0.00 | 41.61 | 100.00 | 0.04 | 660.54 | 100.00 | 0.00 |
| 3.01 | 0.00 | 0.00 | 47.78 | 100.00 | 0.00 | 758.46 | 100.00 | 0.00 |
| 3.46 | 0.01 | 0.01 | 54.86 | 100.00 | 0.00 | 870.89 | 100.00 | 0.00 |
| 3.97 | 0.76 | 0.74 | 63.00 | 100.00 | 0.00 | 1000.00 | 100.00 | 0.00 |

Table A.2c: Droplet Diameter vs. Cumulative (%) and Volume Frequency (%) respectively for conditions of Figure A2.c

| Size (µm) | % < | % In | Size (µm) | % < | % In | Size (µm) | % < | % In |
|---|---|---|---|---|---|---|---|---|
| 0.287 | 0.00 | 0.00 | 4.56 | 10.01 | 8.94 | 72.33 | 100.00 | 0.00 |
| 0.330 | 0.00 | 0.00 | 5.23 | 28.06 | 18.05 | 83.06 | 100.00 | 0.00 |
| 0.378 | 0.00 | 0.00 | 6.01 | 45.29 | 17.22 | 95.37 | 100.00 | 0.00 |
| 0.435 | 0.00 | 0.00 | 6.90 | 55.37 | 10.08 | 109.51 | 100.00 | 0.00 |
| 0.499 | 0.00 | 0.00 | 7.92 | 61.20 | 5.83 | 125.74 | 100.00 | 0.00 |
| 0.573 | 0.00 | 0.00 | 9.10 | 66.39 | 5.19 | 144.38 | 100.00 | 0.00 |
| 0.658 | 0.00 | 0.00 | 10.44 | 72.61 | 6.22 | 165.79 | 100.00 | 0.00 |
| 0.755 | 0.00 | 0.00 | 11.99 | 80.03 | 7.43 | 190.37 | 100.00 | 0.00 |
| 0.867 | 0.00 | 0.00 | 13.77 | 86.75 | 6.72 | 218.59 | 100.00 | 0.00 |
| 0.996 | 0.00 | 0.00 | 15.81 | 91.66 | 4.91 | 250.99 | 100.00 | 0.00 |
| 1.14 | 0.00 | 0.00 | 18.16 | 94.85 | 3.19 | 288.20 | 100.00 | 0.00 |
| 1.31 | 0.00 | 0.00 | 20.85 | 96.85 | 1.99 | 330.92 | 100.00 | 0.00 |
| 1.51 | 0.00 | 0.00 | 23.94 | 98.11 | 1.27 | 379.98 | 100.00 | 0.00 |
| 1.73 | 0.00 | 0.00 | 27.49 | 98.95 | 0.84 | 436.31 | 100.00 | 0.00 |
| 1.99 | 0.00 | 0.00 | 31.56 | 99.49 | 0.54 | 500.99 | 100.00 | 0.00 |
| 2.28 | 0.00 | 0.00 | 36.24 | 99.80 | 0.31 | 575.26 | 100.00 | 0.00 |
| 2.62 | 0.00 | 0.00 | 41.61 | 99.94 | 0.14 | 660.54 | 100.00 | 0.00 |
| 3.01 | 0.00 | 0.00 | 47.78 | 99.98 | 0.05 | 758.46 | 100.00 | 0.00 |
| 3.46 | 0.03 | 0.03 | 54.86 | 100.00 | 0.01 | 870.89 | 100.00 | 0.00 |
| 3.97 | 1.07 | 1.03 | 63.00 | 100.00 | 0.00 | 1000.00 | 100.00 | 0.00 |

Table A.2d: Droplet Diameter vs. Cumulative (%) and Volume Frequency (%) respectively for conditions of Figure A2d

| Size (µm) | % < | % In | Size (µm) | % < | % In | Size (µm) | % < | % In |
|---|---|---|---|---|---|---|---|---|
| 0.287 | 0.00 | 0.00 | 4.56 | 4.45 | 4.38 | 72.33 | 100.00 | 0.00 |
| 0.330 | 0.00 | 0.00 | 5.23 | 24.01 | 19.56 | 83.06 | 100.00 | 0.00 |
| 0.378 | 0.00 | 0.00 | 6.01 | 45.61 | 21.60 | 95.37 | 100.00 | 0.00 |
| 0.435 | 0.00 | 0.00 | 6.90 | 57.14 | 11.53 | 109.51 | 100.00 | 0.00 |
| 0.499 | 0.00 | 0.00 | 7.92 | 62.17 | 5.03 | 125.74 | 100.00 | 0.00 |
| 0.573 | 0.00 | 0.00 | 9.10 | 66.49 | 4.32 | 144.38 | 100.00 | 0.00 |
| 0.658 | 0.00 | 0.00 | 10.44 | 72.59 | 6.09 | 165.79 | 100.00 | 0.00 |
| 0.755 | 0.00 | 0.00 | 11.99 | 81.52 | 8.94 | 190.37 | 100.00 | 0.00 |
| 0.867 | 0.00 | 0.00 | 13.77 | 90.25 | 8.72 | 218.59 | 100.00 | 0.00 |
| 0.996 | 0.00 | 0.00 | 15.81 | 95.90 | 5.65 | 250.99 | 100.00 | 0.00 |
| 1.14 | 0.00 | 0.00 | 18.16 | 98.63 | 2.73 | 288.20 | 100.00 | 0.00 |
| 1.31 | 0.00 | 0.00 | 20.85 | 99.63 | 1.00 | 330.92 | 100.00 | 0.00 |
| 1.51 | 0.00 | 0.00 | 23.94 | 99.91 | 0.28 | 379.98 | 100.00 | 0.00 |
| 1.73 | 0.00 | 0.00 | 27.49 | 99.98 | 0.07 | 436.31 | 100.00 | 0.00 |
| 1.99 | 0.00 | 0.00 | 31.56 | 100.00 | 0.02 | 500.99 | 100.00 | 0.00 |
| 2.28 | 0.00 | 0.00 | 36.24 | 100.00 | 0.00 | 575.26 | 100.00 | 0.00 |
| 2.62 | 0.00 | 0.00 | 41.61 | 100.00 | 0.00 | 660.54 | 100.00 | 0.00 |
| 3.01 | 0.00 | 0.00 | 47.78 | 100.00 | 0.00 | 758.46 | 100.00 | 0.00 |
| 3.46 | 0.00 | 0.00 | 54.86 | 100.00 | 0.00 | 870.89 | 100.00 | 0.00 |
| 3.97 | 0.07 | 0.07 | 63.00 | 100.00 | 0.00 | 1000.00 | 100.00 | 0.00 |

Table A.2e: Droplet Diameter vs. Cumulative (%) and Volume Frequency (%) respectively for conditions of Figure A2e

| Size (µm) | % < | % In | Size (µm) | % < | % In | Size (µm) | % < | % In |
|---|---|---|---|---|---|---|---|---|
| 0.287 | 0.00 | 0.00 | 4.56 | 5.81 | 5.65 | 72.33 | 100.00 | 0.01 |
| 0.330 | 0.00 | 0.00 | 5.23 | 25.99 | 20.18 | 83.06 | 100.00 | 0.00 |
| 0.378 | 0.00 | 0.00 | 6.01 | 47.26 | 21.27 | 95.37 | 100.00 | 0.00 |
| 0.435 | 0.00 | 0.00 | 6.90 | 58.41 | 11.15 | 109.51 | 100.00 | 0.00 |
| 0.499 | 0.00 | 0.00 | 7.92 | 63.48 | 5.07 | 125.74 | 100.00 | 0.00 |
| 0.573 | 0.00 | 0.00 | 9.10 | 67.97 | 4.49 | 144.38 | 100.00 | 0.00 |
| 0.658 | 0.00 | 0.00 | 10.44 | 74.31 | 6.34 | 165.79 | 100.00 | 0.00 |
| 0.755 | 0.00 | 0.00 | 11.99 | 83.43 | 9.12 | 190.37 | 100.00 | 0.00 |
| 0.867 | 0.00 | 0.00 | 13.77 | 91.79 | 8.36 | 218.59 | 100.00 | 0.00 |
| 0.996 | 0.00 | 0.00 | 15.81 | 96.76 | 4.97 | 250.99 | 100.00 | 0.00 |
| 1.14 | 0.00 | 0.00 | 18.16 | 98.96 | 2.20 | 288.20 | 100.00 | 0.00 |
| 1.31 | 0.00 | 0.00 | 20.85 | 99.69 | 0.74 | 330.92 | 100.00 | 0.00 |
| 1.51 | 0.00 | 0.00 | 23.94 | 99.90 | 0.20 | 379.98 | 100.00 | 0.00 |
| 1.73 | 0.00 | 0.00 | 27.49 | 99.95 | 0.05 | 436.31 | 100.00 | 0.00 |
| 1.99 | 0.00 | 0.00 | 31.56 | 99.97 | 0.02 | 500.99 | 100.00 | 0.00 |
| 2.28 | 0.00 | 0.00 | 36.24 | 99.98 | 0.01 | 575.26 | 100.00 | 0.00 |
| 2.62 | 0.00 | 0.00 | 41.61 | 99.98 | 0.00 | 660.54 | 100.00 | 0.00 |
| 3.01 | 0.00 | 0.00 | 47.78 | 99.98 | 0.00 | 758.46 | 100.00 | 0.00 |
| 3.46 | 0.00 | 0.00 | 54.86 | 99.98 | 0.00 | 870.89 | 100.00 | 0.00 |
| 3.97 | 0.16 | 0.16 | 63.00 | 99.99 | 0.01 | 1000.00 | 100.00 | 0.00 |

Table A.2f: Droplet Diameter vs. Cumulative (%) and Volume Frequency (%) respectively for conditions of Figure A2f

| Size (µm) | % < | % In | Size (µm) | % < | % In | Size (µm) | % < | % In |
|---|---|---|---|---|---|---|---|---|
| 0.287 | 0.00 | 0.00 | 4.56 | 14.71 | 10.81 | 72.33 | 99.91 | 0.20 |
| 0.330 | 0.00 | 0.00 | 5.23 | 30.86 | 16.15 | 83.06 | 100.00 | 0.09 |
| 0.378 | 0.00 | 0.00 | 6.01 | 45.80 | 14.95 | 95.37 | 100.00 | 0.00 |
| 0.435 | 0.00 | 0.00 | 6.90 | 55.99 | 10.19 | 109.51 | 100.00 | 0.00 |
| 0.499 | 0.00 | 0.00 | 7.92 | 62.85 | 6.85 | 125.74 | 100.00 | 0.00 |
| 0.573 | 0.00 | 0.00 | 9.10 | 68.64 | 5.79 | 144.38 | 100.00 | 0.00 |
| 0.658 | 0.00 | 0.00 | 10.44 | 74.53 | 5.89 | 165.79 | 100.00 | 0.00 |
| 0.755 | 0.00 | 0.00 | 11.99 | 80.59 | 6.06 | 190.37 | 100.00 | 0.00 |
| 0.867 | 0.00 | 0.00 | 13.77 | 86.01 | 5.42 | 218.59 | 100.00 | 0.00 |
| 0.996 | 0.00 | 0.00 | 15.81 | 90.33 | 4.32 | 250.99 | 100.00 | 0.00 |
| 1.14 | 0.00 | 0.00 | 18.16 | 93.46 | 3.13 | 288.20 | 100.00 | 0.00 |
| 1.31 | 0.00 | 0.00 | 20.85 | 95.57 | 2.11 | 330.92 | 100.00 | 0.00 |
| 1.51 | 0.00 | 0.00 | 23.94 | 96.95 | 1.38 | 379.98 | 100.00 | 0.00 |
| 1.73 | 0.00 | 0.00 | 27.49 | 97.83 | 0.89 | 436.31 | 100.00 | 0.00 |
| 1.99 | 0.00 | 0.00 | 31.56 | 98.41 | 0.58 | 500.99 | 100.00 | 0.00 |
| 2.28 | 0.00 | 0.00 | 36.24 | 98.80 | 0.39 | 575.26 | 100.00 | 0.00 |
| 2.62 | 0.01 | 0.01 | 41.61 | 99.08 | 0.28 | 660.54 | 100.00 | 0.00 |
| 3.01 | 0.07 | 0.06 | 47.78 | 99.30 | 0.22 | 758.46 | 100.00 | 0.00 |
| 3.46 | 0.59 | 0.52 | 54.86 | 99.50 | 0.20 | 870.89 | 100.00 | 0.00 |
| 3.97 | 3.91 | 3.32 | 63.00 | 99.71 | 0.21 | 1000.00 | 100.00 | 0.00 |

Table A.3a: Droplet Diameter vs. Cumulative (%) and Volume Frequency (%) respectively for Conditions of Figure A3a

| Size (µm) | % < | % In | Size (µm) | % < | % In | Size (µm) | % < | % In |
|---|---|---|---|---|---|---|---|---|
| 0.287 | 0.00 | 0.00 | 4.56 | 8.02 | 7.43 | 72.33 | 100.00 | 0.00 |
| 0.330 | 0.00 | 0.00 | 5.23 | 26.81 | 18.79 | 83.06 | 100.00 | 0.00 |
| 0.378 | 0.00 | 0.00 | 6.01 | 46.15 | 19.34 | 95.37 | 100.00 | 0.00 |
| 0.435 | 0.00 | 0.00 | 6.90 | 57.52 | 11.37 | 109.51 | 100.00 | 0.00 |
| 0.499 | 0.00 | 0.00 | 7.92 | 63.53 | 6.01 | 125.74 | 100.00 | 0.00 |
| 0.573 | 0.00 | 0.00 | 9.10 | 68.51 | 4.98 | 144.38 | 100.00 | 0.00 |
| 0.658 | 0.00 | 0.00 | 10.44 | 74.42 | 5.90 | 165.79 | 100.00 | 0.00 |
| 0.755 | 0.00 | 0.00 | 11.99 | 81.72 | 7.30 | 190.37 | 100.00 | 0.00 |
| 0.867 | 0.00 | 0.00 | 13.77 | 88.74 | 7.03 | 218.59 | 100.00 | 0.00 |
| 0.996 | 0.00 | 0.00 | 15.81 | 93.98 | 5.24 | 250.99 | 100.00 | 0.00 |
| 1.14 | 0.00 | 0.00 | 18.16 | 97.19 | 3.21 | 288.20 | 100.00 | 0.00 |
| 1.31 | 0.00 | 0.00 | 20.85 | 98.85 | 1.66 | 330.92 | 100.00 | 0.00 |
| 1.51 | 0.00 | 0.00 | 23.94 | 99.58 | 0.74 | 379.98 | 100.00 | 0.00 |
| 1.73 | 0.00 | 0.00 | 27.49 | 99.87 | 0.29 | 436.31 | 100.00 | 0.00 |
| 1.99 | 0.00 | 0.00 | 31.56 | 99.97 | 0.10 | 500.99 | 100.00 | 0.00 |
| 2.28 | 0.00 | 0.00 | 36.24 | 100.00 | 0.03 | 575.26 | 100.00 | 0.00 |
| 2.62 | 0.00 | 0.00 | 41.61 | 100.00 | 0.00 | 660.54 | 100.00 | 0.00 |
| 3.01 | 0.00 | 0.00 | 47.78 | 100.00 | 0.00 | 758.46 | 100.00 | 0.00 |
| 3.46 | 0.01 | 0.01 | 54.86 | 100.00 | 0.00 | 870.89 | 100.00 | 0.00 |
| 3.97 | 0.60 | 0.59 | 63.00 | 100.00 | 0.00 | 1000.00 | 100.00 | 0.00 |

Table A.3b: Droplet Diameter vs. Cumulative (%) and Volume Frequency (%) respectively for Conditions of Figure A3b

| Size (µm) | % < | % In | Size (µm) | % < | % In | Size (µm) | % < | % In |
|---|---|---|---|---|---|---|---|---|
| 0.287 | 0.00 | 0.00 | 4.56 | 7.91 | 7.51 | 72.33 | 100.00 | 0.00 |
| 0.330 | 0.00 | 0.00 | 5.23 | 28.19 | 20.27 | 83.06 | 100.00 | 0.00 |
| 0.378 | 0.00 | 0.00 | 6.01 | 49.01 | 20.82 | 95.37 | 100.00 | 0.00 |
| 0.435 | 0.00 | 0.00 | 6.90 | 60.76 | 11.75 | 109.51 | 100.00 | 0.00 |
| 0.499 | 0.00 | 0.00 | 7.92 | 66.64 | 5.88 | 125.74 | 100.00 | 0.00 |
| 0.573 | 0.00 | 0.00 | 9.10 | 71.40 | 4.76 | 144.38 | 100.00 | 0.00 |
| 0.658 | 0.00 | 0.00 | 10.44 | 77.04 | 5.64 | 165.79 | 100.00 | 0.00 |
| 0.755 | 0.00 | 0.00 | 11.99 | 83.98 | 6.95 | 190.37 | 100.00 | 0.00 |
| 0.867 | 0.00 | 0.00 | 13.77 | 90.46 | 6.47 | 218.59 | 100.00 | 0.00 |
| 0.996 | 0.00 | 0.00 | 15.81 | 95.05 | 4.60 | 250.99 | 100.00 | 0.00 |
| 1.14 | 0.00 | 0.00 | 18.16 | 97.73 | 2.67 | 288.20 | 100.00 | 0.00 |
| 1.31 | 0.00 | 0.00 | 20.85 | 99.05 | 1.32 | 330.92 | 100.00 | 0.00 |
| 1.51 | 0.00 | 0.00 | 23.94 | 99.63 | 0.58 | 379.98 | 100.00 | 0.00 |
| 1.73 | 0.00 | 0.00 | 27.49 | 99.87 | 0.24 | 436.31 | 100.00 | 0.00 |
| 1.99 | 0.00 | 0.00 | 31.56 | 99.96 | 0.09 | 500.99 | 100.00 | 0.00 |
| 2.28 | 0.00 | 0.00 | 36.24 | 99.99 | 0.03 | 575.26 | 100.00 | 0.00 |
| 2.62 | 0.00 | 0.00 | 41.61 | 100.00 | 0.01 | 660.54 | 100.00 | 0.00 |
| 3.01 | 0.00 | 0.00 | 47.78 | 100.00 | 0.00 | 758.46 | 100.00 | 0.00 |
| 3.46 | 0.00 | 0.00 | 54.86 | 100.00 | 0.00 | 870.89 | 100.00 | 0.00 |
| 3.97 | 0.41 | 0.40 | 63.00 | 100.00 | 0.00 | 1000.00 | 100.00 | 0.00 |

Table A.3c: Droplet Diameter vs. Cumulative (%) and Volume Frequency (%) respectively for Conditions of Figure A3c

| Size (µm) | % < | % In | Size (µm) | % < | % In | Size (µm) | % < | % In |
|---|---|---|---|---|---|---|---|---|
| 0.287 | 0.00 | 0.00 | 4.56 | 6.57 | 6.33 | 72.33 | 100.00 | 0.00 |
| 0.330 | 0.00 | 0.00 | 5.23 | 27.31 | 20.74 | 83.06 | 100.00 | 0.00 |
| 0.378 | 0.00 | 0.00 | 6.01 | 49.60 | 22.29 | 95.37 | 100.00 | 0.00 |
| 0.435 | 0.00 | 0.00 | 6.90 | 62.14 | 12.54 | 109.51 | 100.00 | 0.00 |
| 0.499 | 0.00 | 0.00 | 7.92 | 68.03 | 5.89 | 125.74 | 100.00 | 0.00 |
| 0.573 | 0.00 | 0.00 | 9.10 | 72.63 | 4.60 | 144.38 | 100.00 | 0.00 |
| 0.658 | 0.00 | 0.00 | 10.44 | 78.06 | 5.43 | 165.79 | 100.00 | 0.00 |
| 0.755 | 0.00 | 0.00 | 11.99 | 84.78 | 6.72 | 190.37 | 100.00 | 0.00 |
| 0.867 | 0.00 | 0.00 | 13.77 | 90.96 | 6.18 | 218.59 | 100.00 | 0.00 |
| 0.996 | 0.00 | 0.00 | 15.81 | 95.27 | 4.31 | 250.99 | 100.00 | 0.00 |
| 1.14 | 0.00 | 0.00 | 18.16 | 97.76 | 2.49 | 288.20 | 100.00 | 0.00 |
| 1.31 | 0.00 | 0.00 | 20.85 | 99.00 | 1.24 | 330.92 | 100.00 | 0.00 |
| 1.51 | 0.00 | 0.00 | 23.94 | 99.56 | 0.56 | 379.98 | 100.00 | 0.00 |
| 1.73 | 0.00 | 0.00 | 27.49 | 99.81 | 0.25 | 436.31 | 100.00 | 0.00 |
| 1.99 | 0.00 | 0.00 | 31.56 | 99.92 | 0.11 | 500.99 | 100.00 | 0.00 |
| 2.28 | 0.00 | 0.00 | 36.24 | 99.97 | 0.05 | 575.26 | 100.00 | 0.00 |
| 2.62 | 0.00 | 0.00 | 41.61 | 99.99 | 0.02 | 660.54 | 100.00 | 0.00 |
| 3.01 | 0.00 | 0.00 | 47.78 | 100.00 | 0.01 | 758.46 | 100.00 | 0.00 |
| 3.46 | 0.00 | 0.00 | 54.86 | 100.00 | 0.00 | 870.89 | 100.00 | 0.00 |
| 3.97 | 0.25 | 0.25 | 63.00 | 100.00 | 0.00 | 1000.00 | 100.00 | 0.00 |

Table A.3d: Droplet Diameter vs. Cumulative (%) and Volume Frequency (%) respectively for Conditions of Figure A3d

| Size (µm) | % < | % In | Size (µm) | % < | % In | Size (µm) | % < | % In |
|---|---|---|---|---|---|---|---|---|
| 0.287 | 0.00 | 0.00 | 4.56 | 8.62 | 8.09 | 72.33 | 99.99 | 0.01 |
| 0.330 | 0.00 | 0.00 | 5.23 | 29.29 | 20.67 | 83.06 | 100.00 | 0.01 |
| 0.378 | 0.00 | 0.00 | 6.01 | 49.81 | 20.52 | 95.37 | 100.00 | 0.00 |
| 0.435 | 0.00 | 0.00 | 6.90 | 60.94 | 11.13 | 109.51 | 100.00 | 0.00 |
| 0.499 | 0.00 | 0.00 | 7.92 | 66.53 | 5.59 | 125.74 | 100.00 | 0.00 |
| 0.573 | 0.00 | 0.00 | 9.10 | 71.21 | 4.69 | 144.38 | 100.00 | 0.00 |
| 0.658 | 0.00 | 0.00 | 10.44 | 76.84 | 5.63 | 165.79 | 100.00 | 0.00 |
| 0.755 | 0.00 | 0.00 | 11.99 | 83.63 | 6.79 | 190.37 | 100.00 | 0.00 |
| 0.867 | 0.00 | 0.00 | 13.77 | 89.76 | 6.13 | 218.59 | 100.00 | 0.00 |
| 0.996 | 0.00 | 0.00 | 15.81 | 94.13 | 4.37 | 250.99 | 100.00 | 0.00 |
| 1.14 | 0.00 | 0.00 | 18.16 | 96.79 | 2.65 | 288.20 | 100.00 | 0.00 |
| 1.31 | 0.00 | 0.00 | 20.85 | 98.22 | 1.44 | 330.92 | 100.00 | 0.00 |
| 1.51 | 0.00 | 0.00 | 23.94 | 98.97 | 0.74 | 379.98 | 100.00 | 0.00 |
| 1.73 | 0.00 | 0.00 | 27.49 | 99.36 | 0.40 | 436.31 | 100.00 | 0.00 |
| 1.99 | 0.00 | 0.00 | 31.56 | 99.59 | 0.23 | 500.99 | 100.00 | 0.00 |
| 2.28 | 0.00 | 0.00 | 36.24 | 99.74 | 0.15 | 575.26 | 100.00 | 0.00 |
| 2.62 | 0.00 | 0.00 | 41.61 | 99.84 | 0.10 | 660.54 | 100.00 | 0.00 |
| 3.01 | 0.00 | 0.00 | 47.78 | 99.91 | 0.07 | 758.46 | 100.00 | 0.00 |
| 3.46 | 0.01 | 0.01 | 54.86 | 99.95 | 0.04 | 870.89 | 100.00 | 0.00 |
| 3.97 | 0.53 | 0.52 | 63.00 | 99.98 | 0.03 | 1000.00 | 100.00 | 0.00 |

Table A.3e: Droplet Diameter vs. Cumulative (%) and Volume Frequency (%) respectively for Conditions of Figure A3e

| Size (µm) | % < | % In | Size (µm) | % < | % In | Size (µm) | % < | % In |
|---|---|---|---|---|---|---|---|---|
| 0.287 | 0.00 | 0.00 | 4.56 | 6.60 | 6.12 | 72.33 | 100.00 | 0.00 |
| 0.330 | 0.00 | 0.00 | 5.23 | 26.43 | 19.82 | 83.06 | 100.00 | 0.00 |
| 0.378 | 0.00 | 0.00 | 6.01 | 47.88 | 21.46 | 95.37 | 100.00 | 0.00 |
| 0.435 | 0.00 | 0.00 | 6.90 | 60.21 | 12.32 | 109.51 | 100.00 | 0.00 |
| 0.499 | 0.00 | 0.00 | 7.92 | 66.22 | 6.01 | 125.74 | 100.00 | 0.00 |
| 0.573 | 0.00 | 0.00 | 9.10 | 71.10 | 4.88 | 144.38 | 100.00 | 0.00 |
| 0.658 | 0.00 | 0.00 | 10.44 | 76.87 | 5.78 | 165.79 | 100.00 | 0.00 |
| 0.755 | 0.00 | 0.00 | 11.99 | 83.86 | 6.99 | 190.37 | 100.00 | 0.00 |
| 0.867 | 0.00 | 0.00 | 13.77 | 90.20 | 6.33 | 218.59 | 100.00 | 0.00 |
| 0.996 | 0.00 | 0.00 | 15.81 | 94.69 | 4.49 | 250.99 | 100.00 | 0.00 |
| 1.14 | 0.00 | 0.00 | 18.16 | 97.37 | 2.69 | 288.20 | 100.00 | 0.00 |
| 1.31 | 0.00 | 0.00 | 20.85 | 98.79 | 1.41 | 330.92 | 100.00 | 0.00 |
| 1.51 | 0.00 | 0.00 | 23.94 | 99.47 | 0.68 | 379.98 | 100.00 | 0.00 |
| 1.73 | 0.00 | 0.00 | 27.49 | 99.78 | 0.31 | 436.31 | 100.00 | 0.00 |
| 1.99 | 0.00 | 0.00 | 31.56 | 99.91 | 0.14 | 500.99 | 100.00 | 0.00 |
| 2.28 | 0.00 | 0.00 | 36.24 | 99.97 | 0.06 | 575.26 | 100.00 | 0.00 |
| 2.62 | 0.00 | 0.00 | 41.61 | 99.99 | 0.02 | 660.54 | 100.00 | 0.00 |
| 3.01 | 0.00 | 0.00 | 47.78 | 100.00 | 0.01 | 758.46 | 100.00 | 0.00 |
| 3.46 | 0.02 | 0.02 | 54.86 | 100.00 | 0.00 | 870.89 | 100.00 | 0.00 |
| 3.97 | 0.49 | 0.47 | 63.00 | 100.00 | 0.00 | 1000.00 | 100.00 | 0.00 |

Table A.3f: Droplet Diameter vs. Cumulative (%) and Volume Frequency (%) respectively for Conditions of Figure A3f

| Size (µm) | % < | % In | Size (µm) | % < | % In | Size (µm) | % < | % In |
|---|---|---|---|---|---|---|---|---|
| 0.287 | 0.00 | 0.00 | 4.56 | 3.64 | 3.57 | 72.33 | 100.00 | 0.00 |
| 0.330 | 0.00 | 0.00 | 5.23 | 26.39 | 22.75 | 83.06 | 100.00 | 0.00 |
| 0.378 | 0.00 | 0.00 | 6.01 | 51.94 | 25.55 | 95.37 | 100.00 | 0.00 |
| 0.435 | 0.00 | 0.00 | 6.90 | 64.42 | 12.49 | 109.51 | 100.00 | 0.00 |
| 0.499 | 0.00 | 0.00 | 7.92 | 68.63 | 4.21 | 125.74 | 100.00 | 0.00 |
| 0.573 | 0.00 | 0.00 | 9.10 | 72.21 | 3.57 | 144.38 | 100.00 | 0.00 |
| 0.658 | 0.00 | 0.00 | 10.44 | 77.50 | 5.29 | 165.79 | 100.00 | 0.00 |
| 0.755 | 0.00 | 0.00 | 11.99 | 85.20 | 7.70 | 190.37 | 100.00 | 0.00 |
| 0.867 | 0.00 | 0.00 | 13.77 | 92.06 | 6.86 | 218.59 | 100.00 | 0.00 |
| 0.996 | 0.00 | 0.00 | 15.81 | 96.32 | 4.26 | 250.99 | 100.00 | 0.00 |
| 1.14 | 0.00 | 0.00 | 18.16 | 98.44 | 2.12 | 288.20 | 100.00 | 0.00 |
| 1.31 | 0.00 | 0.00 | 20.85 | 99.33 | 0.89 | 330.92 | 100.00 | 0.00 |
| 1.51 | 0.00 | 0.00 | 23.94 | 99.67 | 0.35 | 379.98 | 100.00 | 0.00 |
| 1.73 | 0.00 | 0.00 | 27.49 | 99.82 | 0.14 | 436.31 | 100.00 | 0.00 |
| 1.99 | 0.00 | 0.00 | 31.56 | 99.88 | 0.07 | 500.99 | 100.00 | 0.00 |
| 2.28 | 0.00 | 0.00 | 36.24 | 99.92 | 0.04 | 575.26 | 100.00 | 0.00 |
| 2.62 | 0.00 | 0.00 | 41.61 | 99.95 | 0.03 | 660.54 | 100.00 | 0.00 |
| 3.01 | 0.00 | 0.00 | 47.78 | 99.97 | 0.02 | 758.46 | 100.00 | 0.00 |
| 3.46 | 0.00 | 0.00 | 54.86 | 99.99 | 0.02 | 870.89 | 100.00 | 0.00 |
| 3.97 | 0.07 | 0.07 | 63.00 | 100.00 | 0.01 | 1000.00 | 100.00 | 0.00 |

Table A.4a: Droplet Diameter vs. Cumulative (%) and Volume Frequency (%) respectively for Conditions of Figure A4a

| Size (µm) | % < | % In | Size (µm) | % < | % In | Size (µm) | % < | % In |
|---|---|---|---|---|---|---|---|---|
| 0.287 | 0.00 | 0.00 | 4.56 | 6.17 | 5.93 | 72.33 | 100.00 | 0.00 |
| 0.330 | 0.00 | 0.00 | 5.23 | 24.95 | 18.78 | 83.06 | 100.00 | 0.00 |
| 0.378 | 0.00 | 0.00 | 6.01 | 45.50 | 20.55 | 95.37 | 100.00 | 0.00 |
| 0.435 | 0.00 | 0.00 | 6.90 | 57.75 | 12.25 | 109.51 | 100.00 | 0.00 |
| 0.499 | 0.00 | 0.00 | 7.92 | 63.95 | 6.20 | 125.74 | 100.00 | 0.00 |
| 0.573 | 0.00 | 0.00 | 9.10 | 68.93 | 4.98 | 144.38 | 100.00 | 0.00 |
| 0.658 | 0.00 | 0.00 | 10.44 | 74.79 | 5.86 | 165.79 | 100.00 | 0.00 |
| 0.755 | 0.00 | 0.00 | 11.99 | 82.00 | 7.22 | 190.37 | 100.00 | 0.00 |
| 0.867 | 0.00 | 0.00 | 13.77 | 88.82 | 6.81 | 218.59 | 100.00 | 0.00 |
| 0.996 | 0.00 | 0.00 | 15.81 | 93.83 | 5.01 | 250.99 | 100.00 | 0.00 |
| 1.14 | 0.00 | 0.00 | 18.16 | 96.91 | 3.08 | 288.20 | 100.00 | 0.00 |
| 1.31 | 0.00 | 0.00 | 20.85 | 98.57 | 1.65 | 330.92 | 100.00 | 0.00 |
| 1.51 | 0.00 | 0.00 | 23.94 | 99.37 | 0.81 | 379.98 | 100.00 | 0.00 |
| 1.73 | 0.00 | 0.00 | 27.49 | 99.74 | 0.37 | 436.31 | 100.00 | 0.00 |
| 1.99 | 0.00 | 0.00 | 31.56 | 99.90 | 0.16 | 500.99 | 100.00 | 0.00 |
| 2.28 | 0.00 | 0.00 | 36.24 | 99.97 | 0.07 | 575.26 | 100.00 | 0.00 |
| 2.62 | 0.00 | 0.00 | 41.61 | 99.99 | 0.02 | 660.54 | 100.00 | 0.00 |
| 3.01 | 0.00 | 0.00 | 47.78 | 100.00 | 0.01 | 758.46 | 100.00 | 0.00 |
| 3.46 | 0.00 | 0.00 | 54.86 | 100.00 | 0.00 | 870.89 | 100.00 | 0.00 |
| 3.97 | 0.24 | 0.24 | 63.00 | 100.00 | 0.00 | 1000.00 | 100.00 | 0.00 |

Table A.4b: Droplet Diameter vs. Cumulative (%) and Volume Frequency (%) respectively for Conditions of Figure A4b

| Size (µm) | % < | % In | Size (µm) | % < | % In | Size (µm) | % < | % In |
|---|---|---|---|---|---|---|---|---|
| 0.287 | 0.00 | 0.00 | 4.56 | 5.62 | 5.43 | 72.33 | 100.00 | 0.00 |
| 0.330 | 0.00 | 0.00 | 5.23 | 25.16 | 19.54 | 83.06 | 100.00 | 0.00 |
| 0.378 | 0.00 | 0.00 | 6.01 | 47.28 | 22.12 | 95.37 | 100.00 | 0.00 |
| 0.435 | 0.00 | 0.00 | 6.90 | 60.58 | 13.29 | 109.51 | 100.00 | 0.00 |
| 0.499 | 0.00 | 0.00 | 7.92 | 66.97 | 6.39 | 125.74 | 100.00 | 0.00 |
| 0.573 | 0.00 | 0.00 | 9.10 | 71.82 | 4.85 | 144.38 | 100.00 | 0.00 |
| 0.658 | 0.00 | 0.00 | 10.44 | 77.33 | 5.52 | 165.79 | 100.00 | 0.00 |
| 0.755 | 0.00 | 0.00 | 11.99 | 84.05 | 6.71 | 190.37 | 100.00 | 0.00 |
| 0.867 | 0.00 | 0.00 | 13.77 | 90.34 | 6.30 | 218.59 | 100.00 | 0.00 |
| 0.996 | 0.00 | 0.00 | 15.81 | 94.89 | 4.54 | 250.99 | 100.00 | 0.00 |
| 1.14 | 0.00 | 0.00 | 18.16 | 97.59 | 2.70 | 288.20 | 100.00 | 0.00 |
| 1.31 | 0.00 | 0.00 | 20.85 | 98.96 | 1.37 | 330.92 | 100.00 | 0.00 |
| 1.51 | 0.00 | 0.00 | 23.94 | 99.58 | 0.62 | 379.98 | 100.00 | 0.00 |
| 1.73 | 0.00 | 0.00 | 27.49 | 99.85 | 0.26 | 436.31 | 100.00 | 0.00 |
| 1.99 | 0.00 | 0.00 | 31.56 | 99.95 | 0.10 | 500.99 | 100.00 | 0.00 |
| 2.28 | 0.00 | 0.00 | 36.24 | 99.99 | 0.04 | 575.26 | 100.00 | 0.00 |
| 2.62 | 0.00 | 0.00 | 41.61 | 100.00 | 0.01 | 660.54 | 100.00 | 0.00 |
| 3.01 | 0.00 | 0.00 | 47.78 | 100.00 | 0.00 | 758.46 | 100.00 | 0.00 |
| 3.46 | 0.00 | 0.00 | 54.86 | 100.00 | 0.00 | 870.89 | 100.00 | 0.00 |
| 3.97 | 0.18 | 0.18 | 63.00 | 100.00 | 0.00 | 1000.00 | 100.00 | 0.00 |

Table A.4c: Droplet Diameter vs. Cumulative (%) and Volume Frequency (%) respectively for Conditions of Figure A4c

| Size (µm) | % < | % In | Size (µm) | % < | % In | Size (µm) | % < | % In |
|---|---|---|---|---|---|---|---|---|
| 0.287 | 0.00 | 0.00 | 4.56 | 4.64 | 4.55 | 72.33 | 100.00 | 0.00 |
| 0.330 | 0.00 | 0.00 | 5.23 | 24.79 | 20.16 | 83.06 | 100.00 | 0.00 |
| 0.378 | 0.00 | 0.00 | 6.01 | 48.02 | 23.22 | 95.37 | 100.00 | 0.00 |
| 0.435 | 0.00 | 0.00 | 6.90 | 61.46 | 13.44 | 109.51 | 100.00 | 0.00 |
| 0.499 | 0.00 | 0.00 | 7.92 | 67.44 | 5.98 | 125.74 | 100.00 | 0.00 |
| 0.573 | 0.00 | 0.00 | 9.10 | 71.96 | 4.53 | 144.38 | 100.00 | 0.00 |
| 0.658 | 0.00 | 0.00 | 10.44 | 77.35 | 5.39 | 165.79 | 100.00 | 0.00 |
| 0.755 | 0.00 | 0.00 | 11.99 | 84.20 | 6.85 | 190.37 | 100.00 | 0.00 |
| 0.867 | 0.00 | 0.00 | 13.77 | 90.69 | 6.49 | 218.59 | 100.00 | 0.00 |
| 0.996 | 0.00 | 0.00 | 15.81 | 95.28 | 4.59 | 250.99 | 100.00 | 0.00 |
| 1.14 | 0.00 | 0.00 | 18.16 | 97.90 | 2.62 | 288.20 | 100.00 | 0.00 |
| 1.31 | 0.00 | 0.00 | 20.85 | 99.16 | 1.25 | 330.92 | 100.00 | 0.00 |
| 1.51 | 0.00 | 0.00 | 23.94 | 99.69 | 0.53 | 379.98 | 100.00 | 0.00 |
| 1.73 | 0.00 | 0.00 | 27.49 | 99.89 | 0.21 | 436.31 | 100.00 | 0.00 |
| 1.99 | 0.00 | 0.00 | 31.56 | 99.97 | 0.08 | 500.99 | 100.00 | 0.00 |
| 2.28 | 0.00 | 0.00 | 36.24 | 99.99 | 0.03 | 575.26 | 100.00 | 0.00 |
| 2.62 | 0.00 | 0.00 | 41.61 | 100.00 | 0.01 | 660.54 | 100.00 | 0.00 |
| 3.01 | 0.00 | 0.00 | 47.78 | 100.00 | 0.00 | 758.46 | 100.00 | 0.00 |
| 3.46 | 0.00 | 0.00 | 54.86 | 100.00 | 0.00 | 870.89 | 100.00 | 0.00 |
| 3.97 | 0.09 | 0.09 | 63.00 | 100.00 | 0.00 | 1000.00 | 100.00 | 0.00 |

Table A.4d: Droplet Diameter vs. Cumulative (%) and Volume Frequency (%) respectively for Conditions of Figure A4d

| Size (µm) | % < | % In | Size (µm) | % < | % In | Size (µm) | % < | % In |
|---|---|---|---|---|---|---|---|---|
| 0.287 | 0.00 | 0.00 | 4.56 | 5.00 | 4.90 | 72.33 | 100.00 | 0.00 |
| 0.330 | 0.00 | 0.00 | 5.23 | 25.50 | 20.50 | 83.06 | 100.00 | 0.00 |
| 0.378 | 0.00 | 0.00 | 6.01 | 48.32 | 22.82 | 95.37 | 100.00 | 0.00 |
| 0.435 | 0.00 | 0.00 | 6.90 | 60.93 | 12.61 | 109.51 | 100.00 | 0.00 |
| 0.499 | 0.00 | 0.00 | 7.92 | 66.52 | 5.59 | 125.74 | 100.00 | 0.00 |
| 0.573 | 0.00 | 0.00 | 9.10 | 70.91 | 4.39 | 144.38 | 100.00 | 0.00 |
| 0.658 | 0.00 | 0.00 | 10.44 | 76.30 | 5.39 | 165.79 | 100.00 | 0.00 |
| 0.755 | 0.00 | 0.00 | 11.99 | 83.20 | 6.90 | 190.37 | 100.00 | 0.00 |
| 0.867 | 0.00 | 0.00 | 13.77 | 89.70 | 6.50 | 218.59 | 100.00 | 0.00 |
| 0.996 | 0.00 | 0.00 | 15.81 | 94.38 | 4.67 | 250.99 | 100.00 | 0.00 |
| 1.14 | 0.00 | 0.00 | 18.16 | 97.17 | 2.79 | 288.20 | 100.00 | 0.00 |
| 1.31 | 0.00 | 0.00 | 20.85 | 98.63 | 1.46 | 330.92 | 100.00 | 0.00 |
| 1.51 | 0.00 | 0.00 | 23.94 | 99.34 | 0.71 | 379.98 | 100.00 | 0.00 |
| 1.73 | 0.00 | 0.00 | 27.49 | 99.68 | 0.34 | 436.31 | 100.00 | 0.00 |
| 1.99 | 0.00 | 0.00 | 31.56 | 99.85 | 0.17 | 500.99 | 100.00 | 0.00 |
| 2.28 | 0.00 | 0.00 | 36.24 | 99.94 | 0.08 | 575.26 | 100.00 | 0.00 |
| 2.62 | 0.00 | 0.00 | 41.61 | 99.98 | 0.04 | 660.54 | 100.00 | 0.00 |
| 3.01 | 0.00 | 0.00 | 47.78 | 99.99 | 0.02 | 758.46 | 100.00 | 0.00 |
| 3.46 | 0.00 | 0.00 | 54.86 | 100.00 | 0.01 | 870.89 | 100.00 | 0.00 |
| 3.97 | 0.10 | 0.10 | 63.00 | 100.00 | 0.00 | 1000.00 | 100.00 | 0.00 |

Table A.4e: Droplet Diameter vs. Cumulative (%) and Volume Frequency (%) respectively for Conditions of Figure A4e

| Size (µm) | % < | % In | Size (µm) | % < | % In | Size (µm) | % < | % In |
|---|---|---|---|---|---|---|---|---|
| 0.287 | 0.00 | 0.00 | 4.56 | 0.00 | 0.00 | 72.33 | 100.00 | 0.13 |
| 0.330 | 0.00 | 0.00 | 5.23 | 10.26 | 10.26 | 83.06 | 100.00 | 0.00 |
| 0.378 | 0.00 | 0.00 | 6.01 | 40.49 | 30.23 | 95.37 | 100.00 | 0.00 |
| 0.435 | 0.00 | 0.00 | 6.90 | 67.52 | 27.04 | 109.51 | 100.00 | 0.00 |
| 0.499 | 0.00 | 0.00 | 7.92 | 68.61 | 1.09 | 125.74 | 100.00 | 0.00 |
| 0.573 | 0.00 | 0.00 | 9.10 | 70.16 | 1.55 | 144.38 | 100.00 | 0.00 |
| 0.658 | 0.00 | 0.00 | 10.44 | 76.90 | 6.74 | 165.79 | 100.00 | 0.00 |
| 0.755 | 0.00 | 0.00 | 11.99 | 96.76 | 19.86 | 190.37 | 100.00 | 0.00 |
| 0.867 | 0.00 | 0.00 | 13.77 | 99.25 | 2.49 | 218.59 | 100.00 | 0.00 |
| 0.996 | 0.00 | 0.00 | 15.81 | 99.53 | 0.28 | 250.99 | 100.00 | 0.00 |
| 1.14 | 0.00 | 0.00 | 18.16 | 99.53 | 0.00 | 288.20 | 100.00 | 0.00 |
| 1.31 | 0.00 | 0.00 | 20.85 | 99.53 | 0.00 | 330.92 | 100.00 | 0.00 |
| 1.51 | 0.00 | 0.00 | 23.94 | 99.53 | 0.00 | 379.98 | 100.00 | 0.00 |
| 1.73 | 0.00 | 0.00 | 27.49 | 99.53 | 0.00 | 436.31 | 100.00 | 0.00 |
| 1.99 | 0.00 | 0.00 | 31.56 | 99.53 | 0.00 | 500.99 | 100.00 | 0.00 |
| 2.28 | 0.00 | 0.00 | 36.24 | 99.53 | 0.00 | 575.26 | 100.00 | 0.00 |
| 2.62 | 0.00 | 0.00 | 41.61 | 99.53 | 0.00 | 660.54 | 100.00 | 0.00 |
| 3.01 | 0.00 | 0.00 | 47.78 | 99.53 | 0.00 | 758.46 | 100.00 | 0.00 |
| 3.46 | 0.00 | 0.00 | 54.86 | 99.53 | 0.00 | 870.89 | 100.00 | 0.00 |
| 3.97 | 0.00 | 0.00 | 63.00 | 99.87 | 0.34 | 1000.00 | 100.00 | 0.00 |

Table A.4f: Droplet Diameter vs. Cumulative (%) and Volume Frequency (%) respectively for Conditions of Figure A4f

| Size (µm) | % < | % In | Size (µm) | % < | % In | Size (µm) | % < | % In |
|---|---|---|---|---|---|---|---|---|
| 0.287 | 0.00 | 0.00 | 4.56 | 0.00 | 0.00 | 72.33 | 99.98 | 0.20 |
| 0.330 | 0.00 | 0.00 | 5.23 | 6.92 | 6.92 | 83.06 | 100.00 | 0.02 |
| 0.378 | 0.00 | 0.00 | 6.01 | 36.51 | 29.58 | 95.37 | 100.00 | 0.00 |
| 0.435 | 0.00 | 0.00 | 6.90 | 65.96 | 29.45 | 109.51 | 100.00 | 0.00 |
| 0.499 | 0.00 | 0.00 | 7.92 | 67.02 | 1.06 | 125.74 | 100.00 | 0.00 |
| 0.573 | 0.00 | 0.00 | 9.10 | 68.36 | 1.34 | 144.38 | 100.00 | 0.00 |
| 0.658 | 0.00 | 0.00 | 10.44 | 74.52 | 6.16 | 165.79 | 100.00 | 0.00 |
| 0.755 | 0.00 | 0.00 | 11.99 | 95.83 | 21.31 | 190.37 | 100.00 | 0.00 |
| 0.867 | 0.00 | 0.00 | 13.77 | 98.96 | 3.13 | 218.59 | 100.00 | 0.00 |
| 0.996 | 0.00 | 0.00 | 15.81 | 99.34 | 0.38 | 250.99 | 100.00 | 0.00 |
| 1.14 | 0.00 | 0.00 | 18.16 | 99.34 | 0.00 | 288.20 | 100.00 | 0.00 |
| 1.31 | 0.00 | 0.00 | 20.85 | 99.34 | 0.00 | 330.92 | 100.00 | 0.00 |
| 1.51 | 0.00 | 0.00 | 23.94 | 99.34 | 0.00 | 379.98 | 100.00 | 0.00 |
| 1.73 | 0.00 | 0.00 | 27.49 | 99.34 | 0.00 | 436.31 | 100.00 | 0.00 |
| 1.99 | 0.00 | 0.00 | 31.56 | 99.34 | 0.00 | 500.99 | 100.00 | 0.00 |
| 2.28 | 0.00 | 0.00 | 36.24 | 99.34 | 0.00 | 575.26 | 100.00 | 0.00 |
| 2.62 | 0.00 | 0.00 | 41.61 | 99.34 | 0.00 | 660.54 | 100.00 | 0.00 |
| 3.01 | 0.00 | 0.00 | 47.78 | 99.34 | 0.00 | 758.46 | 100.00 | 0.00 |
| 3.46 | 0.00 | 0.00 | 54.86 | 99.34 | 0.00 | 870.89 | 100.00 | 0.00 |
| 3.97 | 0.00 | 0.00 | 63.00 | 99.77 | 0.43 | 1000.00 | 100.00 | 0.00 |

Table A.5a: Droplet Diameter vs. Cumulative (%) and Volume Frequency (%) respectively for Conditions of Figure A5a

| Size (µm) | % < | % In | Size (µm) | % < | % In | Size (µm) | % < | % In |
|---|---|---|---|---|---|---|---|---|
| 0.287 | 0.00 | 0.00 | 4.56 | 8.39 | 7.69 | 72.33 | 100.00 | 0.00 |
| 0.330 | 0.00 | 0.00 | 5.23 | 27.08 | 18.69 | 83.06 | 100.00 | 0.00 |
| 0.378 | 0.00 | 0.00 | 6.01 | 46.61 | 19.53 | 95.37 | 100.00 | 0.00 |
| 0.435 | 0.00 | 0.00 | 6.90 | 58.55 | 11.94 | 109.51 | 100.00 | 0.00 |
| 0.499 | 0.00 | 0.00 | 7.92 | 64.77 | 6.22 | 125.74 | 100.00 | 0.00 |
| 0.573 | 0.00 | 0.00 | 9.10 | 69.53 | 4.76 | 144.38 | 100.00 | 0.00 |
| 0.658 | 0.00 | 0.00 | 10.44 | 74.89 | 5.36 | 165.79 | 100.00 | 0.00 |
| 0.755 | 0.00 | 0.00 | 11.99 | 81.70 | 6.81 | 190.37 | 100.00 | 0.00 |
| 0.867 | 0.00 | 0.00 | 13.77 | 88.76 | 7.06 | 218.59 | 100.00 | 0.00 |
| 0.996 | 0.00 | 0.00 | 15.81 | 94.21 | 5.45 | 250.99 | 100.00 | 0.00 |
| 1.14 | 0.00 | 0.00 | 18.16 | 97.49 | 3.28 | 288.20 | 100.00 | 0.00 |
| 1.31 | 0.00 | 0.00 | 20.85 | 99.07 | 1.58 | 330.92 | 100.00 | 0.00 |
| 1.51 | 0.00 | 0.00 | 23.94 | 99.69 | 0.62 | 379.98 | 100.00 | 0.00 |
| 1.73 | 0.00 | 0.00 | 27.49 | 99.90 | 0.21 | 436.31 | 100.00 | 0.00 |
| 1.99 | 0.00 | 0.00 | 31.56 | 99.97 | 0.07 | 500.99 | 100.00 | 0.00 |
| 2.28 | 0.00 | 0.00 | 36.24 | 99.99 | 0.02 | 575.26 | 100.00 | 0.00 |
| 2.62 | 0.00 | 0.00 | 41.61 | 100.00 | 0.01 | 660.54 | 100.00 | 0.00 |
| 3.01 | 0.00 | 0.00 | 47.78 | 100.00 | 0.00 | 758.46 | 100.00 | 0.00 |
| 3.46 | 0.02 | 0.02 | 54.86 | 100.00 | 0.00 | 870.89 | 100.00 | 0.00 |
| 3.97 | 0.71 | 0.69 | 63.00 | 100.00 | 0.00 | 1000.00 | 100.00 | 0.00 |

Table A.5b: Droplet Diameter vs. Cumulative (%) and Volume Frequency (%) respectively for Conditions of Figure A5b

| Size (µm) | % < | % In | Size (µm) | % < | % In | Size (µm) | % < | % In |
|---|---|---|---|---|---|---|---|---|
| 0.287 | 0.00 | 0.00 | 4.56 | 3.54 | 3.50 | 72.33 | 99.90 | 0.01 |
| 0.330 | 0.00 | 0.00 | 5.23 | 23.71 | 20.17 | 83.06 | 99.91 | 0.01 |
| 0.378 | 0.00 | 0.00 | 6.01 | 47.06 | 23.35 | 95.37 | 99.93 | 0.02 |
| 0.435 | 0.00 | 0.00 | 6.90 | 59.69 | 12.63 | 109.51 | 99.96 | 0.03 |
| 0.499 | 0.00 | 0.00 | 7.92 | 64.64 | 4.95 | 125.74 | 100.00 | 0.03 |
| 0.573 | 0.00 | 0.00 | 9.10 | 68.48 | 3.84 | 144.38 | 100.00 | 0.00 |
| 0.658 | 0.00 | 0.00 | 10.44 | 73.66 | 5.18 | 165.79 | 100.00 | 0.00 |
| 0.755 | 0.00 | 0.00 | 11.99 | 81.38 | 7.72 | 190.37 | 100.00 | 0.00 |
| 0.867 | 0.00 | 0.00 | 13.77 | 89.46 | 8.08 | 218.59 | 100.00 | 0.00 |
| 0.996 | 0.00 | 0.00 | 15.81 | 95.14 | 5.68 | 250.99 | 100.00 | 0.00 |
| 1.14 | 0.00 | 0.00 | 18.16 | 98.11 | 2.97 | 288.20 | 100.00 | 0.00 |
| 1.31 | 0.00 | 0.00 | 20.85 | 99.31 | 1.20 | 330.92 | 100.00 | 0.00 |
| 1.51 | 0.00 | 0.00 | 23.94 | 99.70 | 0.39 | 379.98 | 100.00 | 0.00 |
| 1.73 | 0.00 | 0.00 | 27.49 | 99.81 | 0.11 | 436.31 | 100.00 | 0.00 |
| 1.99 | 0.00 | 0.00 | 31.56 | 99.84 | 0.04 | 500.99 | 100.00 | 0.00 |
| 2.28 | 0.00 | 0.00 | 36.24 | 99.86 | 0.02 | 575.26 | 100.00 | 0.00 |
| 2.62 | 0.00 | 0.00 | 41.61 | 99.87 | 0.01 | 660.54 | 100.00 | 0.00 |
| 3.01 | 0.00 | 0.00 | 47.78 | 99.88 | 0.01 | 758.46 | 100.00 | 0.00 |
| 3.46 | 0.00 | 0.00 | 54.86 | 99.88 | 0.01 | 870.89 | 100.00 | 0.00 |
| 3.97 | 0.04 | 0.04 | 63.00 | 99.89 | 0.01 | 1000.00 | 100.00 | 0.00 |

Table A.5c: Droplet Diameter vs. Cumulative (%) and Volume Frequency (%) respectively for Conditions of Figure A5c

| Size (µm) | % < | % In | Size (µm) | % < | % In | Size (µm) | % < | % In |
|---|---|---|---|---|---|---|---|---|
| 0.287 | 0.00 | 0.00 | 4.56 | 8.17 | 7.72 | 72.33 | 98.99 | 0.11 |
| 0.330 | 0.00 | 0.00 | 5.23 | 28.22 | 20.05 | 83.06 | 99.13 | 0.15 |
| 0.378 | 0.00 | 0.00 | 6.01 | 48.06 | 19.84 | 95.37 | 99.36 | 0.23 |
| 0.435 | 0.00 | 0.00 | 6.90 | 58.65 | 10.59 | 109.51 | 99.70 | 0.34 |
| 0.499 | 0.00 | 0.00 | 7.92 | 63.91 | 5.26 | 125.74 | 100.00 | 0.30 |
| 0.573 | 0.00 | 0.00 | 9.10 | 68.51 | 4.60 | 144.38 | 100.00 | 0.00 |
| 0.658 | 0.00 | 0.00 | 10.44 | 74.53 | 6.01 | 165.79 | 100.00 | 0.00 |
| 0.755 | 0.00 | 0.00 | 11.99 | 82.51 | 7.98 | 190.37 | 100.00 | 0.00 |
| 0.867 | 0.00 | 0.00 | 13.77 | 89.86 | 7.35 | 218.59 | 100.00 | 0.00 |
| 0.996 | 0.00 | 0.00 | 15.81 | 94.61 | 4.76 | 250.99 | 100.00 | 0.00 |
| 1.14 | 0.00 | 0.00 | 18.16 | 97.01 | 2.39 | 288.20 | 100.00 | 0.00 |
| 1.31 | 0.00 | 0.00 | 20.85 | 97.98 | 0.98 | 330.92 | 100.00 | 0.00 |
| 1.51 | 0.00 | 0.00 | 23.94 | 98.33 | 0.35 | 379.98 | 100.00 | 0.00 |
| 1.73 | 0.00 | 0.00 | 27.49 | 98.47 | 0.13 | 436.31 | 100.00 | 0.00 |
| 1.99 | 0.00 | 0.00 | 31.56 | 98.53 | 0.06 | 500.99 | 100.00 | 0.00 |
| 2.28 | 0.00 | 0.00 | 36.24 | 98.58 | 0.05 | 575.26 | 100.00 | 0.00 |
| 2.62 | 0.00 | 0.00 | 41.61 | 98.63 | 0.05 | 660.54 | 100.00 | 0.00 |
| 3.01 | 0.00 | 0.00 | 47.78 | 98.69 | 0.06 | 758.46 | 100.00 | 0.00 |
| 3.46 | 0.00 | 0.00 | 54.86 | 98.77 | 0.08 | 870.89 | 100.00 | 0.00 |
| 3.97 | 0.45 | 0.45 | 63.00 | 98.87 | 0.10 | 1000.00 | 100.00 | 0.00 |

Table A.5d: Droplet Diameter vs. Cumulative (%) and Volume Frequency (%) respectively for Conditions of Figure A5d

| Size (µm) | % < | % In | Size (µm) | % < | % In | Size (µm) | % < | % In |
|---|---|---|---|---|---|---|---|---|
| 0.287 | 0.00 | 0.00 | 4.56 | 9.39 | 8.76 | 72.33 | 99.39 | 0.17 |
| 0.330 | 0.00 | 0.00 | 5.23 | 29.29 | 19.90 | 83.06 | 99.54 | 0.15 |
| 0.378 | 0.00 | 0.00 | 6.01 | 47.82 | 18.53 | 95.37 | 99.70 | 0.16 |
| 0.435 | 0.00 | 0.00 | 6.90 | 57.28 | 9.46 | 109.51 | 99.88 | 0.18 |
| 0.499 | 0.00 | 0.00 | 7.92 | 62.20 | 4.92 | 125.74 | 100.00 | 0.12 |
| 0.573 | 0.00 | 0.00 | 9.10 | 66.83 | 4.63 | 144.38 | 100.00 | 0.00 |
| 0.658 | 0.00 | 0.00 | 10.44 | 73.14 | 6.31 | 165.79 | 100.00 | 0.00 |
| 0.755 | 0.00 | 0.00 | 11.99 | 81.61 | 8.47 | 190.37 | 100.00 | 0.00 |
| 0.867 | 0.00 | 0.00 | 13.77 | 89.36 | 7.75 | 218.59 | 100.00 | 0.00 |
| 0.996 | 0.00 | 0.00 | 15.81 | 94.35 | 5.00 | 250.99 | 100.00 | 0.00 |
| 1.14 | 0.00 | 0.00 | 18.16 | 96.86 | 2.51 | 288.20 | 100.00 | 0.00 |
| 1.31 | 0.00 | 0.00 | 20.85 | 97.89 | 1.03 | 330.92 | 100.00 | 0.00 |
| 1.51 | 0.00 | 0.00 | 23.94 | 98.27 | 0.38 | 379.98 | 100.00 | 0.00 |
| 1.73 | 0.00 | 0.00 | 27.49 | 98.42 | 0.15 | 436.31 | 100.00 | 0.00 |
| 1.99 | 0.00 | 0.00 | 31.56 | 98.50 | 0.09 | 500.99 | 100.00 | 0.00 |
| 2.28 | 0.00 | 0.00 | 36.24 | 98.58 | 0.08 | 575.26 | 100.00 | 0.00 |
| 2.62 | 0.00 | 0.00 | 41.61 | 98.68 | 0.10 | 660.54 | 100.00 | 0.00 |
| 3.01 | 0.00 | 0.00 | 47.78 | 98.83 | 0.15 | 758.46 | 100.00 | 0.00 |
| 3.46 | 0.01 | 0.01 | 54.86 | 99.03 | 0.20 | 870.89 | 100.00 | 0.00 |
| 3.97 | 0.63 | 0.62 | 63.00 | 99.22 | 0.19 | 1000.00 | 100.00 | 0.00 |

Table A.5e: Droplet Diameter vs. Cumulative (%) and Volume Frequency (%) respectively for Conditions of Figure A5e

| Size (µm) | % < | % In | Size (µm) | % < | % In | Size (µm) | % < | % In |
|---|---|---|---|---|---|---|---|---|
| 0.287 | 0.00 | 0.00 | 4.56 | 5.61 | 5.36 | 72.33 | 99.71 | 0.19 |
| 0.330 | 0.00 | 0.00 | 5.23 | 25.46 | 19.85 | 83.06 | 99.85 | 0.14 |
| 0.378 | 0.00 | 0.00 | 6.01 | 46.89 | 21.43 | 95.37 | 99.95 | 0.10 |
| 0.435 | 0.00 | 0.00 | 6.90 | 58.34 | 11.45 | 109.51 | 100.00 | 0.05 |
| 0.499 | 0.00 | 0.00 | 7.92 | 63.28 | 4.94 | 125.74 | 100.00 | 0.00 |
| 0.573 | 0.00 | 0.00 | 9.10 | 67.53 | 4.25 | 144.38 | 100.00 | 0.00 |
| 0.658 | 0.00 | 0.00 | 10.44 | 73.51 | 5.98 | 165.79 | 100.00 | 0.00 |
| 0.755 | 0.00 | 0.00 | 11.99 | 82.28 | 8.77 | 190.37 | 100.00 | 0.00 |
| 0.867 | 0.00 | 0.00 | 13.77 | 90.61 | 8.33 | 218.59 | 100.00 | 0.00 |
| 0.996 | 0.00 | 0.00 | 15.81 | 95.65 | 5.04 | 250.99 | 100.00 | 0.00 |
| 1.14 | 0.00 | 0.00 | 18.16 | 97.88 | 2.23 | 288.20 | 100.00 | 0.00 |
| 1.31 | 0.00 | 0.00 | 20.85 | 98.62 | 0.74 | 330.92 | 100.00 | 0.00 |
| 1.51 | 0.00 | 0.00 | 23.94 | 98.83 | 0.21 | 379.98 | 100.00 | 0.00 |
| 1.73 | 0.00 | 0.00 | 27.49 | 98.90 | 0.07 | 436.31 | 100.00 | 0.00 |
| 1.99 | 0.00 | 0.00 | 31.56 | 98.93 | 0.03 | 500.99 | 100.00 | 0.00 |
| 2.28 | 0.00 | 0.00 | 36.24 | 98.96 | 0.03 | 575.26 | 100.00 | 0.00 |
| 2.62 | 0.00 | 0.00 | 41.61 | 99.01 | 0.05 | 660.54 | 100.00 | 0.00 |
| 3.01 | 0.00 | 0.00 | 47.78 | 99.11 | 0.10 | 758.46 | 100.00 | 0.00 |
| 3.46 | 0.00 | 0.00 | 54.86 | 99.30 | 0.19 | 870.89 | 100.00 | 0.00 |
| 3.97 | 0.25 | 0.25 | 63.00 | 99.52 | 0.22 | 1000.00 | 100.00 | 0.00 |

Table A.5f: Droplet Diameter vs. Cumulative (%) and Volume Frequency (%) respectively for Conditions of Figure A5f

| Size (µm) | % < | % In | Size (µm) | % < | % In | Size (µm) | % < | % In |
|---|---|---|---|---|---|---|---|---|
| 0.287 | 0.00 | 0.00 | 4.56 | 9.61 | 8.47 | 72.33 | 100.00 | 0.00 |
| 0.330 | 0.00 | 0.00 | 5.23 | 27.59 | 17.98 | 83.06 | 100.00 | 0.00 |
| 0.378 | 0.00 | 0.00 | 6.01 | 45.62 | 18.04 | 95.37 | 100.00 | 0.00 |
| 0.435 | 0.00 | 0.00 | 6.90 | 56.80 | 11.18 | 109.51 | 100.00 | 0.00 |
| 0.499 | 0.00 | 0.00 | 7.92 | 63.24 | 6.45 | 125.74 | 100.00 | 0.00 |
| 0.573 | 0.00 | 0.00 | 9.10 | 68.68 | 5.44 | 144.38 | 100.00 | 0.00 |
| 0.658 | 0.00 | 0.00 | 10.44 | 74.93 | 6.25 | 165.79 | 100.00 | 0.00 |
| 0.755 | 0.00 | 0.00 | 11.99 | 82.48 | 7.55 | 190.37 | 100.00 | 0.00 |
| 0.867 | 0.00 | 0.00 | 13.77 | 89.66 | 7.18 | 218.59 | 100.00 | 0.00 |
| 0.996 | 0.00 | 0.00 | 15.81 | 94.83 | 5.17 | 250.99 | 100.00 | 0.00 |
| 1.14 | 0.00 | 0.00 | 18.16 | 97.78 | 2.95 | 288.20 | 100.00 | 0.00 |
| 1.31 | 0.00 | 0.00 | 20.85 | 99.14 | 1.36 | 330.92 | 100.00 | 0.00 |
| 1.51 | 0.00 | 0.00 | 23.94 | 99.67 | 0.53 | 379.98 | 100.00 | 0.00 |
| 1.73 | 0.00 | 0.00 | 27.49 | 99.87 | 0.19 | 436.31 | 100.00 | 0.00 |
| 1.99 | 0.00 | 0.00 | 31.56 | 99.94 | 0.07 | 500.99 | 100.00 | 0.00 |
| 2.28 | 0.00 | 0.00 | 36.24 | 99.97 | 0.03 | 575.26 | 100.00 | 0.00 |
| 2.62 | 0.00 | 0.00 | 41.61 | 99.98 | 0.01 | 660.54 | 100.00 | 0.00 |
| 3.01 | 0.00 | 0.00 | 47.78 | 99.99 | 0.01 | 758.46 | 100.00 | 0.00 |
| 3.46 | 0.05 | 0.05 | 54.86 | 100.00 | 0.01 | 870.89 | 100.00 | 0.00 |
| 3.97 | 1.14 | 1.09 | 63.00 | 100.00 | 0.00 | 1000.00 | 100.00 | 0.00 |

Table A.6a: Droplet Diameter vs. Cumulative (%) and Volume Frequency (%) respectively for Conditions of Figure A6a

| Size (µm) | % < | % In | Size (µm) | % < | % In | Size (µm) | % < | % In |
|---|---|---|---|---|---|---|---|---|
| 0.287 | 0.00 | 0.00 | 4.56 | 0.30 | 0.30 | 72.33 | 100.00 | 0.00 |
| 0.330 | 0.00 | 0.00 | 5.23 | 21.44 | 21.15 | 83.06 | 100.00 | 0.00 |
| 0.378 | 0.00 | 0.00 | 6.01 | 49.24 | 27.79 | 95.37 | 100.00 | 0.00 |
| 0.435 | 0.00 | 0.00 | 6.90 | 63.91 | 14.67 | 109.51 | 100.00 | 0.00 |
| 0.499 | 0.00 | 0.00 | 7.92 | 67.03 | 3.12 | 125.74 | 100.00 | 0.00 |
| 0.573 | 0.00 | 0.00 | 9.10 | 69.84 | 2.81 | 144.38 | 100.00 | 0.00 |
| 0.658 | 0.00 | 0.00 | 10.44 | 75.44 | 5.61 | 165.79 | 100.00 | 0.00 |
| 0.755 | 0.00 | 0.00 | 11.99 | 85.72 | 10.28 | 190.37 | 100.00 | 0.00 |
| 0.867 | 0.00 | 0.00 | 13.77 | 94.01 | 8.29 | 218.59 | 100.00 | 0.00 |
| 0.996 | 0.00 | 0.00 | 15.81 | 98.00 | 3.98 | 250.99 | 100.00 | 0.00 |
| 1.14 | 0.00 | 0.00 | 18.16 | 99.43 | 1.44 | 288.20 | 100.00 | 0.00 |
| 1.31 | 0.00 | 0.00 | 20.85 | 99.83 | 0.40 | 330.92 | 100.00 | 0.00 |
| 1.51 | 0.00 | 0.00 | 23.94 | 99.94 | 0.11 | 379.98 | 100.00 | 0.00 |
| 1.73 | 0.00 | 0.00 | 27.49 | 99.97 | 0.03 | 436.31 | 100.00 | 0.00 |
| 1.99 | 0.00 | 0.00 | 31.56 | 99.99 | 0.02 | 500.99 | 100.00 | 0.00 |
| 2.28 | 0.00 | 0.00 | 36.24 | 100.00 | 0.01 | 575.26 | 100.00 | 0.00 |
| 2.62 | 0.00 | 0.00 | 41.61 | 100.00 | 0.00 | 660.54 | 100.00 | 0.00 |
| 3.01 | 0.00 | 0.00 | 47.78 | 100.00 | 0.00 | 758.46 | 100.00 | 0.00 |
| 3.46 | 0.00 | 0.00 | 54.86 | 100.00 | 0.00 | 870.89 | 100.00 | 0.00 |
| 3.97 | 0.00 | 0.00 | 63.00 | 100.00 | 0.00 | 1000.00 | 100.00 | 0.00 |

Table A.6b: Droplet Diameter vs. Cumulative (%) and Volume Frequency (%) respectively for Conditions of Figure A6b

| Size (µm) | % < | % In | Size (µm) | % < | % In | Size (µm) | % < | % In |
|---|---|---|---|---|---|---|---|---|
| 0.287 | 0.00 | 0.00 | 4.56 | 0.16 | 0.16 | 72.33 | 100.00 | 0.00 |
| 0.330 | 0.00 | 0.00 | 5.23 | 15.64 | 15.49 | 83.06 | 100.00 | 0.00 |
| 0.378 | 0.00 | 0.00 | 6.01 | 42.24 | 26.59 | 95.37 | 100.00 | 0.00 |
| 0.435 | 0.00 | 0.00 | 6.90 | 61.45 | 19.22 | 109.51 | 100.00 | 0.00 |
| 0.499 | 0.00 | 0.00 | 7.92 | 65.87 | 4.42 | 125.74 | 100.00 | 0.00 |
| 0.573 | 0.00 | 0.00 | 9.10 | 69.06 | 3.19 | 144.38 | 100.00 | 0.00 |
| 0.658 | 0.00 | 0.00 | 10.44 | 74.37 | 5.31 | 165.79 | 100.00 | 0.00 |
| 0.755 | 0.00 | 0.00 | 11.99 | 83.49 | 9.12 | 190.37 | 100.00 | 0.00 |
| 0.867 | 0.00 | 0.00 | 13.77 | 91.69 | 8.20 | 218.59 | 100.00 | 0.00 |
| 0.996 | 0.00 | 0.00 | 15.81 | 96.36 | 4.67 | 250.99 | 100.00 | 0.00 |
| 1.14 | 0.00 | 0.00 | 18.16 | 98.44 | 2.08 | 288.20 | 100.00 | 0.00 |
| 1.31 | 0.00 | 0.00 | 20.85 | 99.23 | 0.78 | 330.92 | 100.00 | 0.00 |
| 1.51 | 0.00 | 0.00 | 23.94 | 99.53 | 0.30 | 379.98 | 100.00 | 0.00 |
| 1.73 | 0.00 | 0.00 | 27.49 | 99.68 | 0.15 | 436.31 | 100.00 | 0.00 |
| 1.99 | 0.00 | 0.00 | 31.56 | 99.78 | 0.10 | 500.99 | 100.00 | 0.00 |
| 2.28 | 0.00 | 0.00 | 36.24 | 99.86 | 0.09 | 575.26 | 100.00 | 0.00 |
| 2.62 | 0.00 | 0.00 | 41.61 | 99.94 | 0.07 | 660.54 | 100.00 | 0.00 |
| 3.01 | 0.00 | 0.00 | 47.78 | 99.98 | 0.04 | 758.46 | 100.00 | 0.00 |
| 3.46 | 0.00 | 0.00 | 54.86 | 100.00 | 0.02 | 870.89 | 100.00 | 0.00 |
| 3.97 | 0.00 | 0.00 | 63.00 | 100.00 | 0.00 | 1000.00 | 100.00 | 0.00 |

Table A.6c: Droplet Diameter vs. Cumulative (%) and Volume Frequency (%) respectively for Conditions of Figure A6c

| Size (µm) | % < | % In | Size (µm) | % < | % In | Size (µm) | % < | % In |
|---|---|---|---|---|---|---|---|---|
| 0.287 | 0.00 | 0.00 | 4.56 | 7.90 | 7.48 | 72.33 | 100.00 | 0.00 |
| 0.330 | 0.00 | 0.00 | 5.23 | 27.77 | 19.88 | 83.06 | 100.00 | 0.00 |
| 0.378 | 0.00 | 0.00 | 6.01 | 47.89 | 20.12 | 95.37 | 100.00 | 0.00 |
| 0.435 | 0.00 | 0.00 | 6.90 | 59.08 | 11.19 | 109.51 | 100.00 | 0.00 |
| 0.499 | 0.00 | 0.00 | 7.92 | 64.89 | 5.81 | 125.74 | 100.00 | 0.00 |
| 0.573 | 0.00 | 0.00 | 9.10 | 70.04 | 5.15 | 144.38 | 100.00 | 0.00 |
| 0.658 | 0.00 | 0.00 | 10.44 | 76.62 | 6.59 | 165.79 | 100.00 | 0.00 |
| 0.755 | 0.00 | 0.00 | 11.99 | 84.83 | 8.20 | 190.37 | 100.00 | 0.00 |
| 0.867 | 0.00 | 0.00 | 13.77 | 91.54 | 6.71 | 218.59 | 100.00 | 0.00 |
| 0.996 | 0.00 | 0.00 | 15.81 | 95.47 | 3.93 | 250.99 | 100.00 | 0.00 |
| 1.14 | 0.00 | 0.00 | 18.16 | 97.39 | 1.92 | 288.20 | 100.00 | 0.00 |
| 1.31 | 0.00 | 0.00 | 20.85 | 98.26 | 0.86 | 330.92 | 100.00 | 0.00 |
| 1.51 | 0.00 | 0.00 | 23.94 | 98.70 | 0.44 | 379.98 | 100.00 | 0.00 |
| 1.73 | 0.00 | 0.00 | 27.49 | 99.00 | 0.30 | 436.31 | 100.00 | 0.00 |
| 1.99 | 0.00 | 0.00 | 31.56 | 99.27 | 0.27 | 500.99 | 100.00 | 0.00 |
| 2.28 | 0.00 | 0.00 | 36.24 | 99.54 | 0.28 | 575.26 | 100.00 | 0.00 |
| 2.62 | 0.00 | 0.00 | 41.61 | 99.79 | 0.25 | 660.54 | 100.00 | 0.00 |
| 3.01 | 0.00 | 0.00 | 47.78 | 99.94 | 0.15 | 758.46 | 100.00 | 0.00 |
| 3.46 | 0.00 | 0.00 | 54.86 | 99.99 | 0.05 | 870.89 | 100.00 | 0.00 |
| 3.97 | 0.42 | 0.42 | 63.00 | 100.00 | 0.01 | 1000.00 | 100.00 | 0.00 |

Table A.6d: Droplet Diameter vs. Cumulative (%) and Volume Frequency (%) respectively for Conditions of Figure A6d

| Size (µm) | % < | % In | Size (µm) | % < | % In | Size (µm) | % < | % In |
|---|---|---|---|---|---|---|---|---|
| 0.287 | 0.00 | 0.00 | 4.56 | 5.66 | 5.25 | 72.33 | 100.00 | 0.00 |
| 0.330 | 0.00 | 0.00 | 5.23 | 26.40 | 20.74 | 83.06 | 100.00 | 0.00 |
| 0.378 | 0.00 | 0.00 | 6.01 | 47.86 | 21.46 | 95.37 | 100.00 | 0.00 |
| 0.435 | 0.00 | 0.00 | 6.90 | 58.14 | 10.28 | 109.51 | 100.00 | 0.00 |
| 0.499 | 0.00 | 0.00 | 7.92 | 62.60 | 4.46 | 125.74 | 100.00 | 0.00 |
| 0.573 | 0.00 | 0.00 | 9.10 | 67.33 | 4.74 | 144.38 | 100.00 | 0.00 |
| 0.658 | 0.00 | 0.00 | 10.44 | 75.65 | 8.32 | 165.79 | 100.00 | 0.00 |
| 0.755 | 0.00 | 0.00 | 11.99 | 88.26 | 12.60 | 190.37 | 100.00 | 0.00 |
| 0.867 | 0.00 | 0.00 | 13.77 | 94.53 | 6.27 | 218.59 | 100.00 | 0.00 |
| 0.996 | 0.00 | 0.00 | 15.81 | 97.71 | 3.18 | 250.99 | 100.00 | 0.00 |
| 1.14 | 0.00 | 0.00 | 18.16 | 99.21 | 1.50 | 288.20 | 100.00 | 0.00 |
| 1.31 | 0.00 | 0.00 | 20.85 | 99.80 | 0.59 | 330.92 | 100.00 | 0.00 |
| 1.51 | 0.00 | 0.00 | 23.94 | 99.97 | 0.17 | 379.98 | 100.00 | 0.00 |
| 1.73 | 0.00 | 0.00 | 27.49 | 100.00 | 0.03 | 436.31 | 100.00 | 0.00 |
| 1.99 | 0.00 | 0.00 | 31.56 | 100.00 | 0.00 | 500.99 | 100.00 | 0.00 |
| 2.28 | 0.00 | 0.00 | 36.24 | 100.00 | 0.00 | 575.26 | 100.00 | 0.00 |
| 2.62 | 0.00 | 0.00 | 41.61 | 100.00 | 0.00 | 660.54 | 100.00 | 0.00 |
| 3.01 | 0.00 | 0.00 | 47.78 | 100.00 | 0.00 | 758.46 | 100.00 | 0.00 |
| 3.46 | 0.01 | 0.01 | 54.86 | 100.00 | 0.00 | 870.89 | 100.00 | 0.00 |
| 3.97 | 0.42 | 0.41 | 63.00 | 100.00 | 0.00 | 1000.00 | 100.00 | 0.00 |

Table A.6e: Droplet Diameter vs. Cumulative (%) and Volume Frequency (%) respectively for Conditions of Figure A6e

| Size (µm) | % < | % In | Size (µm) | % < | % In | Size (µm) | % < | % In |
|---|---|---|---|---|---|---|---|---|
| 0.287 | 0.00 | 0.00 | 4.56 | 9.66 | 8.51 | 72.33 | 99.92 | 0.16 |
| 0.330 | 0.00 | 0.00 | 5.23 | 28.56 | 18.90 | 83.06 | 100.00 | 0.07 |
| 0.378 | 0.00 | 0.00 | 6.01 | 47.32 | 18.76 | 95.37 | 100.00 | 0.00 |
| 0.435 | 0.00 | 0.00 | 6.90 | 58.34 | 11.02 | 109.51 | 100.00 | 0.00 |
| 0.499 | 0.00 | 0.00 | 7.92 | 64.34 | 6.00 | 125.74 | 100.00 | 0.00 |
| 0.573 | 0.00 | 0.00 | 9.10 | 69.32 | 4.97 | 144.38 | 100.00 | 0.00 |
| 0.658 | 0.00 | 0.00 | 10.44 | 75.26 | 5.94 | 165.79 | 100.00 | 0.00 |
| 0.755 | 0.00 | 0.00 | 11.99 | 82.64 | 7.38 | 190.37 | 100.00 | 0.00 |
| 0.867 | 0.00 | 0.00 | 13.77 | 88.88 | 6.25 | 218.59 | 100.00 | 0.00 |
| 0.996 | 0.00 | 0.00 | 15.81 | 93.30 | 4.42 | 250.99 | 100.00 | 0.00 |
| 1.14 | 0.00 | 0.00 | 18.16 | 96.11 | 2.81 | 288.20 | 100.00 | 0.00 |
| 1.31 | 0.00 | 0.00 | 20.85 | 97.74 | 1.62 | 330.92 | 100.00 | 0.00 |
| 1.51 | 0.00 | 0.00 | 23.94 | 98.60 | 0.86 | 379.98 | 100.00 | 0.00 |
| 1.73 | 0.00 | 0.00 | 27.49 | 99.03 | 0.43 | 436.31 | 100.00 | 0.00 |
| 1.99 | 0.00 | 0.00 | 31.56 | 99.24 | 0.21 | 500.99 | 100.00 | 0.00 |
| 2.28 | 0.00 | 0.00 | 36.24 | 99.36 | 0.12 | 575.26 | 100.00 | 0.00 |
| 2.62 | 0.00 | 0.00 | 41.61 | 99.44 | 0.08 | 660.54 | 100.00 | 0.00 |
| 3.01 | 0.00 | 0.00 | 47.78 | 99.52 | 0.08 | 758.46 | 100.00 | 0.00 |
| 3.46 | 0.07 | 0.07 | 54.86 | 99.62 | 0.10 | 870.89 | 100.00 | 0.00 |
| 3.97 | 1.16 | 1.09 | 63.00 | 99.76 | 0.14 | 1000.00 | 100.00 | 0.00 |

Table A.6f: Droplet Diameter vs. Cumulative (%) and Volume Frequency (%) respectively for Conditions of Figure A6f

| Size (µm) | % < | % In | Size (µm) | % < | % In | Size (µm) | % < | % In |
|---|---|---|---|---|---|---|---|---|
| 0.287 | 0.00 | 0.00 | 4.56 | 9.49 | 8.34 | 72.33 | 100.00 | 0.00 |
| 0.330 | 0.00 | 0.00 | 5.23 | 27.01 | 17.53 | 83.06 | 100.00 | 0.00 |
| 0.378 | 0.00 | 0.00 | 6.01 | 44.30 | 17.29 | 95.37 | 100.00 | 0.00 |
| 0.435 | 0.00 | 0.00 | 6.90 | 54.92 | 10.62 | 109.51 | 100.00 | 0.00 |
| 0.499 | 0.00 | 0.00 | 7.92 | 61.48 | 6.55 | 125.74 | 100.00 | 0.00 |
| 0.573 | 0.00 | 0.00 | 9.10 | 67.60 | 6.12 | 144.38 | 100.00 | 0.00 |
| 0.658 | 0.00 | 0.00 | 10.44 | 75.02 | 7.43 | 165.79 | 100.00 | 0.00 |
| 0.755 | 0.00 | 0.00 | 11.99 | 83.60 | 8.58 | 190.37 | 100.00 | 0.00 |
| 0.867 | 0.00 | 0.00 | 13.77 | 90.80 | 7.20 | 218.59 | 100.00 | 0.00 |
| 0.996 | 0.00 | 0.00 | 15.81 | 95.47 | 4.67 | 250.99 | 100.00 | 0.00 |
| 1.14 | 0.00 | 0.00 | 18.16 | 97.97 | 2.50 | 288.20 | 100.00 | 0.00 |
| 1.31 | 0.00 | 0.00 | 20.85 | 99.11 | 1.14 | 330.92 | 100.00 | 0.00 |
| 1.51 | 0.00 | 0.00 | 23.94 | 99.57 | 0.47 | 379.98 | 100.00 | 0.00 |
| 1.73 | 0.00 | 0.00 | 27.49 | 99.76 | 0.19 | 436.31 | 100.00 | 0.00 |
| 1.99 | 0.00 | 0.00 | 31.56 | 99.85 | 0.09 | 500.99 | 100.00 | 0.00 |
| 2.28 | 0.00 | 0.00 | 36.24 | 99.90 | 0.05 | 575.26 | 100.00 | 0.00 |
| 2.62 | 0.00 | 0.00 | 41.61 | 99.93 | 0.03 | 660.54 | 100.00 | 0.00 |
| 3.01 | 0.00 | 0.00 | 47.78 | 99.96 | 0.03 | 758.46 | 100.00 | 0.00 |
| 3.46 | 0.06 | 0.06 | 54.86 | 99.99 | 0.03 | 870.89 | 100.00 | 0.00 |
| 3.97 | 1.15 | 1.09 | 63.00 | 100.00 | 0.01 | 1000.00 | 100.00 | 0.00 |

Table A.7a: Droplet Diameter vs. Cumulative (%) and Volume Frequency (%) respectively for Conditions of Figure A7a

| Size (µm) | % < | % In | Size (µm) | % < | % In | Size (µm) | % < | % In |
|---|---|---|---|---|---|---|---|---|
| 0.287 | 0.00 | 0.00 | 4.56 | 2.24 | 2.23 | 72.33 | 100.00 | 0.00 |
| 0.330 | 0.00 | 0.00 | 5.23 | 21.34 | 19.10 | 83.06 | 100.00 | 0.00 |
| 0.378 | 0.00 | 0.00 | 6.01 | 44.60 | 23.25 | 95.37 | 100.00 | 0.00 |
| 0.435 | 0.00 | 0.00 | 6.90 | 57.45 | 12.85 | 109.51 | 100.00 | 0.00 |
| 0.499 | 0.00 | 0.00 | 7.92 | 62.30 | 4.85 | 125.74 | 100.00 | 0.00 |
| 0.573 | 0.00 | 0.00 | 9.10 | 66.35 | 4.05 | 144.38 | 100.00 | 0.00 |
| 0.658 | 0.00 | 0.00 | 10.44 | 72.47 | 6.12 | 165.79 | 100.00 | 0.00 |
| 0.755 | 0.00 | 0.00 | 11.99 | 82.30 | 9.83 | 190.37 | 100.00 | 0.00 |
| 0.867 | 0.00 | 0.00 | 13.77 | 91.86 | 9.56 | 218.59 | 100.00 | 0.00 |
| 0.996 | 0.00 | 0.00 | 15.81 | 97.30 | 5.44 | 250.99 | 100.00 | 0.00 |
| 1.14 | 0.00 | 0.00 | 18.16 | 99.40 | 2.10 | 288.20 | 100.00 | 0.00 |
| 1.31 | 0.00 | 0.00 | 20.85 | 99.92 | 0.52 | 330.92 | 100.00 | 0.00 |
| 1.51 | 0.00 | 0.00 | 23.94 | 99.99 | 0.08 | 379.98 | 100.00 | 0.00 |
| 1.73 | 0.00 | 0.00 | 27.49 | 100.00 | 0.01 | 436.31 | 100.00 | 0.00 |
| 1.99 | 0.00 | 0.00 | 31.56 | 100.00 | 0.00 | 500.99 | 100.00 | 0.00 |
| 2.28 | 0.00 | 0.00 | 36.24 | 100.00 | 0.00 | 575.26 | 100.00 | 0.00 |
| 2.62 | 0.00 | 0.00 | 41.61 | 100.00 | 0.00 | 660.54 | 100.00 | 0.00 |
| 3.01 | 0.00 | 0.00 | 47.78 | 100.00 | 0.00 | 758.46 | 100.00 | 0.00 |
| 3.46 | 0.00 | 0.00 | 54.86 | 100.00 | 0.00 | 870.89 | 100.00 | 0.00 |
| 3.97 | 0.01 | 0.01 | 63.00 | 100.00 | 0.00 | 1000.00 | 100.00 | 0.00 |

Table A.7b: Droplet Diameter vs. Cumulative (%) and Volume Frequency (%) Respectively for Conditions of Figure A7b

| Size (µm) | % < | % In | Size (µm) | % < | % In | Size (µm) | % < | % In |
|---|---|---|---|---|---|---|---|---|
| 0.287 | 0.00 | 0.00 | 4.56 | 0.31 | 0.31 | 72.33 | 100.00 | 0.00 |
| 0.330 | 0.00 | 0.00 | 5.23 | 18.88 | 18.57 | 83.06 | 100.00 | 0.00 |
| 0.378 | 0.00 | 0.00 | 6.01 | 44.96 | 26.08 | 95.37 | 100.00 | 0.00 |
| 0.435 | 0.00 | 0.00 | 6.90 | 60.10 | 15.14 | 109.51 | 100.00 | 0.00 |
| 0.499 | 0.00 | 0.00 | 7.92 | 63.30 | 3.20 | 125.74 | 100.00 | 0.00 |
| 0.573 | 0.00 | 0.00 | 9.10 | 66.17 | 2.87 | 144.38 | 100.00 | 0.00 |
| 0.658 | 0.00 | 0.00 | 10.44 | 72.20 | 6.02 | 165.79 | 100.00 | 0.00 |
| 0.755 | 0.00 | 0.00 | 11.99 | 84.51 | 12.32 | 190.37 | 100.00 | 0.00 |
| 0.867 | 0.00 | 0.00 | 13.77 | 94.79 | 10.28 | 218.59 | 100.00 | 0.00 |
| 0.996 | 0.00 | 0.00 | 15.81 | 98.87 | 4.08 | 250.99 | 100.00 | 0.00 |
| 1.14 | 0.00 | 0.00 | 18.16 | 99.88 | 1.01 | 288.20 | 100.00 | 0.00 |
| 1.31 | 0.00 | 0.00 | 20.85 | 100.00 | 0.11 | 330.92 | 100.00 | 0.00 |
| 1.51 | 0.00 | 0.00 | 23.94 | 100.00 | 0.00 | 379.98 | 100.00 | 0.00 |
| 1.73 | 0.00 | 0.00 | 27.49 | 100.00 | 0.00 | 436.31 | 100.00 | 0.00 |
| 1.99 | 0.00 | 0.00 | 31.56 | 100.00 | 0.00 | 500.99 | 100.00 | 0.00 |
| 2.28 | 0.00 | 0.00 | 36.24 | 100.00 | 0.00 | 575.26 | 100.00 | 0.00 |
| 2.62 | 0.00 | 0.00 | 41.61 | 100.00 | 0.00 | 660.54 | 100.00 | 0.00 |
| 3.01 | 0.00 | 0.00 | 47.78 | 100.00 | 0.00 | 758.46 | 100.00 | 0.00 |
| 3.46 | 0.00 | 0.00 | 54.86 | 100.00 | 0.00 | 870.89 | 100.00 | 0.00 |
| 3.97 | 0.00 | 0.00 | 63.00 | 100.00 | 0.00 | 1000.00 | 100.00 | 0.00 |

Table A.7c: Droplet Diameter vs. Cumulative (%) and Volume Frequency (%) Respectively for Conditions of Figure A7c

| Size (µm) | % < | % In | Size (µm) | % < | % In | Size (µm) | % < | % In |
|---|---|---|---|---|---|---|---|---|
| 0.287 | 0.00 | 0.00 | 4.56 | 5.38 | 5.26 | 72.33 | 100.00 | 0.00 |
| 0.330 | 0.00 | 0.00 | 5.23 | 25.69 | 20.31 | 83.06 | 100.00 | 0.00 |
| 0.378 | 0.00 | 0.00 | 6.01 | 47.14 | 21.45 | 95.37 | 100.00 | 0.00 |
| 0.435 | 0.00 | 0.00 | 6.90 | 58.22 | 11.08 | 109.51 | 100.00 | 0.00 |
| 0.499 | 0.00 | 0.00 | 7.92 | 63.58 | 5.36 | 125.74 | 100.00 | 0.00 |
| 0.573 | 0.00 | 0.00 | 9.10 | 69.25 | 5.67 | 144.38 | 100.00 | 0.00 |
| 0.658 | 0.00 | 0.00 | 10.44 | 78.53 | 9.28 | 165.79 | 100.00 | 0.00 |
| 0.755 | 0.00 | 0.00 | 11.99 | 91.37 | 12.84 | 190.37 | 100.00 | 0.00 |
| 0.867 | 0.00 | 0.00 | 13.77 | 97.99 | 6.62 | 218.59 | 100.00 | 0.00 |
| 0.996 | 0.00 | 0.00 | 15.81 | 99.73 | 1.75 | 250.99 | 100.00 | 0.00 |
| 1.14 | 0.00 | 0.00 | 18.16 | 99.99 | 0.26 | 288.20 | 100.00 | 0.00 |
| 1.31 | 0.00 | 0.00 | 20.85 | 100.00 | 0.01 | 330.92 | 100.00 | 0.00 |
| 1.51 | 0.00 | 0.00 | 23.94 | 100.00 | 0.00 | 379.98 | 100.00 | 0.00 |
| 1.73 | 0.00 | 0.00 | 27.49 | 100.00 | 0.00 | 436.31 | 100.00 | 0.00 |
| 1.99 | 0.00 | 0.00 | 31.56 | 100.00 | 0.00 | 500.99 | 100.00 | 0.00 |
| 2.28 | 0.00 | 0.00 | 36.24 | 100.00 | 0.00 | 575.26 | 100.00 | 0.00 |
| 2.62 | 0.00 | 0.00 | 41.61 | 100.00 | 0.00 | 660.54 | 100.00 | 0.00 |
| 3.01 | 0.00 | 0.00 | 47.78 | 100.00 | 0.00 | 758.46 | 100.00 | 0.00 |
| 3.46 | 0.00 | 0.00 | 54.86 | 100.00 | 0.00 | 870.89 | 100.00 | 0.00 |
| 3.97 | 0.13 | 0.13 | 63.00 | 100.00 | 0.00 | 1000.00 | 100.00 | 0.00 |

Table A.7d: Droplet Diameter vs. Cumulative (%) and Volume Frequency (%) Respectively for Conditions of Figure A7d

| Size (µm) | % < | % In | Size (µm) | % < | % In | Size (µm) | % < | % In |
|---|---|---|---|---|---|---|---|---|
| 0.287 | 0.00 | 0.00 | 4.56 | 7.07 | 6.67 | 72.33 | 100.00 | 0.00 |
| 0.330 | 0.00 | 0.00 | 5.23 | 28.59 | 21.52 | 83.06 | 100.00 | 0.00 |
| 0.378 | 0.00 | 0.00 | 6.01 | 48.96 | 20.36 | 95.37 | 100.00 | 0.00 |
| 0.435 | 0.00 | 0.00 | 6.90 | 57.67 | 8.71 | 109.51 | 100.00 | 0.00 |
| 0.499 | 0.00 | 0.00 | 7.92 | 61.63 | 3.97 | 125.74 | 100.00 | 0.00 |
| 0.573 | 0.00 | 0.00 | 9.10 | 65.56 | 3.93 | 144.38 | 100.00 | 0.00 |
| 0.658 | 0.00 | 0.00 | 10.44 | 71.27 | 5.71 | 165.79 | 100.00 | 0.00 |
| 0.755 | 0.00 | 0.00 | 11.99 | 79.24 | 7.98 | 190.37 | 100.00 | 0.00 |
| 0.867 | 0.00 | 0.00 | 13.77 | 87.41 | 8.17 | 218.59 | 100.00 | 0.00 |
| 0.996 | 0.00 | 0.00 | 15.81 | 93.77 | 6.36 | 250.99 | 100.00 | 0.00 |
| 1.14 | 0.00 | 0.00 | 18.16 | 97.50 | 3.73 | 288.20 | 100.00 | 0.00 |
| 1.31 | 0.00 | 0.00 | 20.85 | 99.19 | 1.69 | 330.92 | 100.00 | 0.00 |
| 1.51 | 0.00 | 0.00 | 23.94 | 99.79 | 0.60 | 379.98 | 100.00 | 0.00 |
| 1.73 | 0.00 | 0.00 | 27.49 | 99.96 | 0.17 | 436.31 | 100.00 | 0.00 |
| 1.99 | 0.00 | 0.00 | 31.56 | 99.99 | 0.04 | 500.99 | 100.00 | 0.00 |
| 2.28 | 0.00 | 0.00 | 36.24 | 100.00 | 0.01 | 575.26 | 100.00 | 0.00 |
| 2.62 | 0.00 | 0.00 | 41.61 | 100.00 | 0.00 | 660.54 | 100.00 | 0.00 |
| 3.01 | 0.00 | 0.00 | 47.78 | 100.00 | 0.00 | 758.46 | 100.00 | 0.00 |
| 3.46 | 0.01 | 0.01 | 54.86 | 100.00 | 0.00 | 870.89 | 100.00 | 0.00 |
| 3.97 | 0.40 | 0.39 | 63.00 | 100.00 | 0.00 | 1000.00 | 100.00 | 0.00 |

Table A.7e: Droplet Diameter vs. Cumulative (%) and Volume Frequency (%) Respectively for Conditions of Figure A7e

| Size (µm) | % < | % In | Size (µm) | % < | % In | Size (µm) | % < | % In |
|---|---|---|---|---|---|---|---|---|
| 0.287 | 0.00 | 0.00 | 4.56 | 10.41 | 9.18 | 72.33 | 100.00 | 0.01 |
| 0.330 | 0.00 | 0.00 | 5.23 | 29.07 | 18.65 | 83.06 | 100.00 | 0.00 |
| 0.378 | 0.00 | 0.00 | 6.01 | 46.97 | 17.90 | 95.37 | 100.00 | 0.00 |
| 0.435 | 0.00 | 0.00 | 6.90 | 57.63 | 10.66 | 109.51 | 100.00 | 0.00 |
| 0.499 | 0.00 | 0.00 | 7.92 | 64.14 | 6.51 | 125.74 | 100.00 | 0.00 |
| 0.573 | 0.00 | 0.00 | 9.10 | 70.25 | 6.10 | 144.38 | 100.00 | 0.00 |
| 0.658 | 0.00 | 0.00 | 10.44 | 77.56 | 7.31 | 165.79 | 100.00 | 0.00 |
| 0.755 | 0.00 | 0.00 | 11.99 | 85.66 | 8.10 | 190.37 | 100.00 | 0.00 |
| 0.867 | 0.00 | 0.00 | 13.77 | 92.12 | 6.46 | 218.59 | 100.00 | 0.00 |
| 0.996 | 0.00 | 0.00 | 15.81 | 96.15 | 4.03 | 250.99 | 100.00 | 0.00 |
| 1.14 | 0.00 | 0.00 | 18.16 | 98.21 | 2.07 | 288.20 | 100.00 | 0.00 |
| 1.31 | 0.00 | 0.00 | 20.85 | 99.12 | 0.91 | 330.92 | 100.00 | 0.00 |
| 1.51 | 0.00 | 0.00 | 23.94 | 99.49 | 0.37 | 379.98 | 100.00 | 0.00 |
| 1.73 | 0.00 | 0.00 | 27.49 | 99.65 | 0.16 | 436.31 | 100.00 | 0.00 |
| 1.99 | 0.00 | 0.00 | 31.56 | 99.74 | 0.09 | 500.99 | 100.00 | 0.00 |
| 2.28 | 0.00 | 0.00 | 36.24 | 99.80 | 0.06 | 575.26 | 100.00 | 0.00 |
| 2.62 | 0.00 | 0.00 | 41.61 | 99.85 | 0.05 | 660.54 | 100.00 | 0.00 |
| 3.01 | 0.00 | 0.00 | 47.78 | 99.90 | 0.05 | 758.46 | 100.00 | 0.00 |
| 3.46 | 0.06 | 0.06 | 54.86 | 99.95 | 0.05 | 870.89 | 100.00 | 0.00 |
| 3.97 | 1.23 | 1.18 | 63.00 | 99.99 | 0.04 | 1000.00 | 100.00 | 0.00 |

Table A.7f: Droplet Diameter vs. Cumulative (%) and Volume Frequency (%) Respectively for Conditions of Figure A7f

| Size (µm) | % < | % In | Size (µm) | % < | % In | Size (µm) | % < | % In |
|---|---|---|---|---|---|---|---|---|
| 0.287 | 0.00 | 0.00 | 4.56 | 3.45 | 3.22 | 72.33 | 100.00 | 0.00 |
| 0.330 | 0.00 | 0.00 | 5.23 | 17.83 | 14.37 | 83.06 | 100.00 | 0.00 |
| 0.378 | 0.00 | 0.00 | 6.01 | 33.14 | 15.31 | 95.37 | 100.00 | 0.00 |
| 0.435 | 0.00 | 0.00 | 6.90 | 41.01 | 7.87 | 109.51 | 100.00 | 0.00 |
| 0.499 | 0.00 | 0.00 | 7.92 | 45.28 | 4.27 | 125.74 | 100.00 | 0.00 |
| 0.573 | 0.00 | 0.00 | 9.10 | 50.10 | 4.82 | 144.38 | 100.00 | 0.00 |
| 0.658 | 0.00 | 0.00 | 10.44 | 57.43 | 7.34 | 165.79 | 100.00 | 0.00 |
| 0.755 | 0.00 | 0.00 | 11.99 | 66.49 | 9.05 | 190.37 | 100.00 | 0.00 |
| 0.867 | 0.00 | 0.00 | 13.77 | 75.43 | 8.95 | 218.59 | 100.00 | 0.00 |
| 0.996 | 0.00 | 0.00 | 15.81 | 84.99 | 9.56 | 250.99 | 100.00 | 0.00 |
| 1.14 | 0.00 | 0.00 | 18.16 | 93.54 | 8.55 | 288.20 | 100.00 | 0.00 |
| 1.31 | 0.00 | 0.00 | 20.85 | 98.36 | 4.82 | 330.92 | 100.00 | 0.00 |
| 1.51 | 0.00 | 0.00 | 23.94 | 99.83 | 1.47 | 379.98 | 100.00 | 0.00 |
| 1.73 | 0.00 | 0.00 | 27.49 | 99.99 | 0.16 | 436.31 | 100.00 | 0.00 |
| 1.99 | 0.00 | 0.00 | 31.56 | 100.00 | 0.01 | 500.99 | 100.00 | 0.00 |
| 2.28 | 0.00 | 0.00 | 36.24 | 100.00 | 0.00 | 575.26 | 100.00 | 0.00 |
| 2.62 | 0.00 | 0.00 | 41.61 | 100.00 | 0.00 | 660.54 | 100.00 | 0.00 |
| 3.01 | 0.00 | 0.00 | 47.78 | 100.00 | 0.00 | 758.46 | 100.00 | 0.00 |
| 3.46 | 0.01 | 0.01 | 54.86 | 100.00 | 0.00 | 870.89 | 100.00 | 0.00 |
| 3.97 | 0.23 | 0.22 | 63.00 | 100.00 | 0.00 | 1000.00 | 100.00 | 0.00 |

Table A.8a: Effect of Applied Voltage on Droplet Concentration for a Reynolds Number of 1350 (Run 1)

| Applied Voltage (Kv) | 0 | 10 | 15 | 18 | 20 | 22 | 24 | 26 | 28 |
|---|---|---|---|---|---|---|---|---|---|
| Droplet Concentration ($g/m^3$) | 23.70 | 19.30 | 15.82 | 13.5 | 11.57 | 9.88 | 8.15 | 5.10 | 3.78 |
| Droplet Concentration ($g/m^3$) | 15.80 | 11.80 | 9.65 | 8.75 | 8.06 | 7.42 | 5.96 | 5.31 | 3.35 |
| Droplet Concentration ($g/m^3$) | 8.40 | 7.6 | 5.32 | 5.54 | 4.72 | 4.25 | 3.3 | 3.05 | 3.0 |

Table A.8b: Effect of Applied Voltage on Droplet Concentration for a Reynolds Number of 1350 (Run 2)

| Applied Voltage (Kv) | 0 | 10 | 15 | 18 | 20 | 22 | 24 | 26 | 28 |
|---|---|---|---|---|---|---|---|---|---|
| Droplet Concentration ($g/m^3$) | 24.76 | 18.65 | 15.80 | 13.94 | 11.67 | 9.96 | 8.18 | 5.15 | 3.94 |
| Droplet Concentration ($g/m^3$) | 16.86 | 11.66 | 9.00 | 8.45 | 8.0 | 7.0 | 5.50 | 5.30 | 3.40 |
| Droplet Concentration ($g/m^3$) | 8.25 | 7.01 | 5.50 | 5.28 | 4.50 | 4.10 | 2.8 | 3.0 | 2.80 |

Table A.8c: Effect of Applied Voltage on Droplet Concentration for a Reynolds Number of 1350 (Ave.)

| Applied Voltage (Kv) | 0 | 10 | 15 | 18 | 20 | 22 | 24 | 26 | 28 |
|---|---|---|---|---|---|---|---|---|---|
| Ave. Droplet Concentration ($g/m^3$) | 24.23 | 18.97 | 15.82 | 13.72 | 11.62 | 9.92 | 8.17 | 5.12 | 3.86 |
| Ave. Droplet Concentration ($g/m^3$) | 16.33 | 11.73 | 9.28 | 8.60 | 8.08 | 7.20 | 5.73 | 5.40 | 3.42 |
| Ave. Droplet Concentration ($g/m^3$) | 8.32 | 7.30 | 5.97 | 5.41 | 4.60 | 4.16 | 3.04 | 3.04 | 2.90 |

Table A.9a: Effect of Applied Voltage on Droplet Concentration for a Reynolds Number of 1950 (Run 1)

| Applied Voltage (Kv) | 0 | 10 | 15 | 18 | 20 | 22 | 24 | 26 |
|---|---|---|---|---|---|---|---|---|
| Droplet Concentration ($g/m^3$) | 12.80 | 9.60 | 9.0 | 7.80 | 7.50 | 7.02 | 5.80 | 3.30 |
| Droplet Concentration ($g/m^3$) | 10.00 | 8.75 | 7.45 | 6.25 | 5.0 | 4.0 | 3.30 | 3.25 |
| Droplet Concentration ($g/m^3$) | 8.20 | 7.50 | 5.98 | 4.45 | 4.40 | 3.80 | 3.20 | 3.05 |

Table A.9b: Effect of Applied Voltage on Droplet Concentration for a Reynolds Number of 1950 (Run 2)

| Applied Voltage (Kv) | 0 | 10 | 15 | 18 | 20 | 22 | 24 | 26 |
|---|---|---|---|---|---|---|---|---|
| Droplet Concentration ($g/m^3$) | 13.80 | 9.80 | 9.10 | 8.21 | 7.62 | 7.06 | 5.70 | 3.23 |
| Droplet Concentration ($g/m^3$) | 10.20 | 8.85 | 7.52 | 6.33 | 5.43 | 4.06 | 3.42 | 3.35 |
| Droplet Concentration ($g/m^3$) | 8.00 | 7.10 | 5.75 | 4.73 | 4.42 | 4.06 | 3.40 | 3.30 |

Table A.9c: Effect of Applied Voltage on Droplet Concentration for a Reynolds Number of 1950 (Ave.)

| Applied Voltage (Kv) | 0 | 10 | 15 | 18 | 20 | 22 | 24 | 26 |
|---|---|---|---|---|---|---|---|---|
| Ave. Droplet Concentration ($g/m^3$) | 13.30 | 9.70 | 9.05 | 8.01 | 7.56 | 7.07 | 5.74 | 3.26 |
| Ave. Droplet Concentration ($g/m^3$) | 10.10 | 8.81 | 7.50 | 6.28 | 5.20 | 4.05 | 3.37 | 3.30 |
| Ave. Droplet Concentration ($g/m^3$) | 8.10 | 7.31 | 5.86 | 4.58 | 4.41 | 3.92 | 3.30 | 3.32 |

Table A.10a: Constant Droplet Concentration at Reynolds Numbers of 940, 1350 and 1680 (Run 1)

| Reynolds Numbers | Applied Voltage (kV) | 0 | 10 | 15 | 18 | 20 | 22 | 24 | 26 |
|---|---|---|---|---|---|---|---|---|---|
| 940 | Droplet Concentration ($g/m^3$) | 14.02 | 12.50 | 10.00 | 10.00 | 8.85 | 7.80 | 5.55 | 5.50 |
| 1350 | Droplet Concentration ($g/m^3$) | 14.65 | 11.50 | 9.00 | 8.0 | 7.50 | 7.40 | 5.70 | 5.40 |
| 1680 | Droplet Concentration ($g/m^3$) | 14.50 | 11.25 | 9.65 | 8.25 | 8.00 | 7.00 | 6.10 | 5.8 |

Table A.10b: Constant Droplet Concentration at Reynolds Numbers of 940, 1350 and 1680 (Run 2)

| Reynolds Numbers | Applied Voltage (kV) | 0 | 10 | 15 | 18 | 20 | 22 | 24 | 26 |
|---|---|---|---|---|---|---|---|---|---|
| 940 | Droplet Concentration ($g/m^3$) | 14.97 | 12.86 | 11.00 | 9.98 | 8.98 | 8.00 | 5.90 | 5.65 |
| 1350 | Droplet Concentration ($g/m^3$) | 14.75 | 11.90 | 9.60 | 8.20 | 7.40 | 7.00 | 5.71 | 5.43 |
| 1680 | Droplet Concentration ($g/m^3$) | 14.50 | 11.36 | 9.75 | 8.56 | 8.41 | 7.00 | 6.42 | 6.21 |

Table A.10c: Constant Droplet Concentration at Reynolds Numbers of 940, 1350 and 1680 (Ave.)

| Reynolds Numbers | Applied Voltage (kV) | 0 | 10 | 15 | 18 | 20 | 22 | 24 | 26 |
|---|---|---|---|---|---|---|---|---|---|
| 940 | Ave.Droplet Concentration ($g/m^3$) | 14.5 | 12.7 | 10.5 | 9.9 | 8.9 | 7.9 | 5.7 | 5.7 |
| 1350 | Ave. Droplet Concentration ($g/m^3$) | 14.7 | 11.7 | 9.3 | 8.1 | 7.6 | 7.2 | 5.7 | 5.4 |
| 1680 | Ave. Droplet Concentration ($g/m^3$) | 14.5 | 11.3 | 9.7 | 8.4 | 8.2 | 7.0 | 6.3 | 6.0 |

Table A.11a: Exit Mist Concentrations for Reynolds Numbers of 1230, 1350, and 1680 (Run 1)

| Reynolds Numbers | Applied Voltage (Kv) | 0 | 10 | 15 | 18 | 20 | 22 | 24 | 26 |
|---|---|---|---|---|---|---|---|---|---|
| 1230 | Droplet Concentration ($g/m^3$) | 28.00 | 27.10 | 25.80 | 25.20 | 25.30 | 23.90 | 22.88 | 22.86 |
| 1350 | Droplet Concentration ($g/m^3$) | 29.00 | 27.15 | 24.87 | 24.82 | 25.00 | 24.00 | 23.20 | 22.92 |
| 1680 | Droplet Concentration ($g/m^3$) | 29.00 | 25.10 | 25.00 | 24.00 | 25.70 | 23.92 | 23.85 | 22.86 |

Table A.11b: Exit Mist Concentrations for Reynolds Numbers of 1230, 1350, and 1680 (Run 2)

| Reynolds Numbers | Applied Voltage (Kv) | 0 | 10 | 15 | 18 | 20 | 22 | 24 | 26 |
|---|---|---|---|---|---|---|---|---|---|
| 1230 | Droplet Concentration ($g/m^3$) | 29.75 | 28.70 | 27.35 | 27.53 | 25.94 | 25.36 | 23.32 | 23.34 |
| 1350 | Droplet Concentration ($g/m^3$) | 29.42 | 27.71 | 26.55 | 25.21 | 26.45 | 25.08 | 23.51 | 23.30 |
| 1680 | Droplet Concentration ($g/m^3$) | 29.05 | 28.14 | 26.60 | 25.00 | 23.80 | 24.50 | 24.56 | 24.48 |

Table A.11c: Exit Mist Concentrations for Reynolds Numbers of 1230, 1350, and 1680 (Ave.)

| Reynolds Numbers | Applied Voltage (Kv) | 0 | 10 | 15 | 18 | 20 | 22 | 24 | 26 |
|---|---|---|---|---|---|---|---|---|---|
| 1230 | Ave. Droplet Concentration ($g/m^3$) | 28.87 | 27.90 | 26.56 | 26.36 | 25.60 | 24.63 | 23.09 | 23.09 |
| 1350 | Ave. Droplet Concentration ($g/m^3$) | 29.20 | 27.40 | 25.71 | 25.00 | 25.71 | 24.52 | 23.34 | 23.10 |
| 1680 | Ave. Droplet Concentration ($g/m^3$) | 29.03 | 26.61 | 25.80 | 24.74 | 24.74 | 24.20 | 24.20 | 23.65 |

Table A.12a: Exit Mist Concentrations for Reynolds Numbers of 2400, 2070, 1810, and 940 (Run 1)

| Reynolds Numbers | Applied Voltage (kV) | 0 | 10 | 15 | 18 | 20 | 22 | 24 | 26 |
|---|---|---|---|---|---|---|---|---|---|
| 2400 | Droplet Concentration ($g/m^3$) | 3.10 | 3.00 | 2.78 | 2.65 | 2.45 | 2.20 | 2.80 | 2.75 |
| 2070 | Droplet Concentration ($g/m^3$) | 3.51 | 2.89 | 2.55 | 2.00 | 2.10 | 2.16 | 2.50 | 2.50 |
| 1810 | Droplet Concentration ($g/m^3$) | 3.10 | 2.41 | 2.20 | 2.35 | 2.00 | 1.95 | 2.15 | 2.00 |
| 940 | Droplet Concentration ($g/m^3$) | 3.56 | 2.95 | 2.75 | 1.95 | 1.85 | 1.00 | 2.06 | 1.85 |

Table A.12b: Exit Mist Concentrations for Reynolds Numbers of 2400, 2070, 1810, and 940 (Run 2)

| Reynolds Numbers | Applied Voltage (kV) | 0 | 10 | 15 | 18 | 20 | 22 | 24 | 26 |
|---|---|---|---|---|---|---|---|---|---|
| 2400 | Droplet Concentration ($g/m^3$) | 3.60 | 3.05 | 2.88 | 2.81 | 2.60 | 2.34 | 2.87 | 2.92 |
| 2070 | Droplet Concentration ($g/m^3$) | 3.72 | 3.35 | 2.70 | 2.30 | 2.21 | 2.15 | 2.73 | 2.53 |
| 1810 | Droplet Concentration ($g/m^3$) | 3.50 | 2.65 | 2.51 | 2.00 | 2.20 | 1.98 | 2.14 | 2.32 |
| 940 | Droplet Concentration ($g/m^3$) | 3.58 | 3.22 | 2.80 | 2.38 | 1.97 | 1.22 | 1.90 | 2.06 |

Table A.12c: Exit Mist Concentrations for Reynolds Numbers of 2400, 2070, 1810, and 940 (Ave.)

| Reynolds Numbers | Applied Voltage (kV) | 0 | 10 | 15 | 18 | 20 | 22 | 24 | 26 |
|---|---|---|---|---|---|---|---|---|---|
| 2400 | Ave. Droplet Concentration ($g/m^3$) | 3.30 | 3.02 | 2.83 | 2.72 | 2.53 | 2.26 | 2.83 | 2.83 |
| 2070 | Ave. Droplet Concentration ($g/m^3$) | 3.60 | 3.12 | 2.61 | 2.14 | 2.19 | 2.16 | 2.61 | 2.51 |
| 1810 | Ave. Droplet Concentration ($g/m^3$) | 3.42 | 2.52 | 2.35 | 2.17 | 2.17 | 1.97 | 2.15 | 2.15 |
| 940 | Ave. Droplet Concentration ($g/m^3$) | 3.56 | 3.08 | 2.80 | 2.16 | 1.90 | 1.10 | 1.95 | 1.95 |

Table A.13a: Exit Mist Concentrations for Reynolds Numbers of 2200, 1680, 1350, and 940 (Run 1)

| Reynolds Numbers | Applied Voltage (kV) | 0 | 10 | 15 | 18 | 20 | 22 | 24 | 26 |
|---|---|---|---|---|---|---|---|---|---|
| 2200 | Droplet Concentration ($g/m^3$) | 8.65 | 7.50 | 6.42 | 5.00 | 4.56 | 4.00 | 3.25 | 2.55 |
| 1680 | Droplet Concentration ($g/m^3$) | 8.32 | 7.51 | 6.00 | 5.20 | 5.00 | 4.25 | 3.90 | 2.75 |
| 1350 | Droplet Concentration ($g/m^3$) | 8.25 | 7.58 | 5.50 | 4.20 | 3.42 | 2.85 | 3.00 | 2.72 |
| 940 | Droplet Concentration ($g/m^3$) | 8.55 | 6.80 | 4.90 | 4.85 | 4.25 | 4.00 | 3.50 | 3.45 |

Table A.13b: Exit Mist Concentrations for Reynolds Numbers of 2200, 1680, 1350, and 940 (Run 2)

| Reynolds Numbers | Applied Voltage (kV) | 0 | 10 | 15 | 18 | 20 | 22 | 24 | 26 |
|---|---|---|---|---|---|---|---|---|---|
| 2200 | Droplet Concentration ($g/m^3$) | 8.80 | 8.38 | 7.32 | 5.72 | 5.00 | 4.43 | 3.66 | 3.25 |
| 1680 | Droplet Concentration ($g/m^3$) | 8.90 | 7.66 | 6.86 | 6.22 | 5.62 | 4.72 | 4.00 | 2.98 |
| 1350 | Droplet Concentration ($g/m^3$) | 8.40 | 7.00 | 6.60 | 4.36 | 3.82 | 3.18 | 3.15 | 3.30 |
| 940 | Droplet Concentration ($g/m^3$) | 8.76 | 7.05 | 6.10 | 5.40 | 4.90 | 4.76 | 3.90 | 3.62 |

Table A.13c: Exit Mist Concentrations for Reynolds Numbers of 2200, 1680, 1350, and 940 (Ave.)

| Reynolds Numbers | Applied Voltage (kV) | 0 | 10 | 15 | 18 | 20 | 22 | 24 | 26 |
|---|---|---|---|---|---|---|---|---|---|
| 2200 | Ave. Droplet Concentration ($g/m^3$) | 8.72 | 7.93 | 6.87 | 5.35 | 4.78 | 4.20 | 3.45 | 2.88 |
| 1680 | Ave. Droplet Concentration ($g/m^3$) | 8.61 | 7.65 | 6.42 | 5.70 | 5.31 | 4.48 | 3.95 | 2.80 |
| 1350 | Ave. Droplet Concentration ($g/m^3$) | 8.32 | 7.30 | 6.00 | 4.25 | 3.60 | 3.00 | 3.04 | 3.04 |
| 940 | Ave. Droplet Concentration ($g/m^3$) | 8.65 | 6.97 | 5.30 | 5.13 | 4.56 | 4.37 | 3.93 | 3.50 |

# VITA

Cyrus K. Riahi-Nezhad was born in suburb of the city of Noor (Vanoosh) near the coast of Caspian Sea located in Mazenderan province in the North of Iran (Persia). He attended Reza Pahlavi and Shareef High School in Chalous, Mazenderan and obtained his high-school diploma with honors in 1973. After finishing his tour of duty (Army) in fall of 1976, he came to U.S.A to pursue his undergraduate and graduate studies in Chemical Engineering. In 1990, he earned his B.S in Chemical Engineering from Tennessee Technological University. In December 2001, he obtained his Master of Science in Chemical Engineering from University of Tennessee at Knoxville. He is currently a U.S Citizen and is employed in Chemical Sciences Division at the Oak Ridge National Laboratory. He is a member of American Institute of Chemical Engineers (AIChE).

3784 2850 of 26
08-07-02 MAB